# LEARNING HIDDEN VARIABLES IN PROBABILISTIC GRAPHICAL MODELS

THESIS SUBMITTED FOR THE DEGREE OF "DOCTOR OF PHILOSOPHY"

BY

**Gal Elidan**

SUBMITTED TO THE SENATE OF THE HEBREW UNIVERSITY

DECEMBER 2004

This work was carried out under the supervision of

**Prof. Nir Friedman**

## Abstract

In the past decades, a great deal of research has focused on learning probabilistic graphical models from data. A serious problem in learning such models is the presence of *hidden*, or *latent*, variables. These variables are not observed, yet their interaction with the observed variables has important consequences in terms of representation, inference and prediction. Consequently, numerous works have been directed towards learning probabilistic graphical models with hidden variables. A significantly harder challenge is that of detecting new hidden variables and incorporating them into the network structure. Surprisingly, and despite the recognized importance of hidden variables both in social sciences and the learning community, this problem has received little attention.

In this dissertation we explore the problem of learning new hidden variable in real-life domains. We present methods for coping with the different elements that this task encompasses: the detection of new hidden variables; determining the cardinality of new hidden variables; incorporating new hidden variables into learning model. In addition we also address the problem of local maxima that is common in many learning scenarios, and is particularly acute in the presence of hidden variables.

We present simple and easy to implement methods that work when training data is relatively plentiful as well as a more elaborate framework that is suitable when the model is particularly complex and the data is sparse. We also consider methods specifically tailored at networks with continuous variables and the added challenges in this scenario.

We evaluate all of our methods on both synthetic and real-life data. For the more elaborate methods, we put a particular emphasis on learning complex models with many hidden variables. We demonstrate significant improvement in quantitative prediction on unseen test samples when learning with hidden variables, reaffirming their importance in practice. We also demonstrate that models learned with our methods have hidden variables that are qualitatively appealing and shed light on the learned domain.

# Acknowledgments

I am indebted to my adviser Nir Friedman who had a profound influence on my research. Nir exposed me to the world of graphical models and flamed my ambition to discover hidden variables. I have learned from Nir, a brilliant scientist, an endless collection of scientific skills: how to approach a complex problem; how to take an idea and make it concrete; how to crisply analyze and understand results; how to go back to data where answers (or more questions) are to be found; how to be critical of myself but always in a constructive way; and the list goes on and on. I truly feel that I have learned from a master and I am sure the principles Nir ingrained in me will help me throughout my career. I was always impressed, and through the years came to appreciate even more, how hands-on Nir's mentoring is and how involved he is in every detail of the research from the fundamental ideas to the axis on a figure of a presentation. Finally, while Nir was being my intellectual mentor he was also, often on the same day, a friend. I have gossiped, dined, hiked, biked and dived with Nir. I cannot but feel extremely lucky that I have had such an inspiring adviser.

I would like to thank, from the bottom of my heart, Eli Shamir, my first adviser. An intellectual role-model and a person who constantly thinks of others, Eli had the insight and confidence to direct me to a then new faculty member whose research interest better matched mine. Throughout my studies, he continued to support and advise. I will always remember the kindness Eli showed in taking the time to think of what is best for me, and his wisdom to push me in the right direction.

I want to thank the other members of my research committee. Yehoshua Sagiv was continuously supportive. Dan Geiger, unknowingly, influenced my career when he gave a superb AI course. Special thanks to the people of the Horowitz foundation for the generous support that allowed me to invest myself in research, and to Intel corporation who provided additional support. I would also like to thank Zvi Gilula for giving me insight to real science, for his unfaltering moral support, and for believing in me. He was always there to help, professionally and as a friend.

I had the pleasure of fruitful collaborations with wonderful people. Noam Lotner helped make my first paper happen, and made working together so easy. Daphne Koller, from the start, inspired me by her intellect and impressed me with her genuine desire to listen to the ideas of a young student. Daphne continued to collaborate, influence and support me throughout my studies and graciously took me under her wing as a postdoc. Dana Pe'er and Aviv Regev showed me how exciting computational biology can be and how far you can get when people work together. Matan Ninio knew how to ask dumbfounding questions that constantly improved our work. Dale Schuurmans made us feel like great scientists and helped us do great work. Yoseph Barash and Tommy Kaplan redefined cooperation and, I hope, paved the way for many works still to come. Iftach Nachman was always laid back yet sharp so that writing a serious paper was carefree. Ariel Jaimovich and Hana Margalit made the last paper in my Ph.D. studies such a friendliness based success.

I spent six wonderful years at the computer science department at the Hebrew university and worked with wonderful people. Thank you Yael, Ziva, Silvi, Regina, Rina, Lital, Ayelet, Relly, Hagit, Koby and Eli for your friendliness and for going out of your way to help me, so that I never felt the weight of bureaucracy. I want to thank Eli Shamir, Tali Tishby, Yoram Singer, Nir Friedman and Yair Weiss for creating a world class learning lab that strives for excellence and at the same time maintains a friendly atmosphere, where students are listened to, and faculty doors are always open. I want to thank Yair for giving me an eye-opening experience as his teaching assistant. I was fortunate to be a member of a special lab where friendship invigorates research. All current and former lab members, including Noam S., Ran, Gill, Gal, Amir G., Lavi, Amir N., Yevgeni and Yossi, were there to drink coffee and so much more. Koby "learned learning" with me and were there for endless thought provoking discussions. Shai was willing to advise about linear algebra, Hazzanic music and the nature of god. Ofer was always ready to be passionate about anything and everything. Elon gave me a "glimpse" to political conscience.

I was also lucky to be a part of Nir's group, a small family. Tal and Noam were with me from the beginning and I will always consider them my friends. Ori, Hillel, Omri, Tomer, Yuval and Ilan made every day so enjoyable. Dana was there to talk, support and care. Noa and Ariel, so quickly, naturally and deservedly became a part of us all and made us smile. Matan made everything exciting and was always ready to be a friend. Iftach gave me a fresh perspective on life and inspired me with his big heart. Finally, my roommates, collaborators and friends, Tommy and Yoseph. We talked about everything. Just by being there you made this era of my life so memorable.

I want to thank my wonderful family. My younger sister Orly who gave me constant support by her appreciation of who I am. My big brother Sharon who from an early age encouraged my curiosity and tirelessly challenged me to think. My parents Sara and Yossi who fed the flame within me and somehow found the time to answer my endless questions. It is because of all of you that I have come this far. I will forever be grateful.

Last, I am at a loss for words on how to thank my eternal love Tali. George Eliot once wrote: "What greater thing is there for two human souls than to feel that they are joined... to strengthen each other... to be at one with each other in silent unspeakable memories". How right he was! Tali, I have met you when I started my graduate studies and you have given me all that and more. You have strengthened me and were with me in all moments and memories, silent or not. For everything that was and will be, thank you.

To my parents who supported and loved me unconditionally
and to Itai, my son, who I hope will one day feel as I do.

# Contents

# Chapter 1

# Introduction

The intriguing world around us is endlessly complex and forever surprising. How then, do we humans manage to cope with different tasks? From infancy we learn to identify relevant influencing factors and allow experience to form deep rooted knowledge, which guides our decision making processes: Before going outdoors we listen to the forecast, take a quick glance outside, and somehow combine these observations to decide whether taking an umbrella is worth the hassle; A financial analyst combines his formal knowledge and his "market-sense" experience to explain current changes in the stock market and predict future trends. Real-life problems are further complicated by the fact that we are usually given only a partial view of the world. A physician will typically want to make a diagnosis *before* all possible tests have been carried out; A SWAT squad leader will have to handle a hostage situation without necessarily knowing the full details of the terrorists' strength. In fact, in making decisions for a domain of interest, an influencing factor may *never* be observed. A chess player, for example, will never have access to his opponent's strategy and mood at a particular game, but will constantly try to infer it from the observed moves, the time it took to make them, and the opponent's history of games. Such hidden factors abound in real-life domains, and often play the part of central hidden mechanisms influencing many of the observations. It is the goal of this dissertation, to learn these hidden, or *latent* entities.

## 1.1 Probabilistic Graphical Models

In coping with the challenges outlined above, we rely heavily on our life experience. For example, long before we formally study the constructs of the language, we learn how to talk by hearing those around us speak. A child learn how to ride a bicycle without understanding the fundamentals of mechanical physics. From its early days, computer science has tried to mimic these human capabilities, or least cope successfully with similar tasks. As the availability of structured data grew, a transition

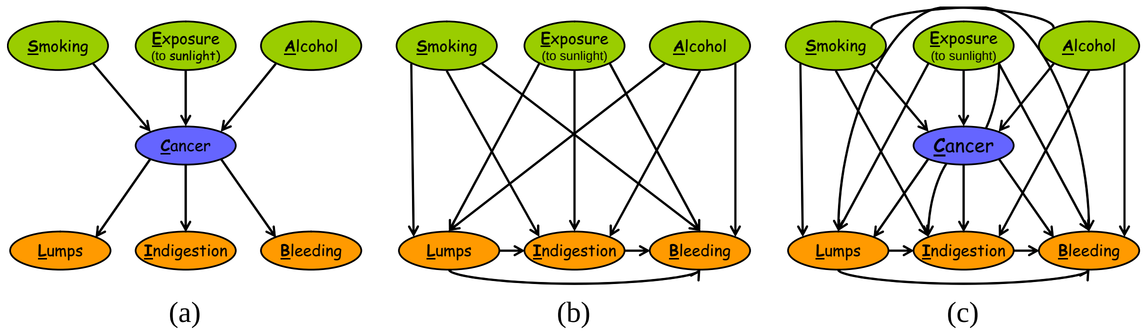

Figure 1.1: Simple network for a cancer domain. (a) shows a plausible structure where Cancer separates its causes from symptoms. (b) shows the resulting structure when Cancer is removed from the model and is no longer able to mediate between its parent and children nodes. (c) shows a possible structure when Cancer is included in the model but its cardinality is too small.

has taken place from classical rule based Artificial Intelligence [Russell and Norwig, 1995] to example based *Machine Learning*. In this field, where our aim is to learn from examples, algorithms are applied to data in order to produce favorable hypothesis, just as we humans apply our inherited skills to the observations of the world around us. A central paradigm in Machine Learning is that of probabilistic graphical models [Pearl, 1988, Jensen, 1996, Lauritzen and Spiegelhalter, 1988] that have become extremely popular in recent years, and are being used in numerous applications (e.g., [Heckerman et al., 1995b]).

Probabilistic graphical models compactly represent a joint distribution over a set of variables in a domain, and facilitate the efficient computation of flexible probabilistic queries. Nodes in the graph of such models denote relevant entities or *random variables*, and the graph structure encodes probabilistic relations between them. Figure 1.1(a) shows the structure of a simple directed graphical model, called a *Bayesian network* [Pearl, 1988] for a cancer domain. One of the most appealing features of the graph representation is that it is easily interpretable, and tells us a lot about the qualitative structure of the domain. For example, it is easy to "read" from the graph that the relation between Smoking and the appearance of Lumps in an x-ray is mediated by the Cancer node. It is also easy to see that Cancer is concurrently effected by several possible direct causes. In contrast, Cancer is the only direct influencing factor on Bleeding.

The parameters of a probabilistic graphical model complement the structure to represent a full joint probability distribution over the variables in the domain. This probability distribution is special in that it takes the form of the structure of the model. For example, the distribution represented by our simple structure of the cancer domain can be written as

$$P(C,S,E,A,L,B,I) = P(S)\cdot P(E)\cdot P(A)\cdot P(C\mid S,E,A)\cdot P(L\mid C)\cdot P(B\mid C)\cdot P(I\mid C)$$

where, for convenience, instead of the variable's full name we use a single letter as shown in Figure 1.1. Notice that the individual terms in the above *decomposition* of the distribution correspond to properties that we intuitively interpreted from the graph structure. For example $P(S)$ encodes the fact that there are no predecessor causes of Smoking. It is this decomposition that gives probabilistic graphical models their unique advantage and facilitates a compact representation of the joint distributions. In the cancer example, naively representing the full joint distribution over 7 binary variables requires $2^7 - 1 = 127$ parameters, each providing the probability to one of the joint assignment of these variables. However, the above decomposition is made up of smaller building blocks requiring just $1 + 1 + 1 + 8 + 2 + 2 + 2 = 17$ parameters, corresponding to the factors $P(S)$,$P(E)$,$P(A)$,$P(C \mid S, E, A)$,$P(L \mid C)$,$P(B \mid C)$, and $P(I \mid C)$, respectively. Obviously, for larger domains the savings can be significantly larger, enabling us to cope with distributions that are otherwise considered “infeasible”.

The decomposition of the distribution has many advantages and its importance cannot be overstated. The compact representation is not only a goal in itself, but also facilitates efficient probabilistic computations [Pearl, 1988, Jensen et al., 1990]. Given a joint distributions, a central task of interest is that of inference, or answering probabilistic queries. For example, we might be interested in the probability of an Anthrax attack given a partial observation on several potential “red flag” factors. Alternatively, given an outcome such as the presence of a disease, we might want to *decode* or diagnose the causes the most probably led to it. We might also examine the influence of one factor on another to quantify the merit of future decisions. All these tasks are typically intractable even for small domains if the joint distribution is naively represented. While inference in general graphical models is NP-hard [Cooper, 1990], the decomposition of the distribution allows us to compute varied probabilistic queries for relatively large and complex domains.

The decomposability of the joint distribution also has important implications on our ability to learn these models from data. In practice, we are given a limited amount of training data and want to learn a hypothesis or model. The performance of practically any method in Machine Learning for doing so, deteriorates as the number of parameters grows larger with respect to the number of samples. Intuitively, if there are many parameters and few samples, each parameter will be supported by little evidence, and its estimation will not be as robust. In this case, the learning procedure will capture specifics of the training data (including noise), rather than the regularities that will enable it to make predictions for unseen samples. That is, the model will *over-fit*, or will be highly adapted, to the training data, rather than have good generalization capabilities. Indeed, the need for a succinct model in Machine Learning is today both theoretically and practically justified. Probabilistic graphical models offer an appealing framework for formulating and learning such models.

Probabilistic graphical models in general, and Bayesian network models in particular, have become popular following the work of Pearl [1988]. Since then numerous works have dealt with the problem of learning these models from the data. When the data is *complete*, so that each variables is observed in each instance, closed form formulas for estimating the *maximum likelihood* parameters are known for many useful distributions. The main challenge in this case is to learn the structure of the network. As the number of possible structures is super-exponential in the number of variables, heuristic greedy procedures are typically used. These explore the space of structures by considering local changes to the structure (e.g., edge addition, deletion or reversal), and are prone to get stuck in local maxima. When some observations are missing or some variables are altogether unobserved, learning is significantly harder: local maxima often trap the learning procedure and lead to inferior models. In fact, the problem of local maxima is common to most learning tasks, and is central in learning probabilistic graphical models. When we consider real-life domains, we also have to cope with the fact that the sheer size of the problem may limit our ability to learn an effective model in practice. Consequently, much of the research in recent years has been directed at learning probabilistic graphical models in complex scenarios where some of the data may be missing (e.g., [Friedman, 1997, Jordan et al., 1998]).

## 1.2 Hidden Variables

In this dissertation, we address the task of learning new hidden variables in probabilistic graphical models for real-life domains. That is, we are interested in hidden variables that are not known to be part of the domain, in contrast to those of which we have prior knowledge. Thus, in addition to the task of learning the parameters and structure of the model, we face the further complication of whether and how to incorporate new hidden variables into the network structure. Why then, should we bother with hidden variables that are never observed and seemingly contribute no new information to the model?

Consider again the model of the Cancer domain shown in Figure 1.1 (a). This simple model encodes the fact that an observation of the Cancer node separates possible causes (smoking, exposure to sunlight, excessive consumption of alcohol) from a few plausible symptoms (lumps,unusual bleeding,chronic indigestion). Now imagine a physician of the 16th century who is yet unaware of the existence of this yet undiscovered disease. Such a physician might be able to recognize a correlation between smoking of a Nargile (a hookah) and the appearance of lumps. He might also be able to deduce a relation between repeated bleeding and chronic indigestion. Slowly, accumulating these correlations, the physician may end up with a model that is similar to the one shown in Figure 1.1(b).

The “true” structure in Figure 1.1(a) is more appealing for several reasons. First, intuitively, it tells us much more about the domain’s structure, and in particular about the way that the different variables influence each other. For example, we can deduce that by refraining from smoking, we can reduce the chances of having cancer and consequently avoid its symptoms. Without the knowledge of the disease, we might think that if we treated our chronic indigestion, we would be able to somehow reduce the life threatening bleeding. In fact, this type of hidden variable exemplifies the process of scientific discovery where a new entity, mechanism or base theory are introduced to explain common correlated phenomena. Second, the structure with the hidden variable offers a much more compact representation of the domain. In contrast to Eq. (1.1), the distribution of the model in Figure 1.1(b) decomposes as

$$\begin{aligned} &P(C,S,E,A,L,B,I) = \\ &\qquad P(S)\cdot P(E)\cdot P(A)\cdot P(L \mid S,E,A)\cdot P(B \mid S,E,H,L)\cdot P(I \mid S,E,H,L,B). \end{aligned}$$

This decomposition is clearly less favorable than the decomposition that follows the original structure. The term $P(I \mid S,E,H,L,B)$ alone, for example, uses $2^5 = 32$ parameters, one for each joint value of $S,E,H,L$ and $B$. Thus, the removal of a hidden variable from the model, may result in a network structure that is significantly more complex and has almost no structure (most nodes are connected to most of the other nodes). Such a model is not only less interpretable, but is also less appealing in terms of inference, and can greatly deteriorate our ability to learn from data.

Let us now reconsider the structure of the cancer domain of Figure 1.1(a), where the Cancer node now has three values: none, mild and severe. A slightly more knowledgeable physician of the 19th century is already aware of the existence of cancer but does not differentiate between different severities, since cancer always leads to death (in his century). Just as in the case of the 16th century physician, this lack of knowledge may result in a skewed understanding of the world. For example, the marginal distribution of Bleeding and chronic Indigestion can be very different for mild and severe cases of cancer. Our physician considers all cancer cases as a whole, and thus might deduce that there is a direct correlation between these two nodes that Cancer cannot mediate. Similar considerations for other variables may lead the physician to construct the model shown in Figure 1.1 (c). This model is even more complex than the model constructed without the Cancer node. It has less structure and significantly more parameters. Thus, knowing the number of distinct values a hidden variable has can be just as important as knowing about its existence and the relation of that hidden variable to the rest of the variables in the domain.

Both of the above examples motivate our goal of learning new hidden variables and correctly determining their cardinality. The benefit of learning such variables is twofold: First, learning these variables effectively can result in a succinct model for representing the distribution over the known entities, which in turn facilitates efficient inference and robust estimation. Second, by learning new hidden variables, we can improve our understanding of the domain, potentially revealing important hidden entities. Considering the above examples, it is not surprising that the importance of incorporating hidden variables in the model was recognized early on in the probabilistic graphical models community (e.g., [Spirtes et al., 1993, Pearl, 2000]), and much earlier in the philosophical, statistical and social sciences and in particular in the use of *Structural Equation Models* [Wright, 1921].

What is surprising, is that despite the influx of research for learning probabilistic graphical models in recent years, few works address the challenge of learning new hidden variables in these models.

Imagine a tool that would have revealed the structure and cardinality of the Cancer variable to those early physicians and the implications of such a tool. It is the goal of this dissertation to present methods that will form the first step towards this goal, in probabilistic graphical models.

## 1.3 Road Map of Our Methods

Learning new hidden variables involves three central challenges. The first is the correct placement of the hidden variable within the structure of the model. Without an initial "intelligent" guess, there is little hope that standard search algorithms will be able to "correct" the structure. On the other hand, it is unreasonable to assume that any method will be able to perfectly position a new hidden. Thus, a good initial placement of a hidden variable must be followed by an effective structure adaptation algorithm. Second, as discussed above, determining the cardinality of a new hidden variable can have an effect on the learned structure that is just as important as the discovery of the hidden variable. We can expect a new hidden variable to be effective only if it is of approximately the correct cardinality. Third, even if a new hidden variable is placed approximately correctly within the structure and with a reasonable cardinality, then the starting point of its parameters can have a significant effect on the network learned by learning algorithm that follow this initial construction.

In coping with these tasks we take a pragmatic view of the problem of learning new hidden variables. That is, unlike *causality* oriented works (e.g., [Spirtes et al., 1993, Pearl, 2000]), we want to add a new hidden variable whenever it improves the predictions of our model. In taking this pragmatic view, we must also consider the possibility that a hidden variable will not be useful if its incorporation into the model is not followed by an effective learning procedure. Thus, to learn hidden variables in practical real-life domains, we must also cope with the practical problem of optimization. Specifically we want to address the problem of local maxima that abound in the presence of hidden variables, and that can trap the learning procedure resulting in inferior models. We now briefly outline the methods explored in this dissertation to handle all of these tasks.

As a preliminary, in Chapter 2 we review the foundations of probabilistic graphical models with an emphasis on a probabilistic interpretation of *Bayesian networks*. We present definitions as well algorithms for inference, parameter estimation and structure learning that are used throughout the rest of the dissertation.

In Chapter 3 we address the problem of local maxima in general parameter estimation and structure learning. The basic idea is that by a re-weighting of samples, e.g., by strengthening of "good" samples and weakening of "bad" ones, we can guide the learning procedure in desirable directions. We present the *Weight Annealing* method that is related both to annealing methods [Kirpatrick et al., 1994, Rose, 1998] and the boosting algorithm [Schapire and Singer, 1999]. We demonstrate the effectiveness of the method for parameter learning with non-linear probability distributions, for structure search with complete data and for structure search in the presence of hidden variables. We also show the applicability of the method to general learning scenarios that are not limited to probabilistic graphical models.

In Chapter 4 we introduce the first and most straightforward method for introducing new hidden variables into the network structure. The motivation for the method comes from the phenomena exemplified in our discussion of the cancer domain in Section 1.2. In that example, the Cancer node was the keystone of a succinct and desirable representation of the domain. When Cancer was hidden, much of the structure was lost. In particular, a clique was formed over all of its children. We show that this phenomena is formally a potential result of the removal of a hidden variable from the domain. Thus, a clique like structure can be used as a structural signature to suggest new putative hidden variables. In our method, we search for such signatures and reverse engineer the hidden variable. We show that this method is able to reconstruct synthetic hidden variables. We further show that in real-life domains, the method is able to introduce new novel hidden variables that improve the prediction of unseen samples, and have an appealing interpretation.

In Chapter 5 we present a complementing technique for determining the cardinality of the hidden variable. Our method starts with an excessive number of states for the hidden variable, and proceeds by bottom up agglomeration of states. Intuitively, two states are merged if their role in the training distribution is similar, and they can be approximated reasonably by a single state. We show how this intuition can be instantiated so that the algorithm is efficient in practice. We demonstrate that this method, in conjunction with the hidden variables discovery algorithm, is further able to improve the quality of the learned model.

In Chapter 6 we present a new approach that concurrently addresses all of the challenges we face. Our method is based on the following idea: a model that performs well on training data is one that captures the behavior of the observed variables in different instances. On the other hand, in order to generalize to unseen samples, we want to forget the specifics of the training data and capture the regularities of the domain. We define a balance between these two competing factors using the *Information Bottleneck* framework of Tishby et al. [1999], and formally show that it is directly related to the standard EM objective [Dempster et al., 1977, Lauritzen, 1995], for learning the parameters of Bayesian networks with hidden variables. This formulation allows us to use continuation [Watson, 2000], where we define a smooth transition between an easily solvable problem to the hard learning objective. By tracking the path of local maximum between these two extremes, the method is able to bypass local maxima and learn preferable models. Importantly, this same approach also facilitates learning of new hidden variables and their cardinality, using emerging information signals. Not unlike the structural signature used in Chapter 4, these signals are information theoretic "evidence" that a hidden variable is potentially missing from the domain. We demonstrate the effectiveness of the method on a range of hard real-life problems.

The final method we present in Chapter 7 specifically addresses the challenge of learning continuous variables networks. In these networks, learning with non-Gaussian conditional probability distributions is often impractical even for relatively small domains. We address this added challenge together with the task of learning new hidden variables. We first present a general method for significantly speeding the search in this scenario, facilitating learning of large scale domains. The basic idea is straightforward: instead of directly evaluating the benefit of different structures (a costly procedure), our method efficiently approximates this benefit, and allows the search procedure to concentrate only on the most promising candidate structures. Importantly, our formulation also offers a guided measure for introducing new hidden variables into the network structure. We demonstrate the effectiveness of the method on large scale problems with linear and non-linear conditional probability distributions.

Finally, in Chapter 8, we summarize and discuss our different methods, their relation to each other, and their relation to other approaches for learning new hidden variables. We conclude with future prospects for the problem of learning new hidden variables, which continues to pose significant theoretical as well as practical challenges.

# Chapter 2

# Probabilistic Graphical Models

Probabilistic graphical models are natural for modeling the rich and complex world around us. Using a graphical model, we can encode the inherent structure of the domain and utilize this structure to perform different task efficiently such as probabilistic inference and learning. Specifically, for a given domain we are interested in modeling the joint distribution over a set of random variables $\mathcal{X} = \{X_1, \ldots, X_N\}$ that are part of the domain. Even for the simplest model where all variables are binary valued, representing the joint distribution over the domain requires the specification of probability for $2^N$ different assignments. Obviously, this is infeasible without taking advantage of regularities in the domain. A key property of all probabilistic graphical models is that they encode conditional independence assumptions in a natural manner, and use these independence properties to compactly represent a joint distribution. Graphical models also facilitate the treatment of uncertainty over these variables via standard probabilistic manipulations and allow us to easily incorporate prior knowledge both about the parameters and structure of the model. Finally, exploring the qualitative graph structure and the quantitative parameterization learned from observed data can reveal inherent regularities and enrich our knowledge of the domain.

Specific forms of graphical models such as *Hidden Markov Models* (HMMs) [Rabiner, 1990] and *Decision Trees* [Buntine, 1993, Quinlan, 1993] have been long used in various fields independently. The foundations for general probabilistic graphical models emerged independently in several communities in the early 80's. In a seminal book, Pearl [Pearl, 1988] set the basis for much of modern research of both directed Bayesian networks and undirected Markov networks. Since then, in addition to a wide variety of applications in numerous fields (see, for example, [Heckerman et al., 1995b]), the field of research of probabilistic graphical models has seen exponential growth, including: a variety of specific forms of graphical models such as *Multinets* [Geiger and Heckerman, 1996] and *Mixture Models* [Cheeseman et al., 1988]; a multitude of algorithmic innovations such as the *Structural EM* (SEM) algorithm [Friedman, 1997, Meila and Jordan, 1998, Thiesson et al.,

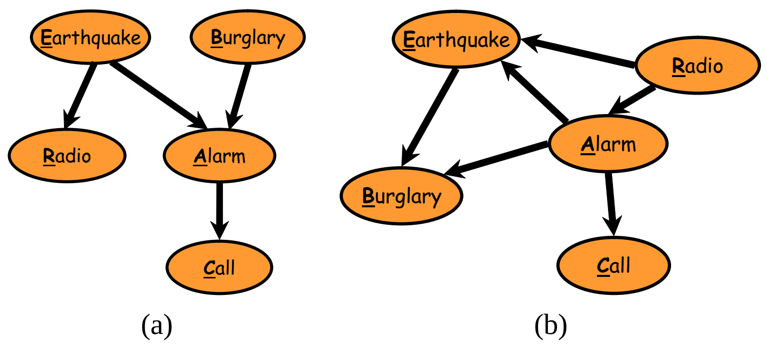

Figure 2.1: (a) An example of a simple Bayesian network structure for a burglary alarm domain. This network structure implies several conditional independence statements: $(E \perp B)$,$Ind(A \perp R \mid B, E)$,$Ind(R \perp A, B, C \mid E)$, and $Ind(C \perp B, E, R \mid A)$. The joint distribution has the product form $P(A, B, C, E, R) = P(B)P(E)P(A|B, E)P(R|E)P(C|A)$. (b) An *I-map* of the distribution defined by (a).

1998] and variational approaches for learning [Jordan et al., 1998]; several generalizing frameworks such as *Chain Graphs* [Lauritzen and Wermuth, 1989], *Dynamic Bayesian Networks* [Dean and Kanazawa, 1989] and *Probabilistic Relational Models* [Friedman et al., 1999a]. Although many of the methods in this dissertation apply to most forms of probabilistic graphical models, most of the results are demonstrated on the framework of directed Bayesian networks. In this chapter we provide a brief overview of this formalism and related algorithms. We describe additional background material throughout the dissertation when relevant.

## 2.1 The Bayesian Network Model

A *Bayesian Network* (BN) is a compact representation of a joint distribution over a set of random variables $\mathcal{X} = \{X_1, \ldots, X_N\}$. The model includes a qualitative graph structure that encodes independence relations between the different variables and quantitative parameters that, together with the graphs structure, define a unique distribution. We start with a brief overview of how a graph encodes the relations between the variables and then formally define the Bayesian network model.

### 2.1.1 Encoding Independencies

At the core of Bayesian networks is the notion of *conditional independence*.

**Definition 2.1.1:** We say that $\mathbf{X}$ is *conditionally independent* of $\mathbf{Y}$ given $\mathbf{Z}$ if

$$P(\mathbf{X}|\mathbf{Y}, \mathbf{Z}) = P(\mathbf{X}|\mathbf{Z}) \quad \text{when } P(\mathbf{Z}) > 0$$

and we denote this statement by $P \models Ind(\mathbf{X} \perp \mathbf{Y} \mid \mathbf{Z})$. ▮

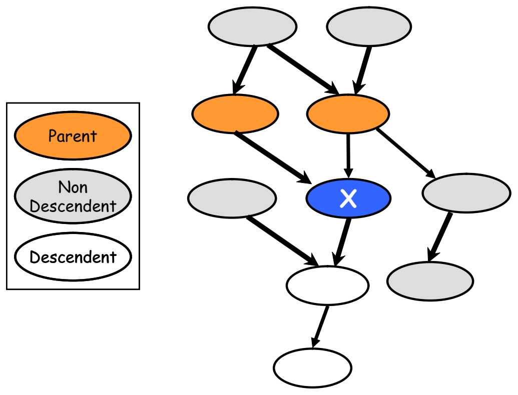

Figure 2.2: Illustrative example of the Markov independence statements. $X$ is independent of all its non-descendents nodes in the graph $\mathcal{G}$, given its parent nodes. In contrast, $X$ is not unconditionally independent of any of its descendent nodes.

We explain this concept as it applies to graphs using the classical example from [Pearl, 1988] shown in Figure 2.1 (a). The graph describes a simple house alarm (A) domain that can be triggered either by burglary (B) or by an earthquake (E). These events are deemed independent. If the alarm is triggered by any of these causes or spontaneously, a call (C) from the neighbor can be expected. In addition, an earthquake is usually followed by a radio report (R). The neighbor's call is, obviously, independent of a cause that might trigger the alarm if we already know whether the alarm was activated. Similarly, a radio report of an earthquake might influence our belief concerning the chances of burglary given that the alarm has been activated, but is no longer relevant if we actually know whether an earthquake occurred. We now formalize these intuitive independence statements that underlie the above example.

**Definition 2.1.2:** Let $\mathcal{G}$ be a *Directed Acyclic Graph* (DAG) whose vertices correspond to random variables $\mathcal{X} = \{X_1, \ldots, X_N\}$. We say the $\mathcal{G}$ encodes a set of *Markov independence statements*: Each variable $X_i$ is independent of its non-descendants, given its parents in $\mathcal{G}$.

$$\forall X_i \;\; Ind(X_i \perp \mathbf{NonDescendants}_{X_i} \mid \mathbf{Pa}_i)$$

and we denote the set of these statements as *Markov*$(\mathcal{G})$. ▮

Figure 2.2 illustrates the concept of the Markov independence statements.

Using the rules of probability, we can infer additional independence statements from *Markov*$(\mathcal{G})$. For example, in Figure 2.1 (a), we can say that $Ind(A \perp R \mid E)$. This is follows from $Ind(R \perp A, B, C \mid E) \Rightarrow Ind(R \perp A \mid E)$ and symmetry of independence. Similarly, it is easy to see that all the independence statements we made in the case of the burglary alarm domain follow directly from the Markov I-statements encoded in that graph.

The ability to infer independencies allow us to characterize the following useful notion

**Definition 2.1.3:** The minimal set of variables in $\mathcal{X}$ that render $X_i$ independent of the rest of the variables given this set is called the *Markov Blanket* (MB) of $X_i$ and is denoted by $\mathbf{MB_i}$. By definition

$$Ind(X_i \perp \mathcal{X} \setminus \{X_i, \mathbf{MB_i}\} \mid \mathbf{MB_i})$$

▮

It follow directly from *Markov*$(\mathcal{G})$ that for any general graph $\mathcal{G}$, $\mathbf{MB_i}$ includes the parents of $X_i$, the children of $X_i$ and all of the children's parents (spouses).

In general, there are numerous independence statements that can be derived from *Markov*$(\mathcal{G})$. The notion of *d-separation* is used to determine whether a specific independence statement $Ind(X \perp Y \mid Z)$ holds. Briefly, $X$ and $Y$ are d-separated given $Z$, if *all* undirected paths between $X$ and $Y$ are *blocked*. A path is blocked if it contains any of the following sub-paths of three nodes

1. $U \rightarrow Z_i \rightarrow V$ such that $Z_i \subset Z$.
2. $U \leftarrow Z_i \rightarrow V$, such that $Z_i \subset Z$.
3. $U \rightarrow W \leftarrow V$, a *v-structure*, where no descendent of $W$ is in $Z$.

If non of these occur in a path, it is not blocked, in which case $X$ and $Y$ are *not* d-separated given $Z$. D-separation can be computed efficiently in time that is linear in the number of variables in the graphs [Geiger et al., 1990]. Note that d-separation only tells us about independencies that must follow from the graph structure that encodes *Markov*$(()\mathcal{G})$. That is, if $X$ and $Y$ are d-separated given $Z$ then $Ind(X \perp Y \mid Z)$ holds in the distribution $P$. However, if they are not d-separated, it is not necessarily the case that $Ind(X \perp Y \mid Z)$ does not hold in $P$. Thus, d-separation cannot rule out additional independencies that may hold in the distribution $P$ and are not encoded in the graph structure.

The following defines graph structures that cannot be distinguished by d-separation (or by any other method that only uses information encoded in the graph structure $\mathcal{G}$):

**Definition 2.1.4:** We say that $\mathcal{G}_1$ and $\mathcal{G}_2$ are *independence equivalent* if

$$\textit{Markov}(\mathcal{G}_1) \Leftrightarrow \textit{Markov}(\mathcal{G}_2)$$

That is, *Markov*$(\mathcal{G}_1)$ and *Markov*$(\mathcal{G}_2)$ imply they same set of independencies. ▮

Chickering [1995] offers an efficient method for testing whether two structures belong to the same equivalence class.

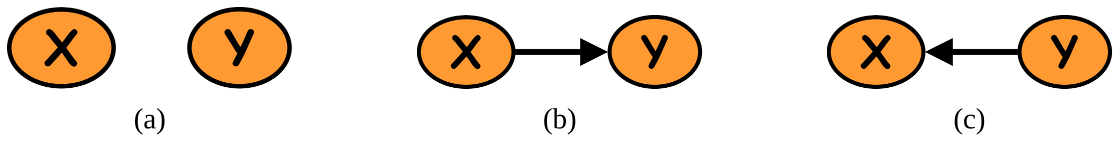

Figure 2.3: Three graph structures that are all *I-map*s of the distribution $P(X, Y) = P(X)P(Y)$ where $X$ and $Y$ are independent. Only (a) is a minimal *I-map* of this distribution.

### 2.1.2 Independence Map (*I-map*)

Since we are interested in graphs that encode a joint distribution $P$ over the random variables, we now define the relation between the graph structure and the probability it encodes.

**Definition 2.1.5:** We say that the graph $\mathcal{G}$ is an *Independence map* (*I-map*) of the distribution $P$ over the random variables $\mathcal{X} = \{X_1, \ldots, X_N\}$ if

$$P \models \mathit{Markov}(\mathcal{G})$$

∎

This implies that all of the independencies that can be derived from *Markov*$(\mathcal{G})$ are satisfied by $P$. Note, however, that $P$ may also include additional independencies. Consequently, the complete graph is an *I-map* of any distribution. Furthermore, the *I-map* of a particular distribution $P$ is not unique. For example, there are three graphs that are *I-map*s of the distribution over two random variables $X$ and $Y$ where $X$ and $Y$ are independent as shown in Figure 2.3.

The above suggest that we might want to define a stricter relation between the graph $\mathcal{G}$ and the distribution $P$. When $\mathcal{G}$ is an *I-map* of $P$ and the distribution does not satisfy any additional independencies that are not encoded by $\mathcal{G}$, we say that $\mathcal{G}$ is a *Perfect Map* (*P-map*) of $P$. This turns out to be too stringent as there are many distributions for which a Bayesian network *P-map* does not exists such as a XOR relation between three random variables. Other distributions can only be captured by directed probabilistic graphical models and cannot be captured by undirected *Markov Networks* [Pearl, 1988]. Instead, we use the following notion

**Definition 2.1.6:** We say that the graph $\mathcal{G}$ is a *minimal* I-map of the distribution $P$ over the random variables $\mathcal{X} = \{X_1, \ldots, X_N\}$ if it is an *I-map* of $P$ and the removal of any edge from it renders it a non-*I-map* of $P$. ∎

It is easy to show that for a given distribution, the minimal *I-map* is not unique and different minimal *I-map*s can vary significantly. Figure 2.1 (b) shows a graph structure that is an *I-map* for the distribution defined by Figure 2.1 (a) (the distribution for which this structure is a *P-map*). An important consequence of *I-map*ness is that it allows us to decompose the distribution $P$. Specifically, the *factorization theorem* states that

**Theorem 2.1.7:** [Pearl, 1988] $\mathcal{G}$ is an *I-map* of $P$ if and only if $P$ can be written as

$$P(X_1, \ldots, X_N) = \prod_{i=1}^{n} P(X_i \mid \mathbf{Pa}_i^{\mathcal{G}}) \tag{2.1}$$

where $\mathbf{Pa}_i^{\mathcal{G}}$ are the parents nodes of the variables $X_i$ in $\mathcal{G}$.

This theorem is a direct consequence of the chain rule of probabilities and properties of conditional independence.

### 2.1.3 Model Defi nition

We can now formally define the Bayesian network model.

**Definition 2.1.8:** [Pearl, 1988] A *Bayesian network* $\mathcal{B} = \langle \mathcal{G}, \theta \rangle$ is a representation of a joint probability distribution over a set of random variables $\mathcal{X} = \{X_1, \ldots, X_N\}$, consisting of two components: A *directed acyclic graph* $\mathcal{G}$ whose vertices correspond to the random variables and that encodes the *Markov independence assumptions Markov*$(\mathcal{G})$; a set of parameters $\theta$ that describe a *conditional probability distribution* (CPD) $P(X_i \mid \mathbf{Pa}_i)$ for each each variable $X_i$ given parents in the graph $\mathbf{Pa}_i$. In addition, we require that $\mathcal{G}$ is an *I-map* of the distribution $P$ represented by the Bayesian network. ▮

Using the factorization theorem, the two components, $\mathcal{G}$ and $\theta$, define a unique probability distribution that can be written as in Eq. (2.1). This is called the *chain rule for Bayesian networks*. This product form makes the Bayesian network representation of a joint probability compact, and economizes the number of parameters. As an example, consider the joint probability distribution $P(B, E, R, A, C)$ represented in Figure 2.1. By the chain rule of probability, without any independence assumptions:

$$P(B,E,R,A,C) = P(B)P(E|B)P(R|B,E)P(A|B,E,R)P(C|B,E,R,A,C)$$

Assuming all variables are binary, this representation requires $1+2+4+8+16 = 31$ parameters. Taking the conditional independencies into account we can write

$$P(B,E,R,A,C) = P(B)P(E)P(R|E)P(A|B,E)P(C|A)$$

which only requires $1+1+2+4+2 = 10$ parameters. More generally, if $\mathcal{G}$ is defined over $N$ binary variables and its indegree (i.e., maximal number of parents) is bounded by $K$, then instead of representing the joint distribution with $2^N - 1$ independent parameters we can represent it with at most $2^K N$ independent parameters.

| $b$ | $e$ | $P(a = \text{false})$ | $P(a = \text{true})$ |
|---|---|---|---|
| false | false | 0.96 | 0.04 |
| false | true | 0.67 | 0.33 |
| true | false | 0.91 | 0.09 |
| true | true | 0.96 | 0.04 |

Table 2.1: A plausible conditional probability table (CPT) encoding the conditional probability distribution (CPD) of $P(A \mid B, E)$ of the alarm domain of Figure 2.1

The graph structure $\mathcal{G}$ encodes independence assumptions and defines the qualitative decomposition form of the distribution. To specify a unique joint distribution over $\mathcal{X}$, a quantitative parameterization $\theta$ defines the conditional probability distributions $P(X_i \mid \mathbf{Pa}_i)$, which can be of any general form. For discrete variables, the most general representation is a *conditional probability table* (CPT). Each row in the table corresponds to a specific joint assignment $\mathbf{pa}_i$ to $\mathbf{Pa}_i$, and specifies the probability vector for $X_i$ conditioned on its parents. For example, if $\mathbf{Pa}_i$ consists of $K$ binary valued variables, the table will specify $2^K$ distributions. Consider again the example of Figure 2.1 and the conditional probability distribution $P(A \mid E, B)$. Table 2.1 encodes the intuition that the alarm is somewhat likely to go off given that there was an earthquake, very likely to be triggered if there was a burglary and will probably not sound if neither of these happened.

A full table form can describe any discrete conditional distribution but comes at a representational price: the number of free parameters is exponential in the number of parents.

Obviously, in many scenarios more compact forms can be considered according to additional regularity that underlies $P(X_i \mid \mathbf{Pa}_i)$, and that is not captured by the structure of $\mathcal{G}$. Several forms try to cope with common scenarios: In some scenarios, once some variables is observed, a previously relevant variable becomes irrelevant. For example, given that we observe heavy rain, our decision to take an umbrella probably does not depend on the morning forecast we hear earlier. This phenomena is captured by a *Context Specific Independence* (CSI) representation for CPDs [Boutilier et al., 1996] that is in fact a limited form of a decision tree. *Default tables* [Friedman and Goldszmidt, 1996b] are suitable for cases where the probability distribution of $X_i$ given $\mathbf{Pa}_i$ has some default value excluding a small number of assignments $\mathbf{pa}_i$; *noisy-OR* CPDs are common in medical domains and capture a scenario where on observation such as a symptom, may be triggered independently by a number of causes such as diseases (e.g., [Diez, 1993]). The representation of noisy-or CPDs is linear in the number of parents which make it suitable for large scale domains (e.g., [Shwe et al., 1991]). Similarly, other form of noisy deterministic functions can be considered for a variety of scenarios.

Unlike the case of discrete variables, when the variable $X$ and some or all of its parents are real valued, there is no representation that can capture all conditional densities. A common choice is the use of *linear Gaussian* conditional densities [Geiger and Heckerman, 1994], where the dependency between a variable and its parents is modeled as linear. When all the variables in a network have linear Gaussian conditional densities, the joint density over $\mathcal{X}$ is a multivariate Gaussian [Lauritzen and Wermuth, 1989]. In many real world domains, such as in neural networks or gene regulation network models, the dependencies are known to be non-linear. One example is a representation that models a saturation effect such as a sigmoid CPD (e.g., [Neal, 1992, Saul et al., 1996]).

### 2.1.4 Inference

A fundamental task in any graphical model is that of inference. That is, we want to be able to answer general queries of the form $P(\mathbf{X} \mid \mathbf{Z})$ where $\mathbf{X}, \mathbf{Z} \subset \mathcal{X}$, as efficiently as possible. Assume for example, that we want to evaluate the probability of getting a call from our neighbor $P(C)$ in the model of Figure 2.1. By the complete probability formula

$$P(c) = \sum_{b,e,a,r} P(b,e,a,r,c)$$

We can improve on this by utilizing the decomposition of the joint probability which results in

$$P(c) = \sum_{a} P(c|a) \sum_{e} P(e) \sum_{b} P(b)P(a|b,e) \sum_{r} P(r|e)$$

which is significantly more efficient. This procedure of *variable elimination* (summation) is the basis of all exact inference methods.

Different method designed for batch query processing at the cost of two variable elimination computations include *Bucket Elimination* [Dechter, 1996] and *Junction Trees* (e.g., [Jensen et al., 1990]), and are widely used in numerous domain. However, these cannot overcome the fact that inference in Bayesian networks is in general (excluding tree structured networks) NP-hard [Cooper, 1990] (it belongs, in fact, to #P).

Consequently, to cope with large scale networks, a range of approximate inference techniques have been developed. These include instance or particle based methods such as *Gibbs sampling* (see [Neal, 1993] for an overview of inference sampling techniques), variational approximation method such as the *Mean Field* approximation (see [Jordan et al., 1998] for an introduction) and *Loopy Belief Propagation* (e.g., [Murphy and Weiss, 1999] and references within). While these methods have shown great success in different scenarios, like exact inference, approximate inference is NP-hard [Dagum and Luby, 1997] and choosing the best method of inference for a particular task remains a challenge.

## 2.2 Learning Parameters with Complete Data

A generative model, such as a probabilistic graphical model, is one that explains, via its inner constructs and parameters, how the observed data could be generated. As such, when learning a probabilistic graphical model from data, we want it to faithfully capture the underlying distribution $P^*$ that gave rise to the observations. That is, we want to learn the minimal decomposition structure $\mathcal{G}$ that is an *I-map* of $P^*$ and we want to correctly quantify its parameters. Our ability to do so is obviously limited by the expressiveness of our model: As discussed above, some generating distributions cannot be captured faithfully by a Bayesian network, and others cannot be captured by the formalism of undirected Markov networks. The choice of the conditional probability distribution representation may also limit our ability to capture $P^*$.

In practice, we face an even more fundamental problem: rather than having access to $P^*$, or equivalently to an infinite number of samples generated by it, we are given a finite *training set* of samples $\mathcal{D} = \{\mathbf{x}[1], \ldots, \mathbf{x}[M]\}$, that are independently drawn from $P^*$. Using the limited knowledge available to us via $\mathcal{D}$, our goal is to somehow learn a model $\mathcal{B} = \langle \mathcal{G}, \theta \rangle$ that best approximates $P^*$. This may require us to take into account particular phenomena that arise in $\mathcal{D}$ and are solely due to its finite nature. In particular, to avoid *over-fitting* (see below), we may not want to capture $\mathcal{D}$ exactly, either in terms of independence statements that hold in $\mathcal{D}$ or in terms of the parameters of the model learned.

In this section we present the essentials of learning the parameters of a Bayesian network when the data is *complete*. That is, we assume that we are given (or have learned) the graph structure $\mathcal{G}$ and structure $\mathcal{G}$ and face the problem of learning the conditional probability distribution parameters $\theta$ or the Bayesian network model $\mathcal{B}$. We start with the *maximum likelihood* approach for learning parameters and then present a more robust Bayesian approach that typically offers better generalization performance. In the next section we present the *score based* approach to learning structure. In Section 2.4, we consider both of these tasks in the presence of missing value or hidden variables and discuss complications that arise in this scenario.

### 2.2.1 Maximum Likelihood Estimation

The *maximum likelihood estimation* (MLE) approach is widely used in all fields of learning. At its core is the intuition that a good model is one that fits the data $\mathcal{D}$ well. That is we want to measure the probability that the model gave rise to the observed data.

**Definition 2.2.1:** The *likelihood function*, $L(\theta : \mathcal{D})$, is the probability of the independently sampled instances of $\mathcal{D}$ given the parameterization $\theta$

$$L(\theta : \mathcal{D}) = \prod_{m=1}^{M} P(\mathbf{x}[m] \mid \theta) \tag{2.2}$$

where $P(\mathbf{x}[m] \mid \theta)$ is the probability of the $m$'th complete instance given the parameter of the network. The log of that function or the the *log-likelihood function* is

$$\ell(\theta : \mathcal{D}) = \sum_{m=1}^{M} \log P(\mathbf{x}[m] \mid \theta) \tag{2.3}$$

∎

In the MLE approach, we want to choose parameters $\widetilde{\theta}$ that maximize the likelihood of the data:

$$\hat{\theta} = \max_{\theta} L(\theta : \mathcal{D}) \tag{2.4}$$

Eq. (2.4) describes optimization in a high dimensional space even for relatively simple network structures since we need to jointly optimize over the parameters of all the conditional probability distributions. As in the case of representation and inference, the Bayesian network representation offers a decomposition of this optimization task. We can use the decomposition property of Eq. (2.1) to write

$$\begin{aligned} L(\theta : \mathcal{D}) &= \prod_{m=1}^{M} P(\mathbf{x}[m] \mid \theta) \\ &= \prod_{m=1}^{M} \prod_{i=1}^{N} P(x_i[m] \mid \mathbf{pa}_i[m] : \theta_{X_i|\mathbf{Pa}_i}) \\ &= \prod_{i=1}^{N} \left[ \prod_{m=1}^{M} P(x_i[m] \mid \mathbf{pa}_i[m] : \theta_{X_i|\mathbf{Pa}_i}) \right] \\ &= \prod_{i=1}^{N} L_i(\theta_{X_i|\mathbf{Pa}_i} : \mathcal{D}) \end{aligned}$$

where $\theta_{X_i|\mathbf{Pa}_i}$ are the parameters that encode the conditional probability distribution of $X_i$ given its parents $\mathbf{Pa}_i$ and

$$L_i(\theta_{X_i|\mathbf{Pa}_i} : \mathcal{D}) \equiv \prod_{m=1}^{M} P(x_i[m] \mid \mathbf{pa}_i[m] : \theta_{X_i|\mathbf{Pa}_i}) \tag{2.5}$$

is the *local likelihood function* for $X_i$. Thus, the global optimization problem is decomposed into significantly smaller problems, where we optimize the parameters of each conditional probability distribution $P(X_i \mid \mathbf{Pa}_i)$ independently of the rest.

In the case of full table CPDs the local likelihood can be further decomposed. Suppose we have a variable $X_i$ with its parents $\mathbf{Pa}_i$, and a parameter $\theta_{x_i|\mathbf{pa}_i}$ for each possible assignment to combination of $x_i$ and its parents. In Eq. (2.5), different assignments for which $X_i = x_i$ and $\mathbf{Pa}_i = \mathbf{pa}_i$ contribute the same term to the product. Thus, if we group similar assignments and denote by $S[x_i, \mathbf{pa}_i]$ the number of these instances, we can write

$$L_i(\theta_{X_i|\mathbf{Pa}_(X_i)} : \mathcal{D}) = \prod_{\mathbf{pa}_i} \prod_{x_i} \theta_{x_i|\mathbf{pa}_i}{}^{S[x_i,\mathbf{pa}_i]} \tag{2.6}$$

where

$$S[x_i, \mathbf{pa}_i] = \sum_m 1\left\{x_i[m] = x_i, \mathbf{pa}_i[m] = \mathbf{pa}_i\right\} \tag{2.7}$$

and $1\{\}$ is the indicator function.

**Proposition 2.2.2:** *The maximal likelihood estimation (MLE) of the parameters of a Bayesian network with multinomial table CPDs is given by:*

$$\widetilde{\theta}_{x_i|\mathbf{pa}_i} = \frac{S[x_i, \mathbf{pa}_i]}{\sum_{x_i} S[x_i, \mathbf{pa}_i]} \tag{2.8}$$

The counts $S[x_i, \mathbf{pa}_i]$ are the *sufficient statistics* of the data $\mathcal{D}$. These summarize all relevant information from the individual data instances $\mathbf{x}[1] \ldots \mathbf{x}[M]$ needed for maximum likelihood parameter estimation of full conditional probability tables. Thus, two different training set may lead to the same maximum likelihood parameters if their marginal empirical counts $S[x_i, \mathbf{pa}_i]$ are the same for all $X_i$ in the structure. Consequently, optimizing the likelihood function is equivalent to finding the best approximation for the empirical distribution constrained by the independence assumptions of $\mathcal{G}$.

### 2.2.2 Bayesian Estimation

MLE estimation follows the *Frequentist* approach to statistics that relies solely on the observed data. This is intuitive since we directly measure the fit of the model to the data. However, in practice when data is both limited and noisy, this approach can suffer from over-fitting. That is, the model might fit the data perfectly but have a poor generalization performance on unseen samples. Consider for example, learning the parameters of the model in Figure 2.1 (a) from alarm sounding in a typical week in a suburb of Los Angeles. Even, in earthquake prone California, there is a good chance that we will have hundreds of burglaries and random alarm sounding and not a single instance of an earthquake. In this case, using MLE would results in $P($alarm=yes $\mid$ Earthquake=yes$) = 0$, which ignores our prior intuition that there is a relation between an earthquake and the chance that the alarm will sound. Conversely, it could be the case that during that same week a 6.8 earthquake indeed sounded all the alarms in the area. In this scenario, MLE would set $P($alarm=yes $\mid$ Earthquake=yes$) = 1$, which would probably not be realistic for the smaller more common earthquakes.

Therefore, in the (realistic) absence of endless and varied data encompassing all facets of the true distribution, we would like to learn models that are more robust to fluctuations in the training data by incorporating prior knowledge into the parameter estimation process. We turn to *Bayesian estimation*, which formulates this concept of prior belief in a principled manner. The core of Bayesian estimation is that, *prior* to seeing the observed data $\mathcal{D}$, we already had some initial prior belief regarding the domain at hand. The prior belief is encoded by a distribution $P(\theta)$. It can be very informative such as a strong belief that it will not rain in the Sahara on any random day even before we are actually "observe" the forecast. On the other hand, a *uninformative* prior can also play an important role. Consider, for example, a toss of a fair coin. Our prior belief is uninformative in the sense that we believe that both *heads* and *tails* are equally likely. In fact, we belief this so strongly that seeing 27 heads and 73 tails in a 100 tosses will not really change this belief. In this case we would like the seemingly uninformative prior belief to constrain MLE that will estimate a probability of $0.73$ for seeing tails. We would like the prior to help us avoid the bias that is a results of any finite dataset. (See [Gelman et al., 1995, Pearl, 1988] and reference within for an overview of the Bayesian formalism and its relation to other approaches.)

Given our prior distribution $P(\theta)$ and the observed data $\mathcal{D}$, we "update" our beliefs and use *Bayes rule* to compute the *posterior distribution*

$$P(\theta \mid D) = \frac{P(\mathcal{D} \mid \theta)P(\theta)}{P(\mathcal{D})}. \tag{2.9}$$

The term $P(\mathcal{D})$, called the *marginal likelihood*, averages the probability of the data over all possible parameter assignments. To estimate a value for the parameters $\hat{\theta}$ that will be used in the prediction of the $(M+1)$th sample, we average over possible values:

$$\hat{\theta} \equiv P(X[M+1] \mid \mathcal{D}) = \int P(X[M+1] \mid \mathcal{D}, \theta)P(\theta \mid \mathcal{D})P(\theta)d\theta \tag{2.10}$$

We now address the issue of choosing a convenient prior. When estimating the parameters of multinomial distributions, the common choice is the use of *Dirichlet Priors* [DeGroot, 1989]. The Dirichlet prior distribution for a multinomial variables $X$ is defined by

$$P(\theta) = Dirichlet(\alpha^1, \ldots \alpha^K) \propto \prod_j \theta_j{}^{\alpha^j - 1} \tag{2.11}$$

where $\alpha^i$ are *hyper-parameters* that correspond to the possible values of $X$.

In the case of MLE for full Bayesian networks, we have seen that the likelihood function decomposes according to the networks structure. This allowed us to estimate the parameters $\theta_{X_i|\mathbf{Pa}_i}$ for each family independently in Eq. (2.4). For Bayesian estimation, we introduce an independence assumption that will lead to a similar decomposability:

**Definition 2.2.3:** [Spiegelhalter and Lauritzen, 1990] A parameter prior $P(\theta)$ for a Bayesian network is said to satisfy *parameter independence* if it can be written as

$$P(\theta) = \prod_{i=1}^{n} \prod_{\mathbf{pa}_i} P(\theta_{x_i|\mathbf{pa}_i})$$

The decomposition according to the network structure is called *global parameter independence*. The further decomposition according to the values $\mathbf{pa}_i$ is called *local parameter independence*. ▮

Assuming parameter independence, for each multinomial CPD in the network, we can assign an independent prior distribution $\theta_i \sim \mathit{Dirichlet}(\alpha_{x_i^1|\mathbf{pa}_i}, \ldots \alpha_{x_i^K|\mathbf{pa}_i})$. The form of the Dirichlet prior defined in Eq. (2.11) is surprisingly similar to that of the likelihood in Eq. (2.6). This leads to the appealing property that Dirichlet is in fact a *conjugate* prior to the multinomial distribution. That is, the form of the posterior and prior distributions are similar:

**Proposition 2.2.4:** *If $P(\theta_i)$ is $\mathit{Dirichlet}(\alpha_{x_i^1|\mathbf{pa}_i}, \ldots \alpha_{x_i^K|\mathbf{pa}_i})$ then the posterior $P(\theta_i \mid \mathcal{D})$ is $\mathit{Dirichlet}(\alpha_{x_i^1|\mathbf{pa}_i} + S[x_{i^1}, \mathbf{pa}_i], \ldots \alpha_{x_i^K|\mathbf{pa}_i} + S[x_{i^K}, \mathbf{pa}_i])$ where $S[x_{i^K}, \mathbf{pa}_i]$ is the sufficient statistics derived from $\mathcal{D}$.*

This important property now allows us, as in the case of Proposition 2.2.2, to compute Eq. (2.10) in closed form:

**Proposition 2.2.5:** *The Bayesian estimation for the parameters of a Bayesian network with multinomial table CPDs using a* Dirichlet *prior is given by:*

$$\widetilde{\theta}_{x_i|\mathbf{pa}_i} \equiv P(X_i[M+1] = x_i \mid \mathbf{Pa}_i[M+1] = \mathbf{pa}_i, \mathcal{D}) = \frac{\alpha_{x_i|\mathbf{pa}_i} + S[x_i, \mathbf{pa}_i]}{\sum_{x_i'} \alpha_{x_i'|\mathbf{pa}_i} + S[x_{i'}, \mathbf{pa}_i]} \tag{2.12}$$

Thus, the hyper-parameters $\alpha_{x_i|\mathbf{pa}_i}$ play a similar role to the empirical counts and are often referred to as *imaginary counts*. $M' \equiv \sum_{x_i} \alpha_{x_i|\mathbf{pa}_i}$ is the *imaginary sample size*. That is, using a Dirichlet prior with the above hyper-parameters is equivalent to seeing $M'$ samples where the different assignment to the variables distribute according to $\alpha_{x_i|\mathbf{pa}_i}$. In order to ensure probabilistic coherence, the hyper-parameters $\alpha_{x_i|\mathbf{pa}_i}$ must satisfy marginalization constraints, in accordance with the network structure. One way to ensure this is to use the BDe prior [Heckerman and Geiger, 1995] to construct these hyper-parameters. We discuss the details of this prior in details in Section 2.3.1 in a more general context.

## 2.3 Structure Learning

In the previous section, we have assumed that the graph structure $\mathcal{G}$ is given. In real-life, however, it is rarely the case that this structure is known and we would like to learn it from data. This task is not only important from the perspective of gaining a better understanding of the domain but also has a significant impact on our ability to learn and the quality of the model's prediction. A missing edge can cut off important influencing factors while spurious edges leads to many parameters which in turn lead to over-fitting and a degradation of the generalization capabilities of the model.

There are two basic paradigms for learning the structure of a Bayesian networks. The first approach is a *constraint based* approach that uses independence tests directly (e.g., [Spirtes et al., 1993]): In short, based on some statistical test or oracle, a set of independence statements forms the constraint set. A network structure to capture this set of constraints to the best extent possible. Although this approach is intuitive since Bayesian networks are, by definition, independence maps of the distribution they represent, it suffers from high sensitivity to the statistical test applied. In this dissertation we adopt the common *score based* approach. In this framework, we define a score that measures the compatibility of the model to the data and then search for the best scoring model. As we will see below, this method is appealing statistically and allows compromises in the choice of edges at the cost of computational complexity.

The problem of searching for the best scoring structure is essentially a *model selection* task and the role of the score is to efficiently guide us towards a beneficial structure. Consequently, all common scores used in structure learning such as BIC [Schwarz], MDL[Lam and Bacchus, 1994], BDe [Heckerman et al., 1995a] and BGe [Geiger and Heckerman, 1994] have certain appealing properties. First, all scores follow *Occam's Razor*: if two models achieve the same likelihood then the simpler one will receive a higher score. The *Minimum Description Length* (MDL) score [Lam and Bacchus, 1994], for example, encodes this directly:

$$\text{Score}_{MDL}(\mathcal{G} \; : \; \mathcal{D}) = \ell(\theta, \mathcal{G} : \mathcal{D}) - \frac{\log M}{2} Dim(\mathcal{G}) - DL(\mathcal{G}) \tag{2.13}$$

where $M$ is the number of instances, $Dim(G)$ is the number of parameters in the model and $DL(G)$ stands for the description length of $\mathcal{G}$ and is the number of bits needed to encode the graph structure. Second, all scores do not distinguish between *independence equivalent* models the are probabilistically indistinguishable (see Definition 2.1.4). Third, given a complete dataset, all scores decompose according to the network structure and facilitate efficient computation of local structure changes. This property is crucial (see Section 2.3.3) when learning the structure of large real-life models. Finally, if $\mathcal{G}^*$ is the generating model, as the number of samples grows to infinity, all scores prefer $\mathcal{G}^*$ (or an equivalent model) to any other structure.

### 2.3.1 The Bayesian Dirichlet Equivalent Sample Size Score

The *Bayesian Dirichlet equivalent sample size* (BDe) or Bayesian score is based on the same principles described in Section 2.2: we explicitly represent uncertainty over both the structure and parameters as a distribution and then combine out prior beliefs $P(\mathcal{G})$ and $P(\theta \mid \mathcal{G})$ to compute a posterior distribution

$$\mathrm{Score}_{BDe}(\mathcal{G} : \mathcal{D}) = \log P(\mathcal{D} \mid \mathcal{G}) + \log P(\mathcal{G})$$

where the *marginal likelihood* $P(\mathcal{D} \mid \mathcal{G})$ averages the probability over all possible parameterizations of $\mathcal{G}$:

$$P(\mathcal{D} \mid \mathcal{G}) = \int P(\mathcal{D} \mid \mathcal{G}, \theta) P(\theta \mid \mathcal{G}) d\theta$$

The integration over all possible parameters gives the Bayesian score a bias towards simpler structures. When the model has many parameters, particularly when the number of sample is small, there are many different parameterizations for which $P(\mathcal{D} \mid \mathcal{G}, \theta)$, and consequently the integral increases. On the other hand, when the probability of the true parameters is peaked (which happens when the sample size is large), the effect of number of parameters is reduced since $P(\mathcal{D} \mid \mathcal{G}, \theta)$ is non-negligible only for few values. Thus the Bayesian score inherently takes care of the problem of over-fitting a complex model to a small sample size. In fact, it can be shown that, as the number of samples grows, that the BDe score is equivalent to the *Minimum Description Length* (MDL) score [Lam and Bacchus, 1994] that encodes this explicitly, up to an additive constant.

As in the case of parameter, estimation, the choice of priors determines not just the score itself but also the form that it can take. We require that the prior satisfy the following intuitive property:

**Definition 2.3.1:** [Heckerman et al., 1995a] A parameter prior satisfies *parameter modularity* if for any two graphs $\mathcal{G}_1$ and $\mathcal{G}_2$, if $\mathbf{Pa}_i^{\mathcal{G}_1} = \mathbf{Pa}_i^{\mathcal{G}_2}$ then:

$$P(\theta_{X_i \mid \mathbf{Pa}_i} \mid \mathcal{G}_1) = P(\theta_{X_i \mid \mathbf{Pa}_i} \mid \mathcal{G}_2)$$

▮

Priors that satisfy parameter modularity are called *factorized* priors [Cooper and Herskovits, 1992, Heckerman et al., 1995a] and facilitate the decomposition of the Bayesian score:

**Proposition 2.3.2:** *If the prior* $P(\theta \mid \mathcal{G})$ *satisfies global parameter independence and parameter modularity then*

$$P(\mathcal{D} \mid \mathcal{G}) = \prod_i \int_{\theta_{X_i \mid \mathbf{Pa}_i}} \prod_m P(x_i[m] \mid \mathbf{pa}_i[m], \theta_{X_i \mid \mathbf{Pa}_i}) P(\theta_{X_i \mid \mathbf{Pa}_i}) d\theta_{X_i \mid \mathbf{Pa}_i}$$

Since $P(\mathcal{D} \mid \mathcal{G})$ already prefers simple structures to complex ones, $P(\mathcal{G})$ is often taken to be uniform and can thus be omitted from the score. In other cases, it is simply given as input and we assume here that it can also be decomposed according to the network structure. We can thus decompose the score into local contributions each depending only on the sufficient statistics of $X_i$ and its parents

$$\mathrm{Score}_{BDe}(\mathcal{G} \,:\, \mathcal{D}) = \sum_i \mathrm{FamScore}_{BDe}(X_i, \mathbf{Pa}_i \,:\, \mathcal{D}) \tag{2.14}$$

This decomposition plays a crucial rule in Section 2.3.3 and enables us to devise efficient search algorithms for network structures of high dimension.

Following Section 2.2.2, we use Dirichlet priors for table CPDs. In addition to the simplification of computation they offer in the case of parameter estimation, they provide a simple closed form expression for the local family score.

**Theorem 2.3.3:** [Heckerman et al., 1995a] Let $\mathcal{G}$ be a network structure and $P(\theta \mid \mathcal{G})$ be a parameter prior satisfying parameter independence and parameter modularity. Using full table CPDs and a Dirichlet prior with hyper-parameters $\{\alpha_{x_i|\mathbf{pa}_i}\}$ then:

$$\mathrm{FamScore}_{BDe}(X_i, \mathbf{Pa}_i \,:\, \mathcal{D}) = \sum_{\mathbf{pa}_i}\left[\log \frac{\Gamma(\alpha_{\mathbf{pa}_i})}{\Gamma(\alpha_{\mathbf{pa}_i} + S[\mathbf{pa}_i])} + \sum_{x_i} \log \frac{\Gamma(\alpha_{x_i|\mathbf{pa}_i} + S[x_i, \mathbf{pa}_i])}{\Gamma(\alpha_{x_i|\mathbf{pa}_i})}\right] \tag{2.15}$$

where $\Gamma$ is the Gamma function and $\alpha_{\mathbf{pa}_i} = \sum_{x_i} \alpha_{x_i|\mathbf{pa}_i}$ and $S[\mathbf{pa}_i] = \sum_{x_i} S[x_i, \mathbf{pa}_i]$

**Proof:** The proof outline is interesting in that it emphasizes the Bayesian perspective of computations. Using the chain rule, the posterior probability of the data can be written as

$$\begin{aligned} P(\mathcal{D} \mid \mathcal{G}) &= \prod_{m=1}^{M} P(X[m] \mid X[1], \ldots, X[m-1], \mathcal{G}) \\ &= \prod_{i=1}^{n} \prod_{\mathbf{pa}_i} \left( \prod_{m:\mathbf{Pa}_i[m]=\mathbf{pa}_i} P(X_i[m] \mid X_i[1], \mathbf{Pa}_i[1], \ldots, X_i[m-1], \mathbf{Pa}_i[m-1], \mathcal{G}) \right) \end{aligned}$$

where the second line follows from decomposition according to the network structure and rearrangement of terms. We have already taken a Bayesian approach to computing each term in this product which resulted in Proposition 2.2.5. Using this results along with some algebraic manipulation we get the desired result. ∎

As noted above, a desired property is that the score reaches its optimum at the true generating structure. That is, given a sufficiently large number of samples, graph structures that exactly capture all independencies in the distribution $P$ (are *P-map*s of $P$), will receive a higher score than all other graphs. This concept is captured in the following definition:

**Definition 2.3.4:** Assume that the structure of the model generating the observations is $\mathcal{G}^*$. We say that our score is *consistent* if, as $M \to \infty$, the following properties hold with probability asymptotic to 1 (over possible choices of dataset $\mathcal{D}$ generated from $\mathcal{G}^*$)

- The structure $\mathcal{G}^*$ will maximize the score
- All structures that are not equivalent to $\mathcal{G}^*$ will have a strictly lower score

∎

Another desired property is that the score be the same for two Bayesian network models that are *independence equivalent*. Such a property is called *structure equivalence* of the score. In order to achieve structure equivalence, we need to devise a set of hyper-parameters so that our prior will not bias the score between equivalent structures. This is achieved using a *BDe prior* [Heckerman and Geiger, 1995]: we define a probability distribution $P'$ over $\mathcal{X}$ and an equivalent sample size $M'$ for our set of imaginary samples. The hyper-parameters are then defined to be:

$$\alpha_{x_i|\mathbf{pa}_i} = M' \cdot P'(x_i, \mathbf{pa}_i)$$

**Theorem 2.3.5:** [Heckerman et al., 1995a] Given complete data, the Bayesian score with BDe prior is both consistent and structure equivalent.

### 2.3.2 Scores For Continuous CPDs

Developing a Bayesian score for network with continuous probability distribution is somewhat more complex. For Gaussian network, the conjugate Normal Wishardt prior (see [DeGroot, 1989]) plays a similar role to Dirichlet priors in the case of discrete variables. Geiger and Heckerman [1994] use this prior to develop a closed form Bayesian score called the BGe score. The specifics of this score are somewhat detailed and we omit these as this score is not used in this thesis.

For general non-linear CPDs, however, there is no simple general form of a Bayesian score. Thus, it is common to to resort to an approximation of the full Bayesian score that is easy to compute in the general case, such as the Bayesian Information Criterion (BIC) score [Schwarz]

$$BIC(\mathcal{D}, G) = \max_\theta \ell(\mathcal{D} : G, \theta) - \frac{\log M}{2}\mathrm{Dim}[G]$$

where $M$ is the number of instances in $\mathcal{D}$, and $\mathrm{Dim}[G]$ is the number of parameters in $G$.

### 2.3.3 Search Algorithm

Given the Bayesian score, or any other commonly used score, learning amounts to finding the structure $\mathcal{G}$ that maximizes the score. Chow and Liu [Chow and Liu, 1968] have shown that learning the ML tree can be done efficiently using a maximum spanning tree approach [Cormen et al., 1990]. A similar method can be used to learn the maximal scoring tree for any decomposable score. Yet, despite extensions to particular scenarios (e.g., [Friedman et al., 1997]), learning the structure for a

**Algorithm 1**: Greedy Hill-Climbing Structure Search for Bayesian Networks

```
Input  : $\mathcal{D}$    // training set
         $\mathcal{G}_0$   // initial structure
Output : A final structure G

$\mathcal{G}_{best} \leftarrow \mathcal{G}_0$
repeat
    G$\leftarrow \mathcal{G}_{best}$
    foreach Add,Delete,Reverse edge in G do
        $\mathcal{G}' \leftarrow$ ApplyOperator($G$)
        if $\mathcal{G}'$ is cyclic then continue
        if $\mathrm{Score}(\mathcal{G}' : \mathcal{D}) > \mathrm{Score}(\mathcal{G}_{best} : \mathcal{D})$ then
            $\mathcal{G}_{best} \leftarrow \mathcal{G}'$
        end
    end foreach
until $\mathcal{G}_{best}$ == G
return $\mathcal{G}_{best}$
```

general Bayesian network, even if the number of parents is limited to two, is NP-hard [Chickering, 1996a].

Thus, we resort to a heuristic greedy search. We define a *search space* where each *state* in this space is a network structure. A set of *operators* manipulate a network structure to generate a set of *successor* states. This defines a graph structure over possible states (networks structures) where neighboring states are two networks that are one operator away. To perform a search, we start with some initial structure (usually the empty graph) and apply a greedy search scheme to traverse the search space in order to locate a high scoring structure.

To facilitate tractable learning, local structure modification operators are considered such as *Add*, *Delete* and *Reverse* an edge. The decomposability of the score allows us to efficiently evaluate the benefit such a local structure change. For example, if we add a parent to $X_i$ we need only recompute the relevant contribution to the score $\mathrm{FamScore}(X_i, \mathbf{Pa}_i : \mathcal{D})$. Furthermore, until an additional parent is added to $X_i$ or an existing parent removed, the contribution of this operator need not be recomputed.

Even when using local modifications, it is still impossible to traverse the full search space even for relatively small domains. Thus, we use a local search procedure such as the greedy hill-climbing algorithm: At each step we evaluate all possible local moves and perform the change that results in the maximal gain, until we reach a local maximum. The procedure is outlined in Algorithm 1.

The greedy nature of the algorithm is necessary to facilitate learning in practice. However, it is also means that we our final local maxima model is an inferior one. This problem is a central issue when learning the structure for practically any real-life domain. Consequently, different methods are applied to cope with this problem in the discrete search space.

One way to reduce the sensitivity to local maxima is to strengthen the power of the greedy algorithm at the cost of computational complexity. This can be done by using search algorithm that are more exhaustive than greedy hill-climbing such as $K$*-best* search and time limited *Iterative Deepening* (see [Cormen et al., 1990] and reference within for on overview of search procedures). An appealing alternative that directly confronts the local maxima is that of Tabu search [Glover and Laguna, 1993]. This method keeps a *tabu list* record of the last $N$ models visited and rather than considering only moves that improve the best (local maxima) model, it also considers moves that improve any of these $N$ models. Tabu search is particularly effective in escaping small local maxima and plateaus, depending on the size of the tabu list.

A different approach to cope with local maxima is to introduce stochasticity into the search procedure. The simplest heuristic of this type is to use *random restarts* when encountering a local maxima or plateau. At each random restart, several random structural changes are applied to the best scoring structure, after which the search procedure continues as usual. This approach suffers from the fact that the "interesting range" of possible random points is typically not known and many of stochastic go to waste. Despite this, it is often extremely useful in practice. Algorithm 2 outlines the extension of the basic greedy hill climbing algorithm of Algorithm 1 to include tabu list and random restarts. This algorithm is the basic search procedure used throughout this dissertation.

Other stochastic methods for escaping local maxima include the bootstrap method [Efron and Tibshirani, 1993, Friedman et al., 1999b] and various annealing algorithms such as Deterministic Annealing [Rose, 1998] and Simulated Annealing [Kirpatrick et al., 1994]. We discuss these methods in more details in Chapter 3 where they are particularly relevant.

## 2.4 Learning with Missing Values and Hidden Variables

In real-life, the observed data is often partial. A patient's record, for example, will probably never contain results for all possible tests. Indeed, one of the advantages of probabilistic graphical models is that, using the ability to perform inference relatively efficiently, we can easily cope with missing values. An important distinction should be made between observations that are *missing at random* (MAR) and observations whose absence influences the domain. For example, the presence or absence of a biopsy result is clearly not random and is related to the result of a preliminary blood test. Yet, the vast majority of learning method adopt the MAR assumption without which the learning problem is practically unapproachable. In this dissertation we adopt the same assumption. We note, however, that one way to partially cope with observation that are not missing at random is to add a "MISSING" state for the relevant variables (see [Rubin, 1976] for a discussion of this issue). In addition to missing values, some of the variables may be hidden or *latent*. That is, we may never observe these variables in the data.[1] Probably the most common scenario involving a hidden variable is that of clustering, where the class assignment of the objects to be clustered is never observed. More interestingly, we may want to take the user's "mood" into account when building a personalized web sales engine, but can expect never to observe the actual state of mind of the Internet surfer.

In this section we give a brief overview of learning *in the presence* of missing values and hidden variables. We assume that the hidden variables, if any, are known to exist and their cardinality is given as input. It is the central goal of the dissertation to explore the significantly harder goal of learning new hidden variables and their cardinality.

### 2.4.1 Parameter Estimation

Learning with missing values is significantly harder than learning with complete data since we no longer have a closed form solution for estimating the parameters of the network. This is a result of the fact that parameter independence does not necessarily hold and the case of unrestricted multinomial distributions can no longer be decomposed into local estimation problems. Optimization is consequently in very high dimension. Furthermore, the parameter space typically contains many local maxima. When some of the variables are hidden (their observation is missing altogether) we further face the problem of multiplicity of both global and local maxima that arises from possible permutations of the values of these variables.

The most straightforward approach for parameter estimation with missing values is to use direct optimization techniques such as gradient ascent and its variants (e.g., [Bishop, 1995]). In the case of maximum likelihood estimation these methods can also take advantage of the network structure in some cases (e.g., [Binder et al., 1997]). Unfortunately, optimization if often computationally demanding due to the large number of parameters and is highly prone to get stuck in inferior local maxima. In the case of Bayesian estimation, we also face the further complication of optimizing a poster over the network parameters $\theta$. This is usually infeasible and an approximation must be used. A common solution is to resort to a *Maximum A-Posteriori* computation which is similar to the maximum likelihood case. Alternatively, we can use a sampled (particle) based stochastic technique that is guaranteed to converge to the true posterior such as *Gibbs sampling* (e.g., [Neal, 1993]). However, such a method can be extremely slow and can take an impractical amount of time to achieve reasonable accuracy.

One commonly used alternative is that is used throughout this dissertation is the *Expectation Maximization* (EM) algorithm [Dempster et al., 1977, Lauritzen, 1995]. The idea of EM is straightforward: since parameter estimation is easy when data is complete, we first "complete" the data

[1]We note that these variables are MAR by definition. Otherwise, a single "MISSING" value will be observed throughout which will render the distribution of the variable not useful in terms of its ability to effect our prediction abilities.

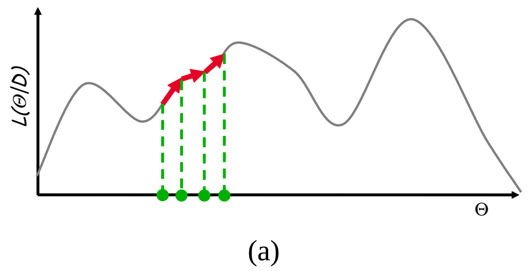

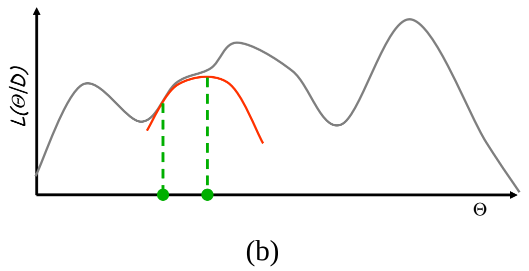

Figure 2.4: Illustration of likelihood optimization using: (a) Gradient Ascent that proceeds in the direction of maximal change; (b) the Expectation Maximization (EM) algorithm that locally approximates the likelihood using a concave function and then optimizes this concave lower-bound.

in the expectation step (E-step) by computing a posterior distribution $Q(H \mid O, \theta_{old})$ of the missing values $H$ given the observations $O$ and the current model at hand. We can then compute the *expected sufficient statistics* by replacing Eq. (2.7) with

$$\boldsymbol{E}_{Q(H|O,\theta_{old})}[S[x_i, \mathbf{pa}_i]] = \sum_m Q(X_i = x_i, \mathbf{Pa}_i = \mathbf{pa}_i \mid \mathbf{o}[m], \theta_{old}) \tag{2.16}$$

where $\mathbf{o}[m]$ is the $m$'th partially observed instance. These complete sufficient statistics can the be used to optimize the parameters in the maximization step (M-step) of the algorithm. The resulting model is then used to repeat the E-step and so on until convergence. It can be shown [Dempster et al., 1977] that EM is equivalent to lower-bounding the likelihood function at the current model parameters via a concave function and then taking the maximum of this function as illustrated in Figure 2.4. Consequently, the EM algorithm is guaranteed to improve the likelihood of the observed data $\mathcal{D}$ at each iteration until convergence to a (typically) local maximum. EM and its variants (e.g., [Neal and Hinton, 1998]) have proved to be surprisingly effective in practice and are typically used when the local distribution functions are in the *exponential family* and sufficient statistics exist. Generalizations of the EM algorithm using variational methods have also been applied for complex non-linear conditional probability distributions (e.g., [Saul et al., 1996, Diez, 1993]).

Like gradient methods, the EM algorithm also suffers from the problem of local maxima and its performance depends on the starting point used. A straightforward method often used to cope with this is simply to run EM from multiple starting points and choose the best of the local maxima solution. While there are no guarantees as to the number of random restarts needed for an effective solution, this method can be surprisingly effective in practice.

### 2.4.2 Structure Learning

When learning structure in the presence of hidden variables we face further complications. If we use either the MDL score or the Bayesian score (BDe) then, at each step in the search procedure, we need to estimate parameters using ones of methods described in the previous section such as the EM algorithm. Consider, for example, adding the first edge to the starting point empty network. Choosing the best such structure change requires that we consider $O(N^2)$ possible candidate structures. Without the decomposability assumption that we had in the case of complete data, even evaluating only the likelihood of each candidate becomes an expensive global optimization procedure. Thus, in the absence of prior constraints on the network structure, that can significantly reduce the search space, straightforward structure search is intractable in any interesting domain.

As in the case of parameter learning, a solution that takes advantage of the relative ease of learning when data is complete is often used. The *Structural Expectation Maximization* (SEM) algorithm [Friedman, 1997] generalizes the idea of EM to the scenario of structure learning. The E-Step is identical to parametric EM where we use the current model to generate the distribution $Q(H \mid O, \theta_{old})$, thus providing complete sufficient statistics as in Eq. (2.16). In the M-Step we need to optimize both the structure of the network and its parameters. Given the "completed" dataset of the E-Step, this is identical in form to structure learning with complete data. It is important to note that the expected benefit by this approach is significant: rather than re-estimating the model parameters and expected statistics after *each* change in structure, the output of a single E-step is used to perform *many* structure adaptations (usually until convergence in the search space) often leading to an order of magnitude and more improvement in running time.

The idea of Structural EM can also be applied for Bayesian learning [Friedman, 1998]. Again, once the expected sufficient statistics are computed in the E-step, we can proceed as if the data were complete. Yet, even with this approximating algorithm, Bayesian learning is particularly challenging in the presence of missing values. Specifically, computation of the marginal likelihood is intractable and we have to resort to one of several possible approximations [Chickering and Heckerman, 1996]. In this dissertation we use the empirically effective and computationally efficient Cheeseman-Stuts approximation [Cheeseman et al., 1988] for this scenario.

**Algorithm 2**: Greedy Hill-Climbing Structure Search for Bayesian Networks with Tabu list and random restarts

```
Input  : $\mathcal{D}$              // training set
         $\mathcal{G}_0$             // initial structure
         T_SIZE          // size of tabu list
         M_EXPAND        // maximum number of expansions
         M_RESTART       // maximum number of restarts
         R_MOVES         // number of random moves at each restart

Output : A final graph G

$\mathcal{G}_{best} \leftarrow \mathcal{G}_0$
qLoops $\leftarrow 0$
eNum $\leftarrow 0$
while qLoops $<$ M_RESTART and eNum $<$ M_EXPAND do
    // GREEDY with TABU
    qSteps $\leftarrow 0$
    G$\leftarrow \mathcal{G}_{best}$
    while qSteps $<$ T_SIZE/2+1 and eNum $<$ M_EXPAND do
        foreach Add,Delete,Reverse edge in G do
            $\mathcal{G}' \leftarrow$ ApplyOperator($G$)
            if $\mathcal{G}'$ is cyclic or in TABU list then continue
            eNum $\leftarrow$ eNum $+1$
            if $\mathrm{Score}(\mathcal{G}' : \mathcal{D}) > \mathrm{Score}(\mathcal{G}_{best} : \mathcal{D})$ then
                $\mathcal{G}_{best} \leftarrow \mathcal{G}'$
                qSteps $\leftarrow 0$
            else
                qSteps $\leftarrow$ qSteps $+1$
            end
        end foreach
    end
    // RANDOM RESTART
    $\mathcal{G}' \leftarrow$ ApplyOperator ($\mathcal{G}_{best}$,R_MOVES)
    if $\mathrm{Score}(\mathcal{G}' : \mathcal{D}) > \mathrm{Score}(\mathcal{G}_{best} : \mathcal{D})$ then
        $\mathcal{G}_{best} \leftarrow \mathcal{G}'$
        qLoops $\leftarrow 0$
    else
        qLoops $\leftarrow$ qLoops $+1$
    end
end
return $\mathcal{G}_{best}$
```

# Chapter 3

# Weight Annealing

Training in machine learning is usually posed as an optimization problem : that is, we search for a hypothesis that maximizes a score on the training data. This is true for regression, classification and density estimation, as well as most other machine learning problems. (The obvious exception we are ignoring is pure Bayesian learning, which involves integration instead of optimization, but that is typically intractable.) Even for straightforward optimization objectives, in interesting hypothesis spaces like decision trees, neural networks, and graphical models, the problem of finding a globally optimal hypothesis is usually intractable. This is true whether one is searching for an optimal combination of hypothesis structure and parameters (e.g., decision tree learning), or just optimizing the parameters for a given structure (where the likelihood function is optimized). Therefore, most training algorithms employ local search techniques such as gradient descent or discrete hill climbing to find locally optimal hypotheses (e.g., [Bishop, 1995]). The drawback is that local maxima are abundant. Thus, local search often yields poor results. This situation is particularly acute when learning probabilistic graphical models in the presence of missing data and hidden variables, as discussed in Section 2.4.

In this chapter we consider annealing like strategies for escaping local maxima. Unlike standard annealing approaches, we perturb the training data rather than the hypothesis space directly. The approach is applicable to a wide range of learning scenarios in general, and for learning Bayesian networks in particular. In Section 3.1, we present a brief background on annealing algorithms. In Section 3.2 we present the basics of our framework, followed by two perturbation strategies in Section 3.3. In Section 3.4 we analyze our approach using a toy learning problem. In Section 3.5 we apply our method to structure search, parameter estimation, and the combined task when learning Bayesian networks. In Section 3.6, we briefly present an application to an inherently different and highly non-linear optimization problem. In Section 3.7 we briefly discuss the relation of our method to other annealing approaches as well as to boosting and bootstrap. We finish with a short discussion in Section 3.8.

**Algorithm 3**: Generic Annealing Algorithm

```
Input  : $\mathcal{D}$     // training set
         $h^0$    // initial hypothesis
         $\tau^0$    // initial temperature
Output : An hypothesis $h$

$i \leftarrow 0$
while $\tau^i > 0$ do
1   | $h^{i+1} \leftarrow$ Optimize($\tau^i$,$h^i$,$\mathcal{D}$)
    | $\tau^{i+1} \leftarrow$ CoolDown($\tau^i$ )
    | $i \leftarrow i + 1$
end
return $h^i$
```

## 3.1 Annealing Algorithms

Tabu list and random restarts for discrete structure search, and multiple starting point EM for parameter estimation were discussed in Chapter 2 as simple and often effective methods for escaping local maxima. When the optimization problem at hand is difficult, as is often the case for real-life domains with hidden variables, more sophisticated tools need also be considered. The annealing family of algorithms are probably the most commonly used tool to avoid local maxima. The basic idea behind these algorithms is to start by optimizing a related, easy to solve problem and gradually converge to a solution of the hard problem of interest. Algorithm 3 shows a generic annealing procedure: At the heart of the algorithm is some *cooling policy* that starts at a high temperature $\tau^0$ and decreases the temperature $\tau$ to $0$. The optimization method involved in Line 1 introduces stochasticity or regularization into the learning process in a magnitude that is a function of the current temperature $\tau^i$. The algorithm gradually converges on a solution of the original optimization problem at $\tau = 0$. Below, we briefly present the two most common annealing methods.

The *Simulated annealing* (SA) algorithm [Kirpatrick et al., 1994] and its variants manipulate the learning algorithm by allowing "illegal" or score decreasing moves. The algorithm follows a "propose, evaluate, reject" scheme: a random move is suggested, evaluated, and then accepted if it improves the score, or with a probability that is proportional to the decrease in score and the current temperature. The acceptance probability is

$$P(\text{Accept}) = \begin{cases} 1 & \Delta\text{Score} > 0 \\ exp\left(-\frac{1}{\tau}\Delta\text{Score}\right) & \text{otherwise} \end{cases}$$

where $\Delta$Score is the difference in score resulting from the move evaluated, and $\tau$ is the current temperature. At high temperatures, practically any move is allowed while at $\tau = 0$, only score increasing moves are accepted. Simulated annealing is in fact a specific instantiation of the Metropolis procedure [Metropolis et al., 1953], and is thus a Markov Chain process where detailed balance holds. Thus, Markov chain theory (see for example [Gilks et al., 1996]), guarantees convergence to the global maximum, if we start at a temperature that is sufficiently high and progress sufficiently slowly. While this may seem promising, the challenge lies in the choice of an effective cooling strategy (see [Laarhoven and Aarts, 1987] for an overview of methods). In practice, it is often not possible to achieve good performance in reasonable time. Simulated annealing has proved beneficial in a variety of optimization tasks such as constraint satisfaction and the traveling salesman problem.

The *Deterministic annealing* (DA) algorithm (e.g., [Rose, 1998]) is an annealing approach that incorporates entropy in the learning objective function, instead of stochasticity in the learning algorithm. As with simulated annealing, the magnitude of the “disturbance” of the true objective is proportional to the temperature $\tau$. When the system is cooled down, the entropy is lowered until at $\tau = 0$ the original objective is optimized. In addition, convergence to the global maxima is again guaranteed in theory, but in practice can be extremely elusive and time consuming. Deterministic annealing has been used successfully for many problems such as clustering (e.g., [Hofmann and Buhmann, 1997]).

Somewhat surprisingly, both of these algorithms, which are often considered as state-of-the-art optimization methods, have not been successful when applied to learning Bayesian networks (see more details in Section 3.7). It is the goal of this chapter to present a different annealing approach that is reminiscent of Boosting [Schapire and Singer, 1999] and Bootstrap [Efron and Tibshirani, 1993], and is effective when learning Bayesian networks.

## 3.2 Weight Annealing

The most common scores used in machine learning are *additive* on training data, which means that the score of a hypothesis $h$ on data $D = \{\mathbf{x}[1], ..., \mathbf{x}[M]\}$ is a sum of local scores on each individual sample, plus an optional regularization penalty

$$\text{Score}(h, D) \quad = \quad \sum_m \text{score}(h, \mathbf{x}[m]) - \text{penalty}(h)$$

Such scores arise naturally in regression or classification problems, where the local score is typically the negated prediction error, and in density estimation, where the local score is typically the log likelihood. Although we will apply our techniques to more general, non-additive scores below, it will be useful to keep additive scores as a simple example.

At the core of our method is a procedure for *reweighting* of the training samples to create useful ascent directions in the hypothesis space. To do this, we augment the score so that it considers a probability distribution $\mathbf{w}$ on the training examples, thus yielding

$$Score(h, D, \mathbf{w}) = M \sum_m \mathbf{w}_m \cdot \text{score}(h, \mathbf{x}[m]) - \text{penalty}(h) \tag{3.1}$$

It is first important to understand intuitively how sample reweighting can help to escape local maxima. The key idea is that we can cause "informed" changes to be made to the current hypothesis, rather than arbitrarily alter it. If the hypothesis is poor, then some training samples which contribute strongly to the score are likely to be outliers that should be down-weighted, whereas other samples that do not contribute strongly should be up-weighted to reflect their true importance in the underlying distribution. That is, a poor hypothesis can fit outliers but under-represent samples that are actually important. Understanding how the score is influenced by training samples can therefore suggest plausible perturbations to the data so that superior hypotheses are favored.

Our goal is to perturb the training data to allow the local search algorithm to escape poor local maxima, under the constraint that we ultimately find a hypothesis that scores well on the original training distribution. Therefore, the perturbations should not move the training data too far from their original state, and eventually the data must be restored to its original form to ensure that the final hypothesis is optimized on the correct distribution. This suggests that we follow an annealing approach, where we allow the instance weights to change freely early in the search, but then eventually "cool" the weights towards the original distribution.

Algorithm 4 outlines the generic *Weight Annealing* (WA) search procedure we suggest, generalizing on the basic annealing procedure of Algorithm 3. The free parameters in this procedure are the annealing schedule or *cooling policy* (Cooldown), the local search method (Optimize), and the example reweighting scheme (Reweight). For the annealing schedule, we follow a standard initialization and decay, starting with temperature $\tau^0$ and setting $\tau^{i+1} = \delta\tau^i$, with $\delta = 0.9$, unless otherwise specified. (Note that this also requires that we set $\tau$ to zero once its value numerically negligble). The optimization procedure depends, naturally, on the learning problem at hand and is different for learning parameters or learning structure. Note however, that the optimization method is used as a black box that does *not* use the temperature parameter. Rather, it is given a weighted data on which it is applied without any need for modification. Another issue to note is that the local search can be interleaved with the example reweighting in many ways. For example, one could perform full local optimization between each reweighting step, or perform only a partial optimization between reweightings. We specify the details of how optimization is applied in section Section 3.5.

The final component of our search procedure is the reweighting method. In the next section we consider two basic techniques for perturbing sample weights to escape local maxima: *random reweighting* where weight profiles (vector of weight values for all instances) are randomly sampled, and *adversarial reweighting* where the weight profile is updated to explicitly punish the current

**Algorithm 4**: Weight Annealing Search Procedure

```
Input  : $\mathcal{D}$      // training set
         $\mathbf{w}^0$     // initial instance weights
         $h^0$     // initial hypothesis
         $\tau^0$     // initial temperature
Output : An hypothesis $h$

$i \leftarrow 0$
while $\tau^i > 0$ do
    $\mathbf{w}^{i+1} \leftarrow$ Reweight($Score$,$\mathbf{w}^i$,$\tau^i$,$h^i$,$D$)
    $h^{i+1} \leftarrow$ Optimize($Score$,$\mathbf{w}^{i+1}$,$h^i$,$\mathcal{D}$)
    $\tau^{i+1} \leftarrow$ CoolDown($\tau^i$ )
    $i \leftarrow i + 1$
end
return $h^i$
```

hypothesis, with the intent of quickly guiding the search to a more promising solution. In both cases, as the temperature is lowered, the weight profile is annealed towards the original weights. This ensures that the search eventually focuses on producing good solutions for the original distribution of training samples.

Our basic approach has several benefits. First, the perturbation schemes are general and can be applied to a large variety of hypothesis spaces, either continuous or discrete. Second, our approach uses *unaltered* standard search procedures to improve hypotheses at each iteration, rather than employ the often wasteful "propose, evaluate, reject" cycle of simulated annealing approaches. Third, because a perturbation of the training data can generate a long chain of search steps in hypothesis space, a single reweighting step can result in a hypothesis that is very different from the one considered at the outset (although its score might not be that different). Finally, in the adversarial variant, the perturbations to the score are not arbitrary. Instead, they force the score to be more attentive to a subset of the training instances, thus allowing the particular problem at hand to explicitly affect the annealing procedure.

## 3.3 Reweighting Strategies

### 3.3.1 Random Reweighting

The first reweighting approach we consider is a randomized method motivated by *iterative local search* methods in combinatorial optimization [Codenotti et al., 1996] and phylogenetic reconstruction [Nixon, 1999]. Instead of performing random steps in the hypothesis space, we perturb the score by randomly reweighting each training example. Candidate hypotheses are then evaluated with respect to the reweighted training set. That is, we use a standard optimization procedure and a score of the form of Eq. (3.1), with the perturbed weights vector $\mathbf{w}$. After each iteration is complete, we repeat the process by independently sampling new example weights, re-optimizing the hypothesis, etc., until the magnitude of the weight perturbation is zero.

For convenience, we require the weights to be a probability distribution over the $M$ data instances. To randomly create a vector of weights, we sample from a *Dirichlet* distribution with parameter $\beta$, so that

$$P(\mathbf{W} = \mathbf{w}) \propto \prod_m w_m^{\beta - 1} \tag{3.2}$$

for legal probability vectors (see, for example [DeGroot, 1989]). When $\beta$ is large, this distribution peaks around the uniform distribution. Thus, if we use $\beta = 1/\tau^i$, the randomly chosen distributions will anneal towards the uniform distribution as $\tau^i$ decreases with the number of iterations $i$. At $\tau^i = 0$ we will converge on the original optimization problem. This scheme, that we call **Random**, can also be applied to datasets with non-uniform initial weights. To do so, we note that for a Dirichlet distribution of the form

$$P(\mathbf{W} = \mathbf{w}) \propto \prod_m w_m^{\alpha_m \beta - 1} \tag{3.3}$$

the maximum is achieved at

$$w_m = \frac{\alpha_m \beta - 1}{\sum_{m'} (\alpha_{m'} \beta - 1)}$$

Thus, if the original weight of sample $m$ is $w_m^0$, we choose $\alpha_m$ so that

$$\frac{\alpha_m \beta - 1}{\sum_{m'} (\alpha_{m'} \beta - 1)} = w_m^0$$

for all $m$. Then, as $\beta$ grows larger and the distribution peaks around its maximum, each weight will converge to its original value. Note that the $\alpha_m$s are easily computed and that Eq. (3.2) is recovered if the weights of all instances are equal.

The **Random** reweighting strategy can be applied to any optimization function problem where the objective can be expressed as a function of samples and their weights. This make this strategy applicable to a large number, if not most, learning problems.

### 3.3.2 Adversarial Reweighting

The second reweighting approach we consider, is to update weights in a way that directly challenges the current hypothesis. This approach is motivated by the exponential gradient search of Schuurmans et al. [2001] for constrained optimization problems. We combine their technique with an annealing process and modify it for a machine learning context. Intuitively, one can challenge a local maxima by calculating the gradient of the score with respect to the weights and then updating the weights to *decrease* the current hypothesis' score. For example, on a training sample $\mathbf{x}[m]$ one could consider the adversarial weight update

$$w_m^{t+1} \leftarrow w_m^t - \eta \frac{\partial Score(h, \mathcal{D}, \mathbf{w})}{\partial w_m}$$

which would explicitly make the current hypothesis appear less favorable and hence less likely to remain a local maximum. In this way, $Score(h, D, \mathbf{w})$ behaves somewhat like a Lagrangian, in the sense that the local search attempts to maximize the score over $h$ whereas the weight update attempts to *minimize* the score over $\mathbf{w}$, in an adversarial min-max fashion.

This general approach still has to be adapted to our needs. First, we want to anneal the weight vector towards the original distribution. Therefore we add a penalty for divergence between $\mathbf{w}^{t+1}$ and the original weights $\mathbf{w}^0$. We use the Kullback-Leibler measure [Kullback and Leibler, 1951] to quantify the divergence between these two weight distributions. We heighten the importance of this term as the temperature is cooled down by using $\beta\, KL(\mathbf{w}^{t+1} \| \mathbf{w}^0)$ where $\beta \propto 1/\tau^{i+1}$. Second, to maintain positive weight values, we follow an exponential gradient strategy and derive a multiplicative update rule in the manner of [Kivinen and Warmuth, 1997]. This adds an additional penalty term of the KL-divergence between successive weight vectors $\mathbf{w}^{t+1}$ and $\mathbf{w}^t$. Combining these leads to the following penalized score target function

$$L(h, \mathcal{D}, \mathbf{w}^{t+1}) = \eta Score(h, \mathcal{D}, \mathbf{w}^{t+1}) + \beta\, KL(\mathbf{w}^{t+1} \| \mathbf{w}^0) + \gamma\, KL(\mathbf{w}^{t+1} \| \mathbf{w}^t) \qquad (3.4)$$

where $1/\beta$ and $1/\gamma$ are proportional to the temperature and enforce proximity to the original weights and the previous weights, respectively.

There are two ways to use this function to derive weight updates. The first is to explicitly minimize the penalized score by solving for $\mathbf{w}^{t+1}$ in $\nabla_{\mathbf{w}^{t+1}} L(\mathcal{D}, h, \mathbf{w}^{t+1}) = 0$. If the score function is convex in $\mathbf{w}$ (as is often the case) the solution can be quickly determined by iteration. A second, more expedient approach, is suggested by Kivinen and Warmuth [1997]: Instead of doing full optimization, we heuristically fix the gradient $\nabla_{\mathbf{w}} L$ to its value at $\mathbf{w}^t$ and *analytically* solve for the minimum of the resulting approximation (up to the step size parameter $\eta$). This is tantamount to approximating the optimal update by taking a fixed step of size $\eta$ in the exponential gradient direction from the current weight vector $\mathbf{w}^t$.

To derive the update formula, we first have to compute the derivative of $L(h, \mathcal{D}, \mathbf{w}^{t+1})$ with respect to each of the instance weights. Using $\frac{\partial x \log x}{\partial x} = \log x + 1$, we can write

$$\frac{\partial KL(w^{t+1} \| w^0)}{\partial w_m^{t+1}} = \frac{\partial \sum_{m'} w_{m'}^{t+1} \log \frac{w_{m'}^{t+1}}{w_{m'}^0}}{\partial w_m^{t+1}} = \log \frac{w_m^{t+1}}{w_m^0} + 1$$

and similarly for the derivative of $KL(w^{t+1} \| w^t)$. Putting these together we get

$$\frac{\partial L(h, \mathcal{D}, \mathbf{w}^{t+1})}{\partial w_m^{t+1}} = \eta \frac{\partial Score(h, \mathcal{D}, \mathbf{w}^{t+1})}{\partial w_m^{t+1}} + (\beta + \gamma) \log w_m^{t+1} - \beta \log w_m^0 - \gamma \log w_m^t + C$$

where $C \equiv \beta + \gamma$ is a constant. Fixing $\frac{\partial Score(h,\mathcal{D},\mathbf{w}^{t+1})}{\partial w_m^{t+1}}$ to $\frac{\partial Score}{\partial w_m}|_{w_m^t}$ and applying some algebraic manipulations, we arrive at the multiplicative update form:

$$w_m^{t+1} = \alpha^{t+1} (w_m^0)^{\frac{\beta}{\beta+\gamma}} (w_m^t)^{\frac{\gamma}{\beta+\gamma}} e^{-\frac{\eta}{\beta+\gamma} \left( \frac{\partial Score}{\partial w_m}|_{w_m^t} \right)} \tag{3.5}$$

where $\alpha^{t+1}$ is a normalization constant. We refer to scheme as **Adversary**. We note that in the update formula $\frac{\eta}{\beta+\gamma}$ can in fact be written as $C \cdot \tau \cdot \eta$ where $C$ is some constant. Thus, we have a degree of freedom that results from interchangeability of the temperature $\tau$ and the learning rate $\eta$. For convenience, we always use $\eta = 1$.

In sum, our second basic reweighting approach is to make adversarial weight updates by following the negative gradient in a well motivated function. This approach can be applied whenever the original weighted score is differentiable *with respect to the weights*, for any fixed hypothesis. Note this is a very weak requirement that is typically satisfied in machine learning scenarios. In particular, differentiability with respect to the weights has nothing to do with the discreteness or continuity of the hypotheses—it is a property of how the instance weights affect the score of a fixed hypothesis. Thus, one could apply the adversarial reweighting approach to decision tree and neural network training problems without modification.

An important distinction from the **Random** reweighting approach is noteworthy: randomness is replaced by a guided methodology where weights are perturbed to minimize an intuitive function. While random may reach the best solution by chance, as we will see in Section 3.5, the **Adeversarial** approach offers a far better average solution due to its objective dependent guidance. This distinction also makes the **Adversarial** approach very different from other annealing approaches that are oblivious to the current hypothesis in the search procedure.

## 3.4 Analysis of a Toy problem

As noted in Section 3.1, Markov chain theory (e.g., [Gilks et al., 1996]) guarantees convergence of the annealing procedure to the global maximum if we start at a sufficiently high temperature and cool down at a sufficiently slow rate. However, we usually do not have any practical guarantees of the performance of any annealing method. This is also the case for our Weight Annealing method. Thus, in this section we analyzed a toy problem to shed some light on situations where we can expect our method to work, and when we can expect it to fail.

Recall that in Section 3.2 we motivated sample reweighting by the fact that strengthening some examples and weakening others can transform the hypothesis toward a profitable direction. With this in mind, we construct a toy example where the direct correspondence between maxima and samples is made explicit. Consider a training dataset of points $\mathcal{D} = \{x_1, \ldots, x_M\}$, a set of corresponding weights $\mathcal{W} = \{w_1, \ldots, w_M\}$, and the following one-dimensional objective function with a single free parameter $\theta$

$$\text{Score}(\theta, \mathcal{D}, \mathbf{w}) = \sum_i w_i \exp\left\{-\frac{1}{2}(x_i - \theta)^2\right\} \tag{3.6}$$

Note that in this objective, each sample can potentially create a local maxima associated with it and that is nearby the value of the sample. Figure 3.1(a) shows this objective when the data set consists of two points $x_1 = 1$ and $x_2 = 5$ with weights $w_1 = 0.8$ and $w_2 = 0.2$, respectively. Also shown are the three extremum points of the function marked by the dashed vertical lines. Our goal is to learn the global maximum $\theta \simeq x_1$.

We now want to analyze how the **Adversary** method will behave given this particular objective. Setting, for convenience, $\beta = \gamma = 0.5/\tau$, the update equation Eq. (3.5) becomes

$$w_1^{t+1} \propto w_1 \exp\left\{-\tau \exp\left\{-\frac{1}{2}(x_1 - \theta)^2\right\}\right\}$$

and similarly for $w_2^{t+1}$, both of which are normalized to sum to 1. If the current parameter $\theta$ is at the local maximum near $x_1$, the inner exponent is approximately zero, and $w_1^{t+1} \propto w_1 \exp\{-\tau\}$. In contrast, $w_2^{t+1} \propto w_2 \exp\{-\tau \cdot c\}$ where $c < 1$. Consequently, the reweighting step will diminish $w_1$ and will enhance $w_2$ thus challenging the current hypothesis. Similarly, if the current hypothesis is in the local maximum near $x_2$, the reweighting step will diminish $w_2$ and enhance $w_1$. Formally, we can guarantee the following:

**Proposition 3.4.1:** *Let $\{x_1, x_2\}$ be two sample points such that $|x_2 - x_1| < \infty$, and $\{w_1, w_2\}$ be their corresponding weights. In addition, let $x_1 < x_2$ and $w_1 > w_2$. Then, using the score defined in Eq. (3.6), there is a range of temperatures $[\tau_l, \tau_h]$ such that:*

1. *If $\theta \simeq x_2$ (is at the local maximum nearest to $x_2$) then, for any $\tau \in [\tau_l, \tau_h]$, after the adversarial reweighting step, the score function will have a single (global) maximum near $x_1$.*
2. *If $\theta \simeq x_1$ then, for any $\tau \leq \tau_h$, after the adversarial reweighting step, the score function will have two maxima near $x_1$ and near $x_2$.*

The consequence of the above proposition is that there exists a range of temperature in which, after adversarial reweighting, using simple gradient ascent optimization will "shift" the parameters in the direction of the true global maximum. Furthermore, if, after such a shift the temperature is only lowered, then the parameters will not "escape" to an inferior maximum. If the temperature is further lowered to zero using *any* cooling policy, then using simple gradient ascent will converge to the true global maximum.

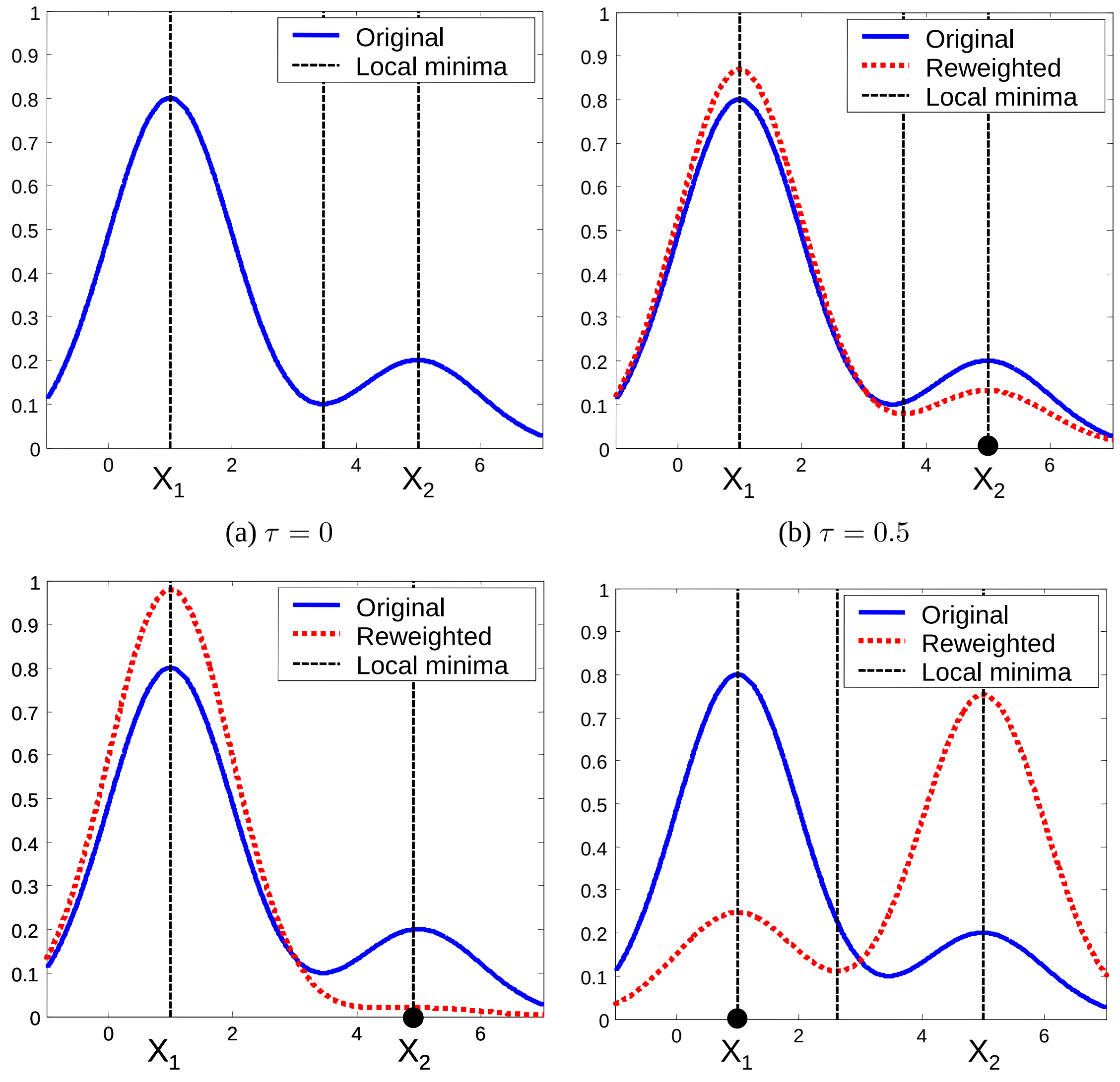

(a) $\tau = 0$ (b) $\tau = 0.5$

(c) $\tau = 2.5$ (d) $\tau = 2.5$

Figure 3.1: Illustration of adversarial reweighting on a toy problem: Two instances $x_1 = 1$ and $x_2 = 5$ are weighted by $w_1 = 0.8$ and $w_2 = 0.2$, respectively. The objective score is $\sum_i w_i exp\{-\frac{1}{2}(x_i - \theta)^2\}$ with one free parameter $\theta$. The figures show the score function before (solid blue) and after (dotted red) adversarial reweighting at different temperatures. The dahsed vertical lines mark the local minima of the reweighted objective. (a)-(c) shows the change when the current hypothesis (black circle) is at $\theta^0 \simeq x_1$. (d) shows the change when the current hypothesis is at $\theta^0 \simeq x_2$.

We illustrate the proposition geometrically in Figure 3.1. (a) shows the original objective function with two local maxima. (b) and (c) show the score function before (solid blue line) and after (dotted red line) reweighting when the current parameters are near $x_2$ (black circle). When the temperature is low as in (b), the score function changes a little and there are still two evident local maxima after reweighting. When the temperature is sufficiently high as in (c), the reweighting causes the rightmost maximum to disappear and gradient ascent will push the parameters towards the true global maximum. (d) shows what happens when the same temperature is used but the current parameters are near $x_1$. In this case, the leftmost maximum is indeed pushed down but not sufficiently to erase the local maximum. It can be computed geometrically that for any $\tau \in [2.4, 5.1]$ the same phenomena occurs. (A similar geometrical computation can be carried out to prove the proposition for any $x_1$ and $x_2$.) The above formal guarantee can be extended to some extent

**Proposition 3.4.2:** *Let $x_1 < x_2 < x_3$ be three distinct points, where $|x_3 - x_1| < \infty$, and $\{w_1, w_2, w_3\}$ be their corresponding weights. Then, for the score of Eq. (3.6), if it* not *the case that $w_1 < w_2 < w_3$ or $w_1 > w_2 > w_3$ then there is is a range of temperatures $(\tau_l, \tau_h]$ for which*

1. *For any $\tau \in (\tau_l, \tau_h]$, adversarial reweighting followed by gradient ascent will converge to the parameters of the global maximum regardless of the initial parameter value*
2. *For any $\tau \leq \tau_h$, adversarial reweighting followed by gradient ascent will not push the parameters away from the global maximum*

**Proof:** (Outline) Assume, w.l.g., that $w_1 > w_2, w_3$ and $w_2 < w_3$. Using Proposition 3.4.1, there is a range $[\tau_l^0, \tau_h^0]$ for which gradient ascent will progress from the parameter at $x_2$ to those at $x_1$ but not the other way around (we loosely use the points here to denote the nearest local maxima). Similarly, there is a range $[\tau_l^1, \tau_h^1]$ for which it is possible to move from the parameters at $x_2$ to those at $x_3$ but not the other way around. In addition, there exists such $\tau_h^1$ so that for any $\tau > \tau_h^1$ it is also possible to move from $x_3$ to $x_2$. Using technical manipulations, it can be shown that $\tau_h^0 > \tau_h^1$. From this we can conclude that there is a range $(\tau_h^1, \tau_h^0]$ of temperatures at which it will be possible to move from $x_3$ to $x_2$ and then to $x_1$ but not the other way around. ∎

It is insightful to understand why the above proposition is guaranteed to work only if the weights are unordered. If, for example $w_1 > w_2 > w_3$, then is could be the case that the temperature that allows the parameters to be pushed from $x_2$ to $x_1$ will also allow it to escape towards $x_3$. At the same time, it could be that at a cold enough temperature, where escape to $x_3$ will no longer be possible, a move towards $x_1$ will no longer be possible as well. We can only still guarantee that if the current parameter is near the global maximum at a low enough temperature, it will stay there.

The above gives us the first clue to where adversary reweighting may fail. In particular, it is not only the magnitude of the local maxima but also their relative size that influences the behavior of the algorithm. Another factor that influences the behavior of the algorithm can be the variance of

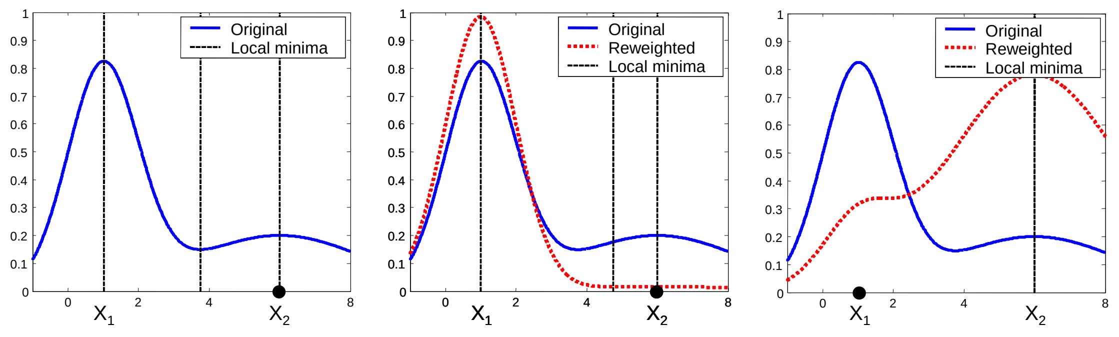

(a) $\tau = 0$ (b) $\tau = 2.66$ (c) $\tau = 2.66$

Figure 3.2: Illustration of adversarial reweighting on a toy problem: Two instances $x_1 = 1$ and $x_2 = 6$ are weighted by $w_1 = 0.8$ and $w_2 = 0.2$, respectively. The objective score is $\sum_i w_i exp\{-\frac{1}{2x_i}(x_i - \theta)^2\}$ with one free parameter $\theta$. The figures show the score function before (solid blue) and after (dotted red) adversarial reweighting at different temperatures. The dotted vertical lines mark the local minima of the reweighted objective. (a) shows the original "cold" function. (b) shows the change when the current hypothesis (black circle) is at $\theta^0 \simeq x_2$ and (c) shows the change when the current hypothesis is at$\theta^0 \simeq x_1$.

each component in the score. Consider, for example, a slightly different score where the variance of each component is proportional to the value of the corresponding sample

$$\text{Score}(\theta, \mathcal{D}, \mathbf{w}) = \sum_i w_i \exp\left\{-\frac{1}{2x_i}(x_i - \theta)^2\right\} \tag{3.7}$$

Figure 3.2 illustrates this example. In (b), we can see that there is a temperature $\tau = 2.66$ for which gradient ascent will not be able to "drift" from the inferior maxima to the global one. (c) shows that a the same temperature it is already possible to move from the global maximum to the inferior one. Intuitively, the narrower a component of the score is, the easier it is to overcome its corresponding maximum. Thus, the algorithm is sensitive not only to the value of the global maximum, but to its *basin of attraction.*

The form of the scores of Eq. (3.6) and Eq. (3.7) we use for the toy example was chosen because of the direct relation between a local maxima and a sample that made some analysis possible. Generalizing Proposition 3.4.2 to more realistic scores of actual problems that arise in machine learning remains a theoretical challenge. Another challenge is to understand how our method behave when multiple local maxima are present. In practice, as we demonstrate in the next sections, adversarial reweighting performs well on complicated and varied target functions with many local maxima.

## 3.5 Learning Bayesian Networks

In this section we apply Weight Annealing to three basic tasks of learning Bayesian networks: structure search, parameter learning in the presence of missing values or hidden variables and the combined challenge of learning both structure and parameters. We finish with evaluation on challenging real-life data sets.

### 3.5.1 Perturbing Structure Search

We start by applying Weight Annealing to the problem of learning the structure of Bayesian networks with complete data $\mathcal{D}$. To guide the search procedure, we use the decomposable BDe score (see Section 2.3.1). A crucial property that we utilize when perturbing instance weights is that this score, like other commonly used scores, is a function of *sufficient statistics* of the data. For models in the exponential family, these sufficient statistics have a canonical form as a sum of functions applied to particular instances. Thus, if $S$ is a sufficient statistic of interest, then

$$S(D) = \sum_m s(\mathbf{x}[m])$$

where $s(\mathbf{x}[m])$ is a function of a particular training instance. For example, if $S(D)$ counts the number of times an event occurred in the data, then $s(\mathbf{x})$ is an indicator function that returns $1$ if $\mathbf{x}$ satisfies the event, and $0$ otherwise. When we perturb the score, we simply need to reweight the contribution of each instance. Thus, the perturbed statistic is

$$S(D, \mathbf{w}) = M \sum_m w_m \cdot s(\mathbf{x}[m]) \tag{3.8}$$

where $M$ is the number of samples and $\mathbf{w}$ is a distribution over the training samples. Although the BDe score itself is not additive, it is nevertheless defined by sufficient statistics of the data and can therefore be easily adapted to the weighted case.

The BDe score is also differentiable with respect to the weights of the training instances, which allows us to apply adversarial reweighting. Using Eq. (2.15) we can write the score for the entire network structure $\mathcal{G}$ as

$$\text{Score}_{BDe}(\mathcal{G} : \mathcal{D}) = \sum_i \sum_{\mathbf{pa}_i} \left[ \log \frac{\Gamma\left(\alpha(\mathbf{pa}_i)\right)}{\Gamma\left(S[\mathbf{pa}_i] + \alpha(\mathbf{pa}_i)\right)} + \sum_{x_i} \log \frac{\Gamma\left(S[x_i, \mathbf{pa}_i] + \alpha(x_i, \mathbf{pa}_i)\right)}{\Gamma\left(\alpha(x_i, \mathbf{pa}_i)\right)} \right]$$

The only expressions in the score that depend on the weights are the sufficient statistics counts $S[\mathbf{pa}_i] = \sum_m w_m \cdot P(\mathbf{Pa}_i = \mathbf{pa}_i \mid e_m)$ where $e_m$ is the evidence of the m'th instance, and similarly for $S[x_i, \mathbf{pa}_i]$. Using the *Digamma function* $\Psi(x) \equiv \frac{\Gamma'(x)}{\Gamma(x)} = (\log \Gamma(x))'$ [DeGroot, 1989], the derivative of the score with respect to a specific weight $w_m$ is given by

$$\frac{\partial \text{Score}_{BDE}(\mathcal{G} : \mathcal{D})}{\partial w_m} = \sum_i \sum_{\mathbf{pa}_i} \sum_{x_i} \Big[\Psi(S[x_i, \mathbf{pa}_i] + \alpha(x_i, \mathbf{pa}_i)) - \Psi(S[\mathbf{pa}_i] + \alpha(\mathbf{pa}_i))\Big] P(x_i, \mathbf{pa}_i \mid e_m)$$

which can readily be evaluated using a numerical approximation to the Digamma function.

## Experimental Evaluation

To evaluate the performance of structure learning with weight annealing we start with the synthetic Alarm network [Beinlich et al., 1989], where we can compare our results to the generating model that has the additional prior knowledge of the true structure. We compare our methods to a greedy hill-climbing procedure that is augmented with a TABU-search mechanism and random restarts as in Algorithm 2 in Section 2.3.3. We use a tabu list of size 200 with 10 random moves at each of the 5 random restarts. This setting allows great flexibility for the learning procedure and is competitive with state-of-the-art methods. We apply our perturbation methods following the outline specified in Algorithm 4. We allow the search procedure to fully optimize with respect to the perturbed weights after each reweighting. When performing Weight Annealing, we limit the tabu list to size 25 and allow no random restart moves.

It is possible to evaluate the results both in terms of scores on training data and generalization performance on test data (average log-loss per instance). In all of our experiments the two measures correlate closely, and therefore we report only test set performance. Figure 3.3 shows the progress of the test set likelihood during iterations of the perturbed runs. Shown are the average performance of 100 runs of the **Random** perturbation method (with the 20%-80% margin in gray) and the **Adversary** method, compared to the best of random restarts without perturbations, and with similar running times. Several conclusions are notable. First, both perturbation methods solidly outperform the random restarts method. In fact, both methods are able to outperform the true structure with parameters that were estimated using the training data (**Silver**). Second, the best model overall is found by **Random**. However, **Adversary** is significantly better than **Random**'s average performance. This allows one to either invest a lot of time and achieve a superior model by performing many random perturbation runs, or obtain a near optimal structure with a single **Adversary** run.

To emphasize this point, Figure 3.4 shows the cumulative performance of two different setups of **Random** (different starting temperatures and cooling factors). The less favorable line has a similar running time to **Adversary**. The superior **Random** takes an order of magnitude longer for each run, and often reaches what appears to be the achievable global maximum.

We also evaluated the performance of our methods for structure search on a real-life data set. Stock Data [Boyen et al., 1999] is a dataset that traces the daily change of 20 major US technology

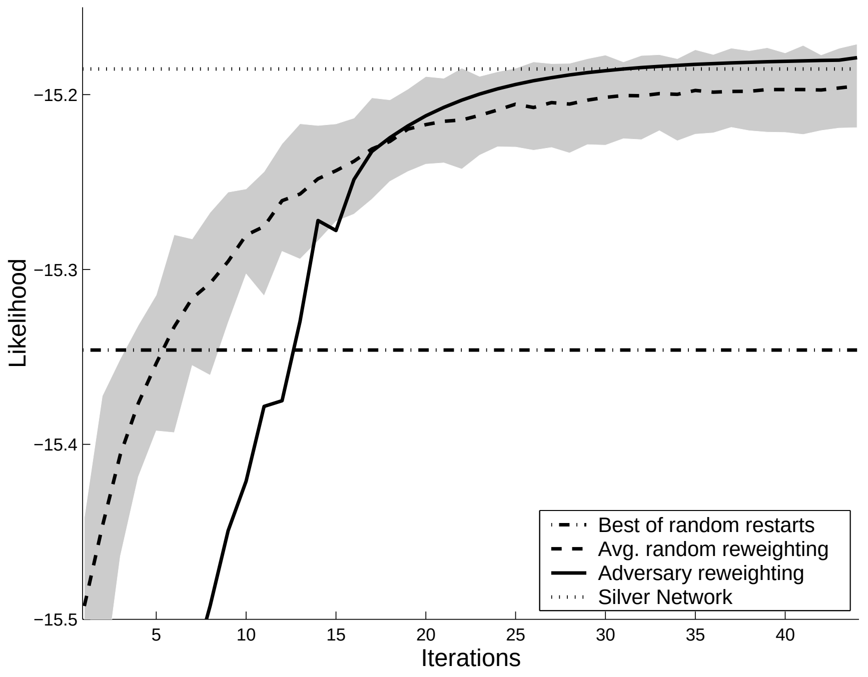

Figure 3.3: The progress of test set likelihood (log-loss per instance) during iterations while learning structure from complete data of the Alarm domain. Compared are the true structure with trained parameters (**Silver**), the best of 100 runs of random restarts search without perturbations, 100 runs of the **Random** perturbation method and a single run of the **Adversary** method. The gray area marks the 20%-80% range of 100 **Random** runs.

stocks for several years (1516 trading days). As shown in Table 3.1, using our Weight Annealing procedure leads to improvement of the performance of the model on unseen test data.

### 3.5.2 Perturbing Parametric EM

We now consider the application of the Weight Annealing framework to parameter estimation of Bayesian networks in the presence of missing data or hidden variables. As discussed in Section 2.4, this scenario raises many complications including our inability to perform maximum likelihood or Bayesian estimation in closed form. However, weight perturbation can easily be applied if we use the *Expectation Maximization* (EM) algorithm to cope with this scenario. In particular, EM uses *expected sufficient statistics* of the data. The perturbed form of these statistics can be obtained by replacing Eq. (3.8) with

$$\boldsymbol{E}_Q[S(D,\mathbf{w})] = M\sum_m w_m \sum_{\mathbf{x}[m]} s(\mathbf{x}[m],\mathbf{o}[m])Q(\mathbf{x}[m] \mid \mathbf{o}[m])$$

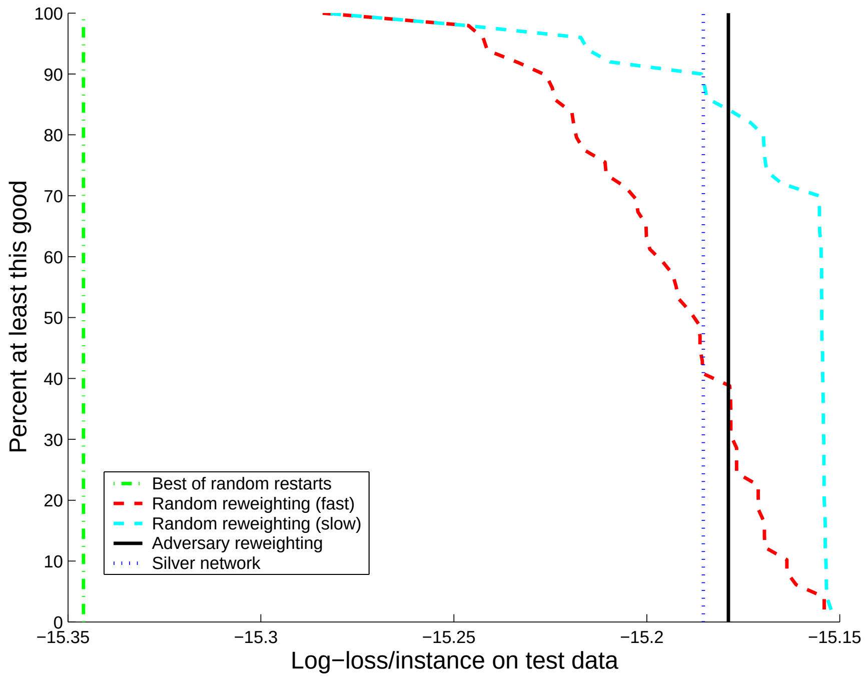

Figure 3.4: Cumulative performance on test data when learning the structure of the network with complete data of the Alarm domain. The $x$-axis shows test-set likelihood (log loss per instance), the $y$-axis shows percent of runs that achieve that likelihood or higher. Compared are the true model with parameters trained (**silver**), the best of 100 random runs of the baseline greedy learning method, 100 random runs two instantiations of the **Random** reweighting method, and a single **Adversary** reweighting run.

where $Q$ is a posterior distribution over $\mathbf{x}[m]$ given the current hypothesis and the partially observed instance $\mathbf{o}[m]$. Note that the above form is a generalization of Eq. (2.16), and enhances the applicability of the approach to general learning scenarios with missing values or hidden variables.

It is clear that the maximum point of the expected score is not the maximum point of the true score (for otherwise one iteration suffices to get to the global maximum). Thus, the expected score is biased. In general, this bias is towards models that are in some sense similar to the one with which we computed the expected sufficient statistics. This suggests that we do not necessarily want to find the optimum of the expected score within EM iterations. Instead, we apply a limited number of EM iterations (e.g., one) within each optimization step of the Weight Annealing procedure shown in Algorithm 4, and then reweight the instances. The general perturbation scheme is otherwise unchanged.

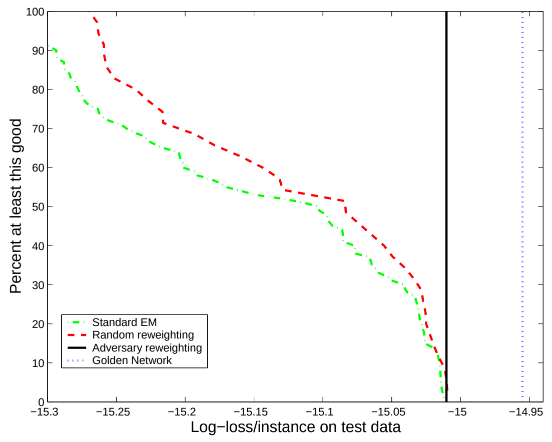

(a) Parametric EM runs

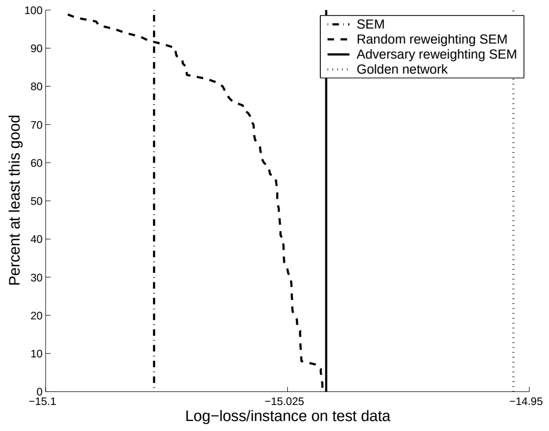

(b) Structural EM runs

Figure 3.5: Cumulative learning performance on test data generated from the synthetic Alarm network. The $x$-axis shows test-set likelihood (log loss/instance), the $y$-axis shows percent of runs that achieve that likelihood or higher. Compared are 100 runs each of the baseline learning method, computationally intensive **Random** perturbations and **Adversary**, as well as the **Golden** model that generated the training and test instances. (a) Shows results for parameter estimation where four central variables were hidden in the training set and true structure is used. (b) Shows results for estimation of the parameters as well as the structure from the same dataset.

#### Experimental Evaluation

We examine our method on the synthetic Alarm network. Figure 3.5(a) compares 100 random runs of standard parametric EM, computationally intensive **Random** perturbation, and an **Adversary** run. Because of the limited number of EM iterations, **Adversary** takes only about 15 times longer than a single parametric EM run, and **Random** takes around 50 times longer than a single EM run. We can clearly see the advantage of the **Adversary** method, which achieves what appears to be the attainable global maximum using the finite training set. This maximum is reached by only a few of the random EM and **Random** perturbation runs, and is not far from the true structure and parameters (**Golden**) that generated the test data.

### 3.5.3 Perturbing Structural EM

The final and most difficult task we explore for Bayesian networks is that of learning both the parameters and the structure of the model. As in the case of parameter estimation, the use of the *Structural EM* (SEM) approach [Friedman, 1997, 1998] facilitates the use of Weight Annealing: Like EM, the algorithm is based on expected sufficient statistics that can be readily perturbed.

**Experimental Evaluation**

The setting is identical to the one used in the EM runs, but we also attempt to learn the topology of the network. The starting point of the search is a structure where all the hidden variables are parents of all the observed nodes. Figure 3.5(b) shows cumulative results for 100 random runs for the synthetic Alarm example. The Structural EM runs have a very low variance and are worse than over 90% of the **Random** perturbation runs. As with parametric EM, but more markedly, the **Adversary** method dominates random reweighting. Note that it halves the distance from the baseline performance to the performance of the true network.

### 3.5.4 Evaluation of real-life domains

To conclude the evaluation of Weight Annealing for learning Bayesian networks, we consider a number of real-life datasets where we learn both the structure and parameters.

- The Soybean [Michalski and Chilausky, 1980] disease database from the UCI machine learning repository contains 35 variables relevant for the diagnosis of 19 possible plant diseases. There are 307 training instances and 376 test instances, with many missing values.
- The Audiology data set [Bareiss and Porter, 1987] from the UCI machine learning repository, contains 69 variables relevant to illnesses relating to audiology disfunctions. There are only 202 training instances an 26 test instances with numerous missing values.
- Rosetta's compendium [Hughes et al., 2000] consists of gene expression data of 6000 *Saccharomyces cerevisiae* genes (variables) and 300 experiments (samples). We used the pre-processing of Pe'er et al. [2001] to discretize the data and concentrated on 37 genes which participate in the *stationary phase* stress response that they identify.

For each data set we performed 5-fold cross validation and compared the log-loss performance on independent test data. Table 3.1 summarizes the results. Shown are results for best of random restarts Structural EM runs, average and 80% values of **Random** perturbation runs, and the **Adversary** method. Both perturbation methods achieve superior results to random restarts Structural EM. Similar to what was observed in structure search, it is sometimes possible to reach a superior model to **Adversary** by performing many **Random** perturbation runs.

In all domains, the perturbation methods improves over the baseline. For the challenging problem of learning structure in the presence of hidden variables this improvement is quite significant. For the Soybean dataset, for example, an average improvement of $0.19$ bits per instance over a test set with 376 test instances, means that the unseen samples are more then $2^{74}$ more likely given the model learned by the adversarial perturbation method, relative to the best of state-of-the-art Structural EM runs with Tabu list and random restarts.

Table 3.1: Summary of results on independent test data for several data sets for the structure search and structural EM problems. Shown are log-loss per instance of improvement in performance with respect to the best of the random restarts baseline. Compared are the mean of the **Random** perturbation method (along with the **80%** mark) and the **Adversary** method.

| | Domain | **Random** | **80%** | **Adversary** |
|---|---|---|---|---|
| Search | Stock | $-0.02$ | $+0.01$ | $+0.03$ |
| | Alarm | $+0.15$ | $+0.18$ | $+0.17$ |
| SEM | Rosetta | $-0.05$ | $+0.27$ | $+0.09$ |
| | Audio | $+0.00$ | $+0.39$ | $+0.23$ |
| | Soybean | $+0.19$ | $+0.32$ | $+0.19$ |
| | Alarm | $+0.25$ | $+0.31$ | $+0.33$ |

## 3.6 Learning Sequence Motifs

All of our case studies so far have addressed unsupervised density estimation problems in the form of learning Bayesian networks. To demonstrate the wide range applicability of Weight Annealing, we now examine a completely different discriminative learning scenario. The problem is to perform non-linear logistic regression in order to find *regulatory motifs* in DNA promoter sequences; i.e., , short subsequences that regulate the expression of genes. In particular, a motif is defined as a relatively short signature of about 8-20 nucleotides (DNA letters) that appears somewhere in the DNA sequence—the exact location of which is unknown and can vary from sequence to sequence. An example of a motif might be the sequence `ACGCGT`. Unfortunately, most known motifs are not preserved perfectly in the DNA, and one generally has to allow for substitutions in one or several positions. Accordingly, the common representation of a motif is as a *weight matrix* [Durbin et al., 1998] which describes the weight of each of the four possible DNA letters for each position within the motif. Intuitively, a subsequence that has a large sum of letter weights is said to match the motif. We use the notation $w_i[x]$ to denote the weight of the letter $x$ in the $i$'th position.

Following Barash et al. [2001] and Segal et al. [2002], we define the basic training problem in discriminative terms. Given $N$ promoter sequences $\mathbf{s}_1, \ldots, \mathbf{s}_N$, where the $n$'th sequence consists of $K$ letters $s_{n,1} \ldots, s_{n,K}$, and a set of of training labels $l_1, \ldots, l_N$, where $l_i$ is 1 if the sequence is regulated by the motif and 0 if it is not (these labels can be obtained from different biological experiments), we wish to maximize the log-loss $\sum_i P(l_n \mid s_n)$ where

$$P(l_n = 1 \mid S_{n,1}, \ldots, S_{n,K}) = \mathit{logistic}\left(\log\left(\frac{v}{K}\sum_j \exp\{\sum_i w_i[S_{n,i+j}]\}\right)\right)$$

and $\mathit{logistic}(x) = \frac{1}{1+e^{-x}}$ is the logistic function and $v$ is a threshold parameter. Segal et al. [2002]

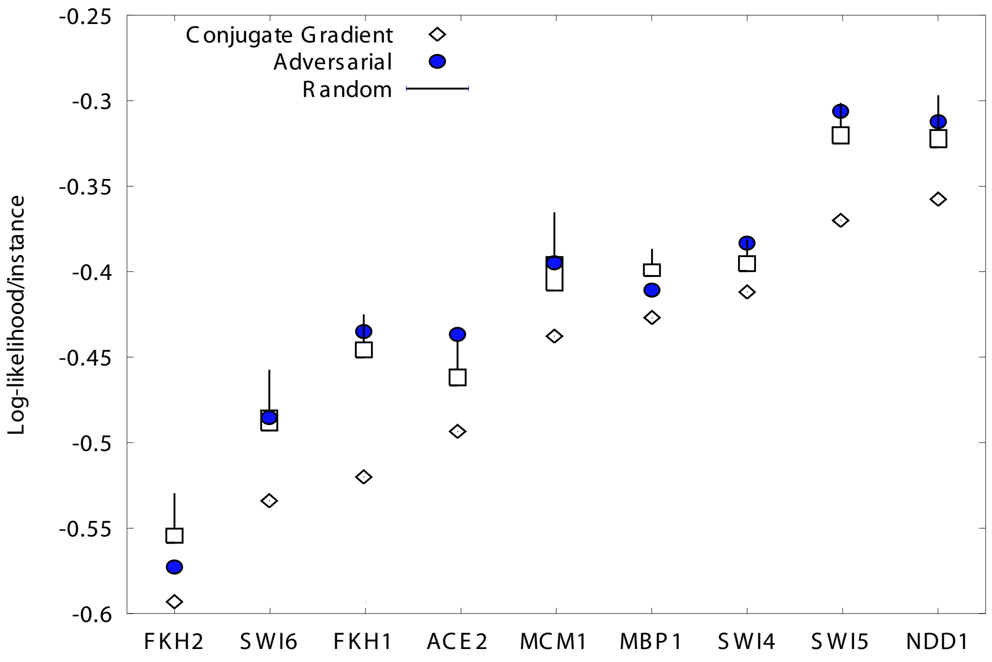

Figure 3.6: Performance of different methods in the motif finding task for 9 data sets. The $x$-axis corresponds to the different datasets, and the $y$-axis reports training log-likelihood per instance. We report the performance of the baseline conjugate ascent method, Adversarial reweighting, and Random reweighting. The box plot show the range between 20% to the 80% of 50 Random reweighting runs, and the narrow lines on top of the box show the best result of these 50 runs.

address this problem in two stages. First, they search for high scoring seeds by considering all short words of length 6 using the method of Barash et al. [2001]. Then, for each seed they construct a weight matrix of 20 positions that embodies the seed consensus sequence in the middle positions (the weights in flanking positions were initialized to 0). Finally, the use conjugate gradient ascent with line search [Price, 1992] to maximize the log-likelihood score.

We adopt the same procedure augmented with our weight perturbation methods. After each weight perturbation, we perform a line search in the direction of the gradient of the likelihood with respect to the reweighted samples. After the end of the cooling schedule, we apply a final conjugate gradient ascent to find the local maxima in the vicinity of the final point of the search.

We applied this procedure to the 9 training sets generated during the analysis that Segal et al. [2002] performed on DNA-binding experiments of Simon et al. [2001]. We report the results in Figure 3.6. As one can see, both Random and Adversarial reweighting are consistently better than the baseline approach. In some cases (ACE2, SWI4, SWI5) the Adversarial reweighting achieves scores better than all of the random runs, in others (FKH1, NDD1) it is better than at least 80% of the random runs, and only in two (FKH2, MBP1) it is worse than 80% of the random runs.

## 3.7 Relation to Other Methods

**Annealing Algorithms**

Both our reweighting strategies share the generic annealing framework outlined in Algorithm 3. Several differences from the standard algorithms are worth noting: Our method changes the optimization space of the learning procedure by perturbing the goal functional. *Simulated Annealing* [Kirpatrick et al., 1994], on the other hand, changes the "rules of the game" by allowing moves that decrease the score with proportion to the current temperature. This approach is often extremely effective when a small number of score decreasing moves is needed to escape an inferior local maxima. However, the approach suffers from two main drawbacks: First, the perturbation is independent from both the problem and the hypothesis in contrast to the guided adversarial reweighting method. Second, the "propose, evaluate, reject" cycle is often wasteful. This is particularly true if the evaluation of candidate hypothesis is costly, as is the case when evaluating the benefit of Bayesian network structures. We have applied simulated annealing as described by Heckerman et al. [1995a] for all the experiments in the previous sections. However, using a range of parameters (around those they suggest), we get significantly worse results than the baseline search method. This is consistent with the results of Chickering [1996b], who demonstrated that using multiple restarts greedy hill-climbing is more effective than simulated annealing when learning Bayesian networks.

*Deterministic Annealing* [Rose, 1998] is even more closely related to our method. Like our approach, it uses a black-box optimizer and applies it to a perturbed problem. The perturbation of the score is done by explicitly introducing entropy into the objective in a magnitude that is proportional to the current temperature. This added component serves as a smoothing factor of the landscape to be optimized. Somewhat surprisingly, despite success in other tasks such as classification, application of Deterministic Annealing for learning Bayesian network Ueda and Nakano [1998] have not been promising. In particular, Whiley and Titterington [2002] have demonstrated why learning Bayesian networks with hidden variables using Deterministic Annealing is problematic. Finally, despite the obvious similarity between our objective function and that of Deterministic Annealing, the rationale for the scores used in the two cases is quite different. It is unclear if there are deeper connections between the two methods.

**Boosting**

There are interesting relationships between the adversarial reweighting and ensemble learning methods such as boosting [Schapire and Singer, 1999]. Both methods share the central idea that at each step the weights of the samples that are not predicted well by the current hypothesis are amplified. However, there are some fundamental differences. On an intuitive level, both methods are inherently different in the motivation for this reweighting. In the case of boosting, the goal is to concentrate on the hard samples. In the case of adversarial reweighting, the goal is to challenge the current hypothesis and put its robustness to a test. Another difference is that boosting attempts to build a weighted ensemble of hypotheses that achieves a good score, whereas we are deliberately seeking a single hypothesis. On a technical level, boosting derives its weight updates by differentiating the loss of an entire ensemble [Mason et al., 2000], whereas our weight updates are derived by taking only the derivative of the score of the most recent hypothesis. Interestingly, although we do not exploit a large ensemble, we find that our method still produces hypotheses that generalize well to unseen test data. Although initially surprising, this phenomenon is explained by the fact that adversarial reweighting of samples discovers hypotheses that obtain good scores while simultaneously being robust against perturbations of the training data, which confers obvious generalization benefits.

**Bootstrap**
Our method is also reminiscent of the Bootstrap approach of Efron and Tibshirani [1993]. Bootstrap is a statistically motivated approach that can be used to provide confidence measures for features of Bayesian networks learned from data [Friedman et al., 1999b]. In short, this approach uses several random re-samplings of the data to learn different networks. Confidence measures from these networks can then be used to learn more robust models bypassing some of the local maxima that are a result of problematic noise in the data. Although both methods manipulate a black-box optimization procedure by effectively altering the weights of instances, there are several inherent differences. Rather than using an annealing procedure, the bootstrap approach learns many models from independent datasets that are sampled from the original training data. This re-sampling procedure is oblivious to the target function as well as to the performance of the hypothesis. Furthermore, instead of a single hypothesis that is a local maximum of the original problem, the bootstrap approach generates an ensemble of hypotheses, each optimizing a different and slightly perturbed problem. These need to be merged into a single hypothesis using several possible approaches (e.g., [Friedman et al., 1999b]).

## 3.8 Discussion

In this chapter we presented a general, annealing like, method for escaping local maxima. The essence of our *Weight Annealing* (WA) approach is to perturb the relative weight of the training instances in a gradually diminishing magnitude. Thus, we perturb the target function rather than the optimization procedure, and look for optimal solutions of the perturbed problem. As we have shown, such perturbations allow one to overcome local maxima in several learning scenarios. On both synthetic and real-life data, our approach seems to lead to significantly improved models when learning the structure of Bayesian networks with complete data, learning parameters with missing data, and learning both parameters and structure. The improvements are particularly impressive for the complex problem of learning both structure and parameters with hidden variables, where the problem of local maxima is acute.

The perturbation of instance weights is particularly attractive in its applicability for a wide range of learning problems. It is not only easy to find reweighted versions of standard learning scores, but sample weights are also easily incorporated into non-trivial learning procedures such as EM. In doing so, one can exploit the expected sufficient statistics for efficient search, and then perturb the expected score to find models that have a better score. We compared two strategies for generating the sequences of weights during annealing: *randomized reweighting* and *adversarial reweighting*. Our results show that both approaches dominate the straw-man of multiple restart search. Randomized reweighting can sometimes achieve better performance, but this might require performing several annealing runs. The deterministic adversarial strategy has the advantage of achieving comparable performance in a single run.

The random reweighting approach we introduced has also been applied in Friedman et al. [2002] as well as Barash and Friedman [2002] for learning phylogenetic trees and context-specific clustering models, respectively. Both papers report significant improvements when using Weight Annealing.

One avenue that we did not explore is the combination of a randomized element within the deterministic adversarial strategy. It is also clear that for realistic applications, we need to tune the implementation to reduce the number of iterations. This can be done by incorporating more sophisticated cooling strategies from the simulated annealing literature (e.g., [Laarhoven and Aarts, 1987]) or the deterministic annealing literature (e.g., [Rose, 1998]). It is also worth exploring improved ways to interleave the maximization and the reweighting steps. This may lead to significant improvement in performance, possibly at a marginal computational cost. Finally, the empirical success of these methods raises the challenge of providing a better theoretical understanding of their effectiveness. This is particularly intriguing for the adversarial reweighting strategy that has similarities to boosting and multiplicative update strategies. Despite the interchangeability of the temperature and the learning rate, the analysis of these methods does not seem to directly apply to our setting.

# Chapter 4

# Discovering Hidden Variables: A Structure-Based Approach

Our main goal in this dissertation is to learn new hidden variables. This involves determining the existence of a variable, inserting it effectively into the network structure, and setting its cardinality in the case of discrete variables. Obviously, all these tasks add significant difficulties to the already complex problem of learning *in the presence* of hidden variables, when they are known to exists. In Chapter 1, we qualitatively discussed why hidden variables should not be ignored: In theory, we can still construct a network that captures all the dependencies in the marginal distribution over the observed variables. However, as we illustrated in Figure 1.1 for the cancer domain, this can result in a model that is less desirable in terms of representation, as it contains significantly more parameters and edges than the succinct model with the hidden variable.

When a hidden variable is known to exist, we can introduce it into the network and apply known Bayesian networks learning algorithms. If the network structure is known, algorithms such as *EM* [Dempster et al., 1977, Lauritzen, 1995] or *gradient ascent* [Binder et al., 1997] can be used to learn parameters. If the structure is not known, the *Structural EM (SEM)* algorithm of [Friedman, 1998] can be used to perform structure learning with missing data. However, we cannot simply introduce a "floating" hidden variable and expect the search algorithm to place it correctly. In fact, if the hidden variable is placed where it does not improve the likelihood of the model, there is a good chance it will be disconnected by the local search algorithm, after which it will never be worthwhile to reconnect it to the network structure. Thus, in applying these algorithms we implicitly assume that some other mechanism introduces the hidden variable in approximately the right location in the network structure. Our goal in this chapter is then to answer the following two questions:

- Should we introduced a new hidden variable into the network structure?
- Where should we initially place it within the network structure?

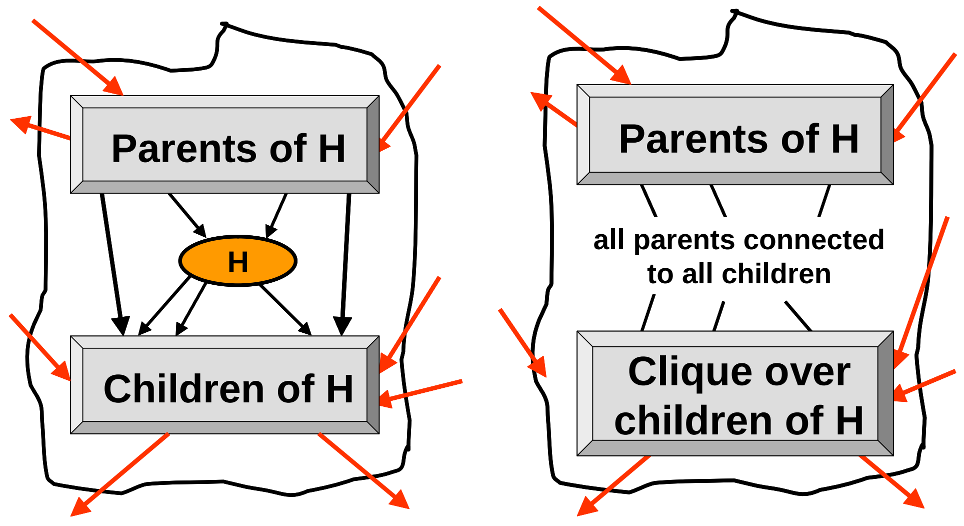
Parents of H
H
Children of H
Parents of H
all parents connected to all children
Clique over children of H

(a) Original network (b) After removal of $H$

Figure 4.1: Schematic illustration of Proposition 4.1.1. (a) shows a network fragment where a hidden variable $H$ separates between some of its parents and children. (b) shows the resulting network fragment when $H$ is not included in the structure and we require that no new independence assumptions are introduced into the network structure.

(We defer the task of learning the cardinality of the hidden variable to Chapter 5.) We investigate what is arguably the most straightforward approach for inducing the existence of a hidden variable. We formally show that the phenomena demonstrated in Figure 1.1, and briefly mentioned in Heckerman [1998], is a typical effect whenever a hidden variable is removed from the network structure. Based on this fact, our approach tries to reverse engineer this phenomena to suggest new hidden variables, and is roughly as follows: We begin by using a standard Bayesian network model selection algorithm to learn a structure over the observed variables. We then search the structure for substructures, which we call *semi-cliques*, that are potentially induced by a hidden variable. We temporarily introduce the hidden variable in a way that alters the sub-structure, and then continue learning based on that new structure. If the resulting structure improves the score, we keep the hidden variable. Surprisingly, this basic technique does not seem to have been pursued. We provide a concrete and efficient instantiation of this approach and show how to integrate it with existing learning algorithms such as the Structural EM algorithm. We apply our approach to several synthetic and real-life datasets, and show that it often provides a good initial placement for the new hidden variable. We can therefore use it as a preprocessing step for Structural EM, substantially reducing the search space of the algorithm.

## 4.1 Detecting Hidden Variables

In the example of Figure 1.1 discussed above and that motivates our approach, the hidden variable "Cancer" is the keystone for the conditional independence assumptions in the network. Without it, many of the independencies of Figure 1.1(a) simply do not hold. As a consequence, the marginal distribution over the remaining variables has almost no structure and includes many edges, creating an undesirable representation. We can show that this phenomena is a typical effect of removing a hidden variables:

**Proposition 4.1.1:** *(see Figure 4.1 for illustration)*
*Let $\mathcal{G}$ be a network over the variables $\mathcal{X} = \{X_1, \ldots, X_N\}, H$. Let $\mathcal{I}$ be the conditional independence statements — statements of the form $Ind(\mathbf{X} \perp \mathbf{Y} \mid \mathbf{Z})$ — that are implied by $\mathcal{G}$ and do not involve $H$. Let $\mathcal{G}'$ be the graph over $X_1, \ldots, X_N$ that contains an edge from $X_i$ to $X_j$ whenever $\mathcal{G}$ contains such an edge, and in addition: $\mathcal{G}'$ contains a clique over the children of $H$, and $\mathcal{G}'$ contains an edge from any parent of $H$ to any child of $H$. Then, there exists a distribution $P(\mathcal{X}, H)$ such that G is an* I-map *of $P(\mathcal{X}, H)$ and $\mathcal{G}'$ is a minimal* I-map *of $P(\mathcal{X}) = \sum_h P(\mathcal{X}, H)$.*

**Proof:** To prove that $\mathcal{G}'$ is an *I-map*, we need to show that the independence statements encoded in $\mathcal{G}'$ indeed hold in $P(\mathcal{X})$. To show that it is a minimal *I-map* we need to prove that removing any edge from $\mathcal{G}'$, renders it a non-*I-map* of $P(\mathcal{X})$.

We start with the latter task. Clearly, any edge $X_i \rightarrow X_j$ in the original network $\mathcal{G}$ must also be included in $\mathcal{G}'$, since the existence of such an edge means that in $P(\mathcal{X}, H)$ (of which $\mathcal{G}$ is an *I-map*), $X_i$ and $X_j$ may be dependent, even when conditioned on all other variables. Thus, only the edges we added in the construction of $\mathcal{G}'$ may be suspected as being redundant. Consider an edge $P_i \rightarrow C_j$, from some a parent $P_i$ of $H$ to some child $C_j$ of $H$. In the original structure there existed a path $P_i \rightarrow H \rightarrow C_j$. To render $P_i$ and $C_j$ independent this path (and possibly others) must be blocked (see discussion of d-separation in Section 2.1.1). This only occurs if $H$ is observed. Thus, when $H$ is not included in the model, we cannot guarantee that these two variables are not dependent making the edge $P_i \leftarrow C_j$ necessary to ensure *I-map*ness of $\mathcal{G}'$ with respect to $P(\mathcal{X})$. Similarly, consider the path $C_i \leftarrow H \rightarrow C_j$ between two children of $H$. The original structure $\mathcal{G}$ implies that unless $H$ is observed, $C_i$ and $C_j$ cannot be declared independent. Thus, either $C_i \rightarrow C_j$ or $C_i \leftarrow C_j$ is requires. This holds for any two children of $H$ in the original structure.

We now show that the independencies encoded in $\mathcal{G}'$ hold in $P(\mathcal{X})$. Obviously we need only consider independencies that were added as a result of the removal of $H$. The removal of $H$ from the structure can only effect independencies of variables if $H$ lies in some path between these variables. All such paths must pass either through parents of $H$, its children, or both. If $H$ is at the bottom of a v-structure $P_i \rightarrow H \leftarrow P_j$ along this path, it blocks the dependency since it is unobserved. This only adds dependencies to those encoded in $\mathcal{G}$ and does not effect *I-map*ness. If $H$ lies along the path so that $P_i \rightarrow H \rightarrow C_j$, the removal of $H$ can introduce a new independency between $P_i$ and

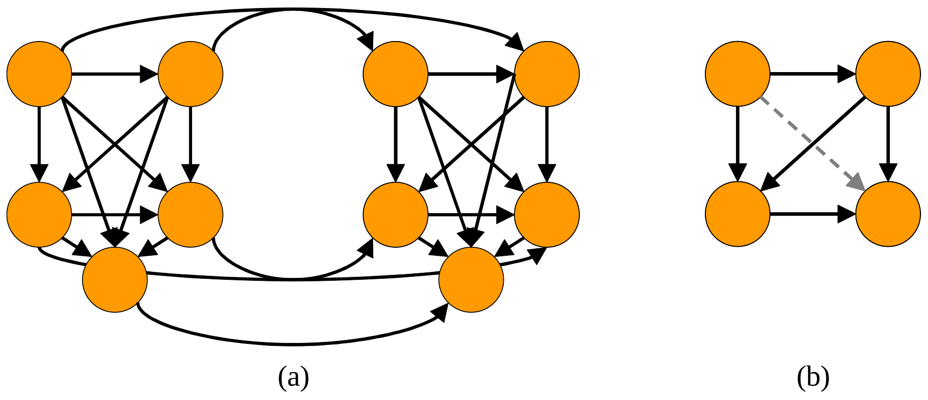

Figure 4.2: (a) A semi clique that is missed by our algorithm and is composed of two 5-cliques that are relatively sparsely connected. (b) A 4-clique structure with one edge missing. This is a slightly relaxed version of a *semi-clique*, that is still accepted by our algorithm.

$C_j$ (or ancestors of $P_i$ and descendants of $C_j$). However, the edge $P_i \rightarrow C_j$ directly cancels this potential independence (which is exactly why it was required for minimality). A similar argument for the case of a path that passes through $C_i \leftarrow H \rightarrow C_j$, shows that no new independencies are introduced in $\mathcal{G}'$, and thus it is an *I-map* of $P(\mathcal{X})$. ∎

Our strategy is to define an approach that will suggest candidate hidden variables by finding structures characterized by the above proposition in the context of a learning algorithm. That is, we will first learn a network using a standard structure learning algorithm, and then look for substructures that are potentially a results of a missing hidden variable. In practice, it is unreasonable to hope that there is an exact mapping between substructures that have the form described in Proposition 4.1.1 and hidden variables: Learned networks are rarely an exact reflection of the minimal I-map for the underlying distribution. We therefore use a somewhat more flexible definition, which allows us to detect potential hidden variables:

**Definition 4.1.2:** A *semi-clique* is a set of nodes $\mathbf{S}$ where each node $X \in \mathbf{S}$ is linked to more than more than half of the nodes in $\mathbf{S}$. That is,

$$|\mathbf{Adj}_X^{\mathcal{G}}(\mathbf{S})| > \frac{1}{2}|\mathbf{S}|$$

where $|\mathbf{S}|$ is the number of elements in the set $\mathbf{S}$ and $\mathbf{Adj}_X^{\mathcal{G}}(\mathbf{S})$ are the adjacent nodes (neighbors) of $X$ in the graph $\mathcal{G}$ that are in the set $\mathbf{S}$. ∎

We propose a simple heuristic for finding semi-cliques in the graph. We first observe that each slightly stricter version of a semi-clique must contain a *seed* which is easy to spot; this seed is a 3-vertex clique.

**Algorithm 5**: FindHidden

```
Input  : $\mathcal{G}$    // a network structure
Output : A list of candidate children sets (semi-cliques) for hidden variables in $\mathcal{G}$

CliqueList ← empty list
SeedList ← all 3-cliques in $\mathcal{G}$
foreach seed in SeedList do
    clique ← ExpandClique(seed,$\mathcal{G}$ )
    if size(clique ) > MIN_CLIQUE_SIZE then
        Insert clique into CliqueList
    end if
end foreach
return CliqueList
```

**Procedure:** ExpandClique

```
Input  : seed // a list of variables
         $\mathcal{G}$    // a network structure
Output : A semi-clique expanded from seed

SemiClique ← seed
repeat
    foreach variable $X$ not in SemiClique do
        if IsSemiClique(SemiClique $\cup X$ ) then
            SemiClique ← SemiClique $\cup X$
        end if
    end foreach
until SemiClique not expanded
return SemiClique
```

**Proposition 4.1.3:** *A set* $\mathbf{S}$ *of* $N$ *nodes where each node has more than* $\lfloor \frac{N}{2} \rfloor$*, must contain a full clique of size 3.*

**Proof:** Consider a semi-clique $\mathbf{S}$ with $N$ nodes, and let $X_i$ be an arbitrary node in it. $X_i$ must have at least $\lfloor \frac{N}{2} + 1 \rfloor$ neighbors in the semi-clique. Let $X_j$ be one of $X_i$'s neighbors (adjacent nodes). $X_j$ must also have at least $\lfloor \frac{N}{2} + 1 \rfloor$ neighbors in the semi-clique. But there are at most $N - \lfloor \frac{N}{2} + 1 \rfloor$ nodes that are not neighbors of $i$. Hence, $\mathbf{Adj}^{\mathcal{G}}_{X_i}(\mathbf{S})$ and $\mathbf{Adj}^{\mathcal{G}}_{X_j}(\mathbf{S})$ cannot be disjoint. Any node in the intersection, together with $X_i$ and $X_j$, forms the required 3-clique. ∎

The first phase of the algorithm is outlined in Algorithm 5: It is starts with an exhaustive search for all 3-cliques in the graph (by definition all of these are also semi-cliques). The algorithm then tries to expand each of them into a maximal semi-clique in a greedy way using the procedure *ExpandClique*. At each iteration this procedure attempts to add a node to the "current" semi-clique. If the expanded set satisfies the semi-clique property, then it is set as the new current semi-clique. These tests are repeated until no additional variable can be added to the semi-clique. The algorithm outputs the expansions found based on the different 3-clique "seeds". We note that this greedy procedure does not find all semi-cliques. The exceptions are typically two semi-cliques that are joined by a small number of edges, making a larger legal semi-clique. These cases, an example of which is illustrated in Figure 4.2(a), are of less interest because they are less likely to arise from the marginalization of a hidden variable. In practice, we allow a little leeway when searching for semi cliques, also accepting structures where each node is connected to exactly half of the other nodes. This allow us to captures structures such as a 4-clique with just one edge missing as shown in Figure 4.2(b).

In the second phase, we convert each of the semi-cliques to a structure *candidate* containing a new hidden node, reverse engineering the phenomena of Proposition 4.1.1. Suppose $\mathbf{S}$ is a semi-clique so that we suspect all of the variables in $Q$ may be the children of an unknown hidden variable $H$. We introduce such an $H$ into the network structure and (ensuring acyclicity)

- make $H$ the parent of all variables in $\mathbf{S}$
- remove all edges between the variables in $\mathbf{S}$
- replace each edge $P_i \rightarrow S_j$, from some parent $P_i$ (that is not in $\mathbf{S}$) to a child $S_j$ by $P_i \rightarrow H$.

This process results in the removal of all intra-clique edges and makes $H$ a proxy for all "outside" influences on the nodes in the semi-clique $\mathbf{S}$.

Our goal is to provide an efficient and effective starting point for the structure learning algorithm that will follow the introduction of a new hidden variables into the network structure. Thus, it is useful to analyze the complexity of our algorithm. The first stage finds all the 3-cliques in the graph. This is done using a greedy algorithm that examines all possible pairs of parents and children for each node. In theory, for a network with $n$ nodes this stage requires the enumeration of the $O(N^3)$ possibilities. In practice, however, since the number of parents and children in a typical network can be bounded by a small constant, the complexity is almost linear in the number of nodes. Next, we try to expand each 3-clique by gradually adding related variables from the network. If the network is represented efficiently, checking the neighborhood criterion is linear in the size of our current semi-clique. The algorithm can, in principle, require $N^2$ iterations before convergence; in practice, the number of iterations is linear in the size of the semi-clique. Thus the actual cost of this stage is typically $O(C^2)$, where $C$ is the size of the semi-clique. Breaking up the semi-clique (the process described above for making $H$ its proxy for outside influence), requires scanning of the edges and deciding which ones to leave and which to change or remove. This requires $O(|E|) + O(C)$ steps, where $E$ is the set of edges of the network.

In the third phase, we evaluate each of the candidate structures constructed with new hidden variables in an attempt to find the most useful one. There are several possible ways in which these candidates can be used by the learning algorithm. We examine three approaches. The simplest assumes that the network structure, after the introduction of the hidden variable, is fixed. In other words, we assume that the true structure of the network is indeed the result of applying our transformation to the input network. We then simply fit the parameters using EM, and score the resulting network. (As discussed in Section 2.4, to score candidates after a hidden variable is added, we need to resort to an approximation of the marginal likelihood. In here, we use the Cheeseman-Stuts approximation [Cheeseman et al., 1988].) To determine if the hidden variable is beneficial, we compare this score to the score of the network without the hidden variable.

We can improve on this method substantially by noting that our simple transformation of the semi-clique does not typically recover the true underlying structure of the original model. In our construction, we chose to make the hidden variable $H$ the parent of *all* the nodes in the semi-clique, and eliminate *all* other incoming edges to variables in the clique. Clearly, this construction is very limited. There might well be cases where some of the edges in the clique are warranted even in the presence of the hidden variable. It might also be the case that some of the edges from $H$ to the semi-clique variables should be reversed. Finally, it is plausible that some nodes were included in the semi-clique accidentally, and should not be directly correlated with $H$. We could therefore allow the learning algorithm to adapt the structure after the hidden variable is introduced. In the second approach we use Structural EM [Friedman, 1998] to fine-tune our model for the part of the network we just changed. More specifically, since $H$ directly effects only its Markov blanket variables $\mathbf{MB_H}$, we allow the structure search to change the parents only of $H$ and each of the variables in $\mathbf{MB_H}$. This restriction substantially reduces the search space of the search algorithm but still offers flexibility of structure adaptation. In the third approach, we allow full structural adaptation over the entire network. This offers greater flexibility, but is computationally more expensive. We examine the merit of these different approaches in Section 4.2.

To summarize our **FindHidden** approach: In the first phase we analyze the network learned using conventional structure search to find semi-cliques that indicate potential locations of hidden variables. In the second phase we convert these semi-cliques into structure candidates (each containing a new hidden variable). Finally, in the third phase we evaluate each of these structures (possibly using them as a seed for further search) and return the best scoring network we find.

## 4.2 Experimental Results

Our aim is to evaluate the success of our procedure in detecting hidden variables. To do so, we evaluated our procedure on both synthetic and real-life data sets. The synthetic data sets were sampled from Bayesian networks that appear in the literature. We then created a training set in which we hid one variable. We chose to hide variables that are "central" in the network (i.e., variables that are the parents of several children). The synthetic data sets allow for a controlled evaluation, and for generating training and testing data sets of any desired size. However, the data is generated from a distribution that indeed has only a single hidden variable. A more realistic benchmark is real data, that may contain many confounding influences. In this case, of course, we do not have a generating model to compare against. We now briefly discuss the different dataset we consider and the variables we hide in the case of synthetic domains.

- **Alarm** is a 37-node network [Beinlich et al., 1989] that models monitoring of ICU patients. We hid the variables HR, Intubation, LVFailure, and VentLung ($H$, $I$, $L$, $V$ in Figure 4.3).
- **Insurance** is a 27-node network developed to evaluate driver's insurance applications [Binder et al., 1997]. We hid the variables Accident, Age, MakeModel, and VehicleYear ($A$, $G$, $M$, $V$ in Figure 4.4).
- **Stock** [Boyen et al., 1999] is a real-life dataset that traces the daily change of 20 major US technology stocks for several years (1516 trading days). These values were discretized to three categories: "up", "no change", and "down".
- **TB** [Behr et al., 1999] is a real-life dataset that records information about 2302 tuberculosis patients in the San Francisco county (courtesy of Dr. Peter Small, Stanford Medical Center). The data set contains demographic information such as gender, age, ethnic group, and medical information such as HIV status, TB infection type, and other test results.

In each data set, we applied our procedure as follows. First, we used a standard model selection procedure to learn a network from the training data (without any hidden variables). In our implementation, we used the standard greedy hill-climbing with TABU search (see Chapter 2). We supplied the learned network as input to the semi-clique detecting algorithm which returned a set of candidate structure with a new hidden variable. We then used each candidate as the starting point

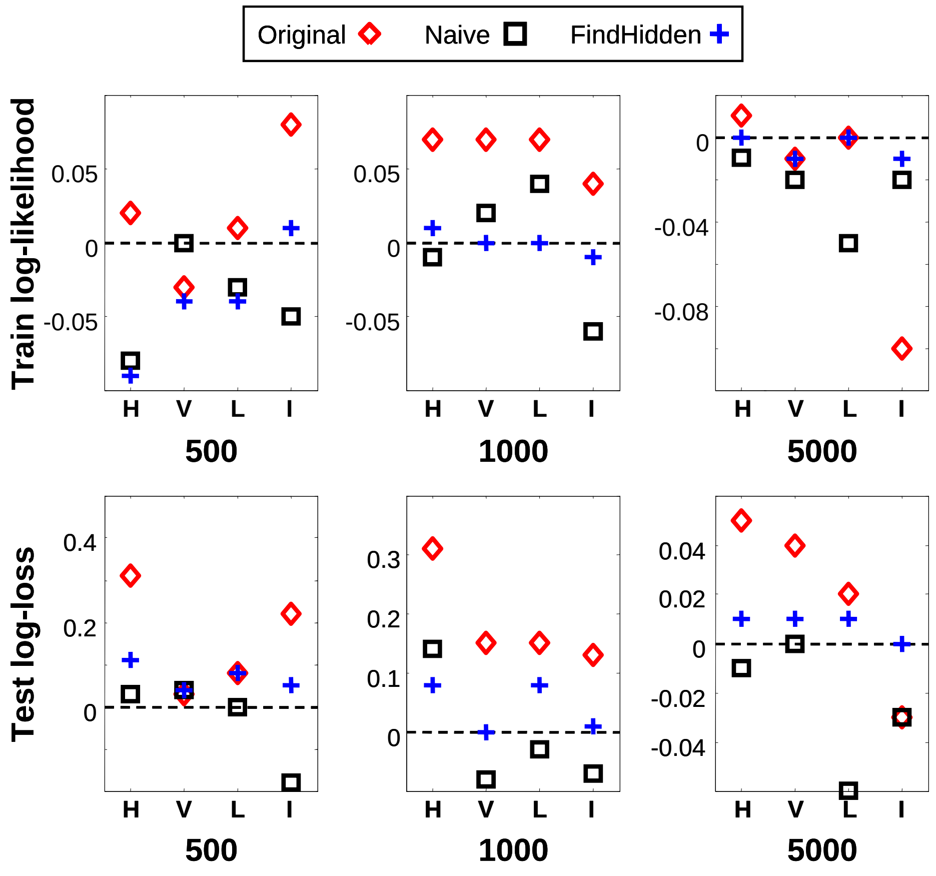

Figure 4.3: Comparison of the different approaches for the **Alarm** domain, where 4 variables were hidden: **H**R, **V**entlung, **L**VFailure and **I**ntubation. Training sets are of sizes 500,1000 and 5000 training instances, and test sets are all with 10,000 samples. Each point corresponds to a network learned by one of the methods. The log-likelihood per instance of train data, and test log-loss per instance appear on the top and bottom row, respectively. In all graphs, the scale is normalized to the performance of the network with no hidden variable (dashed line at “0”).

for a new learning phase. We use the second variant of Structural EM discussed in Section 4.1, where the algorithm is allowed to adapt only the parents of the Markov blanket variables of the new hidden variable (we discuss the other variants below). Our **FindHidden** procedure returns the highest-scoring network that results from evaluating the different putative hidden variables.

To gauge the quality of our learning procedure, we compared it to two straw-man approaches. The **Naive** straw-man [Friedman, 1998] initializes the learning with a network that has a single hidden variable as parent of all the observed variables. It then applies Structural EM to get an improved network. This process is repeated several times, where each time a random perturbation (e.g., edge addition) is applied to help the algorithm escape local maxima (see Algorithm 2 in Section 2.3.3). The **Original** straw-man, which applied only in synthetic data set, is to use the true

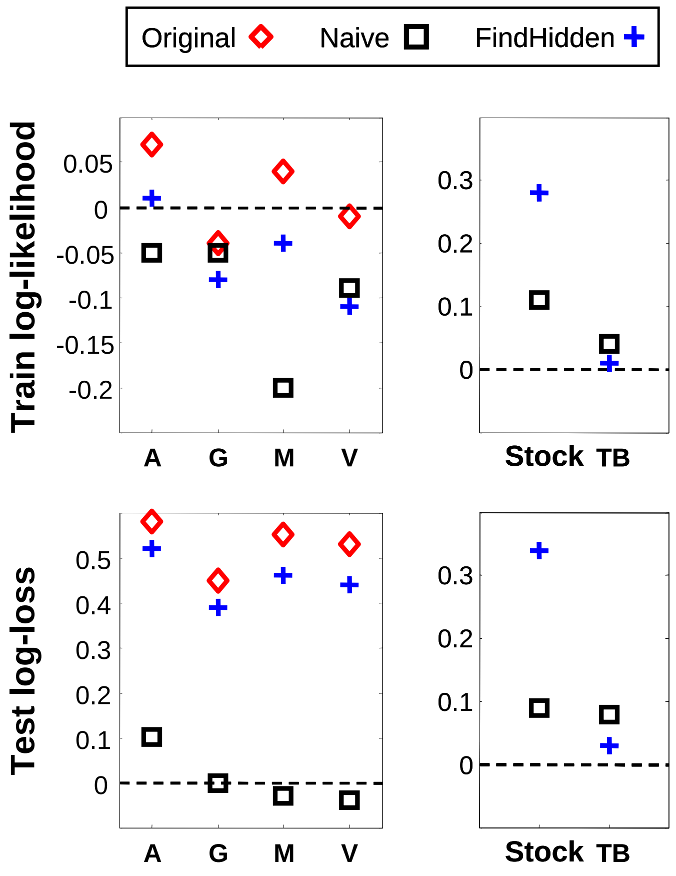

Figure 4.4: Comparison of the different approaches for the **Insurance** domain with 1000 training instance, as well as the real-life datasets **Stock** and **TB**. In the insurance network, 4 variables were hidden: **A**ccident, **A**ge, **M**akeModel and **V**ehicleYear. Each point corresponds to a network learned by one of the methods. The log-likelihood per instance of train data, and test log-loss per instance appear on the top and bottom row, respectively. In all graphs, the scale is normalized to the performance of the network with no hidden variable (dashed line at "0").

generating network structure. That is, we take the original network (that contains the variable we hid) and use standard parametric EM to learn parameters for it. This straw-man corresponds to cases where the learner has additional prior knowledge about the structure of the domain.

Figure 4.3 compares the different methods for four different variables that were hid in the **Alarm** network. Shown are the results of train (top) and test (bottom) performance against the baseline performance of the network with no hidden variables. When compared to our FindHidden model, the **Naive** model is more expressive and it is given greater flexibility in learning the structure. Thus, it is not surprising that on training data, the lesser the samples, the better its performance. However, on unseen test data, our FindHidden method is consistently better than both the baseline method and the **Naive** straw-man (excluding one case). The difference is often quite large: a model that is

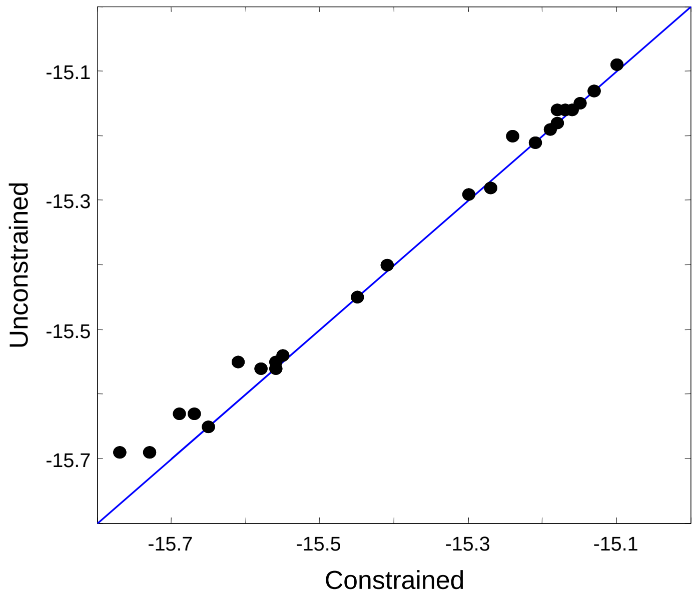

Figure 4.5: Test log-loss per instance of the unconstrained search vs. the constrained search variants of **FindHidden**. Shown are the experiments (each circle) for 4 variables of the **Alarm** network for training sets ranging from 500 to 10000 instances.

better than another by $0.1$ in log-loss per instance, for the test set of $10,000$ samples, is $2^{1000}$ as likely to have generated the unseen test data. The superiority of FindHidden compared to the Naive straw-man supports the hypothesis that it is not only important to add a hidden variable, but also to provide it a reasonable initial placement within the network structure. Note, that as the number of training samples gets larger, and as can be expected, the differences in performance between all methods gets smaller.

The results for 4 different variables that were hidden in the **Insurance** domain as well as the two real-life datasets **Stock** and **TB** are shown in Figure 4.4 and are equally encouraging. However, for the **TB** domain, the **Naive** straw-man was superior to our method. One possible explanation is that because the TB domain is relatively small (11 variables), **Naive** is able to take advantage of its greater flexibility.

As discussed in Section 4.1, there are three ways that a learning algorithm can utilize the original structure proposed by our algorithm. In all of our experiments, the variant that fixed the candidate structure after the introduction of the hidden variables and learned parameters for it resulted in scores that were significantly worse than the networks found by the variants that employed structure search. The networks trained by this variant also performed much worse on test data. This highlights the importance of structure search in evaluating a potential hidden variable. The initial structure candidate is often too simplified; on the one hand, it forces too many independencies among the variables in the semi-clique, and on the other, it can add too many parents to the new hidden variable.

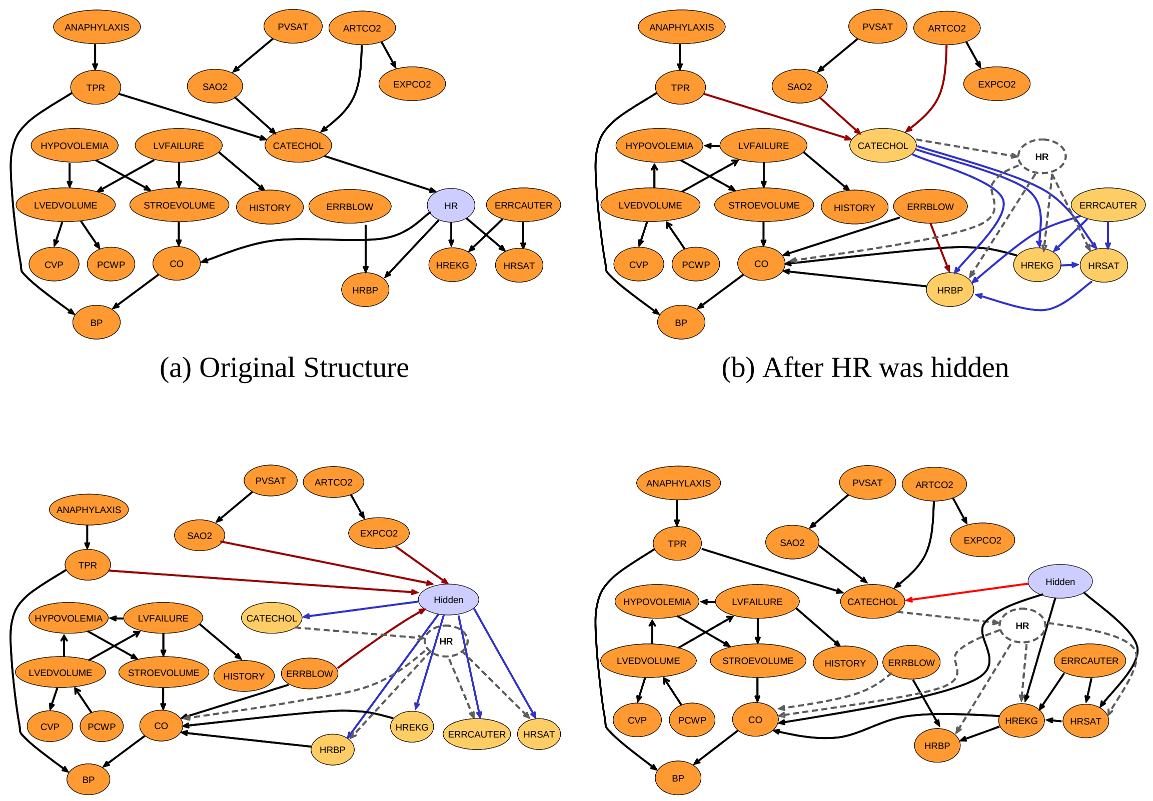

(a) Original Structure

(b) After HR was hidden

(c) After **FindHidden** insertion

(d) After final structure adaptation

Figure 4.6: Structure changes during the **FindHidden** algorithm when applied to the synthetic Alarm network using 1000 training samples. Dashed nodes and edges show those removed from the original structure. (a) the original structure; (b) the structure after HR was hidden and the structure adapted using Structural EM; (c) insertion of a new hidden variable by **FindHidden**; (d) final structure after Structural EM was applied to (c).

To compare the two variants that do use structure search, Figure 4.5 compares the test log-loss performance of the unconstrained variant of our method vs. the variant that adapts the only structure of the Markov blanket of the new hidden variable. In many cases, the variant that gives Structural EM complete flexibility in adapting the network structure did not find a better scoring network than the variant that only searches for edges in the vicinity of the new variable. In the cases it did lead to improvement, the difference in score was relatively small. Since the variant that restricts Structural EM is computationally cheaper (often by an order of magnitude), we believe that it provides a good tradeoff between model quality and computational cost.

We also want to qualitatively evaluate the ability of our method to reconstruct the approximately correct structure. To do so, we examine the performance of **FindHidden** on the synthetic Alarm network. Figure 4.6 shows the progress of the structure during the algorithm in the first such experiment. Starting with the original structure (a), Structural EM was not able to overcome the missing

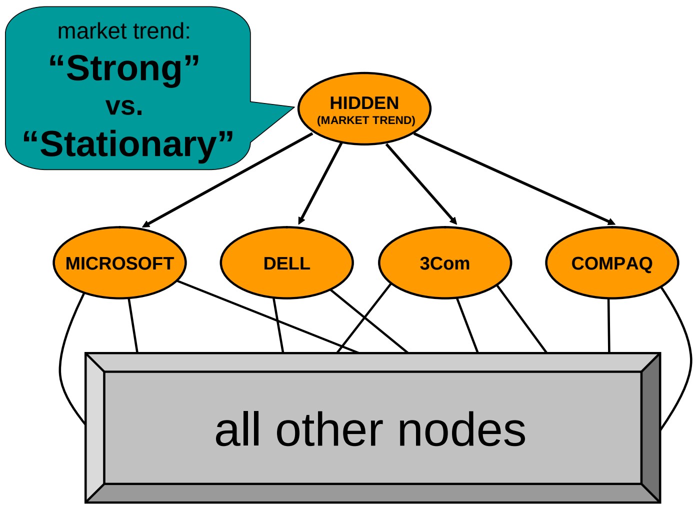

Figure 4.7: Schematic illustration of the model learned by **FindHidden** for the **Stock** dataset.

HR node and a *semi-clique* is clearly evident (b). Insertion of a new hidden variable after detection of **FindHidden** (c) seems reasonable but leaves a lot to be desired when compared to the original structure. Final structure adaptation using Structural EM recovers the original structure almost perfectly (d).

The structures found by our procedure when applied to real-life data are also quite appealing. For example, in the stock market data, our procedure constructs a hidden variable that is the parent of several dominant stocks at the time: Microsoft, Dell, 3COM, and Compaq, as shown in Figure 4.7. A plausible interpretation of this variable is "strong" market vs. "stationary" market. When the hidden variable has the "strong" value, all the stocks have higher probability for going up. When the hidden variable has the "stationary" probability, these stocks have much higher probability of being in the "no change" value. We do note that in the learned networks there were still many edges between the individual stocks. Thus, the hidden variable serves as a general market trend, while the additional edges make better description of the correlations between individual stocks. The model we learned for the TB patient dataset was also interesting and is shown in Figure 4.8. One value of the hidden variable captures two highly dominant segments of the population: older, HIV-negative, foreign-born Asians, and younger, HIV-positive, US-born blacks. The hidden variable's children distinguished between these two aggregated subpopulations using the *HIV-result* variable, which was also a parent of most of them. As we show in Chapter 5, when we allow the hidden variables to have a larger number of states, it is able to improve the division into subpopulations, and leads to overall improvement in prediction.

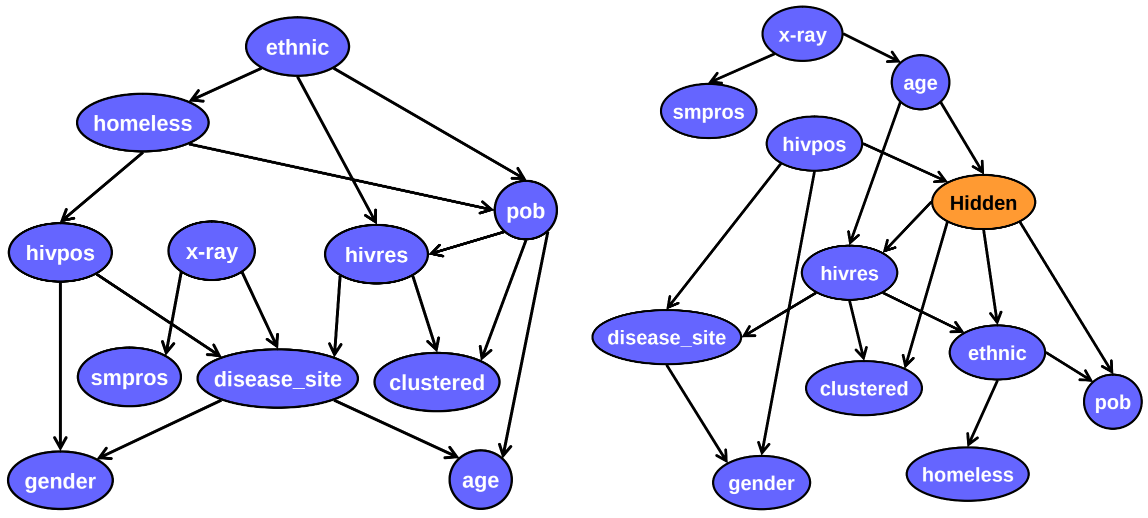

(a) Original Structure (b) After **FindHidden**

Figure 4.8: Structure of the TB patient real-life domain before and after the **FindHidden** algorithm.

## 4.3 Discussion

In this chapter, we proposed a simple and intuitive algorithm for introducing new hidden variables into a Bayesian network structure. First, a standard search algorithm is used to learn the structure over the domain. Our method then searches for structural signatures that are potentially left by a hidden variable that is missing from the network structure. If such signals are found, we propose a candidate hidden variable, after which we allow the structure learning algorithm to fine tune the network structure. We presented synthetic and real-life experiments showing that our approach improves the performance of the models learned, and is a successful guide for the structure learning algorithm.

The main assumption of our approach is that we can find “structural signatures” of hidden variables via semi-cliques. As we discussed above, it is unrealistic to expect the learned network $\mathcal{G}$ to have exactly the structure described in Proposition 4.1.1. On the one hand, learned networks often have spurious edges resulting from statistical noise, which might cause fragments of the network to resemble these structures even if no hidden variable is involved. On the other hand, there might be edges that are missing or reversed. Spurious edges are less problematic: At worst, they will lead us to propose a spurious hidden variable which will be eliminated by the subsequent evaluation step. Our definition of a semi-clique, with its more flexible structure, partially deals with the problem of missing edges. However, if our data is very sparse, so that standard learning algorithms will be very reluctant to produce clusters with many edges, the approach we propose will not work.

Our approach can be further explored in several directions. First, the structural signature a hidden variables “leaves” behind encompasses not just semi-cliques but a larger *many parent – many children* configuration. Detecting this signature effectively might allow us to expand the range of hidden variables we discover. Second, our clique-discovering procedure is based solely on the structure of the network learned. Additional information, such as the confidence of learned edges [Friedman et al., 1999b, Friedman and Koller, 2003], might help the procedure avoid spurious signatures. Finally, as noted above, our method can only be applied when data is sufficient so that the structural signatures manifest. Methods that can deal with sparse data are of great importance and pose a different challenge. In Chapter 6 we explore a method that uses a more flexible information theoretic signature for the presence of a hidden variable.

# Chapter 5

# Adapting the cardinality of hidden variables

In the previous chapter we presented the first method for learning new hidden variables using structural signatures. While the problem of learning the number of states of a hidden variable may seem relatively negligible in respect, this is far from true. In fact, we may be better off ignoring a hidden variable whose dimensionality is too low altogether: A hidden variables that is not expressive enough may not be able to capture the regularities of the original structure. At the same time, by incorporating the hidden variable into the network structure, we needlessly increase the complexity of the model thus limiting our ability to learn. This phenomena is illustrated in Figure 1.1 (c) and can occur, for example, if the independencies in the true structure (a) hold only if the Cancer node has several distinct values such as $\{$ None, Lung, Leukemia, Prostate, Breast $\}$, and do not hold when Cancer is a $\{$ Yes, No $\}$ binary valued variable. A hidden variable that is too expressive can be an equally bad choice — each redundant state can result in many redundant parameters when the variable has many children and parents, leading to estimation that is not robust. Thus, as discussed in Chapter 1, the dimensionality of a hidden variable can have a significant effect on the complexity of the model, its performance and its representation quality. Consequently, the problem of determining the cardinality of a hidden variables is crucial both when the initial (or fixed) structure is supplied by the expert, and when a new hidden variable is introduced into the network structure, e.g., using the method of the previous chapter.

In this chapter, we propose an agglomerative, score-based approach for determining the cardinality of hidden variables. Our approach starts with the maximal number of states possibly needed, and merges states in a greedy fashion. At each iteration of the algorithm, it maintains for each training instance a hard assignment to the hidden variable. Thus, we can score the data using *complete data* scoring functions that are orders of magnitude more efficient than standard EM-based scores for incomplete data. The procedure progresses by choosing the two states whose merger will lead to the best improvement (or least decrease) in the score. These steps are repeated until all the states are merged into one state. Based on the scores of intermediate stages, we choose the cardinality of the hidden variable that corresponds to the best score. We show that networks learned from the intermediate stages are also good initial starting points for EM runs that fine-tune the parameters.

We then move on to consider networks with multiple hidden variables. As we show, we can combine multiple invocations of the single-variable procedure to learn the interactions between several hidden variable. Finally, we combine our method with the method of the previous chapter for learning new hidden variables, and show that this leads to learning models that perform better on synthetic and real-life data.

## 5.1 Learning the Cardinality of a Hidden Variable

As in Section 4.1, we motivate our approach by considering a hidden variable Cancer that is the keystone for the conditional independence assumption encoded in the network of Figure 1.1(a). In addition, we also assume that the presence of the hidden variable by itself is not sufficient: the full expressiveness of the hidden variable is also crucial for the independencies to hold. Without it, many of these independencies simply do not hold, and the marginal distribution over the remaining variables has almost no structure, resulting in an undesirable representation, as shown in Figure 1.1(c). We conjecture that this phenomena is a potential effect of constructing a network with a hidden variable of reduced cardinality

**Conjecture 5.1.1:** *Let $\mathcal{G}$ be a naive Bayes network over the variables $\mathcal{X} = \{X_1, \ldots, X_N\}, H$, where $H$ is of cardinality $K$ and is the parent of all the variables in $\mathcal{X}$. Let $L$ be the number of parameters in the network. Further require that $L$ is not greater than the number of parameters needed to represent the complete marginal distribution over $\mathcal{X}$. That is $L \leq \prod_i |Val(X_i)|$, where $|Val(X_i)|$ is the cardinality of $X_i$.*

*Then, a naive Bayes model $\mathcal{G}'$ where $H$ is replaced by $H'$ with a cardinality smaller than $K$, has less parameters than the degrees of freedom of the marginal distribution over $\mathcal{X}$ of the original model $\mathcal{G}$.*

This conjecture, if true, implies that if the cardinality of $H$ is reduced, and we want to represent the marginal distribution over $\mathcal{X}$, we will not be able to preserve all independencies in $\mathcal{G}$, similarly to the case of Proposition 4.1.1. The exception, of course, is when the cardinality of $H'$ is an over representation, in which case the number of parameters in the model is larger than the number of parameters required to represent *any* marginal distribution over $\mathcal{X}$. To prove the above conjecture, we need to show that the number of parameters in a distribution represented by the new model $P(\mathcal{X}, H') = P(H') \prod_i P(X_i \mid H')$, is smaller than the degrees of freedom in the distribution of the original model. Computing the degrees of freedom of a network is not easy, and we briefly discuss the works that touched on that seemingly simple but challenging task.

Geiger et al. [1996] introduced the notion of *effective dimensionality* of models with hidden variables: They consider the polynomial transformation between the network parameters $\Theta$ and the parameters of the true marginal distribution $P(\mathcal{X})$. For example in the naive Bayes model $P(x_1) = \sum_h \theta_h \theta_{x_1|h}$. The number of degrees of freedom of this transformation is the effective dimensionality of the network, and is equal to the rank of the Jacobian of the transformation. As they show, this rank is a constant almost everywhere in the space of parameters. Thus, by computing the rank of the Jacobian for *some* parameterization, one can numerically determine the effective dimensionality of the network. For a network with a binary hidden variable $H$ with $N$ binary children, they are further able to lower bound the rank by $2N$ which potentially leaves only one redundant parameter. While this implies our conjecture for such networks, this case is trivial from our perspective since lowering the number of states of the hidden variable will results in a useless hidden variable with a single state. Unfortunately, even for simple naive Bayes models with a cardinality greater than two, they are only able to compute the rank of the Jacobian numerically. Settimi and Smith [1998] formally characterizes the case of a single hidden variable with two children and the case of a hierarchical model where each binary hidden variable has at most three neighbors. Other works (e.g., [Geiger and Meek, 1998]) are aimed toward characterizing the differences in the space spanned by different models with hidden variables, but do not provide an analytical alternative to the numerical computation of the effective dimensionality of a model. And so, proving the conjecture formally for any non-trivial model remains a challenge. On the practical side, Kocka and Zhang [2002] suggested a method for combining several simple bounds on the effective dimensionality in order to better evaluate it. In their work, they numerically evaluated the effective dimensionality of many naive Bayes models of different cardinalities of the hidden variable as well as its children. A closer inspection of their results, shows that our conjecture holds empirically in the cases they examine. Intuitively, we also expect the conjecture to hold for more general structures: if the hidden variable is not part of an over-represented structure, we hypothesize that decreasing the number of its states will lead to deterioration of the effective representation strength of the model.

### 5.1.1 The Agglomeration Procedure

The above discussion motivates the need to determine the cardinality of a hidden variable, as it may have a significant effect on the model learned. Our goal is to address the following problem: We are given training data $\mathcal{D}$ of samples from $\mathcal{X} = \{X_1, \ldots, X_N\}$, and a network structure $\mathcal{G}$ over
$X$ and an additional variable $H$. We need to determine what cardinality of $H$ leads to the best scoring network. A straightforward way to solve this problem is as follows: We can examine all possible cardinalities of $H$ up to a certain point. For each cardinality $k$, we can apply the EM

**Algorithm 7**: Agglomeration Tree

```
Input  : $H$        // a hidden variable
         $\mathbf{MB_H}$ // the Markov blanket variables of $H$
         D        // A dataset with M instances where $H$ is unobserved
Output : An agglomeration tree

// initialization
$O_{MB} \leftarrow \{1 \ldots L\}$, an ordering of unique assignments to $\mathbf{MB_H}$ in D
for $m \leftarrow 1$ to $M$ do
    $\sigma_H$ [m] $\leftarrow O_{MB}$ $[\mathbf{MB_H}[\mathbf{m}]]$        // initial value is index of $\mathbf{MB_H}$ assignment
end
for $l \leftarrow 1$ to $L$ do
    Create Node(l)
    Node(l).Children $\leftarrow \emptyset$
end

// agglomeration
for $a \leftarrow 1$ to L-1 do
    $(i, j) \leftarrow$ BestMerge(D,H,$\sigma_H$ )
    Create Node($i \cdot j$)
    Node($ij$).Children $\leftarrow$ { Node($i$) $\cup$ Node($j$) }
    foreach $\sigma_H$ [m] == $i$ or $j$ do
        $\sigma_H$ [m] = $i \cdot j$
    end foreach
end
return last node created
```

algorithm to learn parameters for the network containing $H$ with $k$ states. Since EM might get stuck in local maxima, we should perform several EM runs from different random starting points. Given the parameters for the network, we can approximate the score of the network with $k$ states for $H$ using, say, the Cheeseman-Stutz approximation [Cheeseman et al., 1988]. At the end of the process, we return the cardinality $k$ and network parameters that received the best score.

The above approach is in common use in probabilistic clustering algorithms, e.g., [Cheeseman et al., 1988]. The central problem of this approach is its exhaustiveness. The EM algorithm is time consuming as it requires inference in the Bayesian network. For simple Naive-Bayes networks that are used in clustering, this cost is not prohibitive. However, in other network structures the cost of multiple EM runs can be high. Thus, we strive to find a method that finds the best scoring cardinality (or a good approximation of it) significantly faster. We now suggest an approach that works with hard assignments to the states of the hidden variables. This approach is motivated by *agglomerative clustering methods* (e.g., [Duda and Hart, 1973]) and *Bayesian model merging* techniques from the HMM literature [Stolcke and Omohundro, 1993].

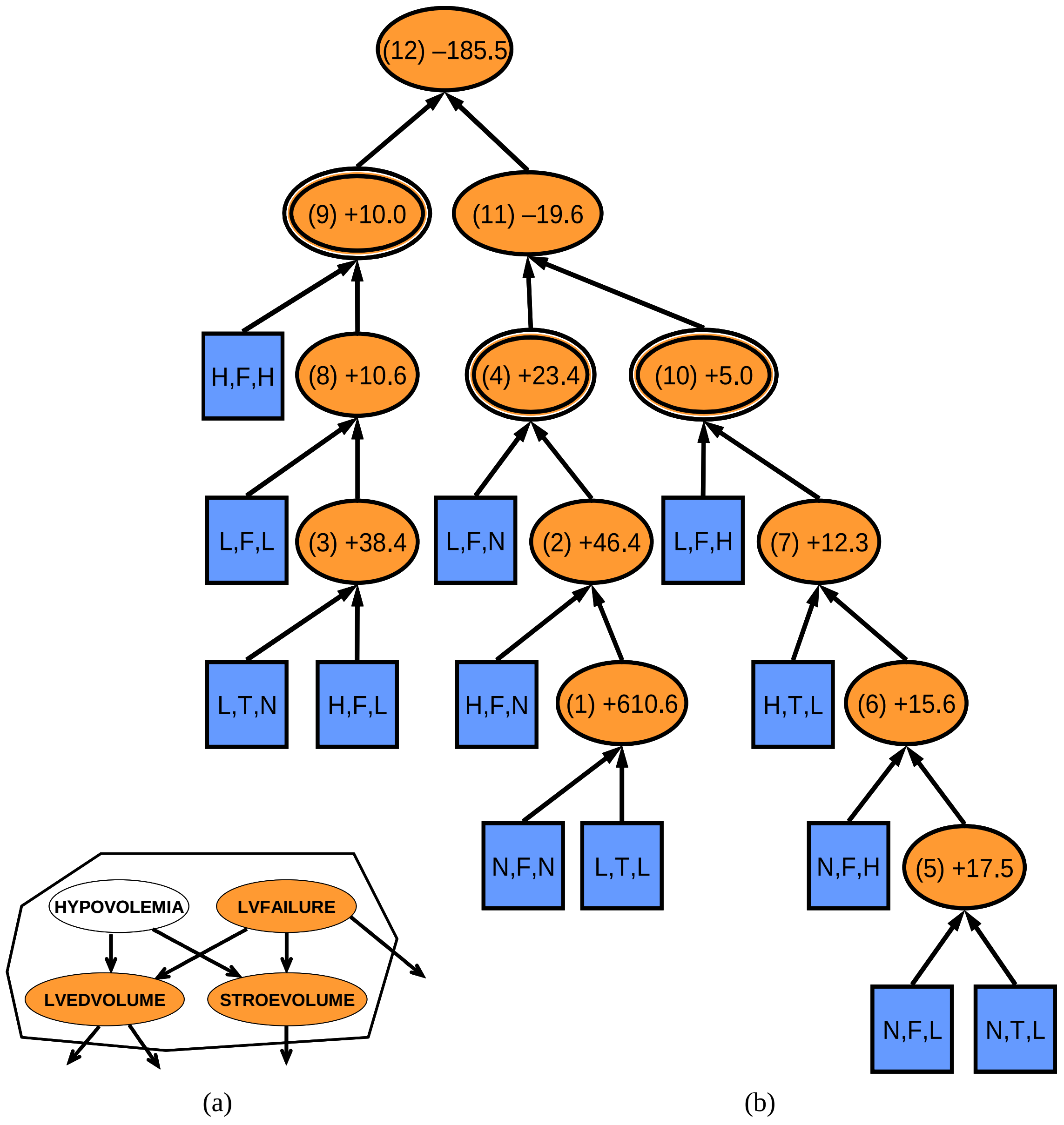

Figure 5.1: (a) fragment of the synthetic Alarm network showing the variable *HYPOVOLEMIA* and its Markov blanket. (b) Trace of the agglomeration process in a simple synthetic experiment: We sampled 1000 instances from the Alarm network, and then hid the observations of the variable *HYPOVOLEMIA* in the data. We then attempted to reconstruct its cardinality. Each leaf in the tree is annotated with the values of the variables in the Markov blanket (LVEDVOLUME,LVFAILURE and STROKEVOLUME). Circle nodes correspond to states that result from merging operations. They are numbered according to the order of the merging operations and are annotated with the change in score incurred by the merge. At each stage, the merge chosen is the one that produces the largest increase (or smallest decrease) to the score. Double bordered nodes correspond to the final cardinality chosen.

The general outline of the approach is as follows: At each iteration we maintain a hard assignment to $H$ in the training data. We initialize the algorithm with a variable $H$ that has many states (we describe the details below). We then evaluate the score of the network with respect to the dataset that is *completed* by the current assignment. Next, we *merge* two states of $H$ to form a variable with smaller cardinality, resulting in a new assignment function. In doing so, we choose the merge that leads to the best improvement (or least decrease) in the score. We repeat this process until $H$ has a single state. Finally, we return the number of states $k$ that received the highest score. The overall algorithm is summarized in Algorithm 7. Figure 5.1 shows a concrete example of the tree built during such an agglomeration process. Given the full agglomeration tree returned by the algorithm, we can easily recover the best scoring cardinality. In the specific example shown in the figure, the cardinality is three, and its states correspond to the double bordered nodes. Note that further merges of these three states lead to a decrease in the score. Next, we consider in more detail the different parts of our algorithm.

### 5.1.2 Scoring of a Merge

We start by describing how merging of states is carried out. We represent an assignment of $H$ in the $M$ instances of $\mathcal{D}$ as a mapping $\sigma_H$ from $\{1, \ldots, M\}$ to the set of values of the hidden variable $Val(H)$. That is, $\sigma_H[m]$ is the value of $H$ assigned to the $m$'th instance.

**Definition 5.1.2:** In a *merge* of two states of $i$ and $j$ of $H$

1. The value $i$ and $j$ of $H$ are replaced with a new state that we denote by $i \cdot j$ (this is in effect a new random variable).

2. A new assignment $\sigma_H(i,j)$ is created.

$$\sigma_H(i,j)[m] = \begin{cases} i \cdot j & \text{if } \sigma_H[m] = i \text{ or } \sigma_H[m] = j \\ \sigma_H[m] & \text{otherwise} \end{cases}$$

▮

Our task now is to evaluate the usefulness of a merge $\sigma_H(i,j)$. In fact, at each iteration of the algorithm we need to evaluate a quadratic number (in the number of states) of these merges, and thus efficient evaluation is crucial. Since, $\sigma_H(i,j)$ assigns a specific state of $H$ for each instance, it *completes* the training data $\mathcal{D}$. Thus, we can apply a standard complete data score function, such as the BDe score (see Section 2.3.1), to our now completed data set. Recall that when the data is complete, the BDe score can be evaluated efficiently in closed form and depends only on simple *sufficient statistics* vectors. In fact, these sufficient statistics, $S[x_i, \mathbf{pa}_i]$, count the number of occurrences of an assignment to a variable $X_i$ and its parents independently for each value of

$X_i$. This makes the BDe score *locally decomposable*. That is, when the distribution of a state changes, we only need to recompute the sufficient statistics corresponding to this state. Thus, when merging states we actually do not need to modify the training data. Instead, we simply apply the merging operation on the sufficient statistics that correspond to $H$ and its children. That is, we set $S[h_{i\cdot j}, \mathbf{pa}_H] = S[h_i, \mathbf{pa}_H] + S[h_j, \mathbf{pa}_H]$ for each assignment $\mathbf{pa}_H$ to the parents of $H$. Similarly we compute the sufficient statistics for $H$'s children and their families.

Concretely, the difference between the BDe score after and before the merge of states $i$ and $j$ is only in the terms where $H$ appears:

$$\begin{aligned}
&\text{Score}_{\text{BDe}}(\mathcal{G}_{i\cdot j} : \mathcal{D}) - \text{Score}_{\text{BDe}}(\mathcal{G}_{i,j} : \mathcal{D}) = \\
&\sum_{\mathbf{pa}_H} \left[ \log \frac{\Gamma(S^+[h_{i\cdot j}, \mathbf{pa}_H])}{\Gamma(\alpha(h_{i\cdot j}, \mathbf{pa}_H))} - \log \frac{\Gamma(S^+[h_i, \mathbf{pa}_H])}{\Gamma(\alpha(h_i, \mathbf{pa}_H))} - \log \frac{\Gamma(S^+[h_j, \mathbf{pa}_H])}{\Gamma(\alpha(h_j, \mathbf{pa}_H))} \right] + \\
&\sum_C \sum_{pa_c} \left[ \log \frac{\Gamma(\alpha(pa_c, H{=}i\cdot j))}{\Gamma(S^+[pa_c, H{=}i\cdot j])} + \sum_c \log \frac{\Gamma(S^+[c, pa_c, H{=}i\cdot j])}{\Gamma(\alpha(c, pa_c, H{=}i\cdot j))} \right. \\
&\quad - \log \frac{\Gamma(\alpha(pa_c, H{=}i))}{\Gamma(S^+[pa_c, H{=}i])} - \sum_c \log \frac{\Gamma(S^+[c, pa_c, H{=}i])}{\Gamma(\alpha(c, pa_c, H{=}i))} \\
&\quad \left. - \log \frac{\Gamma(\alpha(pa_c, H{=}j))}{\Gamma(S^+[pa_c, H{=}j])} - \sum_c \log \frac{\Gamma(S^+[c, pa_c, H{=}j])}{\Gamma(\alpha(c, pa_c, H{=}j))} \right]
\end{aligned}$$

where the first summation corresponds to the family of $H$ and its parents, and the second summation is over all $C$ that are children of $H$ and corresponds to the families of the children of $H$ and their parents. To ensure probabilistic coherence of the BDe prior, similarly to the empirical sufficient statistics, the new prior counts are $\alpha(h_{i\cdot j}) = \alpha(h_i) + \alpha(h_j)$. The counts $S^+[x] = S[x] + \alpha(x)$ correspond to *total* statistics that include both the empirical counts and the imaginary prior counts.

In addition to decomposability, the terms corresponding to the states $i$ and $j$ were already calculated in previous steps and can be cached. Thus the change in the score resulting from a merge only requires computation of the new terms that correspond to the new states $i \cdot j$, which can be computed rapidly in $O(|\mathbf{Pa}_H| + \sum_C |\mathbf{Pa}_C|)$ time. This make our overall cubic (in the number of states) algorithm tractable in practice.

### 5.1.3 Initialization

Having described the agglomeration process and how a merge is scored, we now address the important issue of how to initialize the states of $H$. Naively, we could assign a distinct state of $H$ for each sample in $\mathcal{D}$. In this case we can set $P(\mathbf{x}[m] \mid h[m]) = 1$, in which case knowing the value of $H$ will deterministically determine the values of all other variables in the sample, thus maximizing the likelihood. This may be problematic since bottom up agglomeration takes $O(S^3)$, where $S$ is the number of initial states, and is not practical even for medium size datasets. To improve on this naive approach, recall that, conditioned on the Markov blanket of $H$ ($\mathbf{MB_H}$), $H$ is independent of all other variables in the network. Thus, intuitively, we do not need more states for $H$ then there are distinct assignments to $\mathbf{MB_H}$ in $\mathcal{D}$. To formalize this intuition, we will show that if the algorithm is initialized naively as described above, then the initial merges will necessarily agglomerate states corresponding to instances with identical $\mathbf{MB_H}$. Thus, we will be able to circumvent these initial merges by simply using a single state for all of these instances.

We are interested in comparing different candidate merges at a particular stage of the algorithm to identify the optimal such merge. Since all these merges lead to the same change in terms of model complexity, we are interest in the change to the likelihood that these merges incur. (This is in contrast to the BDe model selection score we used in Section 5.1.1 to identify the overall best cardinality.) We denote by $L(\theta : \mathcal{D}, \sigma_H)$ the likelihood of the data augmented by the assignment to $H$ in the different instances defined by $\sigma_H$. We denote by $\Delta L(\theta : \mathcal{D}, \sigma_H(i,j))$ the change in likelihood resulting from the merge of states $i$ and $j$ of $H$. The following identifies the best merge at a particular point (e.g., start) of the agglomeration process:

**Proposition 5.1.3:** *Let $\mathcal{G}$ be a network over the discrete variables $\mathcal{X} = \{X_1, \ldots, X_N\}, H$. Let $\mathcal{D}$ be a set of $M$ instances, where all the variables in $\mathcal{X}$ are observed, and $H$ is never observed. Let $H$ have $K$ distinct states and $\sigma_H$ be an assignment for each instance $m$ of a value for $H$ such that $\sigma_H[m] = m$ (the value of $H$ in each instance is simply the index of that instance). Finally, let $m_1$ and $m_2$ be two instances, where the assignment to the Markov blanket variables $\mathbf{MB_H}$ of $H$ in both instances is identical.*

*Then, assuming* maximum likelihood *(ML) or* Bayesian estimation *parameters*

$$\Delta L(\theta : \mathcal{D}, \sigma_H(m_1, m_2)) \geq \Delta L(\theta : \mathcal{D}, \sigma_H(m_i, m_j)) \qquad \forall i, j \neq i$$

*That is, merging two states corresponding to two instances with identical $\mathbf{MB_H}$ values, will lead to an improvement in likelihood that is as good or better than any other possible merge of two states.*

**Proof:** For clarity we consider the case of maximum likelihood parameters. The proof for the Bayesian case is identical. Using the factorization theorem (Eq. (2.1)), we can write the log-likelihood of the data given the model (Eq. (2.2)) as

$$\ell(\theta : \mathcal{D}, \sigma_H) = \sum_{m=1}^{M} \left[ \log P(h[m] \mid \mathbf{pa}_h[m] : \theta_{H|\mathbf{Pa}_h}) + \sum_{i=1}^{N} \log P(x_i[m] \mid \mathbf{pa}_i[m] : \theta_{X_i|\mathbf{Pa}_i}) \right]$$

We note the following (using Proposition 2.2.2)

- The only terms that involve $H$ in the last summation correspond to the children of $H$.

- When we merge two states $i$ and $j$, only the likelihood of the corresponding instances changes.

- By construction of $\sigma_H$, each value of $H$ deterministically determines the rest of the variables, so that $P(c[m] \mid \mathbf{pa}_c[m], \sigma_H[m]) = 1$ for all children $C$ of $H$ and all $m$.
- By construction of $\sigma_H$, $P(h[m] \mid \mathbf{pa}_h[m]) = \frac{1}{S[\mathbf{pa}_h[m]]}$ for each $m$, where $S[\mathbf{pa}_h[m]]$ is the number of times that specific assignment appears in $\mathcal{D}$.

We now consider the difference in log-likelihood as a results of a merge of two states $i$ and $j$ in different cases:

**Case 1: The value of $\mathbf{MB_H}$ is identical in both assignments**
In this case, $P(c[m] \mid \mathbf{pa}_c[m], \sigma_H[m]) = 1$ is still true for both the $i$'th and $j$'th instance after the merge, since the value of the children in these two instances is identical. Now, $P(h[i \cdot j] \mid \mathbf{pa}_h[i]) = \frac{2}{S[\mathbf{pa}_h[i]]}$ since the state $i \cdot j$ now appears twice out of $S[\mathbf{pa}_h[i]]$ different instances with the same assignment to $\mathbf{Pa}_H$ (and similarly for the $j$'th instance). Thus, the difference in log-likelihood is:

$$\Delta\ell(\theta : \mathcal{D}) = 2\log\frac{2}{S[\mathbf{pa}_h[i]]} - 2\log\frac{1}{S[\mathbf{pa}_h[i]]} = 2\log 2 \tag{5.1}$$

where we have used the fact that $\mathbf{pa}_h[i] = \mathbf{pa}_h[j]$.

**Case 2: The value of $\mathbf{MB_H}$ is identical in both assignments, except for the value of $\mathbf{Pa}_H$**
Similarly to the previous case, the only change is in the probability of $H$ given its parents. The difference in log-likelihood is:

$$\begin{aligned}\Delta\ell(\theta : \mathcal{D}) &= 2\log\frac{2}{S[\mathbf{pa}_h[i]] + S[\mathbf{pa}_h[j]]} - \left(\log\frac{1}{S[\mathbf{pa}_h[i]]} + \log\frac{1}{S[\mathbf{pa}_h[j]]}\right) \\ &= 2\log 2 - \Big(2\log(S[\mathbf{pa}_h[i]] + S[\mathbf{pa}_h[j]]) - \log S[\mathbf{pa}_h[i]] - \log S[\mathbf{pa}_h[j]]\Big) \\ &< 2\log 2\end{aligned}$$

where the last inequality follows from properties of the $\log$ function.

**Case 3: The value of $\mathbf{MB_H}$ is different in both assignments, but is the same for $\mathbf{Pa}_H$**
In this case $P(h[i] \mid \mathbf{pa}_h[i])$ does not change for either $i$ and $j$, so that the change in likelihood is the same as in Eq. (5.1), except that the first term is multiplied by $P(c \mid \mathbf{pa}_c)$. Since that term can only be smaller or equal to 1, the change in the likelihood must be smaller than in case 1.

**Case 4: The value of both $\mathbf{Pa}_H$ and the rest of $\mathbf{MB_H}$ is different in both assignments**
The fact that the increase in likelihood in this case is smaller than in the first scenario follows immediately from the combination of cases 2 and 3, where the change resulting from $P(h[i] \mid \mathbf{pa}_h[i])$ is further decreased by $P(c \mid \mathbf{pa}_c)$. ∎

Once we merge two states with identical Markov blanket assignments, we can apply the proposition again to the new hidden variable with the revised states. By applying the above proposition repeatedly, it immediately follows that, as long as such a situation exists, the agglomeration procedure will choose to merge two states corresponding to instances where the assignment for the $\mathbf{MB_H}$ is identical. Thus, if there are $L$ distinct assignments for $\mathbf{MB_H}$ in $\mathcal{D}$, we can in fact save $M - L$ agglomeration steps: instead of starting with $M$ states for the hidden variables, we can start with $L$ distinct states, where $\sigma_H[m]$ will be equal to the state corresponding to $\mathbf{MB_H}[\mathbf{m}]$. As the agglomeration procedure is cubic in the number of initial states, the improvement we gain is quite significant as typically we have $M \gg L$.

## 5.2 Properties of the Score

It is worthwhile to consider the properties of score in order to reveal the typical behavior we can expect to see when applying our procedure. Recall that the scoring function trades-off between the likelihood of the data and the complexity of the model. When we consider plots of score vs. $H$'s cardinality, three effects that come into play.

1. When merging states of $H$, the number of parameters in the network is reduced. This gives a positive contribution to the score since the complexity of the model is lowered. The magnitude of this effect is linear in the number of states and it is larger if $H$ has more parents and children. Each additional state of $H$ creates an additional set of parameters for each of the joint assignments of $H$'s parents. Similarly, each additional states of $H$ creates an additional set parameters for each of the joint assignments of the parents of each child $C$ of $H$.
2. When $H$ has fewer states, it is easier to describe its distribution, and thus its entropy given its parents is lower. Thus, the likelihood term associated with the conditional probability distribution of $H$ given its parents $P(H \mid \mathbf{Pa}_H)$ can only improve after each merge operation. This effect rises dramatically as the number of states approaches 1 but effect only a single term in the likelihood.
3. When $H$ has many states, it can provide better prediction of its children. In fact, in our initialization point, $H$'s children are a deterministically determined by $H$'s state (since $H$ has a state for each joint assignment to the Markov blanket). When the number of states is reduced, the predictions of $H$'s children become more stochastic and their likelihood is reduced. Thus, after a merge, the likelihood of $H$'s children can only decrease. This effect is dramatic when the number of states approaches 1, and influences the terms in the likelihood corresponding to *all* of $H$'s children. For interesting hidden variables that have many children, this effect will dominate as the number of states grows smaller.

This suggests that the score will first increase due to the lowered complexity and better representation of $H$, will then slow down but still increase due to the steady decline in model complexity.

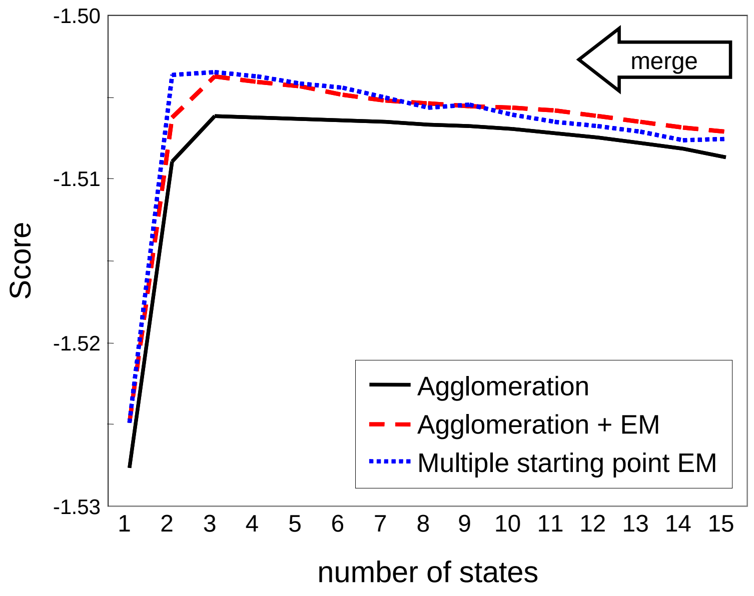

Figure 5.2: Typical behavior of the score as a function of the number of states in an agglomeration run. Shown are the BDe score of the agglomeration method, Cheeseman-Stutz (CS) score of an EM run that starts at agglomeration output, and CS score based on the best EM run from multiple starting points. The result shown are when learning the cardinality of the *STROKEVOLUME* variable in the synthetic Alarm network.

At some point, when $H$ can longer properly predict its children, the score will start to decrease. As we approach a single state and this effect is significantly larger, we expect to see a drastic decrease in the score. Figure 5.2 shows an example of the progression of the score as the number of states is diminished during the iterations of our algorithm. Also shown is the score of EM, invoked independently for each cardinality value. In Section 5.4 we analyze in more detail the relation between the methods.

## 5.3 Learning the Cardinality of Several Hidden Variables

In the previous section we examined the problem of learning the cardinality of a single hidden variable. What happens if our network contains several of these variables? We start by noting that in some cases, we can decouple the problem: If a hidden variable $H$ is d-separated (see Section 2.1.1) from all the other hidden variables given the observed variables, then we can learn it independently. More precisely, if $\mathrm{MB}_{\mathbf{H}}$ consists of observable variables only, we do not need to worry about $H$'s interactions with other hidden variables.

However, when two or more hidden variables interact with each other, the problem is more complex. A decision about the cardinality of one hidden variable can have an effect on the decisions about other hidden variables. The standard EM approach becomes more problematic here since the cardinality space grows exponentially with the number of hidden variables. Thus, we need to consider a joint and efficient decision for all the interacting variables. We now describe a simple heuristic approach that attempts to approximate the cardinality assignment for multiple variables. The ideas are motivated by a similar approach to multi-variable discretization [Friedman and Goldszmidt, 1996a].

The basic idea is to apply the agglomerative procedure of the previous section in a round-robin fashion. At each iteration, we fix the number of states, and the state assignment to instances, for all the hidden variables except for one. We apply the agglomerative algorithm with respect to this hidden variable. At the next iteration, we select another variable and repeat the procedure. It is easy to check that we should reexamine a hidden variable only after one of the variables in its Markov blanket has changed. Thus, we continue the procedure until no hidden variable has changed its cardinality and state assignment.

One crucial issue is the initialization of this procedure. We suggest to start in a network were all hidden variables have a single state. Thus, in the initial rounds of the procedure, each hidden variable will be trained with respect to its observable neighbors. Only in later iterations, the interactions between hidden variables will start to play a role. It is easy to see that each iteration of this procedure will improve the score of the completed data set specified by the state assignment functions of the hidden variables. It immediately follows that it must converge.

## 5.4 Experimental Results and Evaluation

We set out to evaluate the applicability of our approach in various learning tasks. We start by evaluating how well our algorithm determines variable cardinality in synthetic datasets where we know the cardinality of the variable we hid. We sampled instances from the Alarm network [Beinlich et al., 1989], and manually hid a variable from the dataset. We then gave our algorithm the original network and evaluated its ability to reconstruct the variable's cardinality. Figure 5.2 shows a typical behavior of the BDe score vs. the number of states. We repeated this procedure with 24 variables in the Alarm network. (We did not consider variables that were either leafs or had fewer than 3 variables in their Markov blanket.) Using training sets with 10,000 instances, the predictions of cardinality can be broken down as follows:

- For 15 variables, the agglomerative procedure recovered the original cardinality.
- For 2 variables, the estimated cardinality had one state less than the true cardinality.
- For 2 variables, the estimated cardinality had one additional state.
- For 5 variables, the agglomerative procedure suggested a complete collapse into a single state. This is equivalent to removing the variable. A close look at the probabilities in the network

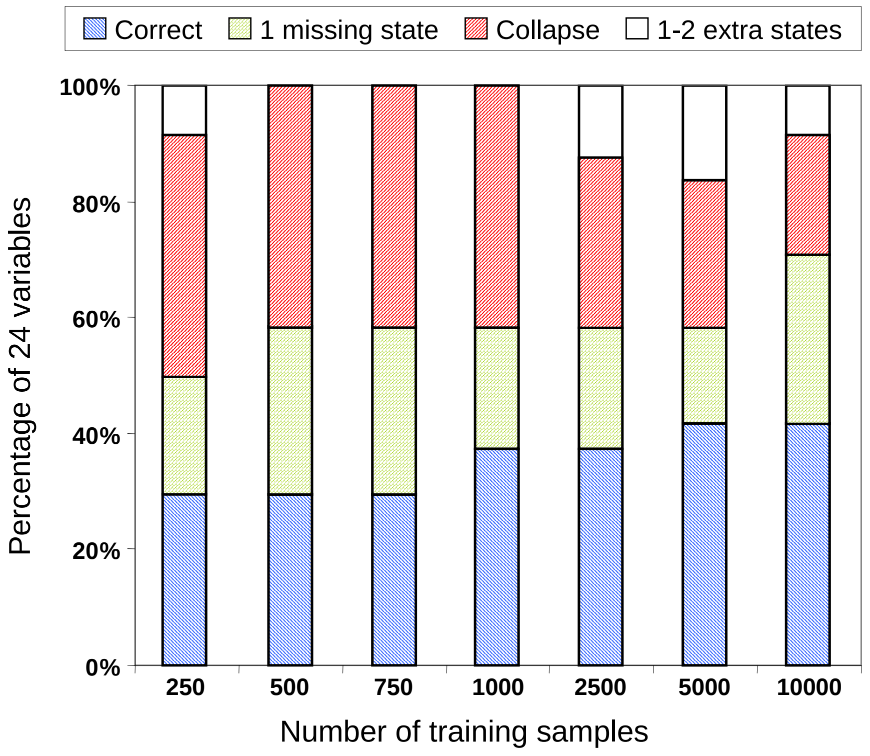

Figure 5.3: Predicted cardinality of the agglomeration method relative to the true cardinality for 24 variables in the Alarm network as a function of the number of instances. For each sample size, shown is the fraction of variables reconstructed correctly, variables with a single states missing, variables collapsed into a single states and other changes (e.g., an extra redundant state).

shows that these variables have little effect if any on their children and thus they indeed seem almost redundant. In order to confirm this claim, for each of the five variables and for each cardinality, we ran EM from multiple starting points to find the best scoring network. For all the variables, the best score was achieved when the variable was collapsed to a single state.

To summarize, for 19 of 24 of the variables we predicted the correct or near-perfect cardinality. For the other 5 variables, the characteristics of the data are two weak to reach statistically significant results. We note that since this happens also when the number of samples is large and the data mirrors the generating distribution, our algorithm was actually able to detect (near) redundancies in the generating distribution.

Next, we tested the effect of the training set size on these decisions. We applied the agglomeration method for all the above variables on training sets with different sizes. Figure 5.3 shows the deviation from the true cardinality as a function of the training set size. We see that even for small sample sizes, the prediction of the cardinality for many variables is either perfect or underestimates the cardinality by one. As the number of samples diminishes, more and more variables are collapsed into a single state. This is no surprise as weaker statistical signals do not manifest when the number of samples is small. In such a scenario, the data can indeed be represented using less states.

We then compared our approach to the standard method of evaluating different cardinalities using EM. We compared two variants of EM. In the first variant, we choose the best of multiple EM runs from 5 different random starting points. In the second variant, we ran a single EM run, starting from the parameters we learn from the completed data during the agglomeration step. Figure 5.2 compares the scores assigned to different cardinalities by the agglomerative approach and these two EM variants for one of the hidden variables. Note that for all methods the case $k = 3$, which is indeed the original cardinality, received the highest score. Also note that the two EM variants give similar scores. This suggests that the agglomerative approach finds useful starting points for EM.

In terms of running time, each EM run for each cardinality in this example takes over 250 seconds. The agglomeration procedure takes a little over one second to agglomerate the 15 initial states. One might claim that for determining cardinality, it suffices to run only few iterations of EM, which are computationally cheaper. To test this, we ran EM with an early stopping rule. This reduced the running time of EM to about 60 seconds for each run. However, this also resulted in worse estimates of the cardinality than those made by the agglomerative method. We conclude that significant time can be saved by using our method to set the number of states and then apply a single EM run for fine-tuning. This typical behavior was observed when we hid other variables in the Alarm network.

Next we wanted to evaluate the performance of our algorithm when dealing with multiple hidden variables. To do so, we constructed a synthetic network, shown in Figure 5.4(a)), with several hidden variables and generated a matching data set. Using the true structure as a starting point, we applied our agglomerative algorithm followed by Structural EM [Friedman, 1998]. As a straw-man we also ran Structural EM with binary values for all hidden variables. Because of the flexibility of Structural EM and the challenging structure of our network, we can expect that a learning algorithm that is not precise, will quickly deviate from the true structure. The resulting structure is shown in Figure 5.4. It is evident that the agglomeration method was able to effectively handle several interacting hidden variable. The cardinality was close to the original cardinality with extra states introduced to better explain stochastic relations that do not appear random in the training data. The structure learned using the binary model emphasizes the importance of determining the cardinality of hidden variables as suggested in the example of Figure 1.1. In terms of log-loss score on test data, the model learned with agglomeration was marginally superior to the original model with parameters trained. Both models were significantly better than the model learned with binary values for the hidden variables.

We now turn to the incorporation of the cardinality determining algorithm into the hidden variable discovery algorithm introduced in the previous chapter. Given a candidate network, FindHidden searches for semi-cliques and offers candidate hidden variables. We then apply our agglomeration method to this candidate network to determine the cardinality of the hidden variable. Finally,

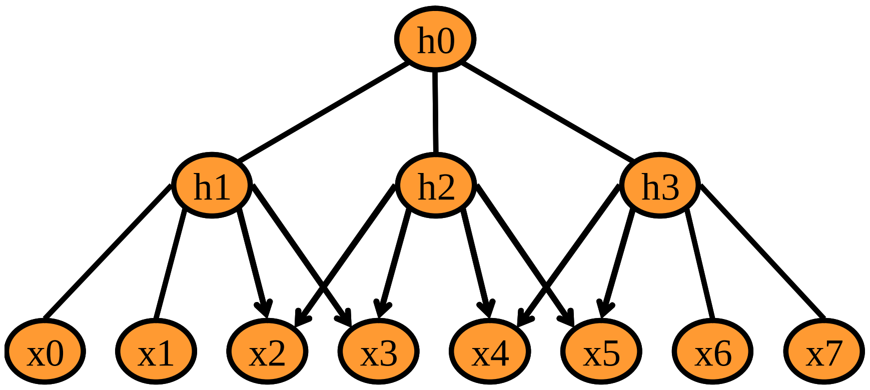

(a) original network

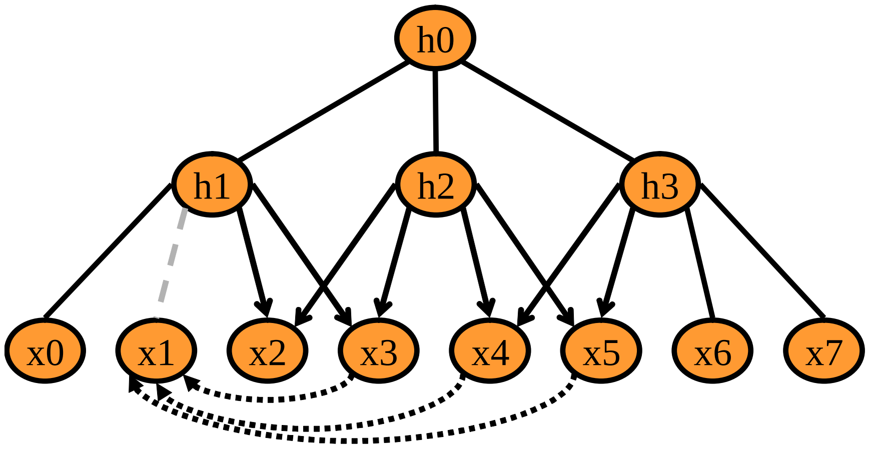

(b) learned with agglomeration

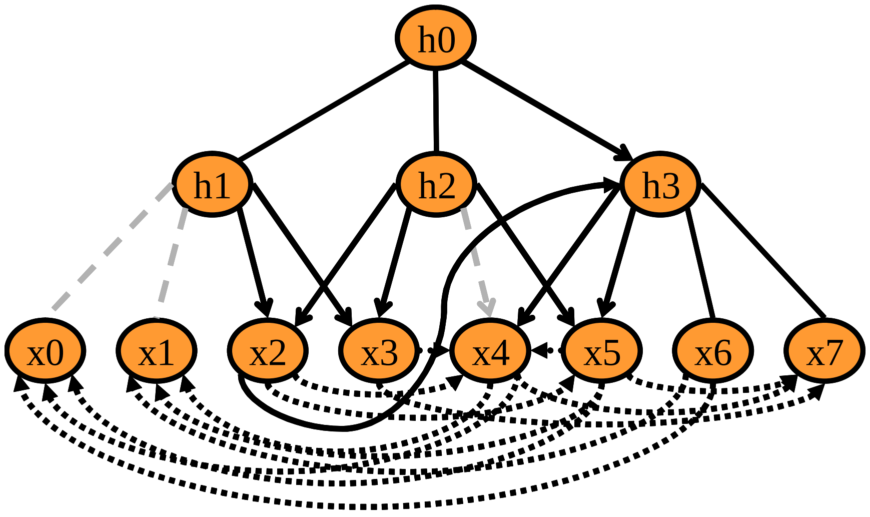

(c) learned with binary states

Figure 5.4: Performance of the agglomeration algorithm on a network with several interacting hidden variables. $h0, h1, h2$ and $h3$ have 3, 2, 4, and 3 states, respectively. The observed nodes are all binary. Edges missing with respect to the original generating structure shown in (a) are dashed. New edges that do not exist in the original model are dotted.

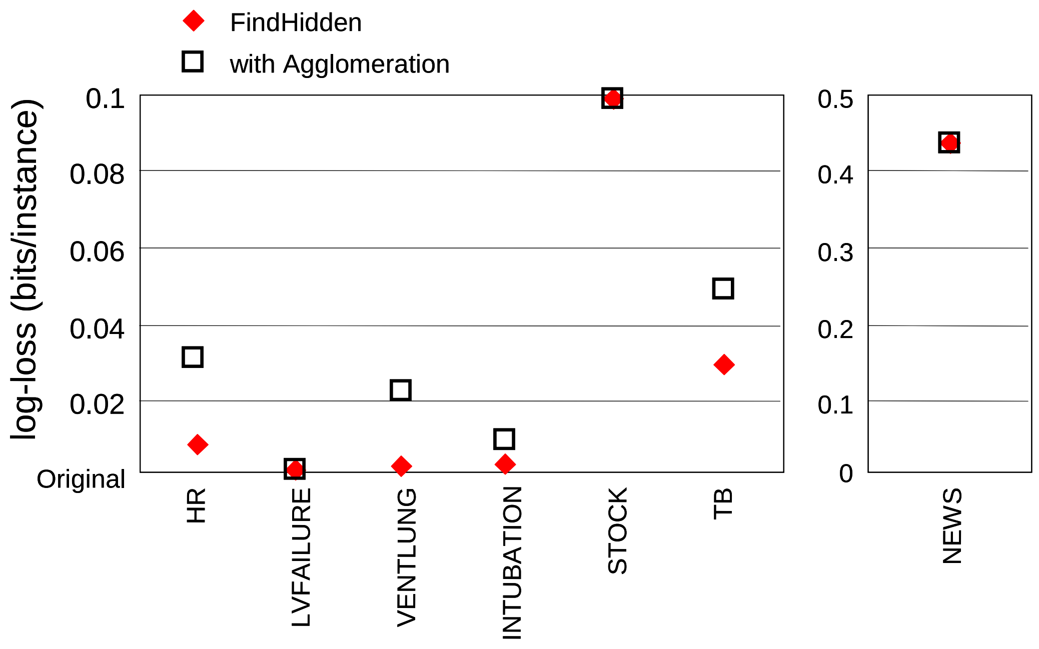

Figure 5.5: Log-loss performance on test data of the FindHidden algorithm with and without agglomeration on synthetic and real-life data. Base line is the performance of the Original network given as an input to FindHidden

we allow Structural EM to fine-tune the candidate network. We applied this to several variables in the synthetic Alarm network. We also experimented on the following real-life data sets:

- The **Stock** [Boyen et al., 1999] dataset traces the daily change of 20 major US technology stocks for several years (1516 trading days). These states were discretized to three categories: “up”, “no change”, and “down”.
- The **TB** [Behr et al., 1999] dataset records information about 2302 tuberculosis patients in the San Francisco county (courtesy of Dr. Peter Small, Stanford Medical Center). The data set contains demographic information such as gender, age, ethnic group, and medical information such as HIV status, TB infection type, and other test results.
- The **News** dataset contains messages from 20 newsgroups [Lang, 1995]. We represent each message as a vector containing one attribute for the newsgroup and attributes for each word in the vocabulary. We removed common stop words, and then sorted words based on their frequency in the whole data set. The data set used here included the group designator and the 99 most common words. We trained on 5,000 messages that were randomly selected.

Figure 5.5 shows the log-loss performance of the different learned networks on test data. The base line is the original network learned without the hidden variable and supplied as input to FindHidden. The solid diamonds mark the score of the network learned with a hidden variable but

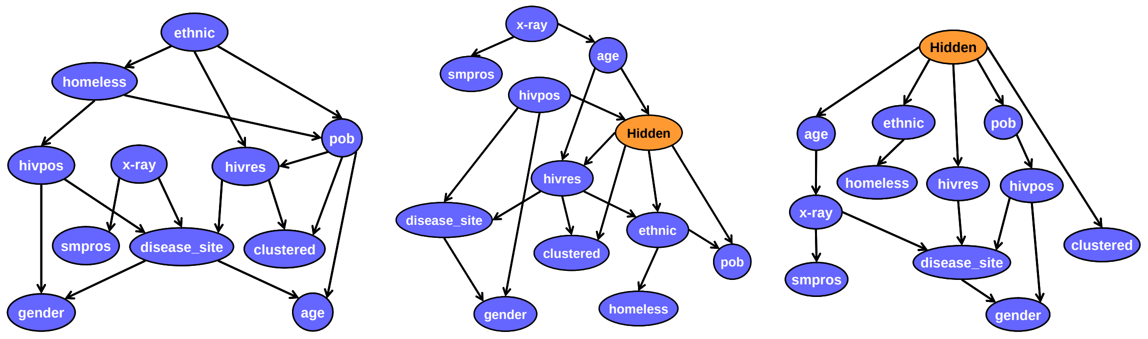

(a) Original Structure (b) After FindHidden (c) With agglomeration

Figure 5.6: Change in structure of the *TB* network due to incorporation of the cardinality determining algorithm into FindHidden. (a) Structure learned using the standard greedy algorithm and given as input to FindHidden; (b) Model learned by **FindHidden** presented in Chapter 4 with a binary hidden variable; (c) Structure learned by **FindHidden** with agglomeration, resulting in a hidden variable with 4 states.

without the agglomeration procedure (hidden variable is arbitrarily set to two states). The squares mark the score of the networks learned with a hidden variable as well as the agglomeration method. As we can see, in all cases, the network with the suggested hidden variable outperformed the original network. The network learned using agglomeration performed better than the learned network with no agglomeration (excluding cases where the agglomeration suggested exactly two states and is thus equivalent to the no agglomeration run).

It is interesting to look at the structures found by our procedure. In the previous chapter, we found an interesting model for the TB patient dataset shown here again for convenience in Figure 5.6(b). Recall that one state of this hidden variable captures two highly dominant segments of the population: older, HIV-negative, foreign-born Asians, and younger, HIV-positive, US-born blacks. Figure 5.6(c) shows the model learned when the FindHidden algorithm of Chapter 4 was combined with the agglomeration procedure. The model does not only perform better on test data (see Figure 5.5) but does indeed define 4 separate populations: US born, under 30 or over 60, HIV-negative; US born, between 30 and 60 years, with higher probability of HIV; Foreign-born, Hispanics, with some probability of HIV; and Foreign-born, Asians, HIV-negative. Clearly, the hidden variable in this case made a succinct but powerful representation plausible.

## 5.5 Discussion and Previous Work

In this chapter, we proposed an agglomerative, score-based approach for determining the cardinality of hidden variables. We compared our method to the exhaustive approach for setting the cardinality using multiple EM runs and showed its successfulness in generating competing learning models.

An important consequence is the plausibility of using the agglomeration method as a preprocessing step to a learning algorithm, potentially saving significant computational effort. The algorithm proved robust to the number of instances in the training set. It was also able to deal effectively with several interacting hidden variables. Finally, we evaluated the method as part of the hidden variable detection algorithm FindHidden on synthetic and real-life data and showed improved performance as well as more appealing structures.

The problem of determining the cardinality of a hidden variable is as old as the use of hidden variables in probabilistic models, as it arises in elementary tasks such as clustering. Consequently, numerous heuristics have been suggested to cope with problem in various clustering methods, ranging from simple K-means to hierarchical and spectral clustering (see [Milligan and Cooper, 1985] for a survey of methods). In the discussion below, we concentrate on methods that are more relevant to general Bayesian networks.

Several authors examined operations of value abstraction and refinement in Bayesian networks [Chang and Fung, 1990, Poh and Horvitz, 1993, Wellman and Liu, 1994]. These works use naive step-by-step refinement and coarsening of hidden variables and are concerned with the impact of these operations on time of inference [Wellman and Liu, 1994] and on decision making in the presence of utilities [Chang and Fung, 1990, Poh and Horvitz, 1993]. This is in contrast to our goal of learning better models in terms of predictions on unseen test data. Decisions about cardinality also appear in the context of discretization. In the case of continuous variables, the discretization of a variable can be modeled as adding a hidden variable. For example, Friedman and Goldszmidt [1996a] incorporated the discretization process into the learning of Bayesian networks by using the score as a measure of the benefit of the particular discretization.

In the context of learning hidden variables, most relevant are the works of Stolcke and Omohundro [1993, 1994], that learn cardinality in HMMs and probabilistic grammars using bottom up state-agglomeration. They start by spanning all possible states and then iteratively merge states using information vs. complexity measures. Our method is a generalization of their method for any Bayesian network structure.

Finally, Bayesian cardinality selection is addressed in graphical models via variational Bayesian learning by Attias [1999] (see more details in Chapter 8) and an ingenious Markov chain approach by Green [1995]. Although in theory applicable to any Bayesian network model, both of these methods are practical only for naive Bayes and simple hierarchical networks, and are intractable for realistic complex domains.

The Structural EM algorithm of Friedman [1998] followed by the method for learning new hidden variables presented in the previous chapter, and along with the agglomeration method presented here, are all aimed toward learning non-trivial structures with hidden variables from data. The incorporation of hidden variables is essential both in improving prediction on new examples, and to gain understanding of the underlying interactions of the domain. These form the first general approach for introducing new hidden variables into Bayesian networks. In the next chapter we present a totally different framework for learning hidden variables, where the addition of new hidden variables relies on information measures.

# Chapter 6

# Information BottleNeck EM

In Chapter 4, we presented a method for learning a hidden variable using structural signatures. One of the drawbacks of this approach is the rigid nature of the signal considered: an edge is either present or it is missing. While this is appropriate when training data is plentiful, in real-life data is often sparse and we need a softer measure that facilitates flexible decisions. In this chapter we introduce a new approach for learning the parameters and structure of Bayesian networks with hidden variables, as well as for learning new hidden variables and their cardinality using soft information-theoretic measures.

We pose the learning problem as an the optimization of a target function that includes a tradeoff between two information theoretic objectives. The first objective is to compress information about the training data. Intuitively, this is required when we want to generalize from the training data to new unseen instances. The second objective is to make the hidden variables informative about the observed attributes to ensure they preserve the *relevant* information. This objective is directly related to maximizing the likelihood of the training data. By exploring different relative weightings of these two objectives, we are able to bypass local maxima and learn better models.

Our approach builds on the *Information Bottleneck* framework of Tishby et al. [1999] and its multivariate extension [Friedman et al., 2001]. This framework provides methods for constructing a set of new variables $\mathbf{T}$ that are stochastic functions of one set of variables $\mathbf{Y}$ and at the same time provide information on another set of variables $\mathbf{X}$. The intuition is that the new variables $\mathbf{T}$ capture the relevant aspects of $\mathbf{Y}$ that are informative about $\mathbf{X}$. We show how to pose the learning problem within the multivariate Information Bottleneck framework and derive a target Lagrangian for the hidden variables. We then show that this Lagrangian is an extension of the Lagrangian formulation of EM of Neal and Hinton [1998], with an additional regularization term. By controlling the strength of this information theoretic regularization term using a *scale parameter*, we can explore a range of target functions. On the one end of the spectrum there is a trivial target where compression of the data is total and all relevant information is lost. On the other extreme is the target function of EM.

This continuum of target functions allow us to learn using a procedure motivated by the *Deterministic annealing* approach [Rose, 1998]. We start with the optimum of the trivial target function and slowly change the scale parameter while tracking the local optimum solution at each step on the way. To do so, we present an alternative view of the optimization problem in the joint space of the model parameters and the scale parameter. This provides an appealing method for scanning the range of solutions as in *homotopy continuation* [Watson, 2000].

We generalize our *Information Bottleneck Expectation Maximization* (IB-EM) framework for multiple hidden variables and any Bayesian network structure. To make learning feasible for large, real-life problems we show how to introduce variational approximation assumptions into the framework. We further show that, similarly to the case of standard parametric EM, there is a formal relation between the Information Bottleneck objective in this case and the *variational EM* functional [Jordan et al., 1998].

We then extend the approach to deal with structure learning. As we show, we can easily incorporate our method into the Structural EM framework to deal with *model selection* with hidden variables. In doing so, we perform continuation interleaved with model selection steps that change the structure and the scope of the model. On top of standard structure modification steps of adding and removing edges, we introduce two model enrichment operators that take advantage of emergent information cues during the continuation process. The first operator can adapt the cardinality of a hidden variable. Specifically, the cardinality of a hidden variable can increase during the continuation process, increasing the likelihood as long as it is beneficial to do so. The second operator introduces new hidden variables into the network structure. Intuitively, a hidden variable is introduced as a parent of a subset of nodes whose interactions are poorly explained by the current model.

We demonstrate the effectiveness of our Information Bottleneck EM algorithm in several learning scenarios. First, we learn parameters in general Bayesian networks for several challenging real-life datasets and show significant improvement in generalization performance on held-out test data. Second, we demonstrate the importance of cardinality adaptation for good generalization. We then show how our operator for enriching the network structure with new hidden variables leads to significantly superior models, for several complex real-life problems. Finally, we show that combining both structure enrichment and cardinality adaptation results in further improvement of test performance.

The chapter is organized as follows. In Section 6.1, we give a short background on the *Multivariate Information Bottleneck* of Friedman et al. [2001]. In Section 6.2, we present the basic framework of our IB-EM algorithm. In Section 6.3, we show how to combine this algorithm with continuation to bypass local maxima. In Section 6.4 we extend the framework to multiple hidden variables. In Section 6.5 we present the proofs of the fix point equation results and the technical computations involved in continuation. In Section 6.6, we demonstrate the method for parameter learning in real-life scenarios. In Section 6.7, we show how our method can be combined with the

Structural EM algorithm to learn the structure of a network with hidden variables. In Section 6.8, we take advantage of emergent structure during the continuation process, and present a method for learning the cardinality of the hidden variables. We apply this method to real-life data in Section 6.9. In Section 6.10, we address the model selection challenge of learning new hidden variables. We present experimental evaluation for several real-life problems in Section 6.11. In Section 6.12, we give a brief overview of relevant works, and in section Section 6.13 we end with a discussion and future directions.

## 6.1 Multivariate Information Bottleneck

The *Information Bottleneck* method [Tishby et al., 1999] is a general non-parametric information-theoretic clustering framework. Given a joint distribution $Q(Y, X)$ of two variables, it attempts to extract the relevant information that $Y$ contains about $X$. We can think of such information extraction as partitioning the possible values of $Y$ into coarser distinctions that are still informative about $X$. (The actual details are more complex, as we shall see shortly). For example, we might want to partition the words ($Y$) appearing in several documents in a way that is most relevant to the topics ($X$) of these documents.

To achieve this goal, we first need a relevance measure between two random variables $X$ and $Y$ with respect to some probability distribution $Q(X, Y)$. The symmetric *mutual information* measure [Cover and Thomas, 1991]

$$\boldsymbol{I}_Q(X;Y) = \sum_{x,y} Q(x,y) \log \frac{Q(x,y)}{Q(x)Q(y)}$$

is a natural choice as it measures the average number of bits needed to convey the information $X$ contains about $Y$ and vice versa. It is bounded from below by zero when the variables are independent, and attains its maximum when one variable is a deterministic function of the other.

The next step is to introduce a new variable $T$. This variable provides the *bottleneck* relation between $X$ and $Y$. In our words and documents example, we want $T$ to maintain the distinctions between words ($Y$) that provide information for determining the topic of a document ($X$). For example, the words 'music' and 'lyrics' typically occur together and are typical of the same topic, and thus the distinction between them does not contribute to the prediction of the topic. At the same time, we want $T$ to distinguish between 'music' and 'politics' as they correlate with markedly different topics. Formally, we define $T$ using a stochastic function $Q(T \mid Y)$. On the one hand we want $T$ to compress $Y$, while on the other hand we want it to preserve information that is relevant to $X$. Using the mutual information defined above, a balance between these two competing goals is

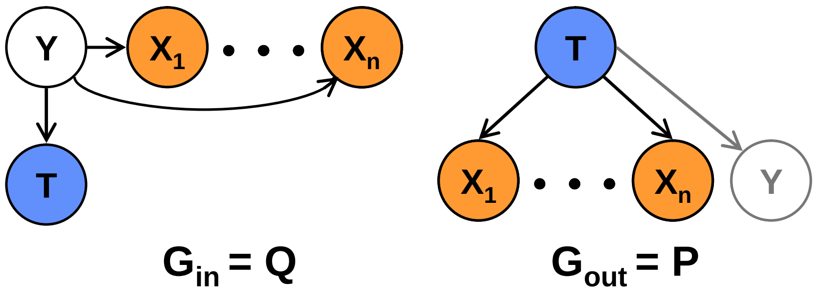

Figure 6.1: Definition of $\mathcal{G}_{in}$ and $\mathcal{G}_{out}$ for the Multivariate Information Bottleneck framework. $\mathcal{G}_{in}$ encodes the distribution $Q$ that compresses $Y$. $\mathcal{G}_{out}$ encodes the distribution $P$ that we want to approximate using $Q$.

achieved by minimization of the Lagrangian

$$\mathcal{L}[Q] = \boldsymbol{I}_Q(Y;T) - \beta \boldsymbol{I}_Q(T;X) \tag{6.1}$$

where the parameter $\beta$ controls the tradeoff. Tishby et al. [1999] show that the optimal partition for a given value of $\beta$ satisfies

$$Q(t \mid y) = \frac{Q(t)}{Z(y,\beta)} \exp\left\{-\beta \boldsymbol{D}(Q(X \mid y) \| Q(X \mid t))\right\}$$

where

$$\boldsymbol{D}(P(\mathbf{X}) \| Q(\mathbf{X})) = \sum_{\mathbf{x}} P(\mathbf{x}) \log \frac{P(\mathbf{x})}{Q(\mathbf{x})}$$

is the Kulback Leibler divergence between the distributions $P$ and $Q$ over the set of random variables $\mathbf{X}$ [Cover and Thomas, 1991]. Repeated iterations of these equations for all $t$ and $y$ converge to a (local) maximum where all equations are satisfied. Practical application of this approach for various clustering problems was demonstrated in several works (e.g., [Slonim and Tishby, 2000, 2001]).

The multivariate extension of this framework [Friedman et al., 2001] allows us to consider the interactions of multiple observed variables using several bottleneck variables. For example, we might want to compress words ($Y$) in a way that preserves information both on the topic of the document ($X_1$) and on the author of that document ($X_2$). In addition, there probably is a strong correlation between the author and the topics he writes about. Evidently, the number of possible interactions may be large, and so the framework allows us to specify the interactions we desire. These interactions are represented via two Bayesian networks. The first, called $\mathcal{G}_{in}$, represents the required compression, and the second, called $\mathcal{G}_{out}$, represents the independencies that we are striving for between the bottleneck variables and the target variables. In Figure 6.1, $\mathcal{G}_{in}$ specifies that $T$ is a stochastic function (compresses) of its parent in the graph $Y$. $\mathcal{G}_{out}$ specifies that we want

$T$ to make $Y$ and the variables $X_i$'s independent of each other.

Formally, the framework of Friedman et al. [2001], attempts to minimize the Lagrangian

$$\mathcal{L}^{(1)}[\mathcal{G}_{in}, Gout] = \mathcal{I}^{\mathcal{G}_{in}} - \beta \mathcal{I}^{\mathcal{G}_{out}}$$

where

$$\mathcal{I}^{\mathcal{G}} = \sum_i \boldsymbol{I}(X_i; \mathbf{Pa}_i^{\mathcal{G}})$$

and the information is computed with respect to the probability distribution represented by the network $\mathcal{G}$. This objective is a direct generalization of Eq. (6.1), and as before, tractable self-consistent equations characterize the optimal partitioning. Note that, as in the basic information bottleneck formulation, the two objective of the above Lagrangian are competing. On the one hand we want to compress the information between all bottleneck variables $\mathbf{T}$ and their parents in $\mathcal{G}_{in}$. On the other hand we want to preserve, or maximize, the information between the variables and their parents in $\mathcal{G}_{out}$.

Friedman et al. [2001] also present an analogous variational principal that will be useful in our framework. Briefly, the problem is reformulated as a tradeoff between compression of mutual information in $\mathcal{G}_{in}$ so that the bottleneck variable(s) $\mathbf{T}$ help us describe a joint distribution that follows that form of a target Bayesian network $\mathcal{G}_{out}$. Formally, they attempt to minimize the following objective function

$$\mathcal{L}^{(2)}[Q, P] = \boldsymbol{I}_Q(Y; T) + \gamma \boldsymbol{D}(Q(Y, T, \mathbf{X}) \| P(Y, T, \mathbf{X})) \tag{6.2}$$

where $Q$ and $P$ are joint probabilities that can be represented by the networks of $\mathcal{G}_{in}$ and $\mathcal{G}_{out}$, respectively. The two principals are analogous under the transformation $\beta = \frac{\gamma}{1+\gamma}$ and assuming $\mathcal{I}^{Gin} = \boldsymbol{I}_Q(Y; T)$. See Friedman et al. [2001] for more details of the relation between the two principals.

The minimization of the above Lagrangian is over possible parameterizations of $Q(T \mid Y)$ (the marginal $Q(Y, \mathbf{X})$ is given and fixed) and over possible parameterizations of $P(Y, T, \mathbf{X})$ that can be represented by $\mathcal{G}_{out}$. In other words, we want to compress $Y$ in such a way that the distribution defined by $\mathcal{G}_{in}$ is as close as possible to desired distribution of $\mathcal{G}_{out}$. The analogous principal gives us a new view on why these two objectives are conflicting: Consider a distribution that is consistent with $\mathcal{G}_{in}$ so that $T$ is independent of $X$ given $Y$. On the other hand, a distribution consistent with a specific choice of $\mathcal{G}_{out}$ may require that $X$ is independent of $Y$ given $T$. Constructing a distribution where both of these requirements actually hold is not useful, may results in $T$ that is equal to either $X$ or $Y$, making this bottleneck variable redundant.

The scale parameter $\gamma$ balances the above two factors. When $\gamma$ is zero we are only interested in compressing the variable $Y$ and we resort to the trivial solution of a single cluster (or an equivalent parameterization). When $\gamma$ is high we concentrate on choosing $Q(T \mid Y)$ that is close to a distribution satisfying the independencies encoded by $\mathcal{G}_{out}$. Returning to our word-document example. We might be willing to forgo the distinction between 'football' and 'baseball' in which case we would set $\gamma$ to a relatively low value. On the other hand, we might even want to make a minute distinction between 'Pentium' and 'Celeron' in which case we would set $\gamma$ to a high value. Obviously, there is no single correct value of $\gamma$ but rather a range of possible tradeoffs. Accordingly, several approaches were devised to explore the spectrum of solutions as $\gamma$ varies. These include Deterministic annealing like approaches that start with small value of $\gamma$ and progressively increase it [Friedman et al., 2001], as well as agglomerative approaches that start with a highly refined solution and gradually compress it [Slonim and Tishby, 2000, 2001, Slonim et al., 2002].

## 6.2 Information Bottleneck Expectation Maximization

The main focus of the Multivariate Information Bottleneck (see is on distribution $Q(T \mid Y)$ that is a local maxima solution of the Lagrangian This distribution can be thought of as a soft clustering of the original data. Our emphasis in here is somewhat different. Given a dataset $\mathcal{D} = \{\mathbf{x}[1], \ldots, \mathbf{x}[M]\}$ over the observed variables $\mathbf{X}$, we are interested in learning a better generative model describing the distribution of the observed attributes $\mathbf{X}$. That is, we want to give high probability to new data instances from the same source. In the learned network, the hidden variables will serve to summarize some part of the data while retaining the relevant information on (some) of the observed variables $\mathbf{X}$.

We start by extending the multivariate Information Bottleneck framework for the task of generalization where, in addition to the task of clustering, we are also interested in learning the generative model $P$. We emphasize that this is a conceptually different task. In particular, the common view of the Information Bottleneck framework is as a non-parametric information-theoretic method for clustering (the obvious exception is the work of Slonim and Weiss [2002] mentioned below). In generative learning, on the other hand, we are interested in modeling the distribution. That is, we are ultimately interested in *parameterizing* a specific model so that our generalization prediction on unseen future instances is improved. We start by considering this task for the case of a single hidden variable $T$ and then, in Section 6.4, extend the framework to several hidden variables.

### 6.2.1 The Information Bottleneck EM Lagrangian

If we were only interested in the *training* data and the cardinality of the hidden variable allows it, each state of the hidden variable would have been assigned to a different instance. Consider, for example, a variable $T$ with $|T|$ states that defines a soft clustering on the specific identity of words ($Y$) appearing in documents while preserving the information relevant to the topic ($X$) of these documents. Now suppose we are given a set of instances $\mathcal{D} = \{word[i], topic[i]\}$ where $i$ goes from

1 to $M$, the number of instances. If $|T| = M$ then we could simply deterministically set $Q(T = i \mid word[i]) = 1$ and then predict $topic[i]$ perfectly. While this model achieves perfect training performance, it will clearly have no generalization abilities. Since we are also interested in unknown future samples, we intuitively require that the learned model "forget" the specifics of the training examples. However, in doing so we will also deteriorate the (previously deterministic) prediction of the observed variables. Thus, there is a tradeoff between the compression of the identity of specific instances and the preservation of the information relevant to the observed variables.

We now formalize this idea for the task of learning a generative model over the variables $\mathbf{X}$ and the hidden variable $T$. We define an additional variable $Y$ to be the instance identity in the training data $\mathcal{D}$. That is, $Y$ takes values in $\{1, \ldots, M\}$ and $Y[m] = m$. We define $Q(Y, \mathbf{X})$ to be the empirical distribution of the variables $\mathbf{X}$ in the data, augmented with the distribution of the new variable $Y$. For each instance $y$, $\mathbf{x}[y]$ are the values $\mathbf{X}$ take in the specific instance. We now apply the Information Bottleneck framework with the graph $\mathcal{G}_{in}$ of Figure 6.1. The choice of the graph $\mathcal{G}_{out}$ depends on the network model that we want to learn. We take it to be the target Bayesian network, augmented by the additional variable $Y$, where we set $T$ as $Y$'s parent. For simplicity, we consider as a running example the simple clustering model of $\mathcal{G}_{out}$ where $T$ is the parent of $X_1, \ldots, X_n$. In practice, and as we show in Section 6.6 any choice of $\mathcal{G}_{out}$ can be used. We now want to optimize the Bottleneck objective as defined by these two networks. This will attempt to define a conditional probability $Q(T \mid Y)$ so that $Q(T, Y, \mathbf{X}) = Q(T \mid Y)Q(Y, \mathbf{X})$ can be approximated by a distribution that factorizes according to $\mathcal{G}_{out}$. This construction will aim to find $T$ that captures the relevant information the instance identity has about the observed attributes. The following proposition concretely defines the objective function for the particular choice of $\mathcal{G}_{in}$ and $\mathcal{G}_{out}$ we are dealing with.

**Proposition 6.2.1:**
*Let*

1. *$Y$ be the instance identity as defined above;*

2. *$\mathcal{G}_{in}$ be a Bayesian network structure such that such that $T$ is independent of $\mathbf{X}$ given $Y$; and*

3. *$\mathcal{G}_{out}$ be a Bayesian network structure such that $Y$ is a leaf with $T$ as its only parent.*

*Then, minimizing the Information Bottleneck objective function in Eq. (6.2) is equivalent to minimizing the Lagrangian*

$$\mathcal{L}_{EM} = \boldsymbol{I}_Q(T;Y) - \gamma \left(\boldsymbol{E}_Q[\log P(\mathbf{X}, T)] - \boldsymbol{E}_Q[\log Q(T)]\right)$$

*as a function of $Q(T \mid Y)$ and $P(\mathbf{X}, T)$.*

Note that once the above conditions are satisfied, we can still arbitrarily choose the structure of $\mathcal{G}_{out}$, which encodes independencies of the distribution $P$ we ultimately wish to learn.

**Proof:** Using the chain rule and the fact that $Y$ and $X$ are independent given $T$ in $\mathcal{G}_{out}$), we can write $P(Y, \mathbf{X}, T) = P(Y \mid T)P(\mathbf{X}, T)$. Similarly, using the chain rule and the fact that $X$ and $T$ are independent given $Y$ in $\mathcal{G}_{in}$, we can write $Q(Y, \mathbf{X}, T) = Q(Y \mid T)Q(T)Q(\mathbf{X} \mid Y)$. Thus,

$$\begin{aligned}
\boldsymbol{D}(Q(Y, \mathbf{X}, T)\|P(Y, \mathbf{X}, T)) &= \boldsymbol{E}_Q\left[\log \frac{Q(Y \mid T)Q(T)Q(\mathbf{X} \mid Y)}{P(Y \mid T)P(\mathbf{X}, T)}\right] \\
&= \boldsymbol{D}(Q(Y \mid T)\|P(Y \mid T)) \\
&\quad + \boldsymbol{E}_Q[\log Q(\mathbf{X} \mid Y)] \\
&\quad + \boldsymbol{E}_Q[\log Q(T)] \\
&\quad - \boldsymbol{E}_Q[\log P(\mathbf{X}, T)]
\end{aligned}$$

By setting $P(Y \mid T) = Q(Y \mid T)$, the first term reaches zero, its minimal value. The second term is a constant since we cannot change the input distribution $Q(\mathbf{X} \mid Y)$. Thus, we need to minimize the last two terms and the result follows immediately. ▮

An immediate question is how this target function relates to standard maximum likelihood learning. To explore the connection, we use a formulation of EM introduced by Neal and Hinton [1998]. Although EM is usually thought of in terms of changing the parameters of the target function $P$, Neal and Hinton show how to view it as a dual optimization of $P$ and an auxiliary distribution $Q$. This auxiliary distribution replaces the given empirical distribution $Q(\mathbf{X})$ with a completed empirical distribution $Q(\mathbf{X}, T)$. Using our notation in the above discussion, we can write the functional defined by Neal and Hinton as

$$\mathcal{F}[Q, P] = \boldsymbol{E}_Q[\log P(\mathbf{X}, T)] + \boldsymbol{H}_Q(T \mid Y) \tag{6.3}$$

where $\boldsymbol{H}_Q(T \mid Y) = \boldsymbol{E}_Q[-\log Q(T \mid Y)]$, and $Q(\mathbf{X}, Y)$ is fixed to be the observed empirical distribution.

**Theorem 6.2.2:** [Neal and Hinton, 1998] *If $(Q^*, P^*)$ is a stationary point of $\mathcal{F}$, then $P^*$ is a stationary point of the log-likelihood function $\boldsymbol{E}_Q[\log P(\mathbf{X})]$.*

Moreover, Neal and Hinton show that an EM iteration corresponds to maximizing $\mathcal{F}[Q, P]$ with respect to $Q(T \mid Y)$ while holding $P$ fixed, and then maximizing $\mathcal{F}[Q, P]$ with respect to $P$ while holding $Q(T \mid Y)$ fixed. The form of $\mathcal{F}[Q, P]$ is quite similar to the IB-EM Lagrangian, and indeed we can relate the two.

**Theorem 6.2.3:** $\mathcal{L}_{EM} = (1 - \gamma)\boldsymbol{I}_Q(T; Y) - \gamma\mathcal{F}[Q, P]$

**Proof:** Plugging the identity $\boldsymbol{H}_Q(T \mid Y) = -\boldsymbol{E}_Q[\log Q(T)] - \boldsymbol{I}_Q(T;Y)$ into the EM functional we can write

$$\mathcal{F}[Q,P] = \boldsymbol{E}_Q[\log P(\mathbf{X},T)] - \boldsymbol{E}_Q[\log Q(T)] - \boldsymbol{I}_Q(T;Y)$$

If we now multiply this by $\gamma$, and re-arrange terms, we get the form of Proposition 6.2.1. ▮

As a consequence, *minimizing* the IB-EM Lagrangian is equivalent to *maximizing* the EM functional combined with an information theoretic regularization term. When $\gamma = 1$, the solutions of the Lagrangian and the EM functional coincide and finding a local minimum of $\mathcal{L}_{EM}$ is equivalent to finding a local maximum of the likelihood function. Slonim and Weiss [2002] provide a similar result for the specific case where the generative model is a mixture model of a univariate $X$. Their formulation is different than ours in several subtle details that do not allow a direct relation between the two methods. Nonetheless, both Slonim and Weiss [2002] and Theorem 6.2.3 show that for a particular value of $\gamma$, the information bottleneck Lagrangian coincides with the likelihood objective of EM. The main difference between the two results is the choice of generative models, in our case general multi-variate Bayesian networks, and in the case of Slonim and Weiss [2002], univariate mixture models.

### 6.2.2 The Information Bottleneck EM Algorithm

Using the above results, we can now describe the *Information Bottleneck EM* algorithm given a specific value of $\gamma$. The algorithm can be described similarly to the EM iterations of Neal and Hinton [1998].

- **E-step**: Maximize $-\mathcal{L}_{EM}$ by varying $Q(T \mid Y)$ while holding $P$ fixed.
- **M-step**: Maximize $-\mathcal{L}_{EM}$ by varying $P$ while holding $Q$ fixed.

Note that the algorithm is formulated in terms of maximizing $-\mathcal{L}_{EM}$ rather than minimizing $\mathcal{L}_{EM}$ to enhance the relation between the Lagrangian and the EM objective.

The M-Step is essentially the standard maximum likelihood optimization of Bayesian networks. To see that, note that the only term that involves $P$ is $\boldsymbol{E}_Q[\log P(\mathbf{X},T)]$. This term has the form of a log-likelihood function, where $Q$ plays the role of the empirical distribution. Since the distribution is over all the variables, we can use sufficient statistics of $P$ for efficient estimates, just as in the case of complete data. Thus, the $M$ step consists of computing expected sufficient statistics given $Q$, and then using a closed form formula for choosing the parameters of $P$.

The E-step is a bit more involved. We need to maximize with respect to $Q(T \mid Y)$. To do this we use the following two results that are variants of Theorem 7.1 and Theorem 8.1 of Friedman et al. [2001] and proved using similar techniques (see Appendix 6.5.1 for the full proof).

**Proposition 6.2.4:** *Let $\mathcal{L}_{EM}$ be defined via $\mathcal{G}_{in}$ and $\mathcal{G}_{out}$ as in Proposition 6.2.1. $Q(T \mid Y)$ is a stationary point of $\mathcal{L}_{EM}$ with respect to a fixed choice of $P$ if and only if for all values $t$ and $y$ of $T$ and $Y$, respectively,*

$$Q(t \mid y) = \frac{1}{Z(y,\gamma)} Q(t)^{1-\gamma} P(\mathbf{x}[y], t])^{\gamma} \tag{6.4}$$

*where $Z(y,\gamma)$ is a normalizing constant:*

$$Z(y,\gamma) = \sum_{t'} Q(t')^{1-\gamma} P(\mathbf{x}[y], t'])^{\gamma}$$

Note that, as can be expected from Theorem 6.2.3, when $\gamma = 1$ the update equation reduces to $Q(t \mid y) \propto P(\mathbf{x}[y], t)$ which is equivalent to the standard EM update equation.

**Proposition 6.2.5:** *A stationary point of $\mathcal{L}_{EM}$ is achieved by iteratively applying the self-consistent equations of Proposition 6.2.4.*

Combining this result with the result of Neal and Hinton that show that optimization of $P$ increases $F(P,Q)$, we conclude that both the E-step and the M-step increase $-\mathcal{L}_{EM}$ until we reach a stationary point. As in standard EM, in most cases the stationary convergence point reached by applying these self-consistent equations will be a local maximum of $-\mathcal{L}_{EM}$, or a local minimum of $\mathcal{L}_{EM}$.

## 6.3 Bypassing Local Maxima using Continuation

As discussed in the previous section, the parameter $\gamma$ balances between compression of the data and the fit of parameters to $\mathcal{G}_{out}$. When $\gamma$ is close to $0$, our only objective is compressing the data and the effective dimensionality of $T$ will be $1$, leading to a trivial solution (or an equivalent parameterization). At larger values of $\gamma$ we pay more and more attention to the distribution of $\mathcal{G}_{out}$, and we can expect additional states of $T$ to be utilized. Ultimately, we can expect each sample to be assigned to a different cluster (if the dimensionality of $T$ allows it), in which case there is no compression of $Y$ and the information about the $X$s is fully preserved. Theorem 6.2.3 also tells us that at the limit of $\gamma = 1$ our solution will actually converge to one of the standard EM solutions. In this section we show how to utilize the inherent tradeoff determined by $\gamma$ to bypass local maxima towards a better solution at $\gamma = 1$.

Naively, we could allow a large cardinality for the hidden variable, set $\gamma$ to a high value and find the solution of the bottleneck problem. There are several drawbacks to this approach. First, we will typically converge to a sub-optimal solution for the given cardinality and $\gamma$, all the more so for $\gamma = 1$ where there are many such maxima. Second, we often do not know the cardinality that should be assigned to the hidden variable. If we use a cardinality for $T$ that is too large, learning will be less robust and might become intractable. If $T$ has too low a dimensionality, we will not

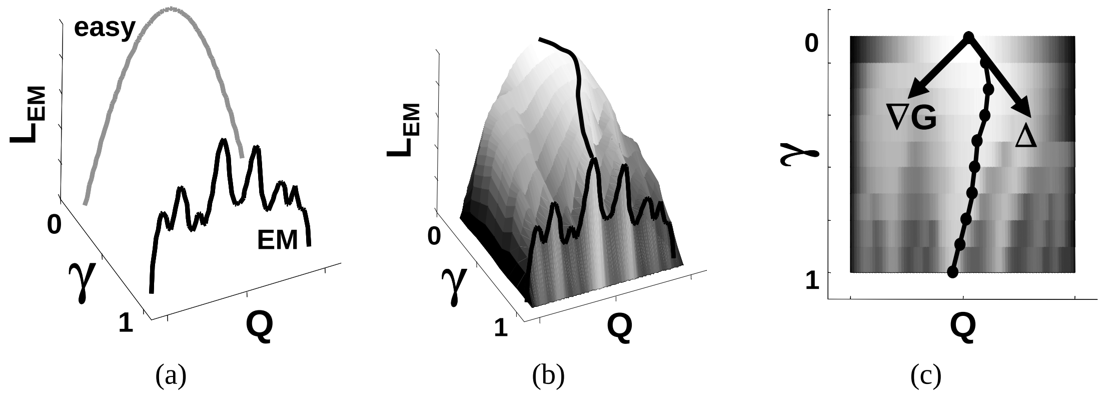

Figure 6.2: Synthetic illustration of the continuation process. (a) shows the easy likelihood function at $\gamma = 0$ and the complex EM function at $\gamma = 1$. (b) spans the full range of functions and marks the desired path for following the maximum. (c) demonstrates a single step in the continuation process. The gradient $\nabla_{Q,\gamma} G$ is computed and then the orthogonal direction is taken.

fully utilize the potential of the hidden variable. We would like to somehow identify the beneficial number of clusters without having to simply try many options.

To cope with this task, we adopt the *Deterministic annealing* strategy [Rose, 1998]. In this strategy, we start with $\gamma = 0$ where a single cluster solution is optimal and compression is total. We then progress toward higher values of $\gamma$. This gradually introduces additional structure into the learned model. Intuitively, the algorithm starts at a place where a single, easy to compute solution exists, and tracks it through various stages of progressively complex solutions hopefully bypassing local maxima by staying close to the optimal solution at each value of $\gamma$. There are several ways of executing this general strategy. The common approach is simply to increase $\gamma$ in fixed steps, and after each increment apply the iterative algorithm to re-attain a (local) maxima with the new value of $\gamma$. On the problems we examine in Section 6.6, this naive approach did not prove successful.

Instead, we use a more refined approach that utilizes *continuation methods* for executing the annealing strategy. This approach automatically tunes the magnitude of changes in the value of $\gamma$, and also tracks the solution from one iteration to the next. To perform continuation, we view the optimization problem in the joint space of the parameters and $\gamma$. In this space we want to follow a smooth path from the trivial solution at $\gamma = 0$ to a solution at $\gamma = 1$. Furthermore, we would like this path to follow a local maximum of $\mathcal{L}_{EM}$. As was shown above, this is equivalent to requiring that the fixed point equations hold at all points along the path. Continuation theory [Watson, 2000] guarantees that, excluding degenerate cases, such a path, free of discontinuities, indeed exists. Figure 6.2 shows a synthetic illustration of the setup. (a) shows the likelihood function of the two extremes of the easy solution at $\gamma = 0$ and the EM function at $\gamma = 1$ in the joint $(\gamma, Q)$-space. (b) shows the range of solutions between these extremes and marks the desired path we would like to follow.

We start by characterizing such paths. Note that once we fix the parameters $Q(T \mid Y)$, the M-step maximization of the parameters in $P$ is fully determined as a function of $Q$. Thus, we take $Q(T \mid Y)$ and $\gamma$ as the only free parameters in our problem. As we have shown in Proposition 6.2.4, when the gradient of the Lagrangian is zero, Eq. (6.4) holds for each value of $t$ and $y$. Thus, we want to consider paths where all of these equations hold. Rearranging terms and taking a log of Eq. (6.4) we define

$$G_{t,y}(Q,\gamma) = -\log Q(t \mid y) + (1-\gamma)\log Q(t) + \gamma \log P(\mathbf{x}[y], y) - \log Z(y,\gamma) \tag{6.5}$$

Clearly, $G_{t,y}(Q,\gamma) = 0$ exactly when Eq. (6.4) holds for all $t$ and $y$. Our goal is then to follow an equi-potential path where all $G_{t,y}(Q,\gamma)$ functions are zero starting from some small value of $\gamma$ up to the desired EM solution at $\gamma = 1$.

Suppose we are at a point $(Q_0, \gamma_0)$, where $G_{t,y}(Q_0,\gamma_0) = 0$ for all $t$ and $y$. We want to move in a direction $\Delta = (dQ, d\gamma)$ so that $(Q_0 + dQ, \gamma_0 + d\gamma)$ also satisfies the fixed point equations. To do so, we want to find a direction $\Delta$, so that

$$\forall t, y, \;\; \nabla_{Q,\gamma} G_{t,y}(Q_0,\gamma_0) \cdot \Delta = 0 \tag{6.6}$$

where $\nabla_{Q,\gamma} G_{t,y}(Q_0,\gamma_0)$ is the gradient of $G_{t,y}(Q_0,\gamma_0)$ with respect to the parameters $Q$ and $\gamma$. Computing these derivatives with respect to each of the parameters results in a derivative matrix

$$H_{t,y}(Q,\gamma) = \left( \begin{array}{c|c} \frac{\partial G_{t,y}(Q,\gamma))}{\partial Q(t|y)} & \frac{\partial G_{t,y}(Q,\gamma)}{\partial \gamma} \end{array} \right) \tag{6.7}$$

Rows of the matrix correspond to each of the $L = |T| \times |Y|$ functions of Eq. (6.5), corresponding to joint combinations of the $|T|$ states of the bottleneck variable $T$ and the $|Y| = M$ number of possible values of the instance identity variable $Y$. The columns correspond to the $L$ parameters of $Q$ as well as $\gamma$. The entries correspond to the partial derivative of the function associated with the row with respect to the parameter associated with the column.

To find a direction $\Delta$ that satisfies Eq. (6.6) we need to satisfy the matrix equation

$$H_{t,y}(Q_0,\gamma_0)\Delta = 0 \tag{6.8}$$

In other words, we are trying to find a vector in the null-space of $H_{t,y}(Q_0,\gamma_0)(Q_0,\gamma_0)$. The matrix $H$ is an $L \times (L+1)$ matrix and its null-space is defined by the intersection of $L$ tangent planes, and is of dimension $L + 1 - \text{Rank}(H_{t,y}(Q,\gamma))$. Numerically, excluding measure zero cases [Watson, 2000], we expect $\text{Rank}(H_{t,y}(Q_0,\gamma_0))$ to be full, *i.e.*, $L$. Thus, a unique line that (up to scaling) defines the null space, and we can choose any vector along it. To follow the path to our target objective at $\gamma = 1$ we choose the direction that always increases $\gamma$ (we discuss the choice of the length of this vector below). Returning to Figure 6.2, (c) illustrates this process. Shown is joint $(\gamma, Q)$-space with the grey-level denoting the value of the likelihood function. At each point in the learning process the gradient of $G$ is evaluated and the orthogonal direction is taken to follow the desired path.

Finding this direction, however, can be costly. Notice that $H_{t,y}(Q,\gamma)$ is of size $L(L+1)$. This number is quadratic in the training set size, and full computation of the matrix is impractical even for small datasets. Instead, we resort to approximating $H_{t,y}(Q,\gamma)$ by a matrix that contains only the diagonal entries $\frac{\partial G_{t,y}(Q,\gamma)}{\partial Q(t|y)}$ and the last column $\frac{\partial G_{t,y}(Q,\gamma)}{\partial \gamma}$. While we cannot bound the extent of this diagonal approximation, we note that the diagonal terms are also the most significant ones and many off diagonal terms are zero. Once we make the approximation, we can solve Eq. (6.8) in time linear in $L$. (See Appendix 6.5.3 for a full development of $H$ and the computation of the orthogonal direction. )

Note that once we find a vector $\Delta$ that satisfies Eq. (6.8), we still need to decide on its length, or the size of the step we want to take in that direction. There are various standard approaches, such as normalizing the direction vector to a predetermined size. However, in our problem, we have a natural measure of progress that stems from the tradeoff defined by the target Lagrangian $\mathcal{L}_{EM}$ , where $\boldsymbol{I}(T;Y)$ increases when $T$ captures more and more information about the samples during the annealing procedure. That is, the “interesting” steps in the learning process occur when $\boldsymbol{I}(T;Y)$ grows. These are exactly the points where the balance between the two terms in the Lagrangian changes and the second term grows sufficiently to allow the first term to increase $\boldsymbol{I}(T;Y)$. Using $\boldsymbol{I}(T;Y)$ to gauge the progress of the annealing procedure is appealing since it is a non-parametric measure that does not involve the form of the particular distribution of interest $P$. In addition, in all runs $\boldsymbol{I}(T;Y)$ starts at $0$, and is upper-bounded by the log of the cardinality of $T$ and we are thus given a scale of progress.

With this intuition at hand, we want to normalize the step size by the expected change in $\boldsymbol{I}(T;Y)$. That is, we calibrate our progress with respect to the *actual* amount of regularization applied at the current value of $\gamma$. At regions where $\boldsymbol{I}(T;Y)$ is not sensitive to changes in the parameters, we can proceed rapidly. On the other hand, if small changes in the parameters result in significant changes of $\boldsymbol{I}(T;Y)$, then we want to carefully track the solution. Figure 6.3 illustrates the difference between using a predetermined step of $\gamma$ and partitioning $\boldsymbol{I}(T;Y)$ in order to determine the step size. It is evident the using $\boldsymbol{I}(T;Y)$ causes the method to concentrate on the region of interest in terms of rapid change of the Lagrangian.

Formally, we compute $\nabla_{Q,\gamma}\boldsymbol{I}(T;Y)$ and rescale the direction vector so that

$$(\nabla_{Q,\gamma}\boldsymbol{I}_Q(T;Y))' \cdot \Delta = \epsilon \tag{6.9}$$

where $\epsilon$ is a predetermined step size that is a fraction of $\log |T|$. We also bound the minimal and

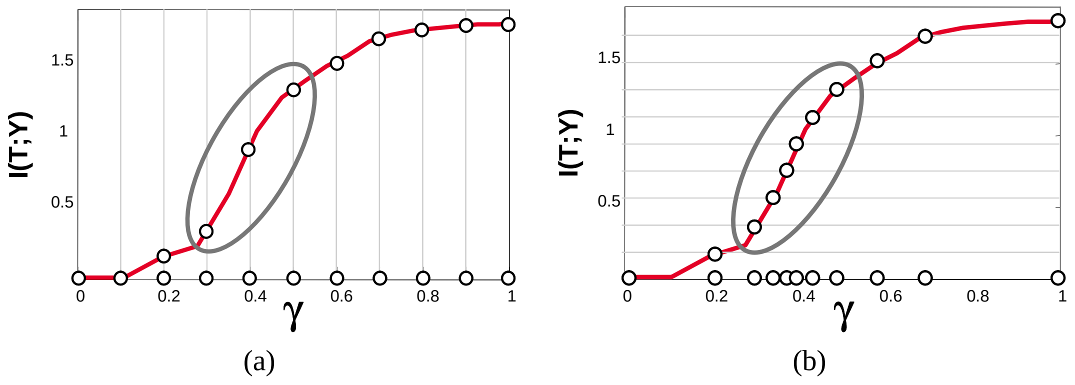

Figure 6.3: Illustration of the step size calibration process. Both graphs show the change in information between $T$ and $Y$ as a function of $\gamma$. The circles denote values of $\gamma$ to be evaluated. (a) shows naive calibration when fixed steps are taken in the $\gamma$ range. (b) shows calibration that uses fixed steps in the information range. The grey circle shows the region of dramatic change of the Lagrangian.

maximal change in $\gamma$ so that we do not get trapped in too many steps or alternatively overlook the regions of change.

Finally, although the continuation method takes us in the correct direction, the approximation as well as inherent numerical instability can lead us to a suboptimal path. To cope with this situation, we adopt a commonly used heuristic used in Deterministic annealing. At each value of $\gamma$, we slightly perturb the current solution and re-iterate the self-consistent equations to converge on a solution. If the perturbation leads to a better value of the Lagrangian, we take it as our current solution.

To summarize, our procedure works as follows: we start with $\gamma = 0$ for which only trivial solutions exists. At each stage we compute the joint direction of $\gamma$ and $Q(T \mid Y)$ that will leave the fixed point equations intact. We then take a small step in this direction and apply IB-EM iterations to attain the fixed point equilibrium at the new value of $\gamma$. We repeat these iterations until we reach $\gamma = 1$.

## 6.4 Multiple Hidden Variables

The framework we described in the previous sections can easily accommodate learning networks with multiple hidden variables simply by treating $T$ as a vector of hidden variables. In this case, the distribution $Q(\mathbf{T} \mid Y)$ describes the *joint* distribution of the hidden variables for each value of $Y$, and $P(\mathbf{T}, \mathbf{X})$ describes their joint distribution with the attributes $\mathbf{X}$ in the desired network. Unfortunately, if the number of variables $\mathbf{T}$ is large, the representation of $Q(\mathbf{T} \mid Y)$ grows exponentially, and this approach becomes infeasible.

One strategy to alleviate this problem is to force $Q(\mathbf{T} \mid Y)$ to have a factorized form. This

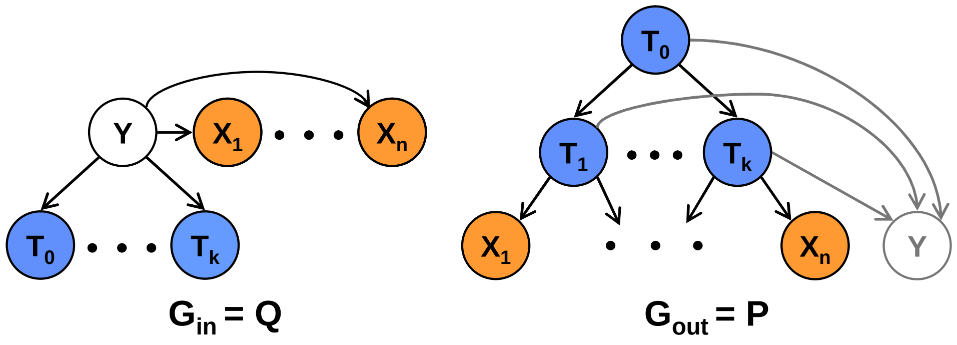

Figure 6.4: Definition of networks for the Multivariate Information Bottleneck framework with multiple hidden variables. Shown are $\mathcal{G}_{in}$ with the *mean field* assumption, and a possible choice for $\mathcal{G}_{out}$.

reduces the cost of representing $Q$ and also the cost of performing inference. As an example, we can require that $Q(\mathbf{T} \mid Y)$ is factored as a product $\prod_i Q(T_i \mid Y)$. This assumption is similar to the *mean field variational approximation* (*e.g.*, Jordan et al. [1998]).

In the Multivariate Information Bottleneck framework, different factorizations of $Q(\mathbf{T} \mid Y)$ correspond to different choices of networks $\mathcal{G}_{in}$. For example, the mean field factorization is achieved when $\mathcal{G}_{in}$ is such that the only parent of each $T_i$ is $Y$, as in Figure 6.4. In general, we can consider other choices where we introduce edges between the different $T_i$'s. For any such choice of $\mathcal{G}_{in}$, we get exactly the same Lagrangian as in the case of a single hidden variable. The main difference is that since $Q$ has a factorized form, we can decompose $\boldsymbol{I}_Q(\mathbf{T}; Y)$. For example, if we use the mean field factorization, we get

$$\boldsymbol{I}_Q(\mathbf{T}; Y) = \sum_i \boldsymbol{I}_Q(T_i; Y)$$

Similarly, we can decompose $\boldsymbol{E}_Q[\log P(\mathbf{X}, \mathbf{T})]$ into a sum of terms, one for each family in $P$. These two factorization can lead to tractable computation of the first two terms of the Lagrangian as written in Proposition 6.2.1. Unfortunately, the last term $\boldsymbol{E}_Q[\log Q(\mathbf{T})]$ cannot be evaluated efficiently. Thus, we approximate this term as $\sum_i \boldsymbol{E}_Q[\log Q(T_i)]$. For the mean field factorization, the resulting Lagrangian (with this lower bound approximation) has the form

$$\mathcal{L}^+_{EM} = \sum_i \boldsymbol{I}_Q(T_i; Y) - \gamma \left( \boldsymbol{E}_Q[\log P(\mathbf{X}, T)] - \sum_i \boldsymbol{E}_Q[\log Q(T_i)] \right) \tag{6.10}$$

The form of $\mathcal{L}^+_{EM}$ is valid, if Proposition 6.2.1 still holds for the case of multiple hidden variables. This is immediate if we make the following requirements, similar to those made for the case of a single hidden variable:

1. $Y$ is the instance identity;

2. $\mathcal{G}_{in}$ is a Bayesian network structure such that all of the variables $\mathbf{T}$ are independent of $X$ given $Y$; and

3. $\mathcal{G}_{out}$ is a Bayesian network structure such that $Y$ is a child of $\mathbf{T}$ and has no other parents. This implies that in $\mathcal{G}_{out}$, $Y$ is independent of all $\mathbf{X}$ given $\mathbf{T}$.

The last requirement is needed so that we can set $P(Y \mid T) = Q(Y \mid T)$ in the proof of Proposition 6.2.1. As in the case of a single hidden variable, we can now characterize fixed point equations that hold in stationary points of the Lagrangian.

**Proposition 6.4.1:** *Let $\mathcal{L}^+_{EM}$ be defined via $\mathcal{G}_{in}$ and $\mathcal{G}_{out}$ as in Eq. (6.10). Assuming a* mean field *approximation for $Q(\mathbf{T} \mid Y)$, a (local) maximum of $\mathcal{L}^+_{EM}$ is achieved by iteratively solving the following self-consistent equations for every hidden variable $i$ independently.*

$$Q(t_i \mid y) \quad = \quad \frac{1}{Z(i,y,\gamma)} Q(t_i)^{1-\gamma} \exp\left\{\gamma \mathbf{EP}\left(t_i, y\right)\right\}$$

*where*

$$\mathbf{EP}\left(t_i, y\right) \equiv \boldsymbol{E}_{Q(\mathbf{T}|t_i,y)}[\log P(\mathbf{x}[y], \mathbf{T})]$$

*where $Z(i,y,\gamma)$ is a normalizing constant and equals to*

$$Z(i,y,\gamma) = \sum_{t'_i} Q(t'_i)^{1-\gamma} \exp\left\{\gamma \mathbf{EP}\left(t'_i, y\right)\right\}$$

See Appendix 6.5.2 for the proof.

The only difference from the case of a single hidden variables is in the form of the expectation $\mathbf{EP}\left(t_i, y\right)$. It is easy to see that when a single hidden variable is considered, and $\mathbf{EP}\left(t_i, y\right) \equiv \log P(\mathbf{x}[y], t)$, the two forms coincide. It is also easy to see that this term decomposes into a sum of expectations, one for each factor in the factorization of $P$. We note that only terms that average over factors that involve $T_i$ are of interest in $\mathbf{EP}\left(t_i, y\right)$. All other terms do not depend on the value of $T_i$, and can be absorbed by the normalizing constant. Thus, $\mathbf{EP}\left(t_i, y\right)$ can still be computed efficiently.

A more interesting consequence (see theorem below) of this discussion is that when $\gamma = 1$, maximizing $\mathcal{L}^+_{EM}$ is equivalent to performing *mean field EM* [Jordan et al., 1998]. Thus, by using the modified Lagrangian we generalize this variational learning principle, and as we show below manage to reach better solutions.

The formulation is easily extensible to a general variational approximation of $Q$ where $\mathcal{G}_{in}$ allows, in addition to the dependence of each $T_i$ on $Y$, dependencies between the different $T_i$'s. In this case, we get

$$\boldsymbol{I}_Q(\mathbf{T}; Y) = \sum_i \boldsymbol{I}_Q(T_i; \mathbf{Pa}_{\mathbf{i}}^{\mathcal{G}_{in}})$$

Similarly, $\boldsymbol{E}_Q[\log P(\mathbf{X}, T)]$ decomposes according to the *joint* families of $T_i$ in $P$ and in $Q$. That is, each term in the decomposition depends on $T_i$, its parents $\mathbf{Pa}_i^{\mathcal{G}_{in}}$ in $\mathcal{G}_{in}$, and its parents $\mathbf{Pa}_i^{\mathcal{G}_{out}}$ in $\mathcal{G}_{out}$. As in the case of the mean field variational approximation, the last term $\boldsymbol{E}_Q[\log Q(\mathbf{T})]$ cannot be evaluated efficiently. We approximate it using a decomposition that follows the structure of $\mathcal{G}_{in}$ as

$$\boldsymbol{E}_Q[\log Q(\mathbf{T})] \approx \sum_i \boldsymbol{E}_Q\left[\log Q(T_i \mid \mathbf{T} \cap \mathbf{Pa}_i^{\mathcal{G}_{in}})\right] \tag{6.11}$$

We can now reformulate the results of Theorem 6.2.3 for this general case

**Theorem 6.4.2:** *Let $Q(\mathbf{T} \mid Y)$ decompose according to any structure $\mathcal{G}_{in}$ where all $T_i$'s are descendents of $Y$ and replace $\boldsymbol{E}_Q[\log Q(\mathbf{T})]$ by a decomposition as defined in Eq. (6.11). Then for the resulting Lagrangian*

$$\mathcal{L}^+_{EM} = (1-\gamma)\sum_i \boldsymbol{I}_Q(T_i; \mathbf{Pa}_\mathbf{i}^{\mathcal{G}_{in}}) - \gamma\mathcal{F}^+\left[Q, P\right]$$

*where $\mathcal{F}^+\left[Q, P\right]$ is defined as in Eq. (6.3), except that the above decomposition for both $\boldsymbol{E}_Q[\log P(\mathbf{X}, T)]$ and $\boldsymbol{H}_Q(T \mid Y)$ is used.*

**Proof:** This is a direct result of the fact that in the proof of Theorem 6.2.3, no assumptions were made of the form of $Q$. ▮

The above theorem extends the formal relation of the Information Bottleneck target Lagrangian and the EM functional for any form of variational approximation encoded by $\mathcal{G}_{in}$. In particular, when $\gamma = 1$, finding a local minimum of $\mathcal{L}^+_{EM}$ is equivalent to finding a local maximum of the likelihood function when the same variational approximation is used in the EM algorithm. Similarly, we can derive the fixed point equations with each for different choices of $\mathcal{G}_{in}$. The change to Proposition 6.4.1 is simply a different decomposition for $\mathbf{EP}\ (i, y)$

To summarize, the IB-EM algorithm of Section 6.2.2 can be easily generalized to handle multiple hidden variables by simply altering the form of $\mathbf{EP}\ (t_i, y)$ in the fixed point equations. All other details, such as the continuation method, remain unchanged.

## 6.5 Proofs and Technical Computations

### 6.5.1 Fixed point equations:Single Hidden Variable

**Proposition 6.2.4:** *Let $\mathcal{L}_{EM}$ be defined via $\mathcal{G}_{in}$ and $\mathcal{G}_{out}$ as in Proposition 1. $Q(T \mid Y)$ is a stationary point of $\mathcal{L}_{EM}$ with respect to a fixed choice of $P$ if and only if for all values $t$ and $y$ of $T$ and $Y$, respectively,*

$$Q(t \mid y) = \frac{1}{Z(y,\gamma)} Q(t)^{1-\gamma} P(\mathbf{x}[y], t])^{\gamma}$$

*where and $Z(y, \gamma)$ is a normalizing constant and equals to*

$$Z(y, \gamma) = \sum_{t'} Q(t')^{1-\gamma} P(\mathbf{x}[y], t'])^{\gamma} \tag{6.12}$$

To prove the proposition we use the following

**Lemma 6.5.1:** *[El-Hay and Friedman, 2001] Let $Q(\mathbf{X})$ be a joint distribution over a set of random variables $\mathbf{X}$, that decomposes according to $Q(\mathbf{X}) = \prod_i Q(X_i \mid \mathbf{U}_i)$. Then*

$$\frac{\partial \boldsymbol{E}_Q[f(\mathbf{X})]}{\partial Q(x_i \mid \mathbf{u}_i)} = Q(\mathbf{u}_i) \boldsymbol{E}_{Q(\cdot|x_i,\mathbf{u}_i)}[f(\mathbf{X})] + \boldsymbol{E}_Q\left[\frac{\partial f(\mathbf{x})}{\partial Q(x_i, \mathbf{u}_i)}\right]$$

The following is an immediate results of that fact that $Q(t) = \sum_{y'} Q(y')Q(t|y')$

$$\frac{\partial Q(T)}{\partial Q(t_0 \mid y_0)} = Q(y_0) 1\{T = t_0\} \tag{6.13}$$

We use this and an instantiation of the above lemma to prove the following:

**Lemma 6.5.2:**

$$\frac{\partial \boldsymbol{I}_Q(T;Y)}{\partial Q(t_0 \mid y_0)} = Q(y_0) \log \frac{Q(t_0|y_0)}{Q(t_0)}$$

**Proof:** We define $f(T, Y) \equiv \log \frac{Q(T,Y)}{Q(T)Q(Y)} = \log \frac{Q(T|Y)}{Q(T)}$ so that using Eq. (6.13), we can write

$$\begin{aligned}
\frac{\partial f(T,Y)}{\partial Q(t_0 \mid y_0)} &= \frac{\partial \log Q(T \mid Y)}{\partial Q(t_0 \mid y_0)} - \frac{\partial \log Q(T)}{\partial Q(t_0 \mid y_0)} \\
&= \frac{1}{Q(t_0 \mid y_0)} 1\{T = t_0, Y = y_0\} - \frac{Q(y_0)}{Q(t_0)} 1\{T = t_0\}
\end{aligned}$$

Plugging this into Lemma 6.5.1, we get

$$\begin{aligned}
\frac{\partial \boldsymbol{I}_Q(T;Y)}{\partial Q(t_0 \mid y_0)} &= Q(y_0) \boldsymbol{E}_{Q(\cdot|t_0,y_0)}\left[\log \frac{Q(T \mid Y)}{Q(T)}\right] + \boldsymbol{E}_Q\left[\frac{\partial \log \frac{Q(T|Y)}{Q(T)}}{\partial Q(t_0, y_0)}\right] \\
&= Q(y_0) \log \frac{Q(t_0 \mid y_0)}{Q(t_0)} + Q(y_0) \frac{Q(t_0 \mid y_0)}{Q(t_0 \mid y_0)} - \sum_y Q(y) Q(t_0 \mid y) \frac{Q(y_0)}{Q(t_0)} \\
&= Q(y_0) \log \frac{Q(t_0 \mid y_0)}{Q(t_0)} + Q(y_0)\left[1 - \frac{1}{Q(t_0)} \sum_y Q(y) Q(t_0 \mid y)\right] \\
&= Q(y_0) \log \frac{Q(t_0 \mid y_0)}{Q(t_0)} + Q(y_0)[1 - 1] \\
&= Q(y_0) \log \frac{Q(t_0 \mid y_0)}{Q(t_0)}
\end{aligned}$$

▮

Using Eq. (6.13) and Lemma 6.5.1 with $f(T,Y) \equiv \log Q(T)$, the following is immediate

**Lemma 6.5.3:**

$$\frac{\partial \boldsymbol{E}_Q[\log Q(T)]}{\partial Q(t_0 \mid y_0)} = Q(y_0)\log Q(t_0) + Q(t_0)\frac{1}{Q(t_0)}Q(y_0) = Q(y_0)\left[\log Q(t_0) + 1\right]$$

**Proof of the proposition:** We want to find $Q(T \mid Y)$ that are stationary points of the Lagrangian $\mathcal{L}_{EM}$ and where the constraints $\sum_t Q(t \mid y) = 1$ hold for any $y$. Thus, using Lagrange multipliers, we want to optimize

$$\mathcal{L} = \boldsymbol{I}_Q(T;Y) - \gamma\left(\boldsymbol{E}_Q[\log P(\mathbf{X},T)] - \boldsymbol{E}_Q[\log Q(T)]\right) + \sum_y \lambda_y \left(\sum_{t'} Q(t' \mid y) - 1\right)$$

Since $P$ is fixed, using Lemma 6.5.1 with $f(Y,\mathbf{X},T) \equiv \log P(\mathbf{X},T)$, we can write

$$\frac{\partial \boldsymbol{E}_Q[\log P(\mathbf{X},T)]}{\partial Q(t_0 \mid y_0)} = Q(y_0)\log P(\mathbf{x}[y_0],t_0)$$

Combining this with Lemma 6.5.2 and Lemma 6.5.3, we get

$$\frac{\partial \mathcal{L}_{EM}}{\partial Q(t_0 \mid y_0)} = Q(y_0)\left[\log Q(t_0 \mid y_0) - (1-\gamma)\log Q(t_0) + \gamma - \gamma \log P(\mathbf{x}[y_0],t_0)\right] + \lambda_{y_0}$$

Dividing by $Q(y_0)$ and equating to $0$, we get after rearranging of terms

$$Q(t_0|y_0) = e^{\lambda_{y_0}/Q(y_0)+\gamma} Q(t_0)^{1-\gamma} P(\mathbf{x}[y_0],t_0)^{\gamma} \tag{6.14}$$

This must hold for any value $t_0$ and $y_0$. Using $\sum_t Q(t \mid y_0) = 1$ we get

$$e^{\lambda_{y_0}/Q(y_0)+\gamma} = \frac{1}{\sum_t Q(t)^{1-\gamma} P(\mathbf{x}[y_0],t)^{\gamma}}$$

We get the desired result by plugging this into Eq. (6.14).

### 6.5.2 Fixed point equations:Multiple Hidden Variable

**Proposition 6.4.1:** *Let $\mathcal{L}^{+}_{EM}$ be defined via $\mathcal{G}_{in}$ and $\mathcal{G}_{out}$ as in Eq. (6.10). Assuming a* mean field *approximation for $Q(\mathbf{T} \mid Y)$, a (local) maximum of $\mathcal{L}^{+}_{EM}$ is achieved by iteratively solving the following self-consistent equations for every hidden variable $i$ independently.*

$$Q(t_i \mid y) \quad = \quad \frac{1}{Z(i,y,\gamma)} Q(t_i)^{1-\gamma} \exp^{\gamma \mathbf{EP}(t_i,y)}$$

*where*

$$\mathbf{EP}\,(t_i, y) \equiv \boldsymbol{E}_{Q(\mathbf{T}|t_i,y)}[\log P(\mathbf{x}[y], \mathbf{T})]$$

*where* $Z(i, y, \gamma)$ *is a normalizing constant and equals to*

$$Z(i, y, \gamma) = \sum_{t'_i} Q(t'_i)^{1-\gamma} \exp^{\gamma \mathbf{EP}\,(t'_i, y)}$$

**Proof:** Using the *mean field* assumption, the information and entropy terms in the Lagrangian decompose as follows

$$\mathcal{L}^+_{EM} = \sum_i \boldsymbol{I}_Q(T_i; Y) - \gamma \left( \boldsymbol{E}_Q[\log P(\mathbf{X}, T)] - \sum_i \boldsymbol{E}_Q[\log Q(T_i)] \right)$$

When computing the derivative with respect to the parameters of a specific variables $T_i$, the only change from the case of single hidden variable, is in the derivative of $\boldsymbol{E}_Q[\log P(\mathbf{X}, T)]$ given fixed $P$. Again using Lemma 6.5.1 with $f(Y, \mathbf{X}, T) \equiv \log P(\mathbf{X}, T)$ we get

$$\frac{\partial \boldsymbol{E}_Q[\log P(\mathbf{X}, \mathbf{T})]}{\partial Q(t_{i0} \mid y_0)} = \boldsymbol{E}_{Q(T|t_{i0}, y_0)}[\log P(\mathbf{x}[y_0], \mathbf{T})]$$

from which we get the change from Proposition 6.2.4 to Proposition 6.4.1 for the case of multiple hidden variables. ▮

### 6.5.3 Computing the Continuation Direction

We now develop the formulas needed to perform continuation as described in Section 6.3 for the case of a single hidden variable $T$. Consider again Eq. (6.5), where we now write the normalization term $Z(y, \gamma)$ explicitly:

$$\begin{aligned} G_{t,y}(Q, \gamma) = \quad & -\log Q(t \mid y) + (1-\gamma) \log Q(t) + \gamma \log P(\mathbf{x}[y], t) \\ & - \underbrace{\log \sum_{t'} \exp^{(1-\gamma) \log Q(t') + \gamma \log P(\mathbf{x}[y], t')}}_{Z(y,\gamma)} \end{aligned} \tag{6.15}$$

We want to compute the derivative of $G_{t,y}(Q, \gamma)$ with respect to the parameters and $\gamma$, and and then use the orthogonal direction for continuation. The will follow a direction in which the fix point equations remain unchanged, and the local maximum is tracked. To do so, we start by expressing $\log P(\mathbf{x}[y], t)$ as a function of the parameters $Q$.

The maximum likelihood parameters of $\log P(\mathbf{X}, T)$ for the conditional distribution of the children $X_i$ of $T$ in $\mathcal{G}_{out}$ are

$$\theta_{x_i|\mathbf{pa}_i,t} = \frac{\sum_y Q(y)Q(t|y)1\{x_i[y] = x_i, \mathbf{pa}_i[y] = \mathbf{pa}_i\} + \alpha(x_i, \mathbf{pa}_i, t)}{\sum_y Q(y)Q(t|y)1\{\mathbf{pa}_i[y] = \mathbf{pa}_i\} + \alpha(\mathbf{pa}_i, t)} \equiv \frac{\mathcal{N}(x_i, \mathbf{pa}_i, t)}{\mathcal{N}(\mathbf{pa}_i, t)} \quad (6.16)$$

where $1\{\}$ is the indicator function, $\alpha()$ are the hyper-parameters of the Dirichlet prior distribution (see Section 2.2.2) and $\mathcal{N}$ are used to denote the total counts (including prior) used for estimation. Similarly the maximum likelihood parameters of the distribution of $T$ given its parents are

$$\theta_{t|\mathbf{pa}_t} = \frac{\sum_y Q(y)Q(t|y)1\{\mathbf{pa}_t[y] = \mathbf{pa}_t\} + \alpha(\mathbf{pa_t}, t)}{\sum_y Q(y)1\{\mathbf{pa}_t[y] = \mathbf{pa}_t\} + \alpha(\mathbf{pa}_t)} \equiv \frac{\mathcal{N}(\mathbf{pa}_t, t)}{\mathcal{N}(\mathbf{pa}_t)} \quad (6.17)$$

We now consider each term in $G_{t,y}(Q, \gamma)$ and compute its derivative with respect to these parameters of $Q$.

**Computation of $\frac{\partial \log P(\mathbf{x}[y],t)}{\partial Q(t_0|y_0)}$**

The derivatives of the parameters expressed in Eq. (6.16) are:

$$\begin{aligned}
&\frac{\partial \theta_{x_i|\mathbf{pa}_i,t}}{\partial Q(t_0|y_0)} \\
&\quad = \frac{Q(y_0)}{\mathcal{N}(\mathbf{pa}_i,t)^2}\Big[\ 1\{x_i[y_0] = x_i, \mathbf{pa}_i[y_0] = \mathbf{pa}_i\}\mathcal{N}(\mathbf{pa}_i, t) - 1\{\mathbf{pa}_i[y_0] = \mathbf{pa}_i\}\mathcal{N}(x_i, \mathbf{pa}_i, t)\ \Big] \\
&\quad = \frac{Q(y_0)1\{\mathbf{pa}_i[y_0]=\mathbf{pa}_i\}}{\mathcal{N}(\mathbf{pa}_i,t)^2}\Big(1\{x_i[y_0] = x_i\}\mathcal{N}(\mathbf{pa}_i, t) - \mathcal{N}(x_i, \mathbf{pa}_i, t)\Big)
\end{aligned} \quad (6.18)$$

for $t = t_0$ and is zero otherwise. Similarly, the derivatives of the parameters of Eq. (6.17) is

$$\frac{\partial \theta_{t|\mathbf{pa}_t}}{\partial Q(t_0 \mid y_0)} = \frac{Q(y_0)}{\mathcal{N}(\mathbf{pa}_t)^2}[1\{\mathbf{pa}_t[y_0] = \mathbf{pa}_t\}\mathcal{N}(\mathbf{pa}_t) - 0] = \frac{Q(y_0)}{\mathcal{N}(\mathbf{pa}_t)}1\{\mathbf{pa}_t[y_0] = \mathbf{pa}_t\} \quad (6.19)$$

for $t = t_0$, and is zero otherwise. The log-probability of a specific instance can be written as

$$\log P(\mathbf{x}[y], t) = \log \theta_{t|\mathbf{pa}_t}[y] + \sum_{i \in Ch_t} \log \theta_{x_i|\mathbf{pa}_i,t}[y] + \sum_{i \neq t, Ch_t} \log \theta_{x_i|\mathbf{pa}_i}[y] \quad (6.20)$$

where $Ch_t$ denotes the children of $T$ in $\mathcal{G}_{out}$ and $\theta_{t|\mathbf{pa}_t}[y]$ is the parameter corresponding to the values appearing in instance $y$. We note that the last summation does not depend on the parameters

$Q(t \mid y)$, and by plugging Eq. (6.18) and Eq. (6.19) into Eq. (6.20), we get

$$
\begin{aligned}
\frac{\partial \log P(\mathbf{x}[y], t)}{\partial Q(t_0 \mid y_0)} &= \frac{1}{\theta_{t|\mathbf{pa}_t}[y]} \frac{\partial \theta_{t|\mathbf{pa}_t}[y]}{\partial Q(t_0 \mid y_0)} + \sum_{i \in Ch_t} \frac{1}{\theta_{x_i|\mathbf{pa}_i,t}[y]} \frac{\partial \theta_{x_i|\mathbf{pa}_i,t}[y]}{\partial Q(t_0 \mid y_0)} \\
&= Q(y_0) \Bigg[ \tfrac{1\{\mathbf{pa}_t[y_0] = \mathbf{pa}_t[y]\}}{\mathcal{N}(\mathbf{pa}_t)\theta_{t|\mathbf{pa}_t}[y_0]} \\
&\qquad + \textstyle\sum_{i \in Ch_t} \tfrac{1\{\mathbf{pa}_i[y_0] = \mathbf{pa}_i[y]\}}{\mathcal{N}(\mathbf{pa}_i,t)^2 \theta_{x_i|\mathbf{pa}_i}[y_0]} \Big( 1\{x_i[y] = x_i[y_0]\} \mathcal{N}(\mathbf{pa}_i, t) - \mathcal{N}(x_i, \mathbf{pa}_i, t) \Big) \Bigg] \\
&\equiv Q(y_0) \mathcal{D}(y, t)
\end{aligned}
\tag{6.21}
$$

where in the last line we use $\mathcal{D}(y,t)$ to denote the expression in the square brackets.

**Computation of $\frac{\partial \log Z(y_0,\gamma)}{\partial Q(t_0|y_0)}$**

Using Eq. (6.13) from Section 6.5.1 and the above, we can write

$$
\frac{\partial \; (1-\gamma)\log Q(t) + \gamma \log P(\mathbf{x}[y], t)}{\partial Q(t_0 \mid y_0)} = Q(y_0) \left[ \frac{1-\gamma}{Q(t)} + \gamma \mathcal{D}(y,t) \right] \tag{6.22}
$$

We can now use Eq. (6.22) to write the derivative of $Z(y,\gamma)$ since it is a summation over similar expressions

$$
\begin{aligned}
\tfrac{\partial \log Z(y_0,\gamma)}{\partial Q(t_0|y_0)} &= \tfrac{1}{Z(y_0,\gamma)} \exp^{(1-\gamma)\log Q(t_0) + \gamma \log P(\mathbf{x}[y],t_0)} Q(y_0) \left[ \tfrac{1-\gamma}{Q(t_0)} + \gamma D(y_0,t_0) \right] \\
&= \tfrac{1}{Z(y_0,\gamma)} Q(y_0) Q(t_0)^{1-\gamma} P(\mathbf{x}[y], t_0)^{\gamma} \left[ \tfrac{1-\gamma}{Q(t_0)} + \gamma D(y_0,t_0) \right] \\
&= Q(y_0) Q(t_0 \mid y_0) \left[ \tfrac{1-\gamma}{Q(t_0)} + \gamma D(y_0,t_0) \right]
\end{aligned}
\tag{6.23}
$$

where the last equality follows from Proposition 6.2.4.

**Computation of $\frac{\partial G_{t,y}(Q,\gamma)}{\partial Q(t_0|y_0)}$**

We combine Eq. (6.22) and Eq. (6.23) to write

$$
\frac{\partial G_{t,y}(Q,\gamma)}{\partial Q(t_0 \mid y_0)} = -1\{y = y_0\} + Q(y_0) \left[1 - Q(t_0 \mid y_0)\right] \left[ \frac{1-\gamma}{Q(t_0)} + \gamma D(y_0, t_0) \right] \tag{6.24}
$$

**Computation of $\frac{\partial \log Z(y,\gamma)}{\partial \gamma}$**

The only term that is not immediate is the derivative of $Z(y,\gamma)$ with respect to $\gamma$

$$
\begin{aligned}
\frac{\partial \log Z(y,\gamma)}{\partial \gamma} &= \frac{1}{Z(y,\gamma)} \sum_{t'} \exp^{(1-\gamma)\log Q(t') + \gamma \log P(\mathbf{x}[y],t')} \left[ -\log Q(t') + \log P(\mathbf{x}[y], t') \right] \\
&= \sum_{t'} \frac{1}{Z(y,\gamma)} Q(t')^{1-\gamma} P(\mathbf{x}[y], t')^{\gamma} \left[ -\log Q(t') + \log P(\mathbf{x}[y], t') \right]
\end{aligned}
$$

$$= \sum_{t'} Q(t'|y) \left[\log P(\mathbf{x}[y], t') - \log Q(t')\right]$$

from which follows

$$\frac{\partial G_{t,y}(Q, \gamma)}{\partial \gamma} = \log P(\mathbf{x}[y], t) - \log Q(t) - \sum_{t'} Q(t'|y) \left[\log P(\mathbf{x}[y], t') - \log Q(t')\right] \quad (6.25)$$

### Computation of the continuation direction

We can now compute all the elements of the derivative matrix of Eq. (6.7)

$$H_{t,y}(Q, \gamma) = \left( \frac{\partial G_{t,y}(Q,\gamma))}{\partial Q(t|y)} \middle| \frac{\partial G_{t,y}(Q,\gamma)}{\partial \gamma} \right)$$

To compute the orthogonal direction to the derivative, we solve Eq. (6.8)

$$H(Q, \gamma)\Delta = 0$$

As noted in Section 6.3, this can be prohibitively expensive and we resort to $H(Q, \gamma)$ with a diagonal approximation for elements of $\frac{\partial G_{t,y}(Q,\gamma)}{\partial Q(t|y)}$ computed in Eq. (6.24). We denote by $h_{y,t}$ the diagonal entry for $Y = y$ and $T = t$ and $h^{\gamma}_{y,t}$ the corresponding derivative with respect to $\gamma$. We then have to solve a set of equations of the form

$$d_{t,y} h_{y,t} + d_{\gamma} h^{\gamma}_{y,t} = 0$$

where $d_{t,y}$ and $d_{\gamma}$ are the elements of $\Delta$. Setting $d_{\gamma} = 1$ (an equivalent solution up to scaling) we get the unique solution

$$d_{t,y} = -\frac{h^{\gamma}_{y,t}}{h_{y,t}}$$

Normalizing $\Delta$ using the derivative of $\boldsymbol{I}_Q(T; Y)$ as described in Eq. (6.9) can now be easily computed given the Lemma 6.5.2 in Section 6.5.1.

### Multiple Hidden Variables

When computing the derivative with respect to the parameters associated with a specific hidden variable $t_i$, the only change in $G_{t,y}(Q, \gamma)$ is that $\log P(\mathbf{x}[y], t)$ is replaced by the term $\boldsymbol{E}_{Q(\mathbf{T}|t_i,y)}[\log P(\mathbf{x}[y], \mathbf{T})]$. In this case we simply compute the expectation of Eq. (6.21) over the $T$'s that are in the Markov blanket of $t_i$. The rest of the details remain the same.

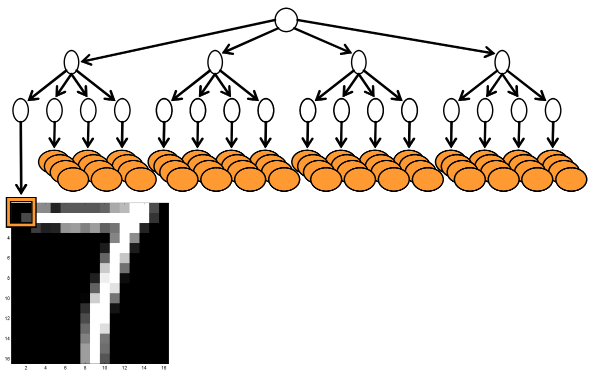

(a)

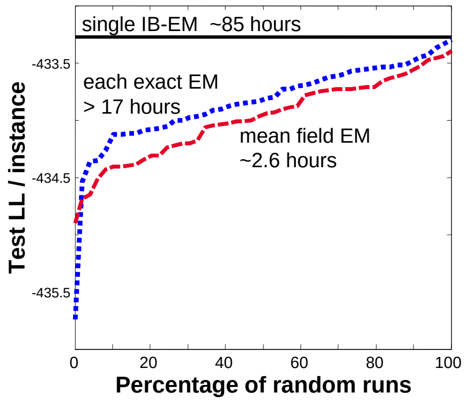

(b)

Figure 6.5: (a) A quadrant based hierarchy structure with 21 hidden variables for modeling $16 \times 16$ images in the Digit domain. (b) Test log-loss of the **IB-EM** algorithm for the model of (a) compared to the cumulative performance of 50 random EM and mean field EM runs.

## 6.6 Experimental Validation: Parameter Learning

To evaluate the IB-EM method for the task of parameter learning, we examine its generalization performance on several types of models on three real-life datasets. In each architecture, we consider networks with hidden variables of different cardinality, where for now we use the same cardinality for all hidden variables in the same network. We now briefly describe the datasets and the model architectures we use.

- The Stock dataset records up/same/down daily changes of 20 major US technology stocks over a period of several years [Boyen et al., 1999]. The training set includes 1213 samples and the test set includes 303 instances. We trained a Naive Bayes hidden variable model where the hidden variable is a parent of all the observations.

- The Digits dataset contains 7291 training instances and 2007 test instances from the USPS (US Postal Service) dataset of handwritten digits (see http://www.kernel-machines.org/data.html). An image is represented by 256 variables, each denoting the gray level of one pixel in a $16\times16$ matrix. We discretized pixel values into 10 equal bins.

  On this dataset we tried several network architectures. The first is a Naive Bayes model with a single hidden variable. In addition, we examined more complex hierarchical models. In these models we introduce a hidden parent to each quadrant of the image recursively. The 3-level hierarchy has a hidden parent to each 8x8 quadrant, and then another hidden variable that is the parent of these four hidden variables. The 4-level hierarchy starts with 4x4 pixel blocks each with a hidden parent. Every 4 of these are joined into an 8x8 quadrant by another level of hidden variables, totaling 21 hidden variables, as illustrated in Figure 6.5(a).

- The Yeast dataset contains measurements of the expression of the Baker's yeast genes in 173 experiments [Gasch et al., 2000]. These experiments measure the yeast response to changes in its environmental conditions. For each experiment the expression of 6152 genes were measured. We discretized the expression levels of genes into ranges down/same/up by using a threshold of one standard deviation from above and below the gene's mean expression across all experiments. In this dataset, we treat each gene as an instance that is described by its behavior in the different experiments. We randomly partitioned the data into 4922 training instances (genes) and 1230 test instances.

  The model we use for this dataset has an hierarchical structure with 19 hidden variables in a 4-level hierarchy that was determined by the biological expert based on the nature of the different experiments, as illustrated schematically in Figure 6.6. In this structure, 5–24 similar conditions (filled nodes) such as different hypo-osmotic shocks are children of a common hidden parent (unfilled nodes). These hidden parents are in their turn children of further abstraction of conditions. For example, the heat shock and heat shock with oxidative stress hidden nodes, are both children of a common more abstract heat node. A root hidden variable is the common parents of these high-level abstractions. Intuitively, each hidden variable encodes how the specific instance (a gene) is altered in the relevant groups of conditions.

As a first sanity check, for each model (and each cardinality of hidden variables) we performed 50 runs of EM with random starting points. The parameter sets learned in these different runs have a wide range of likelihoods both on the training set and the test set. These results (on which we elaborate below), indicate that these learning problems are challenging in the sense that EM runs can be trapped in markedly different local maxima.

Next, we considered the application of IB-EM on these problems. We performed a single IB-EM run on each problem and compared it to the 50 random EM runs, and also to 50 random mean field EM runs. For example, Figure 6.5 compares the test set performance (log-likelihood per instance) of these runs on the Digit dataset with a 4-level hierarchy of 21 hidden variables with 2 states each. The solid line shows the performance of the IB-EM solution at $\gamma = 1$. The two dotted lines show the cumulative performance of the random runs. As we can see, the IB-EM model is superior to all the mean field EM runs, as well as all of the exact EM runs. Figure 6.6 shows the result for the biological expert constructed hierarchy of Yeast dataset with binary variables. As can be seen, in this harder domain, the superiority of the exact EM runs over mean field EM runs is more evident. Yet, the IB-EM run which also use the mean field approximation, is still able to surpass all of the 50 random exact EM runs.

It is important to note the time required by these runs, all on a Pentium IV 2.4 GHz machine. For the Digit dataset, a single mean field EM run requires approximately 2.5 hours, an exact EM run requires roughly 17 hours, and the single IB-EM run requires just over 85 hours. As the IB-EM

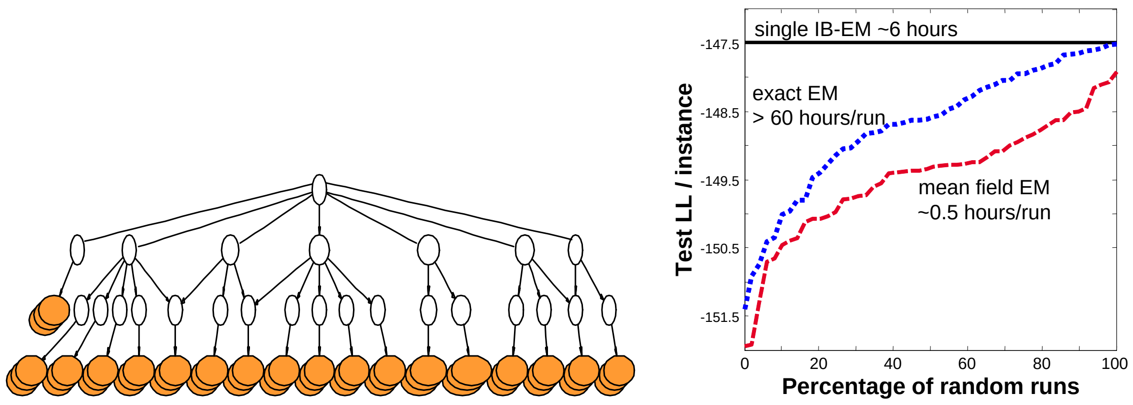

(a) (b)

Figure 6.6: (a) A structure constructed by the biological expert for the Yeast dataset based on properties of different experiments. 5-24 similar conditions (filled nodes) are aggregated by a common hidden parent (unfilled nodes). These hidden nodes are themselves children of further abstraction nodes of similar experiments, which in their turn are children of the single root node. (b) Comparison of test performance when learning the parameters of the structure of (a) with binary variables. Shown is test log-likelihood per instance of the **IB-EM** algorithm and the cumulative performance of 50 random EM as well as 50 random mean field EM runs.

run reaches a solution that is better than all of this runs, it offers an appealing performance to time tradeoff. This is even more evident for the Yeast dataset where the structure is somewhat more complex and the difference between exact learning and the mean field approximation is greater. For this dataset, the single IB-EM is still superior and takes significantly less time than a single exact EM.

Figure 6.7 compares the test log-likelihood per instance performance of our IB-EM algorithms and 50 random EM runs for a range of models for the Stock, Digit and Yeast datasets. In most cases, IB-EM is better than 80% of the EM runs and is often as good or better than the best of them. The advantage of IB-EM is particularly pronounced for the more complex models with higher cardinalities. Table 6.1 provides more details of these runs including train performance and comparison to 50 random mean field EM runs.

We also compared the IB-EM method to the perturbation method of Elidan et al. [2002]. Briefly, their method alters the landscape of the likelihood by perturbing the relative weight of the samples and progressively diminishing this perturbation as a factor of the temperature parameter. In the **Stock** dataset, the perturbation method initialized with a starting temperature of $4$ and cooling factor of $0.95$, had performance similar to that of IB-EM. However, the running time of the perturbation method was an order of magnitude longer. For the other datasets we considered above, running the perturbation method with the same parameters proved to be impractical. When we used more efficient parameter settings, the perturbation method's performance was significantly inferior to

| | Train Log-Likelihood | | | | | | | Test Log-Likelihood | | | | | | |
|---|---|---|---|---|---|---|---|---|---|---|---|---|---|---|
| Model | **IB-EM** | **Random EM** | | | **Mean Field EM** | | | **IB-EM** | **Random EM** | | | **Mean Field EM** | | |
| | | %< | 100% | 80% | %< | 100% | 80% | | %< | 100% | 80% | %< | 100% | 80% |
| **Stock** | | | | | | | | | | | | | | |
| C=3 | -19.91 | 62% | -19.90 | -19.90 | | | | -19.90 | 76% | -19.88 | -19.89 | | | |
| C=4 | -19.47 | 98% | -19.46 | -19.52 | | | | -19.52 | 96% | -19.52 | -19.62 | | | |
| C=5 | -19.16 | 94% | -19.15 | -19.24 | | | | -19.31 | 98% | -19.30 | -19.39 | | | |
| **Digit** | | | | | | | | | | | | | | |
| C=5 | -429.95 | 36% | -428.67 | -429.11 | | | | -439.91 | 56% | -439.03 | -439.47 | | | |
| C=10 | -411.44 | 100% | -411.72 | -413.96 | | | | -425.33 | 100% | -425.36 | -427.05 | | | |
| **DigH3** | | | | | | | | | | | | | | |
| C=2 | -442.02 | 100% | -442.02 | -442.29 | 100% | -442.03 | -442.20 | -450.812 | 92% | -450.76 | -450.92 | 82% | -450.76 | -450.84 |
| C=3 | -428.77 | 100% | -428.85 | -429.02 | 100% | -428.83 | -429.02 | -437.798 | 98% | -437.74 | -438.20 | 98% | -437.74 | -438.04 |
| **DigH4** | | | | | | | | | | | | | | |
| C=2 | -425.43 | 100% | -425.54 | -425.81 | 100% | -425.61 | -425.94 | -433.279 | 100% | -433.30 | -433.55 | 100% | -433.40 | -433.71 |
| C=3 | -407.60 | 100% | -407.75 | -408.56 | 100% | -408.49 | -408.83 | -415.798 | 100% | -415.88 | -416.48 | 100% | -416.37 | -416.77 |
| **Yeast** | | | | | | | | | | | | | | |
| C=2 | -148.13 | 100% | -148.32 | -148.79 | 100% | -148.89 | -149.71 | -147.48 | 100% | -147.51 | -147.87 | 100% | -147.92 | -148.78 |
| C=3 | -139.44 | 100% | -139.58 | -140.05 | 100% | -140.09 | -140.87 | -138.38 | 100% | -138.57 | -139.00 | 100% | -139.06 | -139.92 |
| C=4 | -136.36 | 100% | -136.72 | -136.97 | 100% | -137.72 | -138.28 | -135.65 | 100% | -135.96 | -136.16 | 100% | -136.92 | -137.34 |

Table 6.1: Comparison of the IB-EM algorithm, 50 runs of EM with random starting points, and 50 runs of mean field EM from the same random starting points. Shown are train and test log-likelihood per instance for the best and 80th percentile of the random runs. Also shown is the percentile of the runs that are worse than the IB-EM results. Datasets shown include a Naive Bayes model for the Stock dataset and the Digit dataset; a 3 and 4 level hierarchical model for the Digit dataset (DigH3 and DigH4); and an hierarchical model for the Yeast dataset. For each model we show several cardinalities for the hidden variables, shown in the first column.

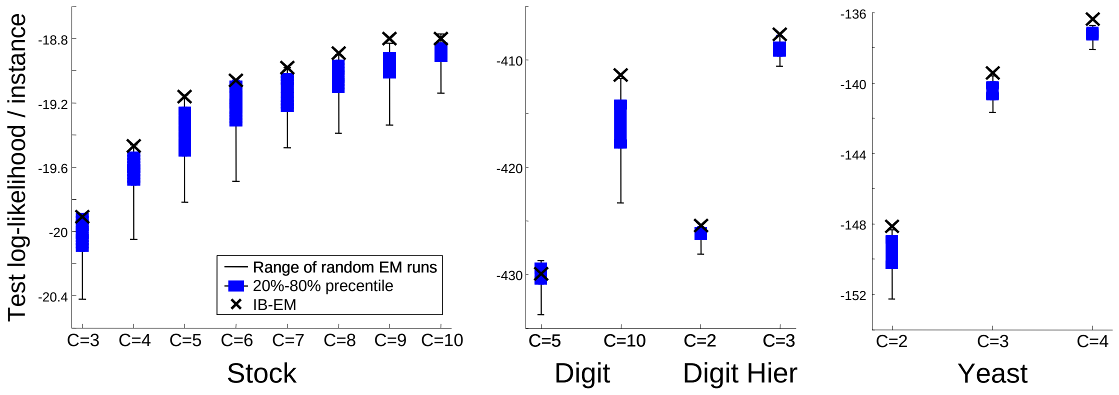

Figure 6.7: Comparison of log-likelihood per instance test performance of the IB-EM algorithm (black 'X') and 50 runs of EM with random starting points. The vertical line shows the range of the random runs and boxes mark the 20%-80% range. Datasets shown (x-axis) include a Naive Bayes model for the Stock dataset and the Digit dataset; a 4 level hierarchical model for the Digit dataset (Digit Hier); a hierarchical model for the Yeast dataset. For each model we show several cardinalities for the hidden variables, shown in the x-axis.

that of IB-EM. These results do not contradict those of Elidan et al. [2002] who showed some improvement for the case of parameter learning but mainly focused on structure learning, with and without hidden variables.

To demonstrate the effectiveness of the continuation method we examine **IB-EM** during the progress of $\gamma$. Figure 6.8 illustrates the progression of the algorithm on the Stock dataset. (a) shows training log-likelihood per instance of parameters in intermediate points in the process. This panel also shows the values of $\gamma$ evaluated during the continuation process (circles). These were evaluated using the predicted change in $\boldsymbol{I}(T;Y)$ shown in (b). As we can see, the continuation procedure focuses on the region where there are significant changes in $\boldsymbol{I}(T;Y)$ approximately corresponding the areas of significant changes in the likelihood. For both the Stock and Digit datasets, we also tried changing $\gamma$ naively from $0$ to $1$ as in standard annealing procedures, without performing continuation. This procedure often "missed" the superior local maxima even when a large number (1000) of $\gamma$ values were used in the process. In fact, in most runs the results were no better than the average random EM run emphasizing the importance of the continuation in the annealing process.

## 6.7 Learning Structure

Up until now, we were only interested in parameter learning. However, in real life it is often not the case that the structure is given. A structure that is too simple will not be able to faithfully capture the distribution, while an overly complex structure will deteriorate our ability to learn. In this

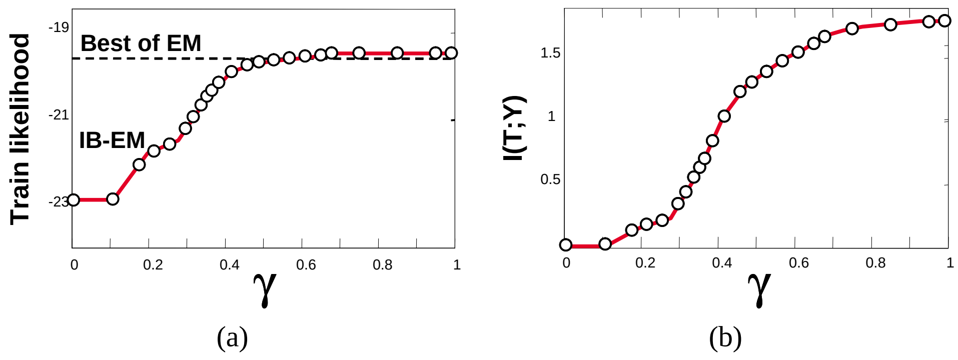

Figure 6.8: The continuation process for a Naive Bayes model on the Stock data set. (a) Shows the progress of training likelihood as a function of $\gamma$ compared to the best of 50 EM random runs. Black circles illustrate the progress of the continuation procedure by denoting the value of $\gamma$ at the end of each continuation step. Calibration is done using information between the hidden variable $T$ and the instance identity $Y$ shown in (b) as a function of $\gamma$.

section we consider the case where the set of hidden variables is fixed and their cardinalities are known, and we want to learn the network structure. Clearly, this problem is harder than simple parameter learning, which is just one of the tasks we have to perform in this scenario. The common approach to this model selection task is to use a *score-based approach* where we search for a structure that maximizes some score. Common scores such as the BDe score [Heckerman et al., 1995a] balance the likelihood achieved by the model and its complexity. Thus, model selection is achieved independently of the search procedure used (see Section 2.3 for more details).

We now aim to extend the **IB-EM** framework for the task of structure learning using a score-based approach. Naively, we could simply consider different structures and for each one apply the IB-EM procedure to estimate parameters, and then evaluate its generalization ability using the score. Such an approach is extremely inefficient, since it spends a non-trivial amount of time to evaluate each potential candidate structure. In this work we advocate a strategy that is based on the Structural EM framework of Friedman [1997]. In Structural EM (see Section 2.4), we use the completion distribution $Q$ that is a result of the E-Step to compute *expected sufficient statistics*. That is, instead of Eq. (2.7) we use Eq. (2.16), where in our case the completion distribution $Q(H \mid O, \theta_{old})$ is simply $Q(\mathbf{T} \mid Y)$. These statistics are then used in the *M-step* when structure modification steps are evaluated. Thus, instead of assuming that the target structure $\mathcal{G}_{out}$ is fixed, we define the Lagrangian as a function of the pair $(\mathcal{G}_{out}, \theta)$. Then, in the M-step, we can consider different choices of $\mathcal{G}_{out}$ and evaluate how each of them changes the score. Given the expected statistics, the problem is identical in form to learning from a fully observed dataset and computation of the score is similar. This facilitates an efficient greedy search procedure that uses local edge modification to the network structure. The EM procedure of Section 6.2.2 is thus revised as follows:

- **E-step** : Maximize $-\mathcal{L}_{EM}$ by varying $Q(\mathbf{T} \mid Y)$ while holding $P$ fixed.
- **M-step**: While holding $Q$ fixed:
  - Search for the structure $\mathcal{G}_{out}$ of $P$ that maximizes $\text{Score}_{\text{BDe}}(\mathcal{G} : \mathcal{D})$, using the sufficient statistics of $Q$.
  - Maximize $-\mathcal{L}_{EM}$ by varying the parameters of $P$ using the structure $\mathcal{G}_{out}$ selected.

In practice, since the BDe score is not a linear function of the sufficient statistics, we approximate it in the **M-step** using the Cheeseman-Stutz [Cheeseman et al., 1988] approximation. It is important to note the distinction between the optimization of the Lagrangian and that of the score. Specifically, optimizing the Lagrangian involves maximization of the likelihood along with an information theoretic regularization term that does not depend on $P$. On the other hand, optimization of the structure is performed using the BDe model selection score. This is mathematically valid since each optimization step is ignorant of the inner mechanics of the other step. However, one might wonder why the use of a score is needed at all if regularization is already present in the form of the information theoretic term in the Lagrangian. It is easy to understand the reason for this if we look at the final stage of learning when $\gamma = 1$. At this point, as we have shown, optimizing the Lagrangian is equivalent to optimizing the EM objective. Using the same objective to adapt structure will result in dense structures. In particular, it will be beneficial to add an edge between any two variables that are not perfectly independent in the training data. Thus, while the regularization encoded in the Lagrangian is needed to smooth the parametric EM problem, a model selection regularization via a score is also needed to constrain the network structure.

Using the Structural EM framework allows us to apply our framework to structure learning and to use various search operators as simple plug-ins. For general Bayesian networks, for example, one can consider the standard add, delete and reverse edge operators. The only requirement in this case is that a hidden variable is constrained to be non-leaf, in which case it becomes redundant and can be marginalized out. In addition, as in the case of learning parameters, we are still guaranteed to converge for a given value of $\gamma$. However, as in parametric EM, convergence is typically to a local maximum. In fact, the problem now has two facets: First, local maxima that result from evaluation of $Q$ in the E-step. Second, local maxima in the discrete structure search space due to the greedy nature of the search algorithm.

Although the method described above applies for any Bayesian network structure, for concreteness we focus on learning *hierarchies* of hidden variables in the following sections. In this sub-class of networks each variable has at most one parent, and that parent has to be a hidden variable. This implies that the hierarchy of hidden variables captures the dependencies between the observed attributes. Since we are dealing with hierarchies we consider search steps that replace the parent of a

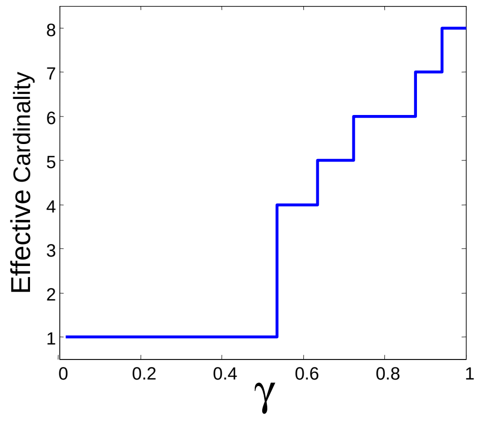

Figure 6.9: Effective cardinality as a function of $\gamma$ during the learning process for the Stock dataset using a Naive Bayes model. Cardinality is evaluated using local decomposition of the BDe score.

variable by one of the hidden variables. Such moves preserve the overall hierarchy structure, repositioning a single observed variable, or a sub-hierarchy. We apply these steps in a greedy manner, from the one that leads to the largest improvement, as long as the resulting hierarchy is acyclic.

## 6.8 Learning Cardinality

In real life, it is often the case that we do not know the cardinality of a hidden variable. In a clustering application, for example, we typically do not know of a beneficial number of clusters and need to either use some arbitrary choice or spend time evaluating several possibilities. Naively, we might try to set a high cardinality so that we can capture all potential clusters. However, this approach can lead to bad generalization performance due to over-representation. The discussion in Section 6.3 on the behavior of the model as a function of $\gamma$ provides insight on the effect of cardinality selection. When examining the models during the continuation process, we observe that for lower values of $\gamma$ the *effective* cardinality of the hidden variable is smaller than its cardinality in the model (we elaborate on how this is measured below). Figure 6.9 shows an example of this phenomenon for the Naive Bayes model of the Stock dataset. Thus, limiting the cardinality of the hidden variable is in effect similar to stopping the continuation process at some $\gamma < 1$. This is, by definition, equivalent to using a regularized version of the EM objective, which can avoid overfitting.

The most straightforward approach to learning the cardinality of a hidden variable is simply to try a few values, and for each value apply IB-EM independently. We can then compare the value of the EM objective (at $\gamma = 1$) corresponding to the different cardinalities. However, models with higher cardinality will achieve a higher likelihood and will thus always be chosen as preferable by the Lagrangian, at the risk of overfitting the training data. In the previous section we discussed the use of a model selection score as a measure for preferring one network structure over another.

The same score can also be readily applied for this scenario of cardinality selection. Whether the complexity is a result of a dense structure or an increased number of parameters due to a high cardinality of a variable, all common scores balance the likelihood with the model complexity, either explicitly as in the case of the MDL score [Lam and Bacchus, 1994] or implicitly as in the case of the Bayesian (BDe) score [Heckerman et al., 1995a]. Thus, similarly to structure learning, we use the Lagrangian when estimating parameters and turn to the score when performing the black-box model selection step. One problem with this simple approach is that it can be extremely time consuming. If we want to try $K$ different cardinalities for each hidden variable, we have to carry out $|H|^K$ independent IB-EM runs, where $|H|$ is the number of hidden variables.

The intuition that the "effective" cardinality of the hidden variable will increase as we consider larger values of $\gamma$ suggests that we increasing the model complexity during the continuation process. A simple method is as follows. At each stage allow the model an extra, seemingly redundant, state for the hidden variable. As soon as this state is utilized, we increase the cardinality by adding a new "spare" state. The annealing process, by nature, automatically utilizes this new state when it is beneficial to do so. The task we face is to determine when all the states of a hidden variables are being utilized and therefore a new redundant state is needed. Intuitively, a state of a variable is being used if it captures a distinct behavior that is not captured by other states. That is, for any state $i$, no other state $j$ is similar.

To determine whether state $i$ is different than all other states, we start by evaluating the cost that we incur due to the merging of state $i$ with another state $j$. We denote by $\widehat{ij}$ a new state that combines both $i$ and $j$ and alter $Q$ so that

$$Q(T = \widehat{ij} \mid Y = y) = Q(T = i \mid Y = y) + Q(T = j \mid Y = y) \tag{6.26}$$

We then use this to reestimate the parameters of $P$ in the M-step, and examine the resulting change to the Lagrangian. As shown in Slonim et al. [2002], the difference in the Lagrangian before and after the merge is a sum of Jensen-Shannon divergence terms that measure the difference between the conditional distribution of each child variable given the two states of the hidden variable. This is in fact the change in likelihood of the model resulting from merging the states and can be computed efficiently.

Now that we have the change in the Lagrangian due to the merging of state $i$ with state $j$, we have to determine whether this change is significant. As already noted, using more states will always improve the likelihood so that the difference in the Lagrangian is not sufficient for model selection. Instead, we can use the BDe score to take into account both the improvement to the likelihood and the change in the model complexity as in Elidan and Friedman [2001]. One appealing property of the BDe score is that it is *locally decomposable*. That is, Eq. (2.15) decomposes according to the different values of each variables. Thus, the difference between the BDe score after and before the merge of states $i$ and $j$ is only in the terms where $T$ appears.

$$
\begin{aligned}
&\text{Score}_{\text{BDe}}(\mathcal{G}_{\widehat{ij}} : \mathcal{D}) - \text{Score}_{\text{BDe}}(\mathcal{G}_{i,j} : \mathcal{D}) = \\
&\sum_{pa_t} \left[ \log \frac{\Gamma(N^+(T{=}i,j,pa_t))}{\Gamma(\alpha(T{=}i,j,pa_t))} - \log \frac{\Gamma(N^+(T{=}i,pa_t))}{\Gamma(\alpha(T{=}i,pa_t))} - \log \frac{\Gamma(N^+(T{=}j,pa_t))}{\Gamma(\alpha(T{=}j,pa_t))} \right] + \\
&\sum_C \sum_{pa_c} \Bigg[ \log \frac{\Gamma(\alpha(pa_c,T{=}i,j))}{\Gamma(N^+(pa_c,T{=}i,j))} + \sum_c \log \frac{\Gamma(N^+(c,pa_c,T{=}i,j))}{\Gamma(\alpha(c,pa_c,T{=}i,j))} \\
&\qquad - \log \frac{\Gamma(\alpha(pa_c,T{=}i))}{\Gamma(N^+(pa_c,T{=}i))} - \sum_c \log \frac{\Gamma(N^+(c,pa_c,T{=}i))}{\Gamma(\alpha(c,pa_c,T{=}i))} \\
&\qquad - \log \frac{\Gamma(\alpha(pa_c,T{=}j))}{\Gamma(N^+(pa_c,T{=}j))} - \sum_c \log \frac{\Gamma(N^+(c,pa_c,T{=}j))}{\Gamma(\alpha(c,pa_c,T{=}j))} \Bigg]
\end{aligned}
$$

where the first summation correspond to the family of $T$ and its parents, and the second summation is over all **C** that are children of $T$ and corresponds to the families of the children of $T$ and their parents. $N^+(x) = N(x) + \alpha(x)$ and correspond to *total* count statistics that include the imaginary prior counts (see Section 2.2.2). As all the terms are functions of these simple sufficient statistics, the above difference can be computed efficiently. Moreover, as in the case of the likelihood computation, the sufficient statistics needed when merging two states are simply the sum of the statistics needed for scoring the individual states. Thus, we can easily evaluate all pairwise state merges to determine if *any* two states of $T$ are similar.

To summarize, the resulting procedure is as follows. We start with a binary cardinality for the hidden variables at $\gamma = 0$. At each stage, before $\gamma$ is increased, we determine for each hidden variable if all its states are utilized: For each pair of states we evaluate the BDe score difference between the model with the two states and the model with the states merged. If the difference is positive for all pairs of states then all states are considered utilized and a new state is added. Optimizing the Lagrangian using IB-EM will utilize this new state automatically when it will be beneficial to do so, causing the introduction of a new "spare" state, and so on.

In an early work leading to the formulation of the Information Bottleneck framework, [Pereira et al., 1993] used a similar idea to gauge the effective number of clusters. Briefly, for each cluster a slightly perturbed cluster (twin state) was incorporated in the model allowing each cluster to split into two distinct ones. Similar procedures were used in Deterministic annealing [Rose, 1998] and later Information Bottleneck implementations [Tishby et al., 1999, Slonim et al., 2002]. The method we presented in this section differs in two important aspects. First, we use a model selection score to determine when it is beneficial to declare that a redundant cluster is actually being used. This allows us to avoid using an arbitrary distance measure to determine if two clusters diverge. Second, the above allows us to use a single redundant cluster rather than a twin for each state, which significantly reduces the model complexity. While this may not be crucial in standard clustering scenario, it is of great importance for the large models with many hidden variables that we consider in this paper.

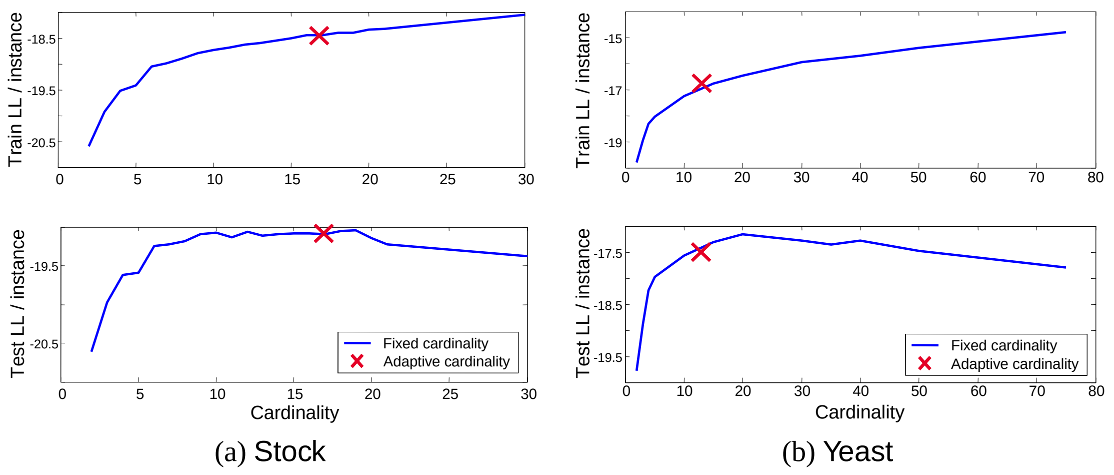

Figure 6.10: Evaluating adaptive cardinality selection for the Stock and the Yeast datasets with a Naive Bayes model. The 'X' marks the performance of runs with adaptive cardinality selection. The line shows performance of individual runs with a fixed cardinality. The top panel shows training set performance, and the bottom one test set performance.

## 6.9 Experimental Validation: Learning Cardinality

We now want to evaluate the effectiveness of our method for adapting cardinality during the annealing process. For this, we would like to compare the cardinality and model achieved by the method to naive selection of the cardinality. To make this feasible, we look at the context of a Naive Bayes model with a single hidden variable for the Stock and the Yeast dataset introduced in Section 6.6. We trained the models using the IB-EM algorithm where the hidden variable was assigned a fixed cardinality, and repeated this for different cardinalities. We then applied our adaptive cardinality method to the same model. Figure 6.10 compares the adaptive cardinality selection run ('X' mark) vs. the fixed cardinality runs for both datasets. As we can see, the adaptive run learns models that generalize nearly as well as the best models learned with fixed cardinality. These results indicate that our method manages to increase cardinality while tracking a high likelihood solution, and that the decision when to add a new state manages to avoid adding spurious states.

A more complex scenario is where, for the Yeast dataset, we learn the hierarchy supplied by the biological expert for 62 of the experiments. In this hierarchy there are 6 hidden variables that aggregate similar experiments, a *Heat* node that aggregates 5 of these hidden variables and a root node that is the parent of both *Heat* and the additional *Nitrogen Depletion* node. Figure 6.11 shows the structure along with the cardinalities of the hidden variables learned by our method and compares the performance of our method to model learned with different fixed cardinalities. As can be seen in (b), the performance of our final model is close to the optimal performance with fixed cardinality. (c) shows that this is achieved with a similar complexity to the simpler of the superior models (at a fixed cardinality of 10).

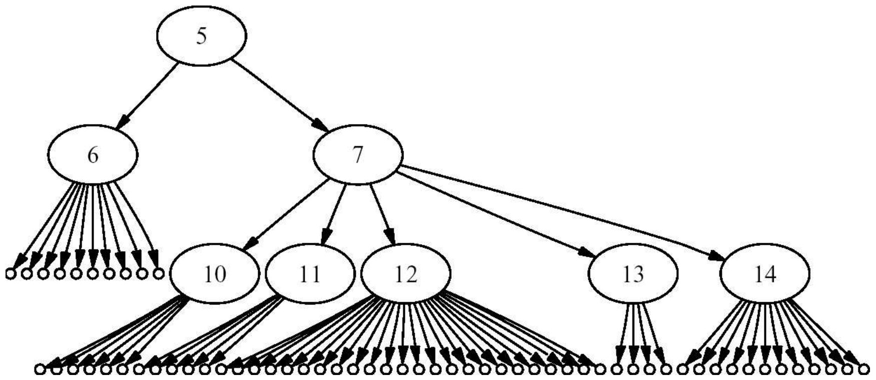

(a)

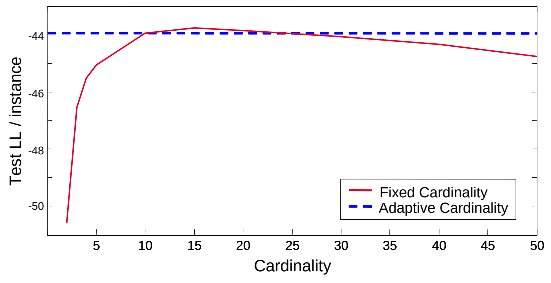

(b)

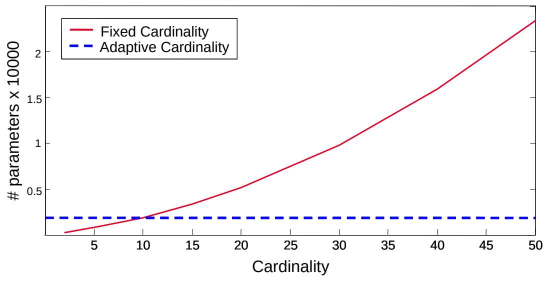

(c)

Figure 6.11: Cardinality learning for the Yeast dataset on the structure provided by the biological expert. (a) shows the structure along with the nodes annotated with the cardinality learned by our adaptive approach. (b) shows the test set log-likelihood performance of models learned with different fixed cardinalities (solid line). The horizontal dashed line marks the performance of our adaptive cardinality method. (c) shows plot the number of parameters for each of these models (solid line) with the dashed horizontal line marking the number of parameters of the model learned by our method.

## 6.10 Learning New Hidden Variables

The ideas presented in Section 6.7 are motivated by the fact that in real life we are typically not given the structure of the Bayesian network. The situation is often even more complex. Hidden variables, as their name implies, are not only unobserved but can also be unknown entities. In this case, we do not even know which variables to include in our model. Thus, we want to determine the number of hidden variables, their cardinality, their relation to the observed variables, and their inter-dependencies. This situation is clearly much more complex than structure learning and might seem hopeless at first. However, as in the case of cardinality adaptation discussed in Section 6.8, we can use emergent cues of the continuation process to suggest an effective method.

Recall the behavior of our target Lagrangian as a function of $\gamma$. For small values of $\gamma$, the emphasis of the Lagrangian is on compressing the instance identity, and the hidden variables are (almost) independent of the observed attributes. Thus, at this stage, a simple model would be able

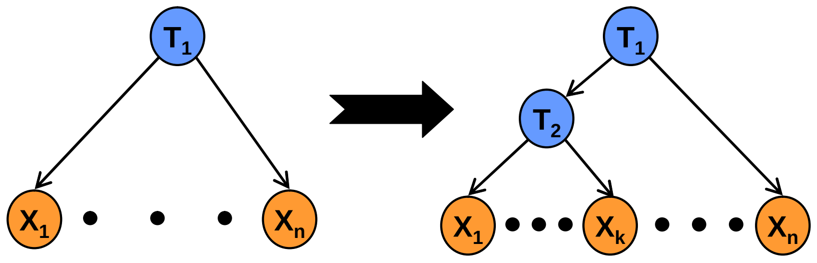

Figure 6.12: Example of enrichment with new hidden variables $T_2$ as parent of a subset $\mathbf{C}$ of the observed variables $X_1 \ldots X_n$.

to perform just as well as a complex one. In fact, to increase learning robustness, we will want to favor the simpler model and avoid redundant representational complexity. As we increase $\gamma$, the hidden variables start capturing properties of the data. In this scenario the need for the more complex structure becomes relevant as it will allow the learning procedure to improve performance.

The above intuition suggests that at small values of $\gamma$ we start with a simple hierarchy (say, one with only a single hidden variable). When the continuation reaches larger values of $\gamma$, the Lagrangian can tolerate more complex structures. Thus, we want to adapt the complexity of the hierarchy as we progress. To do so, we consider a search operator that enriches the structure of hierarchy with a new hidden variable. (This operator is much in the spirit of the "top-down" strategy explored by Adachi and Hasegawa [1996] in learning evolutionary trees.)

Suppose that we want to consider the addition of a new hidden variables into the network structure. For simplicity, consider the scenario shown in Figure 6.12, where we start with a Naive Bayes network with a hidden variable $T_1$ as root and want to add a hidden variable $T_2$ as a parent of a subset $\mathbf{C}$ of $T_1$'s children. Intuitively, we want to select a subset $\mathbf{C}$ that is not "explained well" by $T_1$ and where we expect to gain a lot by the introduction of $T_2$. Formally, we evaluate the change in our target Lagrangian as the result of inserting $T_2$ into the network structure

$$\mathcal{L}_{EM} - \mathcal{L}'_{EM} =$$
$$-\boldsymbol{I}_Q(T_2;Y) + \gamma \boldsymbol{E}_Q\left[\log P'(T_2 \mid T_1) - \log Q(T_2) + \textstyle\sum_{i \in \mathbf{C}} [\log P'(X_i \mid T_2) - \log P(X_i \mid T_1)]\right]$$

where $P$ and $P'$ are the models before and after the change to the network, respectively. The term $\log P(X_i \mid T_1)$ can be readily evaluated from the current model for each $X \in \mathbf{C}$ and the terms $\boldsymbol{I}_Q(T_2;Y)$ and $\boldsymbol{E}_Q[\log Q(T_2)]$ can be easily bounded. However, to evaluate $\log P'(T_2 \mid T_1)$ or $\sum_{i \in \mathbf{C}} \log P'(X \mid T_2)$ we need to actually choose $\mathbf{C}$, add $T_2$ to the current structure and optimize $Q(T_2 \mid Y)$. This can be too costly as the number of possible subsets $\mathbf{C}$ can be large even for a relatively small number of variables. Thus, we want to somehow approximate the above terms efficiently using only the current model. The following bound allows us to do so by bounding the contribution of a hidden variable.

**Proposition 6.10.1:** *Let $P$ be a Bayesian network model with a hidden variable $T_1$ and denote by $\mathbf{C}$ an observed subset of $T_1$'s children. Let $P'$ be the result of replacing $T_1$ as a parent of $\mathbf{C}$ by $T_2$, making $T_2$ a child of $T_1$ and optimizing the parameters of the model using the IB-EM algorithm for any value of $\gamma$. Then*

$$\boldsymbol{E}_Q[\log Q(\mathbf{C} \mid T_1)] \geq \boldsymbol{E}_Q\left[\sum_{i \in \mathbf{C}} \log P'(X_i \mid T_2) + \log P'(T_2 \mid T_1)\right]$$

**Proof:** Using the chain rule and positivity of entropy, we can write

$$\begin{aligned}
\boldsymbol{E}_Q[\log Q(\mathbf{C} \mid T_1)] &\equiv -\boldsymbol{H}_Q(\mathbf{C} \mid T_1) \\
&= -\Big[\boldsymbol{H}_Q(\mathbf{C}, T_2 \mid T_1) - \boldsymbol{H}_Q(T_2 \mid \mathbf{C}, T_1)\Big] \\
&\geq -\boldsymbol{H}_Q(\mathbf{C}, T_2 \mid T_1) \\
&= -\Big[\boldsymbol{H}_Q(\mathbf{C} \mid T_2, T_1) + \boldsymbol{H}_Q(T_2 \mid T_1)\Big] \\
&= -\Big[\sum_{i \in \mathbf{C}} \boldsymbol{H}_Q(X_i \mid X_1 \ldots X_{i-1}, T_2, T_1) + \boldsymbol{H}_Q(T_2 \mid T_1)\Big] \\
&\geq -\Big[\sum_{i \in \mathbf{C}} \boldsymbol{H}_Q(X_i \mid T_2) + \boldsymbol{H}_Q(T_2 \mid T_1)\Big] \\
&\equiv \boldsymbol{E}_Q\left[\sum_{i \in \mathbf{C}} \log P'(X_i \mid T_2) + \log P'(T_2 \mid T_1)\right]
\end{aligned}$$

The last inequality result from the fact that entropy conditioned on less variables can only increase. The final equivalence is a result of the construction of the M-Step of IB-EM, where $Q$ is used when in the optimization of the parameters of $P'$. ▮

The above proposition provides a bound on the extent to which a hidden variable induces correlations in the marginal distribution. The result is intuitive — the contribution of insertion of a new hidden variable cannot exceed the entropy of its children given their current hidden parent. If we use the bound instead of the original term, we get an over-optimistic estimate of the potential profitability of adding a new hidden variable. However, the scenarios we are interested in are those in which the information between the hidden variable and its children is high and the entropy of the hidden variable is low (or there would be no need for it in the network). In such cases, we can expect the bound to be tight in both inequalities.

The above bound provides us with an information signal for putative new hidden variables. In practice, searching for the best subset $\mathbf{C}$ can be impractical even for relatively small networks. Instead, we use the following greedy approach: first, for each hidden variable, we limit our attention to up to $K$ (we use 20) of its children with the highest entropy individually. We then consider *all*

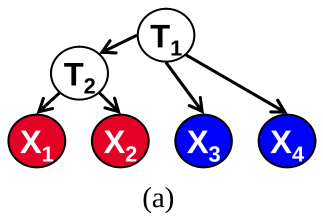

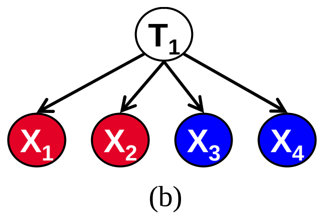

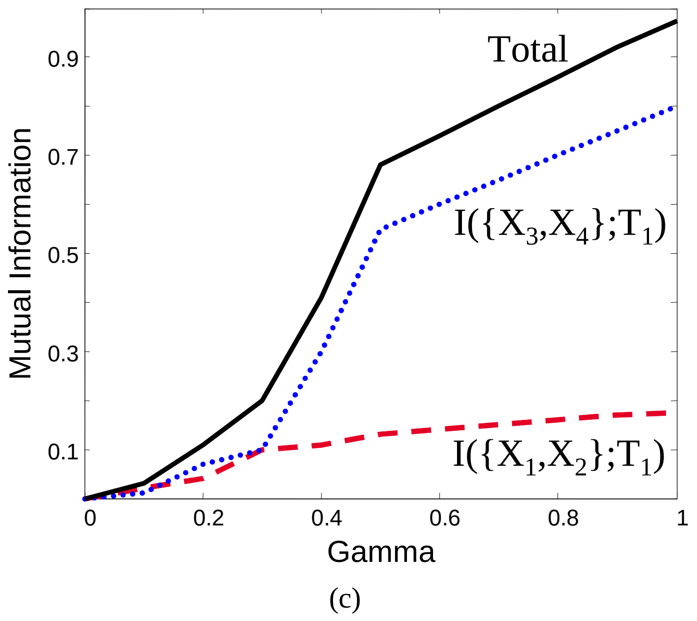

Figure 6.13: Synthetic example demonstrating the information signal for adding new hidden variables. (a) shows the original structure that generated the samples. (b) shows the structure used in learning without the hidden variable $T_2$. (c) shows the information as a function of $\gamma$ between the hidden variables and the observed variables. As learning progresses, the total information rises and the distribution of the direct children of $T_1$ is captured significantly better (dotted). The information with the original children of $T_2$ (dashed) remains small.

three-node subsets of these children whose entropy level passes some threshold (see details in the experiments below). Intuitively, such seeds will capture the core of the signal needed to attract other nodes when structure change is allowed.[1]

Another complication in using the above signal is a consequence of the annealing process itself. For small values of $\gamma$ we can expect, and indeed we want, $Q$ to smooth out all statistical signals. This will make most subsets appear equally appealing for adding a hidden variable, since $T_1$ will not be informative about them. In Section 6.3, we have shown that $\boldsymbol{I}_Q(Y;T)$ is a natural measure for the progress of the continuation process. To demonstrate the phenomenon in the structure learning scenario, Figure 6.13 shows a simple synthetic experiment where the samples were generated from the structure shown in (a) and a Naive Bayes model without $T_2$ was used when learning. (c) shows the information between the hidden variable $T_1$ and the observed children (solid), its direct children in the generating distribution (dotted) and the children of $T_2$ (dashed). Up to some point in the annealing process, the information content of the hidden variable is low and the information with both subsets of variables is low. When the hidden variable starts to capture the distribution of

[1]In synthetic experiments for different structures where the network size still made computations feasible, these three node seeds always included two or three variables of the optimal larger subset.

the observed variables, the two subsets diverge and while $T_1$ captures its original direct children significantly better, the children of $T_2$ still have high entropy given $T_1$. Thus, we want to start considering our information "cue" only when the hidden parent becomes meaningful, that is only when $\boldsymbol{I}_Q(Y;T_1)$ passes some threshold.

Finally, we note that although the discussion so far assumed that we have a Naive Bayes model and considered the addition of a single new hidden variable, it is easily generalized for any forms of $P$ where in $P'$ we separate a hidden variables in $P$ from its observed children by introducing a new hidden variable.

To summarize, our approach for learning a new hidden variable $T$ (or several such variables) is as follows: At each value of $\gamma$, we first evaluate $\boldsymbol{I}_Q(Y;T)$ to determine if it is above the threshold, signifying that the hidden variable is capturing some of the distribution over the rest of the variables. If this is the case, we greedily search for subsets of children of the hidden variable that have high entropy. These are subsets that are not predicted well by their hidden parent. For the subset with the highest entropy, we suggest a putative new hidden variable that is the parent of the variables in the subset. The purpose of this new variable is to improve the prediction of the subset variables, which are not sufficiently explained by the current model. We then continue with the parameter estimation and structure learning procedure as is. If, after structure search, a hidden variable has at most one child, it is in fact redundant and can be removed from the structure. We iterate the entire procedure until no more hidden variable are added and the structure learning procedure converges.

## 6.11 Full Learning — Experimental Validation

We want to evaluate the effectiveness of our method when learning structure with and without the introduction of new hidden variables into the model. We examined two real-life data sets: The Stock dataset and the Yeast dataset (see Section 6.6). For the Yeast dataset we look at a subset of 62 experiments related to heat conditions and Nitrogen depletion.

In Figure 6.14 we consider average test set performance on the Stock dataset. To create a baseline for hierarchy performance, we train a Naive hierarchy with a single hidden variable and cardinality of 3 totaling 122 parameters. We start by evaluating structure learning without the introduction of new hidden variables. To do this, we generated 25 random hierarchies with 5 binary hidden variables that are parents of the observed variables and a common root parent totaling 91 parameters. We then use Structural EM [Friedman, 1997] to adapt the structure by using a *replace-parent* operator where at each local step an observed node can replace its hidden parents. As can be seen in Figure 6.14, standard structure learning applied to the IB-EM framework significantly improves the model's performance. In fact, many of the 25 random runs with the Search operator surpass the performance of the Naive model using fewer parameters.

Next, we evaluate the ability of the new hidden variable enrichment operator to improve the

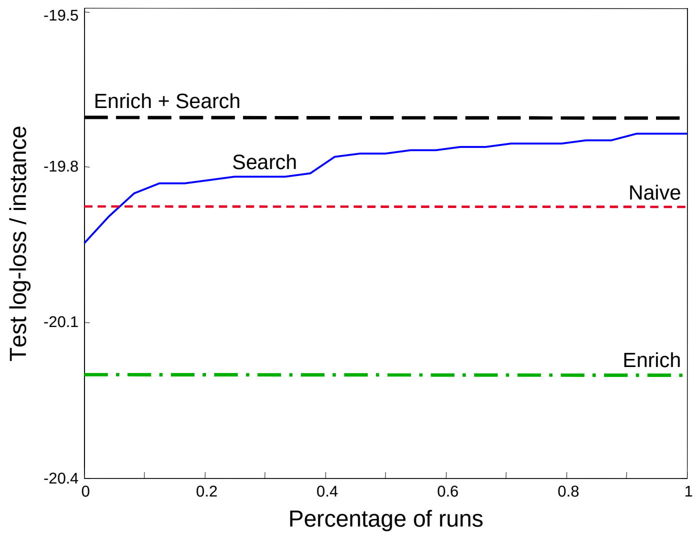

Figure 6.14: Comparison of performance on the Stock data set of Naive hierarchy (Naive), 25 hierarchies with replace-parent search (Search) , hierarchy learned with enrichment operator (Enrich) and hierarchy learned with enrichment and replace-parent search (Enrich+).

model. We denote by Enrich the IB-EM run with the automatic enrichment operator. We denote by Enrich+Search the run with this operator augmented with structure search operators in the M-steps. As can be seen in Figure 6.14, the performance of Enrich by itself was not able to compete with the Naive or the Search method. This is not surprising as we cannot expect the information signal to introduce "perfect" hidden variables into the hierarchy. Indeed, when combining the enrichment operator with structure adaptation (Enrich+Search), our method was able to exceed all other runs. The learned hierarchy had only two hidden variables (requiring only 85 parameters). These results show the enrichment operator effectively added useful hidden variables and that the ability to adapt the structure of the network is crucial for utilizing these hidden variables to the best extent.

There are two thresholds used by our algorithm for learning new hidden variables. First, as noted in Section 6.10, due to the nature of the annealing process we consider adding new hidden variable only when the information $\boldsymbol{I}_Q(Y;T)$ of a hidden variable $T$ in the current structure passes some threshold. In the results presented in this section we use a threshold of 20% of the maximum value the information can reach which is limited by the cardinality of $T$. Lowering this threshold to as far as 10% or raising it to 40% had negligible effect on the results. We hypothesize that this robustness is caused by the fact that, typically, the cardinality of $T$ will be much lower than $Y$. Thus, when $T$ undergoes the transition from being redundant to being informative, its information content rises drastically, even if it captures only a small aspect of $Y$.

The threshold used to limit the number of candidate subsets, however, is more interesting. Recall from Section 6.10 that the greedy procedure only considers subsets whose entropy passes some

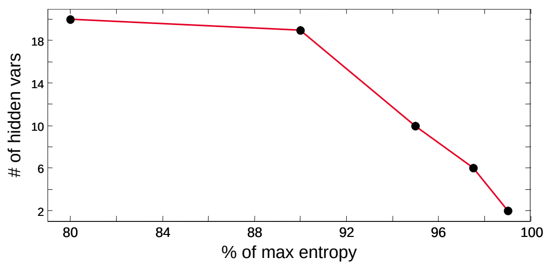

(a)

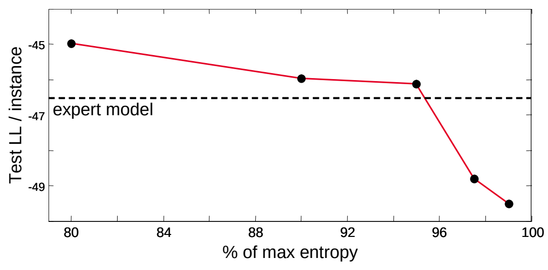

(b)

Figure 6.15: Learning new hidden variables for the Yeast data set. (a) shows the number of variables learned as a function of the threshold on the percentage of entropy of a subset used in the greedy procedure. (b) shows the corresponding test set log-likelihood per instance performance and the performance of the model supplied by the biological expert.

threshold. More precisely, we consider only subsets whose entropy passes some percentage of the maximum entropy possible for this subset. Thus, using a lower threshold potentially allows more hidden variables. This is observed empirically in Figure 6.15(a) for the Yeast dataset. A possible concern is that lowering the threshold too much will results in many hidden variables leading to overfitting. However, as is evident in Figure 6.15(b), even when the number of hidden variables is 20, these new variables are effective in that they improve the generalization performance on unseen test data. In fact, with just a few extra variables, our method successfully surpassed the performance of the structure supplied by the biological expert. Obviously, at some point, having too many variables will lead to overfitting. We could not examine this scenario due to the running time required to learn such large networks.

To qualitatively assess the value of our method, we show in Figure 6.16 the structure learned for the Stock dataset with binary variables and the entropy threshold set at 95% (structures at 92.5% and 97.5% were almost identical for this dataset). The emergent structure is evident with the "High-tech giants" and "Internet" group dominating the model. The "Varied" group contains "Canon" and "Sony" that manufacture varied technology products such as electronics, photographic, computer peripheral, etc. The "Japanese" relation of "Toyota" to these companies was interestingly stronger than the relation to the "Car" group.

Finally, we applied runs that combine both automatic cardinality adaptation and enrichment of the structure with new hidden variables. Table 6.2 shows the train and test performance for the Stock dataset. Shown are several runs with the Enrich operator and fixed cardinality. For each run, the number of hidden variables added during the learning process (excluding the initial root node) is noted. Also shown is the automatic cardinality method using the BDe score along with the different cardinalities of the 6 hidden variables introduced into the network structure. The combined method was able to surpass the best of the fixed cardinality models in terms of test set performance with fewer than 70% of the parameters. In addition, the fact that the combined method improves test

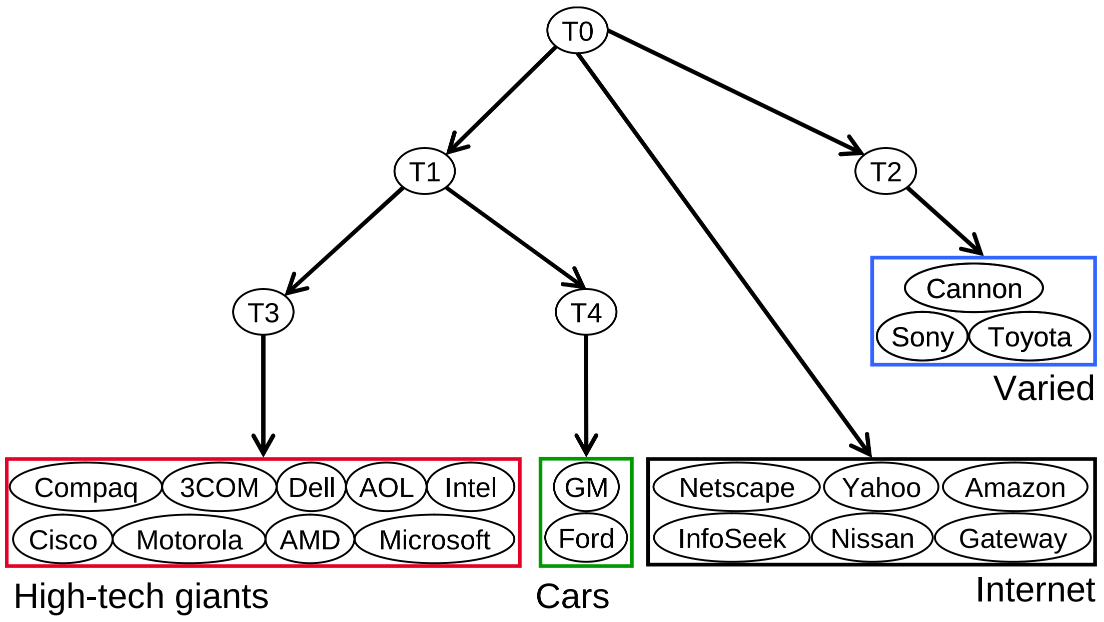

Figure 6.16: Structure learned for the Stock dataset using the enrichment operator augmented with structure search that use the replace-parent operator. All the hidden variables (circles) are binary and the subset entropy threshold was set at 95%. The children of each leaf are annotated with a plausible interpretation.

performance but has worse training likelihood, demonstrates its ability to avoid overfitting.

## 6.12 Related Work

To define the IB-EM algorithm, we introduced a formal relation between the Information Bottleneck (IB) target Lagrangian and the EM functional. This allowed us to formulate an information-theoretic regularization for our learning problem. Given this objective, we used two central ideas to make learning feasible. First, following all annealing methods, we slowly diminish the level of “perturbation” as a way to reach a solution of the hard objective. Second, we use continuation to define a stable traversal from an easy problem to our goal problem.

A multitude of regularization forms are used in machine learning, typically depending on the specific form of the target function (see Bishop [1995] and references within). Information-theoretic regularization has been used for classification with partially labeled data by Szummer and Jaakkola [2002] and for general scenarios in Deterministic annealing [Rose, 1998].

Of the annealing methods, the well known *Simulated annealing* [Kirkpatrick et al., 1983] is least similar to ours. Rather than changing the form of the objective function, Simulated annealing allows the search procedure to make “downhill” moves with some diminishing probability. This

| Cardinality | Log-likelihood Train | Test | # of hiddens | # of parameters |
|---|---|---|---|---|
| 2 | -19.62 | -19.62 | 5 | 89 |
| 3 | -19.32 | -19.37 | 5 | 146 |
| 5 | -18.87 | -19.04 | 6 | 304 |
| 10 | **-18.53** | **-18.96** | **5** | **769** |
| 20 | -18.43 | -18.98 | 5 | 2340 |
| BDe (9,6,7,7,7,7) | **-18.65** | **-18.94** | **6** | **526** |

Table 6.2: Effect of cardinality when inserting new hidden variables into the network structure with the Enrich operator for the Stock dataset. A 95% entropy threshold was used for the hidden variable discovery algorithm. The table shows results for several fixed cardinalities as well as the automatic cardinality method using the BDe score. Shown is the log-likelihood per instance for training as well as test data, the number of hidden variables and the number of parameters in the model. For the automatic method, the cardinalities of each hidden variable is noted.

changes the way the procedure traverses the search space and allows it to potentially reach previously unattainable solutions. Several papers [Heckerman et al., 1994, Chickering, 1996b, Elidan et al., 2002] have shown that Simulated annealing is not effective when learning Bayesian networks.

*Weight annealing* [Elidan et al., 2002], on the other hand, skews the target function directly by perturbing the weights of instances in diminishing magnitudes. Thus, like our method it changes the form of $Q$ directly but does not use an information-theoretic regularization. Weight annealing can actually be applied to a wider variety of problems than our method, including structure search with complete data. However, like other annealing methods, it requires a cooling scheme. For the large problems with hidden variables we explored in this paper, Weight annealing proved inferior with similar running times, and impractical with the settings of Elidan et al. [2002].

Finally, like our method, Deterministic annealing [Rose, 1998] alters the problem by explicitly introducing an information-theoretic regularization term. Specifically, following the widely recognized *maximum entropy principle* [Jaynes, 1957], deterministic annealing penalizes the objective with a term that is the entropy of the model. A concrete application of deterministic annealing to graphical models was suggested by Ueda and Nakano [1998]. However, when learning graphical models, the deterministic annealing was not found to be superior to standard EM (e.g., [Smith and Eisner, 2004]).[2] In particular, Whiley and Titterington [2002], Smith and Eisner [2004]) show why applying deterministic annealing to standard unsupervised learning of Bayesian networks with hidden variables is problematic. One possible explanation for why our method works well for these methods is the difference in motivation of the regularization term. Specifically, our term was motivated by the need for generalization where one want to compress the identity of specific instances.

[2]Smith and Eisner [2004] also suggest a variant of the deterministic annealing algorithm that appears to work well but is only applicable in the context of semi-supervised learning or when an initial informed starting point for the EM algorithm is at hand.

Another important difference between the two methods is that, like Weight annealing, deterministic annealing requires the specification of a cooling policy which makes it potentially impractical for large generative problems. This problem may be avoided using a method similar to the one we used in this work. We leave this prospect as well as the challenge of better understanding the relation between the entropy and information regularization terms for future study.

Continuation methods are a well developed field in mathematics [Watson, 2000]. While these methods are used extensively and successfully to solve practical engineering challenges such as complex polynomial systems, they have not been frequently used in machine learning. Recently, Corduneanu and Jaakkola [2002] used continuation to determine a beneficial balance between labeled and unlabeled data. To our knowledge this is the first work in learning graphical models to use continuation to traverse from an easy solution to the desired maximum likelihood problem.

A complementary aspect of our work is the introduction of modification operators for hidden variables. Our method both for learning the cardinality of a hidden variable, and for introducing new hidden variables into the network structure, relies on the annealing process and utilizes emergent signals. The problem of evaluating the cardinality of a hidden variable in a graphical model was explored in several works (*e.g.*, Chang and Fung [1990], Elidan and Friedman [2001]). The work of Stolcke and Omohundro [1993] for HMMs was the first to use evaluation of pairwise state merges to determine adapt the cardinality. In Elidan and Friedman [2001], we extend their method for general Bayesian networks, and Slonim et al. [2002] used a similar approach within the Information Bottleneck framework. All of these methods start with a large number of states, and then apply bottom-up agglomeration to merge overlaps in the state space and reduce redundancies. By contrast, our method is able to take an "add-when-needed" approach and state mergers are evaluated not to collapse states but rather to determine if a new one is needed. Several papers also explored methods for introducing new hidden variables into the network structure, either for specific classes of Bayesian networks (*e.g.*, Martin and VanLehn [1995], Spirtes et al. [1993], Zhang [2004]) or for general models using a structural signature approach [Elidan et al., 2001]. Our contribution in enriching the structure with new hidden variables is twofold. First, we suggested a natural information signature as a "cue" for the presence of a hidden variable. Unlike the structural signature this signature is flexible and is able to weight the influence of different child nodes. Second, we use the enrichment approach in conjunction with the continuation approach for bypassing local maxima. As in cardinality learning, we are able to utilize emergent signals allowing the introduction of new hidden variables into simpler models rendering them more effective.

## 6.13 Discussion and Future Work

In this chapter we addressed the challenge of learning models with hidden variables in real-life scenarios. We presented a general approach for learning the parameters of hidden variables in

Bayesian networks and introduced model selection operators that allow learning of new hidden variables and their cardinality. We showed that the method achieves significant improvement on challenging real-life problems.

The contribution of this chapter is threefold. First, we made a formal connection between the objective functionals of the Information Bottleneck framework [Tishby et al., 1999, Friedman et al., 2001] and maximum likelihood learning for graphical models. The Information Bottleneck and its extensions are originally viewed as methods to understand the structure of a distribution. We showed that in some sense the Information Bottleneck and maximum likelihood estimation are two sides of the same coin. The Information Bottleneck focuses on the distribution of variables in each instance, while maximum likelihood focuses on the projection of this distribution on the estimated model. This understanding extends to general Bayesian networks the recent results of Slonim and Weiss [2002] that relate the original Information Bottleneck and maximum likelihood estimation in univariate mixture distributions.

Second, the introduction of the IB-EM principle allowed us to use an approach that starts with a solution at $\gamma = 0$ and progresses toward a solution in the more complex landscape of $\gamma = 1$. This general scheme is common in *Deterministic annealing* approaches [Rose, 1998, Ueda and Nakano, 1998]. These approaches "flatten" the posterior landscape by raising the likelihood to the power of $\gamma$. The main technical difference of our approach is the introduction of a regularization term that is derived from the structure of the approximation of the probability of the latent variables in each instance. This was combined with a continuation method for traversing the path from the trivial solution at $\gamma = 0$ to a solution at $\gamma = 1$. Unlike standard approaches in Deterministic annealing and Information Bottleneck, our procedure can automatically detect important regions where the solution changes drastically and ensure that they are tracked closely. In preliminary experiment the continuation method was clearly superior to standard annealing strategies.

Third, we introduced model enrichment operators for inserting new hidden variables into the network structure and adapting their cardinality. These operators were specifically geared toward utilizing the emergent cues resulting from the annealing procedure. This resulted in models that generalize better and achieve equivalent or better results with a relatively simple model.

The methods presented here can be extended in several directions. First, we can improve the introduction of new hidden variables into the structure by formulating better "signals" that can be efficiently calculated for larger clusters. Second, we can use alternative variational approximations as well as adaptive approximation during the learning process. Third, we want to explore methods for stopping at $\gamma < 1$ as an alternative way for improving generalization performance.

## Chapter 7

# The "Ideal Parent" method for Continuous Variable Networks

Up until now, we were mostly concerned with learning new hidden variables and coping with the difficulties of attaining a favorable model in the presence of multiple local maxima. In real-life domains, we might have to start by facing the more fundamental problem of computational complexity. This is particularly true when learning networks with continuous variables and varied conditional probability distributions, which are being used in a wide range of applications, including fault detection (*e.g.,* [U. Lerner and Koller, 2000]), modeling of biological systems (*e.g.,* [Friedman et al., 2000]) and medical diagnosis (*e.g.,* [Shwe et al., 1991]). Just as in Chapter 6 we addressed the problem on learning hidden variables in conjunction with the problem of local maxima, in this chapter we address the problem of hidden variables in conjunction with the problem of computational complexity, when applied to networks with continuous variables.

When learning probabilistic graphical models, the task of structure learning is particularly demanding. As discussed in Chapter 2, this task is typically treated as a combinatorial optimization problem. This problem is typically addressed by heuristic search procedures, such as greedy hill climbing, that traverses the space of candidate structure. Even this greedy approach can be extremely time consuming due to the time required to score each candidate structure, particularly in the presence of missing data or hidden variables. The situation can be even more acute if we want to learn networks with continuous variables: If we limit ourselves to networks with *linear Gaussian* conditional probability distributions [Geiger and Heckerman, 1994], we can use sufficient statistics to summarize the data, as is the case for discrete variables, and use a closed form equation to evaluate the score of candidate families. In general, however, we are also interested in non-linear interactions. These do not have sufficient statistics, and require costly parameter optimization to evaluate the score of a candidate family. These difficulties severely limit the applicability of standard heuristic structure search procedures to rich non-linear models.

We present a general method for speeding search algorithms for structure learning in continuous variable networks. Our method can be applied to many forms of a unimodal parametric conditional distribution, including the linear Gaussian model as well as many non-linear models. The ideas are inspired from the notion of *residues* in regression [McCullagh and Nelder, 1989], and involve the notion of “ideal parents”. For each variable, we construct an *ideal parent profile* of a new hypothetical parent that would lead to the best possible prediction of the variable. We then use this profile to efficiently select potential candidate parents that have a similar profile of values. Using basic principles, we derive a similarity measure that can be computed efficiently and that approximates the improvement in score that will result from the addition of a candidate parent. This provides us with a fast method for scanning many potential parents and focus more careful evaluation (exact scoring) to a smaller number of promising candidates.

The ideal parent profiles we construct during search also provide new leverage on the problem of introducing new hidden variables during structure learning. Basically, if the ideal parent profiles of several variables are sufficiently similar, and are not similar to one of their current parents, we can consider adding a new hidden parents for all these variables. The ideal profile allows us to estimate the impact this new variable will have on the score, and suggest the values it takes in each instance. Thus, our method provides a guided approach for introducing new variables during search, and allows to contrast this with alternative search steps in a computationally efficient manner.

## 7.1 The “Ideal parent” Concept

We start with the task of speeding up the structure search algorithm for a Bayesian network with continuous variables. The complexity of any such algorithm is rooted in the need to score each candidate structure change, which in turn may require non-linear parameter optimization. Thus, we want to somehow efficiently approximate the benefit of each candidate and score only the most promising of these. The manner in which this will help us to discover new hidden variables will become evident in Section 7.3.

### 7.1.1 Basic Framework

Consider adding $Z$ as a new parent of $X$ whose current parents in the network are $\mathbf{U}$. Given a training data $\mathcal{D}$ of $M$ instances, to evaluate the change in score, when using the BIC score (see Section 2.3.2), we need to compute the change in the log-likelihood (see Section 2.2.1)

$$\Delta_{X|\mathbf{U}}(Z) = \ell_X(\mathbf{U} \cup \{Z\}, \theta' : \mathcal{D}) - \ell_X(\mathbf{U}, \theta : \mathcal{D}) \tag{7.1}$$

where $\theta$ are the current maximum likelihood parameters for the family of $X$, and $\theta'$ are the maximum likelihood parameters after the addition of $Z$. The change in the BIC score is this difference combined with the change in the model complexity penalty terms. Thus, to evaluate this difference, we need to compute the maximum likelihood parameters $X$ given the new choice of parents. Our goal is to speed up this computation.

The basic idea of our method is straightforward — for a given variable, we want to construct a hypothetical “ideal parent” $Y$ that would best predict the variable. We will then compare each existing candidate parent $Z$ to this imaginary one using a similarity measure $C(\vec{y}, \vec{z})$ (which we instantiate below) and fully score only the most promising candidates. In order for this approach to be beneficial, we will want the similarity score to approximate the actual change in likelihood defined in Eq. (7.1).

**Conditional Probability Distribution**

To make our discussion concrete, we focus on networks where we represent $X$ as a function of its parents $\mathbf{U} = \{U_1, \ldots, U_k\}$ with a conditional probability distribution (CPD) that has the following general form:

$$X = g(\alpha_1 \mathbf{u}_1, \ldots, \alpha_k \mathbf{u}_k : \theta) + \epsilon \tag{7.2}$$

where $g$ is a *link function* that integrates the contributions of the parents with additional parameters $\theta$, $\alpha_i$ that are scale parameters applied to each of the parents, and $\epsilon$ that is a noise random variable with zero mean. In here, we assume that $\epsilon$ is Gaussian with variance $\sigma^2$.

When the function $g$ is the sum of its arguments, this CPD is the standard linear Gaussian CPD. However, we can also consider non-linear choices of $g$. For example,

$$g(\alpha_1 \mathbf{u}_1, \ldots, \alpha_k \mathbf{u}_k : \theta) \equiv \theta_1 \frac{1}{1 + e^{-\sum_i \alpha_i u_i}} + \theta_0 \tag{7.3}$$

is a sigmoid function where the response of $X$ to its parents’ values is saturated when the sum is far from zero.

**Likelihood Function**

Given the above form of CPDs, we can now write a concrete form of the log-likelihood function

$$\begin{aligned}
\ell_X(\mathbf{U}, \theta : \mathcal{D}) &= -\frac{1}{2} \sum_{m=1}^{M} \left[ \log(2\pi) + \log(\sigma^2) + \frac{1}{\sigma^2}(x[m] - g(\mathbf{u}[m]))^2 \right] \\
&= -\frac{1}{2} \left[ M \log(2\pi) + M \log(\sigma^2) + \frac{1}{\sigma^2} \sum_m (x[m] - g(\mathbf{u}[m]))^2 \right]
\end{aligned}$$

where, for simplicity, we absorbed each coefficient $\alpha_j$ into each value of $u_j[m]$. Similarly, when the new parent $Z$ is added with coefficient $\alpha_z$, the new likelihood is

$$\ell_X(\mathbf{U} \cup \{Z\}, \theta' : \mathcal{D}) = -\frac{1}{2} \left[ M \log(2\pi) + M \log(\sigma_z^2) + \frac{1}{\sigma_z^2} \sum_m (x[m] - g(\mathbf{u}[m], \alpha_z z[m]))^2 \right]$$

Consequently, the difference in likelihood of Eq. (7.1) takes the form of

$$\begin{aligned}\Delta_{X|\mathbf{U}}(Z) = & -\frac{M}{2}\left[\log\sigma_z^2 - \log\sigma^2\right] \\ & -\frac{1}{2}\left[\frac{1}{\sigma_z^2}\sum_m (x[m]-g(\mathbf{u}[m],\alpha_z z[m]))^2 - \frac{1}{\sigma^2}\sum_m (x[m]-g(\mathbf{u}[m]))^2\right]\end{aligned} \tag{7.4}$$

**The “Ideal Parent”**

We now define the ideal parent for $X$

**Definition 7.1.1:** Given a dataset $\mathcal{D}$, and a CPD for $X$ given its parents $\mathbf{U}$, with a link function $g$ and parameters $\theta$ and $\alpha$, the *ideal parent* $Y$ of $X$ is such that for each instance $m$,

$$x[m] = g(\alpha_1 u_1[m], \ldots, \alpha_k u_k[m], y[m] : \theta) \tag{7.5}$$

▮

Under mild conditions, the *ideal parent profile* (i.e., value of $Y$ in each instance) can be computed for almost any unimodal parametric conditional distribution. The only requirement from $g$ is that it should be invertible w.r.t. each one of the parents. Note that in this definition, we implicitly assume that $x[m]$ lies in the image of $g$. If this is not the case, we can substitute $x[m]$ with $x_g[m]$, the point in $g$’s image closest to $x[m]$. This guarantees that the prediction’s mode for the current set of parents and parameters is as close as possible to $X$.

The resulting profile for the hypothetical ideal parent $Y$ is the optimal set of values for the $k+1$’th parent, in the sense that it would maximize the likelihood of the child variable $X$. This is true since by definition, $X$ is equal to the mode of the function of its parents defined by $g$. Intuitively, if we can efficiently find a candidate parent $Z$ that is similar to the hypothetically optimal parent, we can improve the model by adding an edge from this parent to $X$. We are now ready to instantiate the similarity measure $C(\vec{y},\vec{z})$. Below, we demonstrate how this is done for the case of a linear Gaussian CPD. We extend the framework for non-linear CPDs in Section 7.5.

### 7.1.2 Linear Gaussian

Let $X$ be a variable in the network with a set of parents $\mathbf{U}$, and a *linear Gaussian* conditional distribution. In this case, $g$ in Eq. (7.2) takes the form

$$g(\alpha_1\mathbf{u}_1, \ldots, \alpha_k\mathbf{u}_k : \theta) \equiv \sum_i \alpha_i\mathbf{u}_i + \theta_0$$

To choose promising candidate parents for $X$, we start by computing the ideal parent $Y$ for $X$ given its current set of parents. This is done by inverting the linear link function $g$ with respect to this additional parent $Y$ (note that we can assume, without loss of generality, that the scale parameter of this additional parent is 1). This results in

$$y[m] = x[m] - \sum_j \alpha_j u_j[m] - \theta_0 \tag{7.6}$$

We can summarize this in vector notation, by using $\vec{x} = \langle x[1], \ldots, x[M] \rangle$, and so we get

$$\vec{y} = \vec{x} - \mathcal{U}\vec{\alpha}$$

where $\mathcal{U}$ is the matrix of parent values on all instances, and $\vec{\alpha}$ is the vector of scale parameters.

Having computed the *ideal parent profile*, we now want to efficiently evaluate its similarity to the profile of candidate parents. Intuitively, we want the similarity measure to reflect the likelihood gain by adding $Z$ as a parent of $X$. Ideally, we want to evaluate $\Delta_{X|\mathbf{U}}(Z)$ for each candidate parent $Z$. However, instead of reestimating all the parameters of the CPD after adding $Z$ as a parent, we approximate this difference by only fitting the scaling factor associated with the new parent and freezing all other parameters of the CPD (the coefficient parameters of the current parents $\mathbf{U}$ and the variance parameter $\sigma$).

**Theorem 7.1.2** *Suppose that $X$ has parents $\mathbf{U}$ with a set $\vec{\alpha}$ of scaling factors. Let $Y$ be the ideal parent as described above, and $Z$ be some candidate parent. Then the change in the log-likelihood of $X$ in the data, when adding $Z$ as a parent of $X$, while freezing all parameters except the scaling factor of $Z$, is*

$$\begin{aligned} C_1(\vec{y}, \vec{z}) &\equiv \max_{\alpha_Z} \ell_X(\mathbf{U} \cup \{Z\}, \theta \cup \{\alpha_Z\} : \mathcal{D}) - \ell_X(\mathbf{U}, \theta : \mathcal{D}) \\ &= \frac{1}{2\sigma^2} \frac{(\vec{y} \cdot \vec{z})^2}{\vec{z} \cdot \vec{z}} \end{aligned}$$

**Proof:** In the linear Gaussian case $y[m] = x[m] - g(\mathbf{u}[m])$ by definition and $g(\mathbf{u}[m], \alpha_z z[m]) = g(\mathbf{u}[m]) + \alpha_z z[m]$ so that Eq. (7.4) can be written as

$$\begin{aligned} \Delta_{X|\mathbf{U}}(Z) &= -\frac{M}{2}\left[\log \sigma_z^2 - \log \sigma^2\right] - \frac{1}{2}\left[\frac{1}{\sigma_z^2}\sum_m (y[m] - \alpha_z z[m])^2 - \frac{1}{\sigma^2}\sum_m y[m]^2\right] \\ &= -\frac{M}{2}\left[\log \sigma_z^2 - \log \sigma^2\right] - \frac{1}{2}\left[\frac{1}{\sigma_z^2}\left(\vec{y} \cdot \vec{y} - 2\alpha_z \vec{z} \cdot \vec{y} + \alpha_z^2 \vec{z} \cdot \vec{z}\right) - \frac{1}{\sigma^2}\vec{y} \cdot \vec{y}\right] \end{aligned} \tag{7.7}$$

Since $\sigma_z = \sigma$ this reduces to

$$\begin{aligned} \Delta_{X|\mathbf{U}}(Z : \alpha_z) &\equiv \ell_X(\mathbf{U} \cup \{Z\}, \theta \cup \{\alpha_Z\} : \mathcal{D}) - \ell_X(\mathbf{U}, \theta : \mathcal{D}) \\ &= -\frac{1}{2\sigma^2}\left(-2\alpha_z \vec{z} \cdot \vec{y} + \alpha_z^2 \vec{z} \cdot \vec{z}\right) \end{aligned} \tag{7.8}$$

To optimize our only free parameter $\alpha_z$, we use

$$\frac{\partial \Delta_{X|\mathbf{U}}(Z:\alpha_z)}{\partial \alpha_z} = -\frac{1}{2\sigma^2}\left(-2\vec{z}\cdot\vec{y} + 2\alpha_z \vec{z}\cdot\vec{z}\right) = 0 \quad \Rightarrow \quad \alpha_z = \frac{\vec{z}\cdot\vec{y}}{\vec{z}\cdot\vec{z}}$$

Plugging this into Eq. (7.8), we get

$$\begin{aligned} C_1(\vec{y},\vec{z}) &\equiv \max_{\alpha_z} \Delta_{X|\mathbf{U}}(Z:\alpha_z) \\ &= -\frac{1}{2\sigma^2}\left(-2\frac{\vec{z}\cdot\vec{y}}{\vec{z}\cdot\vec{z}}\vec{z}\cdot\vec{y} + \left(\frac{\vec{z}\cdot\vec{y}}{\vec{z}\cdot\vec{z}}\right)^2 \vec{z}\cdot\vec{z}\right) \\ &= \frac{1}{2\sigma^2}\frac{(\vec{z}\cdot\vec{y})^2}{\vec{z}\cdot\vec{z}} \end{aligned}$$

The form of the similarity measure can be even further simplified

**Proposition 7.1.3** *Let $C_1(\vec{y},\vec{z})$ be as defined above and let $\sigma$ be the maximum likelihood parameter* before *$Z$ is added as a new parent of $X$. Then*

$$C_1(\vec{y},\vec{z}) = \frac{M}{2}\frac{(\vec{y}\cdot\vec{z})^2}{(\vec{z}\cdot\vec{z})(\vec{y}\cdot\vec{y})} = \frac{M}{2}\cos^2\phi_{\vec{y},\vec{z}}$$

*where $\phi_{\vec{y},\vec{z}}$ is the angle between the ideal parent profile vector $\vec{y}$ and the candidate parent profile vector $\vec{z}$.*

**Proof:** To recover the maximum likelihood parameter of $\sigma$ we differentiate the log-likelihood function as written in Eq. (7.4)

$$\begin{aligned} \frac{\partial \ell_X(\mathbf{U},\theta:\mathcal{D})}{\partial \sigma^2} &= -\frac{M}{2\sigma^2} + \frac{1}{\sigma^4}\sum_m (x[m]-g(\mathbf{u}[m]))^2 = 0 \\ &\Rightarrow \sigma^2 = \frac{1}{M}\sum_m (x[m]-g(\mathbf{u}[m]))^2 = \frac{1}{M}\vec{y}\cdot\vec{y} \end{aligned}$$

where the last equality follows from the definition of $\vec{y}$. The result follows immediately by plugging this into Theorem 7.1.2 and the fact that $\cos^2\phi_{\vec{y},\vec{z}} \equiv \frac{(\vec{y}\cdot\vec{z})^2}{(\vec{z}\cdot\vec{z})(\vec{y}\cdot\vec{y})}$ ∎

Thus, there is an intuitive geometric interpretation to the measure $C_1(\vec{y},\vec{z})$: we prefer a profile $\vec{z}$ that is similar to the ideal parent profile $\vec{y}$, regardless of its norm: It can easily be shown that $\vec{z} = c\vec{y}$ (for any constant $c$) maximizes this similarity measure. We retain the less intuitive form of $C_1(\vec{y},\vec{z})$ in Theorem 7.1.2 for compatibility with later developments.

Note that, by definition, $C_1(\vec{y},\vec{z})$ is a *lower bound* on $\Delta_{X|\mathbf{U}}(Z)$, the improvement on the log-likelihood by adding $Z$ as a parent of $X$: When we add the parent we optimize all the parameters, and so we expect to attain a likelihood as high, or higher, than the one we attain by freezing some of the parameters. This is illustrated in Figure 7.1(a) that plots the true likelihood improvement

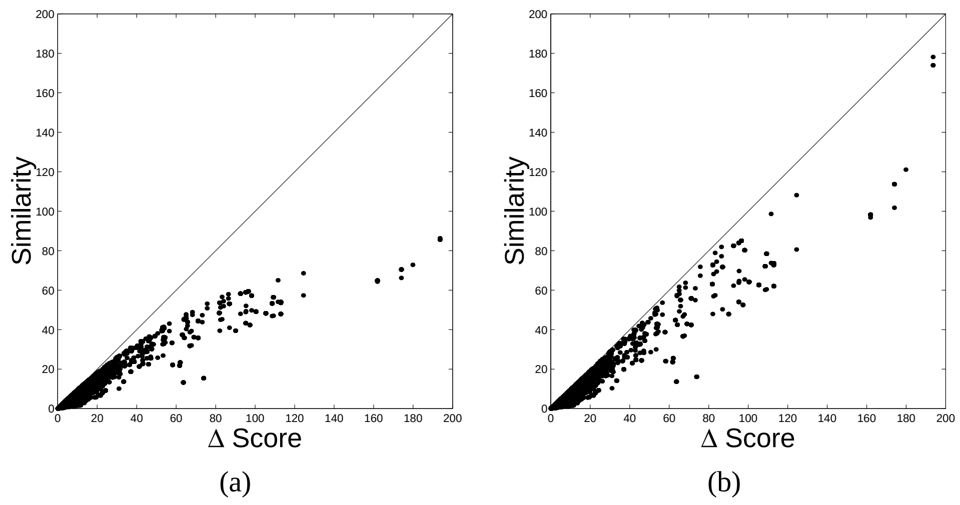

Figure 7.1: Demonstration of the (a) $C_1$ and (b) $C_2$ bounds for linear Gaussian CPDs. The $x$-axis is the true change in score as a result of an edge modification. The $y$-axis is the lower bound of this score. Points shown correspond to several thousand edge modifications in a run of the ideal parent method on real-life Yeast gene expressions data.

vs. $C_1$ for several thousand edge modifications taken from an experiment using real life Yeast gene expression data (see Section 7.6).

We can get a better lower bound by optimizing additional parameters. In particular, after adding a new parent, the errors in predictions change, and so we can readjust the variance term. As it turns out, we can perform this readjustment in closed form.

**Theorem 7.1.4** *Suppose that $X$ has parents $\mathbf{U}$ with a set $\vec{\alpha}$ of scaling factors. Let $Y$ be the ideal parent as described above, and $Z$ be some candidate parent. Then the change in the log-likelihood of $X$ in the data, when adding $Z$ as a parent of $X$, while freezing all other parameters except the scaling factor of $Z$ and the variance of $X$, is*

$$\begin{aligned} C_2(\vec{y},\vec{z}) &\equiv \max_{\alpha_Z,\sigma} \ell_X(\mathbf{U}\cup\{Z\},\theta\cup\{\alpha_Z\}:\mathcal{D}) - \ell_X(\mathbf{U},\theta:\mathcal{D}) \\ &= -\frac{M}{2}\log\sin^2\phi_{\vec{y},\vec{z}} \end{aligned}$$

*where $\phi_{\vec{y},\vec{z}}$ is the angle between $\vec{y}$ and $\vec{z}$.*

**Proof:** To optimize $\sigma_z$ we again consider Eq. (7.4) and set

$$\frac{\partial\Delta_{X|\mathbf{U}}(Z)}{\partial\sigma_z} = -\frac{M}{\sigma_z} + \frac{1}{\sigma_z^3}\left[\vec{y}\cdot\vec{y} - 2\alpha_z\vec{z}\cdot\vec{y} + \alpha_z^2\vec{z}\cdot\vec{z}\right] = 0$$

Solving for $\sigma_z$ and plugging the maximum likelihood parameter $\alpha_z$ from the development of $C_1(\vec{y},\vec{z})$, we get

$$\sigma_z^2 = \frac{1}{M}\left[\vec{y}\cdot\vec{y} - 2\alpha_z \vec{z}\cdot\vec{y} + \alpha_z^2 \vec{z}\cdot\vec{z}\right] = \frac{1}{M}\left[\vec{y}\cdot\vec{y} - \frac{(\vec{z}\cdot\vec{y})^2}{\vec{z}\cdot\vec{z}}\right]$$

As we have shown above $\sigma = \frac{1}{M}\vec{y}\cdot\vec{y}$ and similarly the variance term $\sigma_z^2$ "absorbs" the sum of squared errors when optimized. Thus, the second term in Eq. (7.4) becomes zero and we can write

$$\begin{aligned} C_2(\vec{y},\vec{z}) &= -\frac{M}{2}\left[\log(\sigma_z^2) - \log(\sigma^2)\right] \\ &= \frac{M}{2}\log\left(\frac{\vec{y}\cdot\vec{y}}{\vec{y}\cdot\vec{y} - \frac{(\vec{z}\cdot\vec{y})^2}{\vec{z}\cdot\vec{z}}}\right) = \frac{M}{2}\log\left(\frac{1}{1 - \frac{(\vec{z}\cdot\vec{y})^2}{(\vec{z}\cdot\vec{z})(\vec{y}\cdot\vec{y})}}\right) = \frac{M}{2}\log\left(\frac{1}{1-\cos^2\phi_{\vec{y},\vec{z}}}\right) \\ &= -\frac{M}{2}\log\sin^2\phi_{\vec{y},\vec{z}} \end{aligned}$$

∎

It is important to note that both $C_1$ and $C_2$ are monotonic functions of $\frac{(\vec{y}\cdot\vec{z})^2}{\vec{z}\cdot\vec{z}}$, and so they consistently rank candidate parents of the same variable. However, when we compare changes that involve different ideal parents, such as adding a parent to $X_1$ compared to adding a parent to $X_2$, the ranking by these two measures might differ. And so, $C_2$ can provide better guidance to some search algorithms since

$$C_1(\vec{y},\vec{z}) \le C_2(\vec{y},\vec{z}) \le \Delta_{X|\mathbf{U}}(Z)$$

This that this is true due to the choice of parameters we freeze in each of these measures. Indeed, Figure 7.1(b) clearly shows that $C_2$ is a tighter bound than $C_1$, particularly for promising candidates.

## 7.2 Ideal Parents in Search

The technical developments of the previous section show that we can approximate the score of candidate parents for $X$ by comparing them to the ideal parent $Y$ using the similarity measure. Is this approximate evaluation useful?

When performing a local heuristic search, at each iteration we have a current candidate structure and we consider some operations on that structure. These operations might include edge addition, edge replacement, edge reversal and edge deletion. We can readily use the ideal profiles and similarity measures developed to speed up two of these: edge addition and edge replacement. In a network with $N$ nodes, there are in the order of $O(N^2)$ possible edge additions, $O(E\cdot N)$ edge replacement where $E$ is the number of edges in the model, and only $O(E)$ edge deletions and reversals. Thus our method can be used to speed up the bulk of edge modifications considered by a typical search algorithm.

When considering adding an edge $Z \to X$, we use the ideal parent profile for $X$ and compute its similarity to $Z$. We repeat this for every other candidate parent for $X$. We then compute the full score only for the K most similar candidates, and insert them (and the associated change in score) to a queue of potential operations. In a similar way, we can utilize the ideal parent profile for considering edge replacement for $X$. Suppose that $U_i \in \mathbf{U}$ is a parent of $X$. We can define the ideal profile for replacing $U$ while freezing all other parameters of the CPD of $X$.

**Definition 7.2.1:** Given a dataset $\mathcal{D}$, and a CPD for $X$ given its parents $\mathbf{U}$, with a link function $g$, parameters $\theta$ and $\alpha$, the *replace ideal parent* $Y$ of $X$ and $U_i \in \mathbf{U}$ is such that for each instance $m$,

$$x[m] = g(\alpha_1 u_1[m], \ldots, \alpha_{i-1}u_{i-1}, \alpha_{i+1}u_{i+1}, \ldots, \alpha_k u_k[m], y[m] : \theta) \tag{7.9}$$

▮

The rest of the developments of the previous section remain the same. For each current parent of $X$ we compute a separate ideal profile - one corresponding to replacement of that parent with a new one. We then use the same policy as above for examining replacement of each one of the parents.

For both operations, we can tradeoff between the accuracy of our evaluations and the speed of the search, by changing $K$, the number of candidate changes per family for which we compute a full score. Using $K = 1$, we only score the best candidate according to the ideal parent method ranking, thus achieving the largest speedup, However, since our ranking only approximates the true score difference, this strategy might miss good candidates. Using higher values of $K$ brings us closer to the standard search algorithm both in terms of move selection quality but also in terms of computation time.

In the experiments in Section 7.6, we integrated the changes described above into a greedy hill climbing heuristic search procedure. This procedure also examines moves that remove an edge and reverse and edge, which we evaluate in the standard way. The greedy hill climbing procedure applies the best available move at each iteration (among those that were chosen for full evaluation) as in Algorithm 1. The ideal parent method is independent of the specifics of the search procedure and simply pre-selects promising candidates for the search algorithm to consider.

## 7.3 Adding New Hidden Variables

Somewhat unexpectingly, the “ideal parent” method also offer a natural solution to the difficult challenge that is in the heart of this thesis - that of detecting new hidden variables. Specifically, the ideal parent profiles provide a straightforward way to find when and where to add hidden variables to the domain in continuous variable networks. The intuition is fairly simple: if the ideal parents of several variables are similar to each other, then we know that a similar input is predictive of all of them. Moreover, if we do not find a variable in the network that is close to these ideal parents, then we can consider adding a new hidden variable that will serve as their combined input, and, in addition, have an informed initial estimate of its profile.

To introduce a new hidden variable, we would like to require that it will be beneficial for several children at once. The difference in log-likelihood due to adding a new parent with profile $\vec{z}$ is the sum of differences between the log-likelihoods of families it is involved in:

$$\Delta_{X_1,\ldots,X_L}(Z) = \sum_i^L \Delta_{X_i|\mathbf{U}_i}(Z)$$

where we assume, without loss of generality, that the members of the cluster are $X_1, \ldots, X_L$. To score the network with $Z$ as a new hidden variable, we also we need to deal with the difference in the complexity penalty term, and the likelihood of $Z$ variable as a root variable. These terms, however, can be readily evaluated. The difficulty is in finding the profile $\vec{z}$ that maximizes $\Delta_{X_1,\ldots,X_L}(Z)$. Using the ideal parent approximation, we can lower bound this improvement by

$$\sum_i^L C_1(\vec{y}_i, \vec{z}) \equiv \sum_i^L \frac{1}{2\sigma_i^2} \frac{(\vec{z} \cdot \vec{y}_i)^2}{\vec{z} \cdot \vec{z}} \leq \Delta_{X_1,\ldots,X_L}(Z) \tag{7.10}$$

and so we want to find $\vec{z^*}$ that maximizes this bound. We will then use this optimized bound as our approximate cluster score. That is we want to find

$$\vec{z^*} = \arg\max_{\vec{z}} \sum_i \frac{1}{2\sigma_i^2} \frac{(\vec{z} \cdot \vec{y}_i)^2}{\vec{z} \cdot \vec{z}} \equiv \arg\max_{\vec{z}} \frac{\vec{z}^T \mathcal{Y}\mathcal{Y}^T \vec{z}}{\vec{z}^T \vec{z}} \tag{7.11}$$

where $\mathcal{Y}$ is the matrix whose columns are $y_i/\sigma_i$. $\vec{z^*}$ must lie in the *column span* of $\mathcal{Y}$ since any component orthogonal to this span increases the denominator of the right hand term but leaves the numerator unchanged, and therefore does not obtain a maximum. We can therefore express the solution as:

$$\vec{z^*} = \sum_i v_i \frac{y_i}{\sigma_i} = \mathcal{Y}\vec{v} \tag{7.12}$$

where $\vec{v}$ is a vector of coefficients. Furthermore, the objective in Eq. (7.11) is known as the *Rayleigh quotient* of the matrix $\mathcal{Y}\mathcal{Y}^T$ and the vector $\vec{z}$. The optimum of this quotient is achieved when $\vec{z}$ equals the eigenvector of $\mathcal{Y}\mathcal{Y}^T$ corresponding to its largest eigenvalue [Wilkinson, 1965]. Thus, to solve for $\vec{z^*}$ we want to solve the following eigenvector problem

$$(\mathcal{Y}\mathcal{Y}^T)\vec{z^*} = \lambda \vec{z^*}$$

Note that the dimension of $\mathcal{Y}\mathcal{Y}^T$ is $M$ (the number of instances), so that, in practice, this problem cannot be solved directly. However, by plugging in Eq. (7.12), multiplying on the right by $\mathcal{Y}$, and defining $A \equiv \mathcal{Y}^T\mathcal{Y}$, we get a reduced generalized eigenvector problem [1]

$$AA\vec{v} = \lambda A\vec{v}$$

Although this problem can now be solved directly, it can be further simplified by noting that $A$ is only singular if the residue of observations of two or more variables are linearly dependent along *all* of the training instances. In practice, for continuous variables, $A$ is indeed non-singular, and we can multiply both sides $A^{-1}$ and end up with a simple eigenvalue problem:

$$A\vec{v} = \lambda\vec{v}$$

which is numerically simpler and easy to solve as the dimension of $A$ is $L$, the number of variables in the cluster, which is typically relatively small. Once we find the $L$ dimensional eigenvector $\vec{v}^*$ with the largest eigenvalue $\lambda^*$, we can express with it the desired parent profile $\vec{z^*}$.

We can get a better bound of $\Delta_{X_1,\ldots,X_L}(Z)$ if we use $C_2$ similarity rather than $C_1$. Unfortunately, optimizing the profile $\vec{z}$ with respect to this similarity measure is a harder problem that is not solvable in closed form. Since the goal of the cluster identification is to provide a good starting point for the following iterations that will eventually adapt the structure, we use the closed form solution for Eq. (7.11). Note that once we optimized the profile $z$ using the above derivation, we can still use the $C_2$ similarity score to provide a better bound on the quality of this profile as a new parent for $X_1, \ldots, X_L$.

Now that we can approximate the benefit of adding a new hidden parent to a cluster of variables, we still need to consider different clusters to find the most beneficial one . As the number of clusters is exponential, we adapt a heuristic *agglomerative clustering* approach (*e.g.*, [Duda and Hart, 1973]) to explore different clusters. We start with each variable as an individual cluster and repeatedly merge the two clusters that lead to the best expected improvement in the BIC score (or the least decrease). This procedure potentially involves $O(N^3)$ merges, where $N$ is the number of possible variables. We save much of the computations by pre-computing the matrix $\mathcal{Y}^T\mathcal{Y}$ only once, and then using the relevant sub-matrix in each merge. In practice, the time spent in this step is insignificant in the overall search procedure.

## 7.4 Learning with Missing Values

Once we add a hidden variable to the network structure, in subsequent structure search, we have to cope with missing values, even if the original training data was complete. Similar considerations can arise if the dataset contains partial observations of some of the variables. To deal with this

[1] In the *Generalized Eigenvector Problem*, we want to find eigenpairs $(\lambda, \vec{v})$ so that $B\vec{v} = \lambda A\vec{v}$ holds.

problem, we use the Expectation Maximization approach [Dempster et al., 1977] and its application to network structure learning [Friedman, 1997] (see Section 2.4 for more details).

How can we combine the ideal parent method into this structural EM search? Since we do not necessarily observe neither $X$ nor all of its parents, the definition of the ideal parent cannot be applied directly. Instead, we define the ideal parent to be the profile that will match the expectations given $Q$. That is, we choose $y[m]$ so that

$$\boldsymbol{E}_Q[x[m] \mid \mathcal{D}_o] = \boldsymbol{E}_Q[g(\alpha_1 u_1[m], \ldots, \alpha_k u_k[m], y[m] : \theta) \mid \mathcal{D}_o]$$

In the case of linear CPDs, this implies that

$$\vec{y} = \boldsymbol{E}_Q[\vec{x} \mid \mathcal{D}_o] - \boldsymbol{E}_Q[\mathcal{U} \mid \mathcal{D}_o]\vec{\alpha}$$

Once we define the ideal parent, we can use it to approximate changes in the expected BIC score (given $Q$). For the case of a linear Gaussian, we get terms that are similar to $C_1$ and $C_2$ of Theorem 7.1.2 and Theorem 7.1.4, respectively. The only change is that we apply the similarity measure on the expected value of $\vec{z}$ for each candidate parent $Z$. This is in contrast to exact evaluation of $\boldsymbol{E}_Q\left[\Delta_{X|\mathbf{U}}Z \mid \mathcal{D}_o\right]$, which requires the computation of the expected sufficient statistics of $\mathbf{U}$, $X$, and $Z$. To facilitate efficient computation, we adopt an approximate variational *mean-field* form (*e.g.*, [Jordan et al., 1998, Murphy and Weiss, 1999]) for the posterior. This approximation is used both for the ideal parent method and the standard greedy approach used in Section 7.6. This results in computations that require only the first and second moments for each instance $z[m]$, and thus can be easily obtained from $Q$.

Finally, we note that the structural EM iterations are still guaranteed to converge to a local maximum. In fact, this does *not* depend on the fact that $C_1$ and $C_2$ are lower bounds of the true change to the score, since these measures are only used to pre-select promising candidates which are scored before actually being considered by the search algorithm. Indeed, the ideal parent method is a modular structure candidate selection algorithm and can be used as a black-box by any search algorithm.

## 7.5 Non-linear CPDs

We now address the important challenge of non-linear CPDs. In the class of CPDs we are considering, this non-linearity is mediated by the link function $g$, which we assume here to be invertible. Examples of such functions include the sigmoid function shown in Eq. (7.3) and hyperbolic functions that are suitable for modeling gene transcription regulation [Nachman et al., 2004], among many others. When we learn with non-linear CPDs, parameter estimation is harder. To evaluate a potential parent $P$ for $X$ we have to perform non-linear optimization (*e.g.*, conjugate gradient) of all of the $\alpha$ coefficients of all parents as well as other parameters of $g$. In this case, a fast approximation can boost the computational cost of the search significantly.

As in the case of linear CPDs, we compute the ideal parent profile $\vec{y}$ by inverting $g$. (We assume that the inversion of $g$ can be performed in time that is proportional to the calculation of $g$ itself as is the case for the CPDs considered above.) Suppose we are considering the addition of a parent to $X$ in addition to its current parents $\mathbf{U}$, and that we have computed the value of the ideal parent $y[m]$ for each sample $m$ by inversion of $g$. Now consider a particular candidate parent $Z$ whose value at the $m$'th instance is $Z[m]$. How will the difference between the ideal value and the value of $Z$ reflect in prediction of $X$ for this instance?

As we have seen in Section 7.1, in the linear case, the difference $z[m] - y[m]$ translated through $g$ to a prediction error. In the non-linear case, the effect of the difference on predicting $X$ depends on other factors, such as the values of the other parents. To see this, consider again the sigmoid function $g$ of Eq. (7.3). If the sum of the arguments to $g$ is close to $0$, then $g$ locally behaves like a sum of its arguments. On the other hand, if the sum is far from $0$, the function is in one of the saturated regions, and big differences in the input almost do not change the prediction. This complicates our computations and does not allow the development of similarity measures as in Theorem 7.1.2 and Theorem 7.1.4 directly.

We circumvent this problem by approximating $g$ with a linear function around the value of the ideal parent profile. We use a first-order Taylor expansion of $g$ around the value of $\vec{y}$ and write

$$g(\vec{\mathbf{u}}, \vec{z}) \approx g(\vec{\mathbf{u}}, \vec{y}) + (\vec{z} - \vec{y}) \frac{\partial g(\vec{\mathbf{u}}, \vec{y})}{\partial \vec{y}}$$

As a result, the “penalty” for a distance between $\vec{z}$ and $\vec{y}$ depends on the gradient of $g$ at the particular value of $\vec{y}$, given the value of the other parents. In instances where the derivative is small, larger deviations between $y[m]$ and $z[m]$ have little impact on the likelihood of $x[m]$, and in instances where the derivative is large, the same deviations may lead to worse likelihood.

To understand the effect of this approximation in more detail we consider a simple example with a sigmoid Gaussian CPD as defined in Eq. (7.3), where $X$ has no parents in the current network and $Z$ is a candidate new parent. Figure 7.2(a) shows the sigmoid function (dotted) and its linear approximation at $Y = 0$ (solid) for an instance where $X = 0.5$. The computation of $Y = \log\left(\frac{1}{0.5} - 1\right) = 0$ by inversion of $g$ is illustrated by the dashed lines. (b) is the same for a different sample where $X = 0.85$. In (c),(d) we can see the effect of the approximation for these two different samples on our evaluation of the likelihood function. For a given probability value, the likelihood function is more sensitive to changes in the value of $Z$ around $Y$ when $X = 0.5$ when compared to the instance $X = 0.85$. This can be seen more clearly in (e) where equi-potential contours are plotted for the sum of the approximate log-likelihood of these two instances. To recover the setup where our sensitivity to $Z$ does *not* depend on the specific instance as in the linear

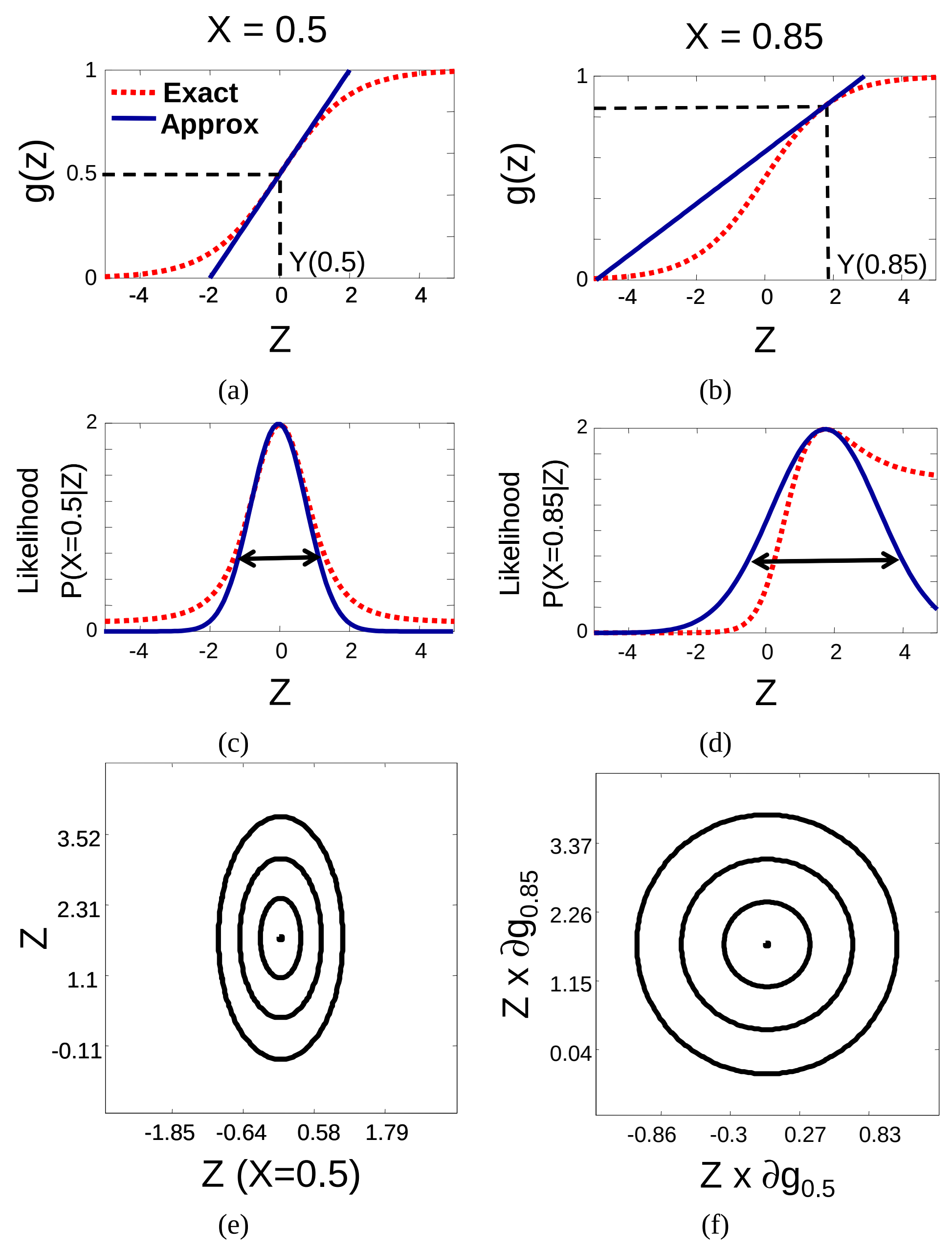

Figure 7.2: A simple example of the effect of the linear approximation for a sigmoid CPD where $X$ has no parents in the current network and $Z$ is considered as a new candidate parent. Two samples (a) and (b) show the function $g(y_1, \ldots, y_k : \theta) \equiv \theta_1 \frac{1}{1+e^{-\sum_i y_i}} + \theta_0$ for two instances where $X = 0.5$ and $X = 0.85$, respectively, along with their linear approximation at the ideal parent value $Y$ of $X$. (c) and (d) show the corresponding likelihood function and its approximation. (e) shows the equi-potential contours of the sum of the log-likelihood of the two instances as a function of the value of $Z$ in each of these instances. (f) is the same as (e) when the axis are skewed using the gradient of $g$ with respect to the value of $Y$.

case, we consider a skewed version of $Z \cdot \partial g/\partial y$ rather than $Z$ directly. The result is shown in Figure 7.2(f). We can generalize the example above to develop a similarity measure for the general non-linear case

**Theorem 7.5.1** *Suppose that $X$ has parents $\mathbf{U}$ with a set $\vec{\alpha}$ of scaling factors. Let $Y$ be the ideal parent as described above, and $Z$ be some candidate parent. Then the change in log-likelihood of $X$ in the data, when adding $P$ as a parent of $X$, while freezing all other parameters, is approximately*

$$C_1(\vec{y} \circ g'(\vec{y}), \vec{z} \circ g'(\vec{y})) - \frac{1}{2\sigma^2}(k_1 - k_2). \tag{7.13}$$

*where $g'(\vec{y})$ is the vector whose $m$'th component is $\partial g(\vec{\alpha}\mathbf{u}, y)/\partial y \mid_{\vec{\mathbf{u}}[m], y[m]}$, and $\circ$ denotes component-wise product. Similarly, if we also optimize the variance, then the change in log-likelihood is approximately*

$$C_2(\vec{y} \circ g'(\vec{y}), \vec{z} \circ g'(\vec{y})) - \frac{M}{2} \log \frac{k_1}{k_2} \tag{7.14}$$

*In both cases,*

$$k_1 = (\vec{y} \circ g'(\vec{y})) \cdot (\vec{y} \circ g'(\vec{y})) \ ; \ k_2 = (\vec{x} - g(\vec{\mathbf{u}})) \cdot (\vec{x} - g(\vec{\mathbf{u}}))$$

*do not depend on $\vec{z}$.*

Thus, we can use exactly the same measures as before, except that we “distort” the geometry with the weight vector $g'(y)$ that determines the importance of different instances. To approximate the likelihood difference, we also add the correction term which is a function of $k_1$ and $k_2$. This correction is not necessary when comparing two candidates for the same family, but is required for comparing candidates from different families, or when adding hidden values. Note that unlike the linear case, our theorem now is approximate by definition due to the linear approximation of $g$.

**Proof:** Using the general form of the Taylor linear approximation for a non-linear link function $g$, Eq. (7.4) can be written as

$$\begin{aligned}
&\Delta_{X|\mathbf{U}}(Z) \\
&\approx -\frac{M}{2}\log\frac{\sigma_z^2}{\sigma^2} - \frac{1}{2}\left[\frac{1}{\sigma_z^2}\left[\vec{x} - g(\vec{\mathbf{u}}, \vec{y}) - (\alpha_z\vec{z} - \vec{y}) \circ \partial g\right]^2 - \frac{1}{\sigma^2}\left[\vec{x} - g(\vec{\mathbf{u}})\right]^2\right] \\
&= -\frac{M}{2}\log\frac{\sigma_z^2}{\sigma^2} - \frac{1}{2\sigma_z^2}\left[\alpha_z^2(\vec{z} \circ \partial g)^2 - 2\alpha_z(\vec{z} \circ \partial g) \cdot (\vec{y} \circ \partial g) + (\vec{y}\partial g)^2\right] + \frac{1}{2\sigma^2}\left[\vec{x} - g(\vec{\mathbf{u}})\right]^2 \\
&= -\frac{M}{2}\log\frac{\sigma_z^2}{\sigma^2} - \frac{1}{2\sigma_z^2}\left[\alpha_z^2\vec{z}_\star \cdot \vec{z}_\star - 2\alpha_z\vec{z}_\star \cdot \vec{y}_\star + \vec{y}_\star \cdot \vec{y}_\star\right] + \frac{1}{2\sigma^2}\left[\vec{x} - g(\mathbf{u})\right]^2
\end{aligned} \tag{7.15}$$

where we use the fact that $\vec{x} - g(\vec{\mathbf{u}}, \vec{y}) = 0$ by construction of $\vec{y}$, and we denote for clarity $\vec{y}_\star \equiv \vec{y} \circ \partial g$

and $\vec{z}_\star \equiv \vec{z} \circ \partial g$. To optimize $\alpha_z$ we use

$$\frac{\partial \Delta_{X|\mathbf{U}}(Z)}{\partial \alpha_z} \approx -\frac{1}{2\sigma}\left[2\alpha_z \vec{z}_\star \cdot \vec{z}_\star - 2\vec{z}_\star \cdot \vec{y}_\star\right] \qquad \Rightarrow \qquad \alpha_z = \frac{\vec{z}_\star \cdot \vec{y}_\star}{\vec{z}_\star \cdot \vec{z}_\star}$$

Plugging this into Eq. (7.15) we get

$$\begin{aligned}\Delta_{X|\mathbf{U}}(Z) &\approx \frac{1}{2\sigma^2}\frac{(\vec{z}_\star \cdot \vec{y}_\star)^2}{\vec{z}_\star \cdot \vec{z}_\star} - \frac{1}{2\sigma^2}\vec{y}_\star \cdot \vec{y}_\star + \frac{1}{2\sigma^2}\left[\vec{x} - g(\vec{\mathbf{u}})\right]^2 \\ &= C_1(\vec{y}_\star, \vec{z}_\star) - \frac{1}{2\sigma^2}(k_1 - k_2)\end{aligned}$$

which proves Eq. (7.13). When we also optimize that variance, as noted before, the variance terms absorbs the sum of squared errors, so that

$$\sigma_z = \frac{1}{M}\left[\vec{y}_\star \cdot \vec{y}_\star - \frac{(\vec{z}_\star \cdot \vec{y}_\star)^2}{\vec{z}_\star \cdot \vec{z}_\star}\right]$$

Plugging this into Eq. (7.15) results in

$$\begin{aligned}\Delta_{X|\mathbf{U}}(Z) &\approx -\frac{M}{2}\log\frac{\sigma^2}{\sigma_z^2} \\ &= \frac{M}{2}\log\frac{[\vec{x} - g(\mathbf{u})]^2}{\vec{y}_\star \cdot \vec{y}_\star - \frac{(\vec{z}_\star \cdot \vec{y}_\star)^2}{\vec{z}_\star \cdot \vec{z}_\star}} = \frac{M}{2}\log\frac{[\vec{x} - g(\mathbf{u})]^2}{\vec{y}_\star \cdot \vec{y}_\star\left[1 - \frac{(\vec{z}_\star \cdot \vec{y}_\star)^2}{\vec{z}_\star \cdot \vec{z}_\star \vec{y}_\star \cdot \vec{y}_\star}\right]} \\ &= \frac{M}{2}\log\frac{1}{1 - \frac{(\vec{z}_\star \cdot \vec{y}_\star)^2}{\vec{z}_\star \cdot \vec{z}_\star \vec{y}_\star \cdot \vec{y}_\star}} + \frac{M}{2}\log\left[\vec{x} - g(\mathbf{u})\right]^2 - \frac{M}{2}\log(\vec{y}_\star \cdot \vec{y}_\star) \\ &= C_2(\vec{y}_\star, \vec{z}_\star) - \frac{M}{2}\log\frac{k_1}{k_2}\end{aligned}$$

▮

As in the linear case, the above theorem allows us to efficiently evaluate promising candidates for the *add edge* step in the structure step, and the *replace edge* step can also be approximated with minor modifications. As before, the significant gain in speed is that we only perform few parameter optimizations (that are expected to be costly as the number of parents grows), rather than $O(N)$ such optimizations.

Adding a new hidden variable with non-linear CPDs introduces further complications. We want to use, similarly to the case of a linear model, the structure score of Eq. (7.10) with the distorted $C_1$ measure. Optimizing this measure has no closed form solution in this case and we need to resort to an iterative procedure or an alternative approximation. We use an approximation where the correction terms of Eq. (7.13) are omitted so that a form that is similar to the linear Gaussian case is used, with the “distorted” geometry of $\vec{y}$. Having made this approximation, the rest of the details are the same as in the linear Gaussian case.

## 7.6 Experiments

We now examine the impact of the ideal parent method in two settings. In the first setting, we use this method for pruning the number of potential moves that are evaluated by greedy hill climbing structure search. We apply this learning procedure to complete data (and data with some missing values) to learn dependencies between the observed variables. In the second setting, we use the ideal parent method as a way of introducing new hidden variables, and also as a guide to reduce the number of evaluations when learning structure that involves hidden variables and observed ones, using a Structural EM search procedure.

In the first setting, we applied standard greedy hill climbing search (Greedy) and greedy hill climbing supplemented by the ideal parent method as discussed in Section 7.2 (Ideal). In using the ideal parent method, we used the $C_2$ similarity measure (Section 7.1) to rank candidate edge additions and replacements, and then applied full scoring only to the top $K$ ranking candidates per variable.

To evaluate the impact of the method, we start with a synthetic experiment where we know the true underlying network structure. In this setting we can evaluate the magnitude of the performance cost that is the result of the approximation we use. (We examine the speedup gain of our method on more interesting real-life examples below.) We used a network learned from real data (see below) with 44 variables. From this network we can generate datasets of different sizes and apply our method with different values of $K$. Figure 7.3 compares the ideal parent method and the standard greedy procedure for linear Gaussian CPDs (left column) and sigmoid CPDs (right column). Using $K = 5$ is, as we expect, closer to the performance of the standard greedy method both in terms of training set [(a),(e)] and test set [(b),(f)] performance then $K = 2$. For linear Gaussian CPDs test performance is essentially the same for both methods. Using sigmoid CPDs we can see a slight advantage for the standard greedy method. When considering the percent of true edges recovered [(c),(g)], as before, the standard method shows some advantage over the ideal method with $K = 5$. However, by looking at the total number of edges learned [(d),(h)], we can see that the standard greedy method achieves this by using close to 50% more edges than the original structure for sigmoid CPDs. Thus, advantage in performance comes at a high complexity price (and as we demonstrate below, at a significant speed cost).

We now examine the effect of the method on learning from real-life datasets. We base our datasets on a study that measures the expression of the baker’s yeast genes in 173 experiments [Gasch et al., 2000]. In this study, researchers measured expression of 6152 yeast genes in its response to changes in the environmental conditions, resulting in a matrix of $173 \times 6152$ measurements. In the following, for practical reasons, we use two sets of genes. The first set consists of 639

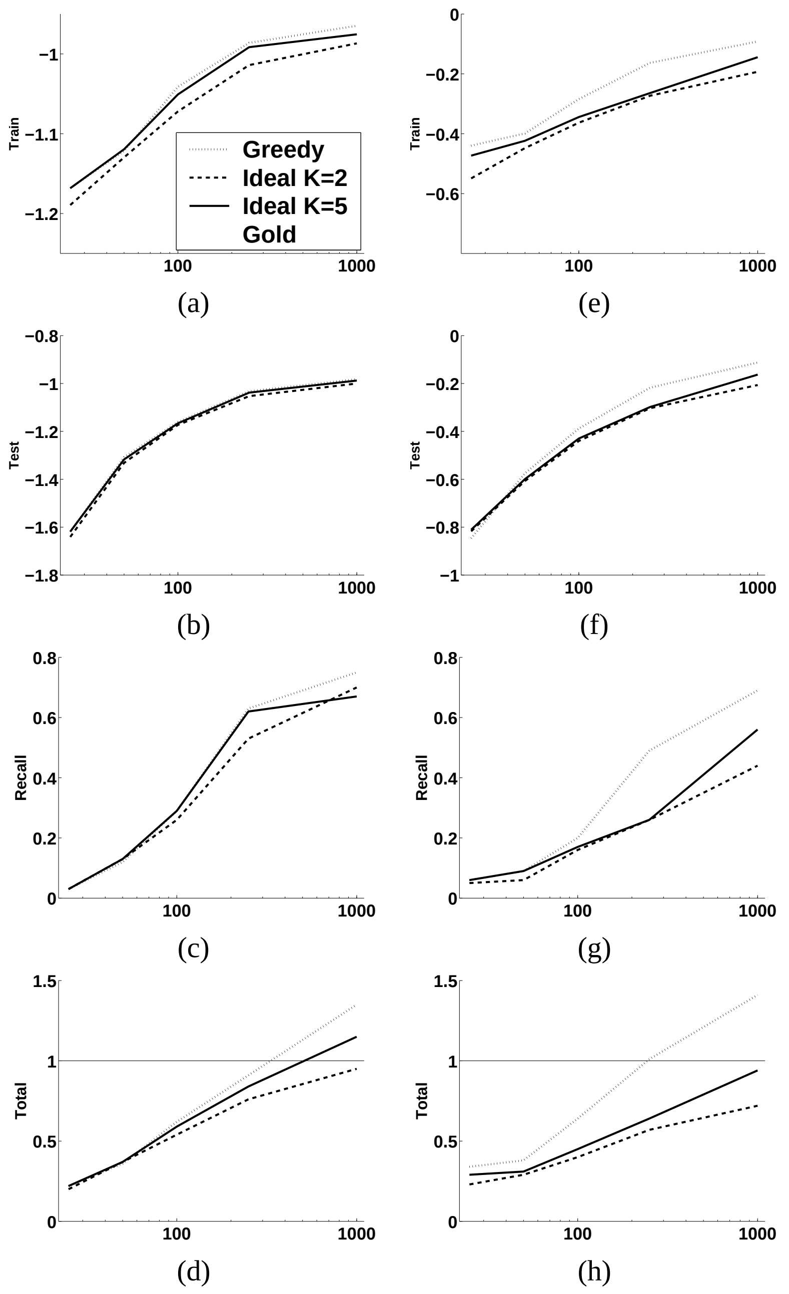

Figure 7.3: Evaluation of Ideal search on synthetic data generated from a real-life like network with 44 variables. We compare Ideal search with $K = 2$ (dashed) and $K = 5$ (solid), against the standard Greedy procedure (dotted). The figures show, as a function of the number of instances ($x$-axis), for linear Gaussian CPDs: (a) average training log likelihood per instance per variable; (b) same for test; (c) fraction of true edges obtained in learned structure; (d) total number of edges learned as fraction of true number of edges. (e)-(h) same for sigmoid CPDs.

| | | | Ideal $K = 2$ vs Greedy | | | | | | Ideal $K = 5$ vs Greedy | | | | | |
|---|---|---|---|---|---|---|---|---|---|---|---|---|---|---|
| Dataset | vars | inst | train | test | edge | move | eval | sp | train | test | edge | move | eval | sp |
| Linear Gaussian with complete data | | | | | | | | | | | | | | |
| AA | 44 | 173 | -0.024 | 0.006 | 87.1 | 96.5 | 3.6 | 2 | -0.008 | 0.007 | 94.9 | 96.5 | 9.3 | 2 |
| AA Cond | 173 | 44 | -0.038 | 0.082 | 92.2 | 92.6 | 1.2 | 2 | -0.009 | 0.029 | 96.9 | 98.2 | 2.9 | 2 |
| Met | 89 | 173 | -0.033 | -0.024 | 88.7 | 91.5 | 1.6 | 3 | -0.013 | -0.016 | 94.5 | 96.9 | 4.4 | 2 |
| Met Cond | 173 | 89 | -0.035 | -0.015 | 91.3 | 98.0 | 1.0 | 2 | -0.007 | -0.023 | 98.9 | 98.5 | 2.4 | 2 |
| Linear Gaussian with missing values | | | | | | | | | | | | | | |
| AA | 354 | 173 | -0.101 | -0.034 | 81.3 | 95.2 | 0.4 | 5 | -0.048 | -0.022 | 90.7 | 96.0 | 0.9 | 5 |
| AA Cond | 173 | 354 | -0.066 | -0.037 | 74.7 | 87.5 | 0.4 | 14 | -0.033 | -0.021 | 86.3 | 101.1 | 1.6 | 11 |
| Sigmoid with complete data | | | | | | | | | | | | | | |
| AA | 44 | 173 | -0.132 | -0.065 | 49.7 | 59.4 | 2.0 | 38 | -0.103 | -0.046 | 60.4 | 77.6 | 6.1 | 18 |
| AA Cond | 173 | 44 | -0.218 | 0.122 | 62.3 | 76.7 | 1.0 | 36 | -0.150 | 0.103 | 73.7 | 79.4 | 2.3 | 21 |
| Met | 89 | 173 | -0.192 | -0.084 | 47.9 | 58.3 | 0.9 | 65 | -0.158 | -0.059 | 56.6 | 69.8 | 2.6 | 29 |
| Met Cond | 173 | 89 | -0.207 | -0.030 | 60.5 | 69.5 | 0.8 | 53 | -0.156 | -0.042 | 69.8 | 77.7 | 2.2 | 29 |

Table 7.1: Performance comparison of the Ideal parent search with $K = 2$, $K = 5$ and Greedy on real data sets. *vars* - number of variables in the dataset; *inst* - the number of instances in the dataset; *train* - average difference in training set log-likelihood per instance per variable; *test* - same for test set; *edges* - percent of edges learned by Ideal with respect to those learned by Greedy. *moves* - percent of structure modifications taken during the search; *eval* - percent of moves evaluated; *speedup* - speedup of Ideal over greedy method. All numbers are averages over 5 fold cross validation sets.

genes that participate in general metabolic processes (Met), and the second is a subset of the first with 354 genes which are specific to amino acid metabolism (AA). We choose these sets since part of the response of the yeast to changes in its environment is in altering the activity levels of different parts of its metabolism. For some of the experiments below, we focused on subsets of genes for which there are no missing values, consisting of 89 and 44 genes, respectively). On these datasets we can consider two tasks. In the first, we treat genes as variables and experiments as instances. The learned networks indicate possible regulatory or functional connections between genes [Friedman et al., 2000]. A complementary task is to treat the 173 experiments as variables (Cond). In this case the network encodes relationships between different conditions.

In Table 7.1 we summarize differences between the Greedy search and the Ideal search with $K$ set to 2 and 5, for the linear Gaussian CPDs as well as sigmoid CPDs. Since the $C_2$ similarity is only a lower bound of the $BIC$ score difference, we expect the candidate ranking of the two to be different. As most of the difference comes from freezing some of the parameters, a possible outcome is that the Ideal search is less prone to over-fitting. Indeed as we see, though the training set log likelihood in most cases is lower for Ideal search, the test set performance is only marginally different than that of the standard greedy method, and often surpasses it.

Of particular interest is the tradeoff between accuracy and speed when using the ideal parent method. In Figure 7.4 we examine this tradeoff in four of the data sets described above using linear Gaussian and sigmoid CPDs. For both types of CPDs, the performance of the ideal parent method approaches that of Greedy as $K$ is increased. As we can expect, in both types of CPDs the ideal

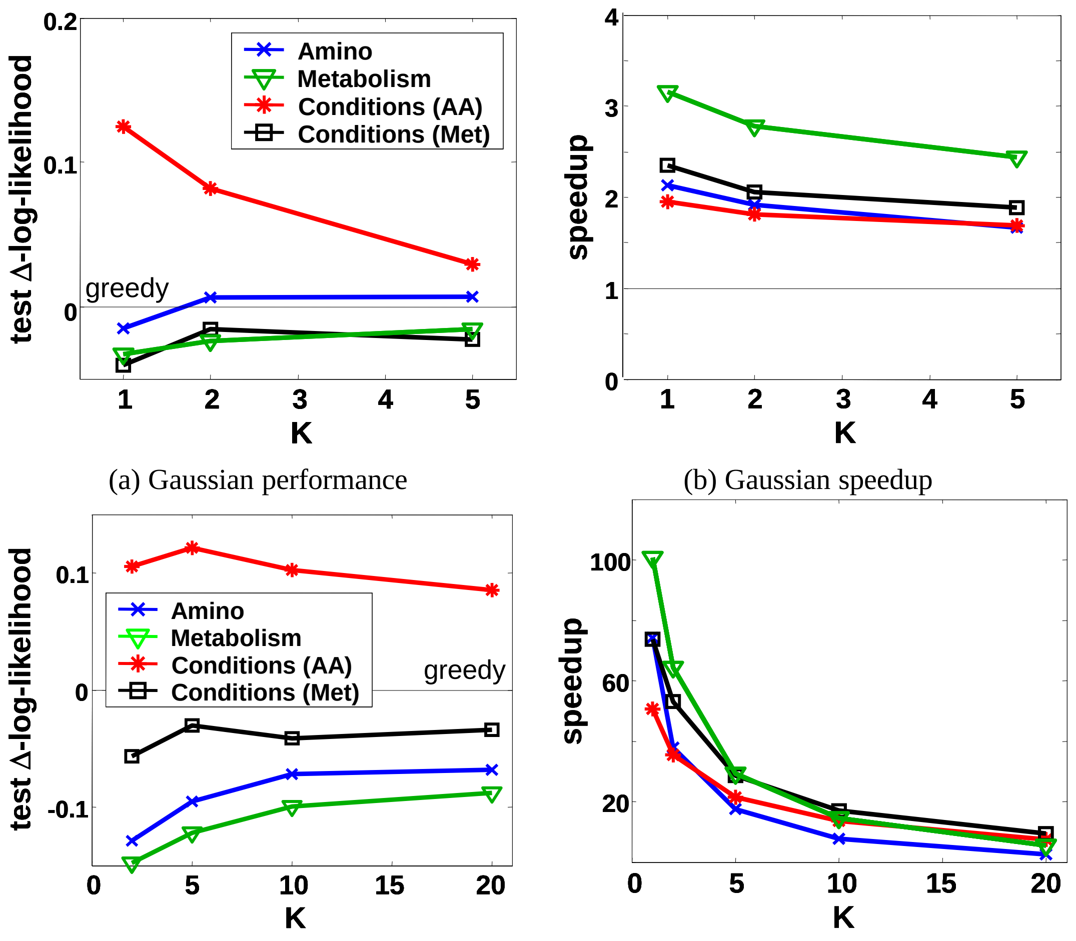

(a) Gaussian performance (b) Gaussian speedup

(c) sigmoid performance (d) sigmoid speedup

Figure 7.4: Evaluation of Ideal search on real-life data using 5-fold cross validation. (a) average difference in log likelihood per instance on test data when learning with linear Gaussian CPDs relative to the Greedy baseline ($y$-axis) vs. the number of ideal candidates for each family $K$ ($x$-axis). (b) Relative speedup over Greedy ($y$-axis) against $K$ ($x$-axis). (c),(d) same for sigmoid CPDs.

parent method is faster even for $K = 5$. However, the effect on total run time is much more pronounced when learning networks with non-linear CPDs. In this case, most of the computation is spent in optimizing the parameters for scoring candidates. And so, reducing the number of candidates evaluated results in a dramatic effect. This speedup in non-linear networks makes previously “intractable” real-life learning problems (like gene regulation network inference) more accessible.

In the second experimental setting, we examine the ability of our algorithm to learn structures that involve hidden variables and introduce new ones during the search. In this setting, we focus on *two layered networks* where the first layer consists of hidden variables, all of which are assumed to be roots, and the second layer consists of observed variables. Each of the observed variables is a

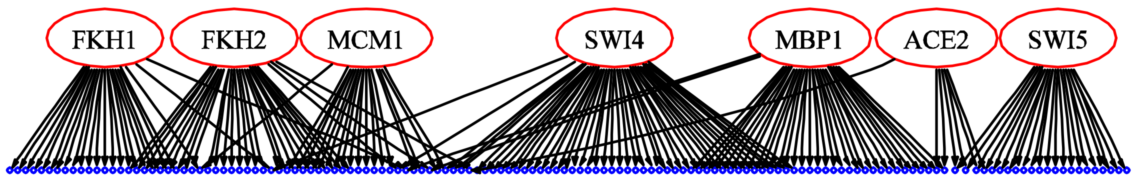

(a)

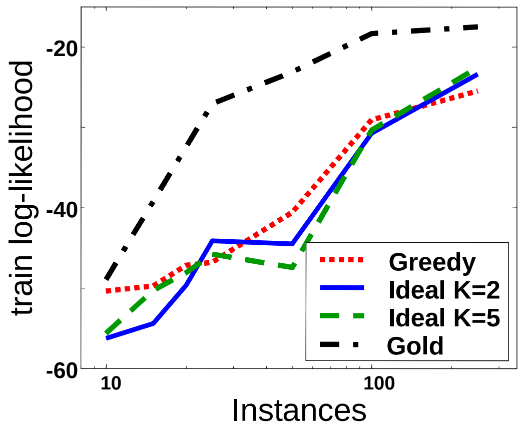

(b)

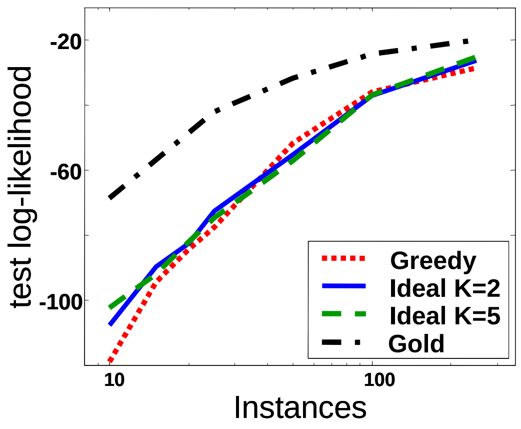

(c)

Figure 7.5: Evaluation of performance in two-layer network experiments using synthetic data generated from the Gold structure with 141 variables shown in (a), which was curated by a biological expert. (b) average log likelihood per instance on *training* data ($y$-axis) for Greedy , Ideal search with $K = 2$ and Ideal search with $K = 5$, when learning with linear Gaussian CPDs against the number of training samples ($x$-axis). (c) Same for *test* set.

leaf and can depend on one or more hidden variables. Learning such networks involves introducing different hidden variables, and determining for each observed variable which hidden variables it depends on.

To test the performance of our algorithm, we used a network topology that is curated [Nachman et al., 2004] from biological literature for the regulation of cell-cycle genes in yeast. This network involves 7 hidden variables and 141 observed variables. We learned the parameters for the network from a cell cycle gene expression dataset [Spellman et al., 1998]. From the learned network we then sampled datasets of varying sizes, and tried to recreate the regulation structure using either greedy search or ideal parent search. In both search procedures we introduce hidden variables in a gradual manner. We start with a network where a single hidden variable is connected as the only parent to all observed variables. After parameter optimization, we introduce another hidden variable - either as a parent of all observed variables (in greedy search), or to members of the highest scoring cluster (in ideal parent search, as explained in Section 7.3). We then let the structure search modify

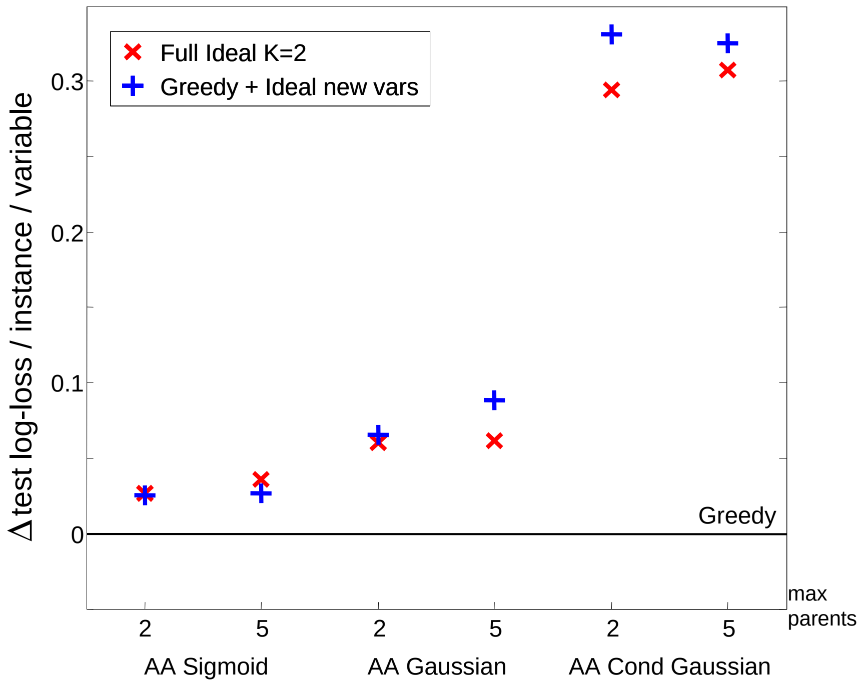

Figure 7.6: Structure learning of bipartite networks where the parents are new hidden variables and the children are the observed variables. The different datasets of the baker’s Yeast include: AA with 44 variables for both Gaussian and sigmoid Gaussian CPDs; AA Cond with 173 variables and Gaussian CPDs. For each datasets a structure with up to 2 and 5 parents was considered. Shown are the test log-likelihood per instance per variable relative to the baseline of the standard greedy structure learning algorithm.

edges (subject to the two-layer constraints) until no beneficial moves are found, at which point we introduce another hidden variable, and so on. The search terminates when it is no longer beneficial to add a new variable.

Figure 7.5 shows the performance of the ideal parent search and the standard greedy procedure as a function of the number of instances, for linear Gaussian CPDs. As can be seen, although there are some differences in training set likelihood, the performance on test data is essentially the same. Thus, as in the case of the yeast experiments considered above, there was no degradation of performance due to the approximation made by our method.

We then considered the application of the algorithms to real-life datasets. Figure Figure 7.6 shows the test set results for several of the datasets of the baker’s yeast [Gasch et al., 2000] described above, for both Gaussian and sigmoid Gaussian CPDs. The full ideal parent method (blue ’+’) with $K = 2$ and the ideal method for adding new hidden variables is consistently better than the baseline greedy procedure. To demonstrate that the improvement is in large part due to the guided method for adding hidden variables we also ran the baseline greedy procedure for structure changes augmented with the ideal method for adding new hidden variables (red ’X’). As can be seen, the performance of this method is typically slightly better than the full ideal method, since it does not approximate the structural adaptation stage. In this setup, the only difference from the greedy baseline is the way that new hidden variables are introduced. Thus, these results support our hypothesis that the ideal method is able to introduce effective new hidden variables, that are preferable to a hidden variables that are naively introduced into the network structure.

We also considered the application of our algorithm to the real-life cell-cycle gene expression data described above with linear Gaussian CPDs. Although this data set contains only 17 samples, it is of high interest from a biological perspective to try and infer from it as much as possible on the structure of regulation. We performed leave-one-out cross validation and compared the ideal parent method with $K = 2$ and $K = 5$ to the standard greedy method. To help avoid over-fitting, we limited the number of hidden parents for each observed variable to 2. In terms of training log-likelihood per instance per variable, the greedy method is better than the ideal method by $0.4$ and $0.42$ bits per instance, for $K = 5$ and $K = 2$, respectively. However, its test log-likelihood performance is significantly worse as a result of high over-fitting of two particular instances, and is worse by $0.72$ bits per instance than the ideal method with $K = 5$ and by $0.88$ bits per instance than the ideal method with $K = 2$. As we have demonstrated in the synthetic example above, the ability of the ideal method to avoid over-fitting via a guided search, does not come at the price of diminished performance when data is more plentiful. When the observed variables were allowed to have up to 5 parents, all methods demonstrated over-fitting, which for Greedy was by far more severe.

The superiority of the sigmoid Gaussian over the Gaussian model for the AA dataset (in the order of 1 bit per instance per variable) motivates us to pursue learning of models with non-linear CPDs. We could not compare the different methods for the larger datasets as the greedy method did not complete runs given several days of CPU time. We believe that the ability of the ideal method to avoid over fitting will only increase its strength in these more challenging cases.

## 7.7 Discussion and Future Work

In this chapter we set out to learn continuous variable networks with hidden variables. Our contribution is twofold: First, we showed how to speed up structure search, particularly for non-linear conditional probability distributions. This speedup is essential as it makes structure learning feasible in many interesting real life problems. Second, we presented a principled way of introducing new hidden variables into the network structure. We used the concept of an “ideal parent” for both of these tasks and demonstrated its benefits on both synthetic and real-life biological domains. In particular, we showed that our method is able to learn new hidden variables that improve the performance. In addition, it allowed us to cope with domains where the greedy method proved too time consuming.

The unique aspect of the Ideal Parent approach is that it leverages on the parametric structure of the conditional distributions. In here, we applied this approach in conjunction with a greedy search algorithm. However, it can also be supplemented to many other search procedures, such as simulated annealing, as a way of speeding up evaluation of candidate moves. Of particular interest is how our method can help methods that inherently limit the search to promising candidates such as the “Sparse Candidate” method of Friedman et al. [1999c].

Both of the CPDs we examined are specific instances of *generalized linear models* (GLMs) [McCullagh and Nelder, 1989]. This class of CPDs uses a function $g$ that is applied to the sum of its arguments, called the *link function* in the GLM literature. However, we can also consider more complex functions, as long as they are well defined for any desired number of parents. For example, in [Nachman et al., 2004] models based on chemical reaction models are considered, where the function $g$ does not have a GLM form. An example of a two variable function of this type is:

$$g(y_1, y_2 : \theta) = \theta \frac{y_1 y_2}{(1 + y_1)(1 + y_2)}$$

We also note that GLM literature deals extensively with different forms of noise. While we focus here on the case of additive Gaussian noise, the ideas we propose here can be extended to many of these noise distributions.

Few works touched on the issue of when and how to add a hidden variable in the network structure (*e.g.,* [Elidan et al., 2001, Elidan and Friedman, 2003, Martin and VanLehn, 1995, Zhang, 2004]). Only some of these method are potentially applicable to continuous variable networks, and none have been adapted to this context. To our knowledge, this is the first method to address this issue in a general context of continuous variable networks.

Many challenges remain. First, we can further improve the speed of our method by considering the $K$ most promising candidates over *all* possible structure change rather than for each family independently. This can potentially lead to another order of magnitude speedup in the search procedure. Second, the Ideal Parent method can be combined as a plug-in for candidate selection with other innovative search procedures. Third, we want to adapt our method for additional and more complex conditional probability distributions (e.g., [Nachman et al., 2004]), and extending it to multi-modal distributions. Fourth, we want to improve the approximation for adding new hidden variables in the non-linear case. Finally, it might be possible to leverage on the connection to Generalized Linear Models for handling more elaborate noise models.

# Chapter 8

# Discussion

## 8.1 Summary

In this dissertation we have addressed the challenge of learning new hidden variables in probabilistic graphical models in general, and Bayesian network in particular. In doing so we were interested in answering three main questions:

- Whether a new hidden variable is needed?
- How a hidden variable should be integrated into the network structure?
- What cardinality should be assigned to a discrete hidden variable?

In addition, we were also concerned with the problem of local maxima that is present in practically any learning scenario of Bayesian networks, and that is particularly acute in the presence of hidden variables.

We first presented an annealing like strategy for coping with local maxima in a general setting. Our *Weight Annealing* method is based on re-weighting of samples in a gradually diminishing magnitude, and is reminiscent both of boosting algorithms and the bootstrap method. The approach is applicable for most sample based algorithms and its scope goes beyond probabilistic graphical models. We demonstrated its effectiveness both for learning Bayesian network and for an unrelated optimization problem.

In Chapter 4, we presented what is arguably the most straightforward approach for learning new hidden variables. Our *FindHidden* approach reverse engineers structural signatures that are potentially left by a hidden variable. We demonstrated how FindHidden is able to improve both the quantitative prediction and the qualitative appeal of models learned from real-life data. This approach was complemented in Chapter 5 by a simple agglomeration approach for automatically determining the cardinality of a hidden variable. We showed that this method, in conjunction with the basic FindHidden algorithm, is able to further improve the quality of the models learned.

A completely different approach for learning hidden variables is the *Information Bottleneck EM* (IB-EM) algorithm presented in Chapter 6. This approach formally relates the Information Bottleneck framework [Tishby et al., 1999] and the EM algorithm [Dempster et al., 1977]. This facilitates an annealing like continuation approach for learning the parameters of a Bayesian network with hidden variables. Furthermore, "information signatures" are used both to introduce new hidden variables into the network structure and adapt their cardinality. We generalized our framework to handle multiple hidden variables and variational approximations enabling us to cope with large scale domains. The main benefit of our construction is that it deals with the problem of learning hidden variables and local maxima concurrently. We assessed different aspects of our approach on several challenging real-life datasets and showed its effectiveness in learning state-of-the-art models.

In the final chapter, we explored a framework specifically geared toward domains with continuous variables. In this scenario, when dealing with interesting non-linear conditional probability distributions, we also face the problem of computational complexity even for relatively small networks. Our *Ideal Parent* method is able to significantly speed up structure search in this scenario by approximating the true score of candidates structures. We then allow the black-box search procedure to consider only the approximately best candidates. Importantly, the same construction also offers a guided method for inserting new continuous hidden variables into the network structure, and initializing their parameters. We demonstrated the effectiveness of the method on several complex datasets.

## 8.2 The Method of Choice

The different characteristics of the methods presented in this dissertation make them applicable in different scenarios. Thus, when approaching a new domain, we need to consider the method of choice for the particular task at hand.

Once the decision to insert a hidden variable is made, and its initial placement in the network is determined, we have several ways of proceeding to learn the best possible model. Aside from standard methods for escaping local maxima (see Chapter 2), we can augment the search procedure both with the *Weight Annealing* method of Chapter 3 and with the *Information Bottleneck* (IB-EM) framework of Chapter 6. Both of these method are similar in that they manipulate the data distribution, albeit in quite different forms. In Weight Annealing this is done directly by perturbing the weight of the training instances. In the IB-EM framework, the data distribution is regularized by an information-theoretic term that competes with the standard EM learning objective. In comparing these methods on small domains, as discussed in Chapter 6, Weight Annealing was similar in performance to IB-EM. However, the significantly slower running time of Weight Annealing made it impossible to evaluate its effectiveness on large scale problems. The source of this difference is rooted in the use of guided continuation in the IB-EM method, rather than an arbitrary cooling policy in the case of Weight Annealing. In fact, in early experiments of the IB-EM method itself, a naive annealing approach required significantly more cycles of learning to reach models that are comparable with those learned using the continuation approach. Still, *Weight Annealing* has several important merits: First, unlike IB-EM, it can be applied to the problem of structure learning of Bayesian networks even when the data is complete with effective results. Second, it is applicable to a wide range of learning problem beyond the scope of learning probabilistic graphical models. Third, it is simple to implement and can be combined with most black-box optimization algorithms.

We also presented a few possible approach for learning new hidden variables. The *FindHidden* approach of Chapter 4 is based on structural signatures and has two significant benefits: First, it can be applied to any domain, be it discrete, continuous or hybrid. Second, it is simple to implement and can be used as a modular “add-on” to the search procedure. However, there are also several drawbacks: First, the approach is rigid in nature, and is thus sensitive to the presence or absence of edges. Second, it is effective only when the structural signatures manifest. That is, the method is expected to work only when the data is not too sparse. When the number of samples relative to the number of parameters is small, we need to consider a more flexible measure for the presence of hidden variables. This is likely to occur when our domain contains many variables. It is in this same scenario that we can also expect the problem of local maxima to be more pronounced. The IB-EM method of Chapter 6 offers a measure for detecting new hidden variables that is based on “soft” information-theoretic signatures for the case of discrete hidden variables. It also copes explicitly with the problem of local maxima, via a continuation approach, and can incorporate variational approximations such as *mean field* to facilitate learning in complex domains. Just as the information bottleneck framework was recently generalized for Gaussian distributions [Chechik et al., 2003], the IB-EM framework can be theoretically generalized to the case of linear Gaussian networks, as long as we can bound the information and entropy terms. However, generalization of the Information Bottleneck to additional types of distributions requires further research. The *Ideal Parent* method of Chapter 7, is specifically geared toward networks with continuous variables, and in particular to models that use a complex conditional probability distribution such as a sigmoid. In addition to offering an appealing method for learning new hidden variables in continuous variable networks, this method also offers a significant speedup in the search procedure. This can be extremely important in complex continuous domains due to the non-linear nature of the parameter optimization procedure. In summary, when the data is relatively plentiful, using FindHidden is a simple and effective choice. In this scenario, we also expect the problem of local maxima to be less acute so that using standard methods such as random restarts should be sufficient. When the number of variables is large and the data is relatively sparse, we have to resort to more complex techniques such as IB-EM or *Ideal Parent*, depending on the type of variables in the domain.

Another choice we have to make in the case of a discrete hidden variable is how to set its cardinality. The agglomeration technique of Chapter 5, is straightforward, easy to implement, and can be used independently of the search procedure or the method by which new hidden variables are introduced. For example, it can be used in conjunction with the FindHidden algorithm for detecting new hidden variables. While the agglomeration procedure can be potentially slow, we used Markov blanket properties to significantly reduce its complexity in practice, making the procedure efficient compared to the other components of the learning procedure. Unlike the bottom up agglomeration approach, IB-EM can take advantage of the annealing process to adapt the cardinality in a top-down fashion. Aside from this, the methods are similar and both use a likelihood vs. model complexity score to determine if the cardinality of hidden variable should be changed. An important benefit that the agglomeration method offers, is that it suggests a useful starting point for the parameterization of the hidden variable. As was shown in Chapter 5, this is important in guiding the EM algorithm toward superior models. The top-down approach, on the other hand has the benefit of an “add when needed” approach offering greater robustness during the learning process. Limited experiments with IB-EM, but when the agglomeration method was used to determine the cardinality of the hidden variable, produced similar results to IB-EM’s top-down approach for determining the cardinality, but at a greater computational cost. Further research is needed in order to characterize the differences between these two approaches.

## 8.3 Previous Approaches for Learning Hidden Variables

Hidden variables can have a profound effect on how we interpret “cause” and “effect”. Consider an extremely simplistic example of a cancer domain shown in Figure 8.1, where we want to determine whether (a) smoking is a direct effect of cancer or, (b) there exists a hidden genetic tendency causing both to appear correlated. The answer to this question has been debated endlessly in U.S. courts and has monumental financial consequences. It is also of great importance in terms of our understanding of the domain. Obviously, practically any causal and statistical treatment of a domain must account for the possibility of unknown hidden variables that affect the observed entities. Consequently, it is no surprise that the importance of hidden variables in influencing and often enabling *causal identifiability* was recognized long before the ‘birth” of probabilistic graphical models in the 1980s. Hidden, or *latent* variables play an important role in many statistical models, and in particular in *Structural Equation Models* (SEM) [Wright, 1921], that have dominated causal analysis in the social and behavioral sciences in the past decades. The basic ideas formulated by these models were later extended into the more general setting of probabilistic graphical models, whether they are given a causal interpretation or not (see [Pearl, 1998] on the relation between the two frameworks).

The importance of hidden variables was also widely recognized in early research of probabilistic graphical model research [Pearl, 1988, Spirtes et al., 1993]. Pearl [2000] presents many causal constructs in which hidden variables play an integral part, and these variable are the basis of many common and empirically successful models such as *Hidden Markov Models* (e.g., [Rabiner,

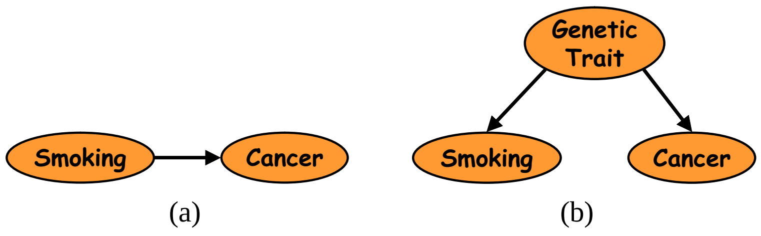

Figure 8.1: Two plausible causal networks: In (a), a Smoking is a direct cause of Cancer. In (b), a common hidden genetic trait influences the tendency both to smoke and to have cancer.

1990]), as well as various clustering models (e.g., [Duda and Hart, 1973]). As in statistics, it is usually assumed that the decision of whether to include a hidden variable into the model or not, is a preprocessing step that relies on expert prior knowledge. Techniques such as the *Structural EM* algorithm [Friedman, 1997], allow manipulation of the structure with a hidden variable in such a scenario. This can enable us to learn useful models even if the prior knowledge about the hidden variable is not precise.

The fundamental question addressed in this dissertation, however, is more demanding. The question of whether it is worthwhile to deal with hidden variables of which we have no knowledge, has received little attention. Not surprisingly, the first works to tackle this challenge treat Bayesian networks as causal models. In our work we have taken a more pragmatic approach to hidden variables, and refrain from causal interpretation of the graph structure. Yet, it is worthwhile to note some of these works, several of which can be applied directly to a Bayesian network, whether it is interpreted causally, or solely as an independence map. The question of determining the cardinality of a hidden variable has been given significantly more attention as it inherently arises in common tasks such as clustering. We discussed the most relevant of these methods in Chapter 5, and elaborate here only on methods for learning new hidden variables.

In theory, the full Bayesian framework (e.g., [Cooper and Herskovits, 1992, Heckerman et al., 1995a]) is all we need for learning networks with hidden variables: We can consider a probability distribution over all possible sets of parameters and structures, as well as the number of hidden variables and their cardinality. Unfortunately, computations within the full Bayesian framework are typically intractable, due to the need to integrate over all possible models. To compute the posterior of a model, two major schemes are typically used. First, Markov Chain Monte Carlo methods (e.g., [Gilks et al., 1996]) potentially achieve exact results and can offer an *anytime* solution. For non trivial models, however, these methods require vast computational resources to achieve reasonable accuracy. This is particularly true in the presence of hidden variables and if the number of such variables and their cardinality is unknown (e.g., [Green, 1995]). Second, the Laplace approximation and its variants (see [Chickering and Heckerman, 1997] for a comparison of different methods), offer efficient closed form posterior computations. However, these methods assume that the posterior is a normal distribution, and are only asymptotically accurate. In practice, both scheme are used for relatively simple cases, such as mixture models. More recently, Attias [1999] has suggested a theoretically elegant approach for learning new hidden variables and estimating their cardinality. He suggests a *Variational Bayes* approach that draws on variational algorithms in graphical models (e.g., [Jordan et al., 1998]) and Bayesian methods for mixture models [Waterhouse et al., 1996]. The idea is to assume independence of the posterior of the hidden variables and the unknown parameters, and use an EM like algorithm for iteratively and analytically estimate the full posterior. Thus, the approach assumes a decomposition of the distribution rather than choosing a specific (e.g., normal) functional form. The method is successfully applied to mixture models and the source separation problem when the number of sources is unknown, but it is still limited to relatively simple models with few variables. Unfortunately, all of the above attempts to approximate the full Bayesian approach are still limited by the computational needs of the algorithm when applied to real-life network. Thus, practical heuristic methods were developed in order to cope with the challenge of learning new hidden variables in practice.

Spirtes et al. [1993] suggest an approach that is based on constraint-based model selection. Their algorithm defines a set of conditional independencies that (above some significance threshold) hold in the data. They then try to find a structure consistent with these constrains, and are able to detects patterns of conditional independencies that can only be generated in the presence of hidden variables. A hidden variable is then introduced to account for these independencies, and parameters of the augmented structure are estimated. This approach suffers from several limitations. First, as for all constraint-based techniques, the dependencies in the data that are going to be used are selected using a fixed a priori threshold. Second, the approach is sensitive to failure in few of the multiple independence tests it uses. In contrast, score based methods allow a smoother trade-off between fit to the data and model complexity. Third, their method only detects hidden variables that are *forced* by the qualitative independence constraints. It cannot detect situations where the hidden variable provides a more succinct model of a distribution that can be described by a network without a hidden variable as in the example of Figure 1.1.

Later, in a series of works, Spirtes et al. [1995] suggested an alternative framework for learning with hidden variables. Rather than learning structure in the space of *Directed Acyclic Graphs* (DAGs), where there are infinitely many possibilities to incorporate hidden variables, they use a representation called a *Partial Ancestral Graph* (PAG). Briefly, a PAG represents a subset of an equivalence class of DAGs that may include (infinitely many) hidden variables and selection bias variables. All DAGs represented by a PAG share a common characteristics: they are *d-separation* equivalent over the *observed* set of variables. Unlike DAGs with hidden variables, the number of PAGs is finite, and like DAGs they facilitate a relatively efficient search. PAGs are used mostly to learn causal ancestor-descendant relations and to estimate the effect of interventions. The main drawback becomes evident when we want to treat graphical models as probabilistic independence maps, rather than as causal models. In this case, a single PAG can represent many DAG models that are quite different in terms of the distribution they represent (they are d-separation equivalent only over the observed set of variables). In particular, both models of the cancer domain shown in Figure 1.1(a,b) and that motivated the need for hidden variables, are d-separation equivalent over the observed variables. Thus, while learning a PAG for these two models may be effective for asserting properties such as “smoking precedes lumps”, it cannot prefer Figure 1.1(a) that is more succinct, and is desirable both in terms of learning robustness and in terms of qualitative modeling.

Martin and VanLehn [1995] use an approach that is based on pair-wise correlations. First, a “dependency” graph is built in which there is an edge from $X$ to $Y$ if their correlation is above a predetermined threshold. They then construct a two-layered network that contains independent hidden variables in the top level, and observable nodes in the bottom layer, such that every dependency between two observed variables is “explained” by at least one common hidden parent. This approach suffers from three important drawbacks. First, it does not eliminate from consideration correlations that can be explained by direct edges between the observed nodes. Thus, redundant clusters are formed even in cases where the dependencies can be fully explained without them. Second, since it only examines pairwise dependencies, it cannot detect conditional independencies, such as $Ind(X \perp Y \mid Z)$ that can be the result of data created from a $X \rightarrow Z \rightarrow Y$ structure. (In this case, it would learn a hidden variable that is the parent of all three variables.) Finally, this approach learns a restricted form of networks that requires many hidden variables to represent dependencies among variables. Thus, it has limited utility in distinguishing “true” hidden variables from artifacts of the representation. Furthermore, in doing so, one of the basic motivations for using hidden variables — to achieve an effective and succinct representation – is lost.

Finally, in a series of works, Zhang [2004] explored search operators that are specifically tailored for learning *Hierarchical Latent Class* (HLC) models. They define equivalence of HLC models and suggest operators of parsimonious HLCs that change the graph locally and efficiently. As they, show, a structural EM like variant can be used for learning HLCs in practice. While their method is appealing in its approach, it is not clear that it is superior to simple methods for learning hierarchical clustering models. Furthermore, their method cannot be generalized to structures with hidden variables that are not hierarchical.

The common limitation of the above works is that they are applicable, either by definition or because of practical considerations to specific scenarios and limited network structures. It was the primary goal of this dissertation to present general methods that can be applied to relatively large scale models, and without the controversial treatment of the model as a causal one.

## 8.4 Future Prospects

The task of learning new hidden variables in probabilistic graphical model in general, and Bayesian networks in particular, is a central and elusive challenge. This dissertation offers the first step toward methods that treat this problem in a general context (e.g., Bayesian networks) without posing restrictive constraints on the model.

The next natural step is to consider the application of the methods presented here for a wider variety of models. This includes extensions to both undirected models (e.g., [Pearl, 1998]) and *Probabilistic Relational Models* (PRMs) [Friedman et al., 1999a]. In the case of *IB-EM*, such extensions appear more subtle than for the other methods presented in this dissertation. Specifically, in relational models, the instance identity takes on a different meaning: each object of each class has an identity value and the data involves a single instance. This requires some adaptations to the framework that change the semantics of the hidden variable. For undirected models we can use a *Chain Graph* [Buntine, 1995] for $\mathcal{G}_{out}$ to encode the independencies of the target model and those required by the IB-EM framework. This somewhat complicates computations but may lead to an effective way of learning challenging undirected models using continuation.

— as a compression mechanism for the instance identity. The *Information Bottleneck* framework, on which this method relies, is inherently directed in its construction, and need to be revisited for undirected models.

Less clear, but of significant importance, is the extension to the hybrid models that allows both discrete and continuous variables. Despite recent progress in learning methods for these networks (e.g., [Lerner, 2002]), our understanding of how such a domain should be approached remains limited. Adapting methods for learning new hidden variables in this scenario remains an important challenge.

Several drawbacks of the different methods discussed in Section 8.2, may be overcome with further investigations: Instead of the rigid structural signature currently used by *FindHidden* to detect new hidden variables, we might be able to use soft confidence measures of edges and a weighted measure for clique like structures. This will potentially result in an algorithm that is still simple and easy to implement and that at the same time can be applied in the case of sparse data. Another direction is to extend our *Weight Annealing* approach to utilize continuation. This will rid the algorithm of an arbitrary cooling policy and will potentially results in comparable running times to IB-EM. This can have important ramifications as Weight Annealing is already used successfully in various learning problems [Friedman et al., 2001, Barash and Friedman, 2002].

Another important avenue of research is to improve our theoretical understanding of the methods presented in the dissertation. The *Weight Annealing* toy problem presented in Chapter 3, hints of a possibility of characterizing families of distributions for which the algorithm provably works; The *IB-EM* framework offers the potential of adapting the theory to relational models; The *Ideal Parent* approach can be extended to encompass a wider family of conditional probability distributions, such as those that use multiplicative Gaussian noise.

Today, numerous challenging applications of graphical models use manually constructed hidden variables to augment the expressiveness of the model. It is our belief that the methods presented in this dissertation will pave the way to learning flexible probabilistic models with effective hidden variables. It is our hope, that in this process, the hidden variables learned will not only increase measurable qualitative performance, but also shed light on new and interesting domains.

# Notation

| | |
|---|---|
| $X, Y, Z \ldots$ | random variables or their corresponding nodes in the network |
| $\mathbf{X}, \mathbf{Y}, \mathbf{Z} \ldots$ | sets of random variables or their corresponding nodes in the network |
| $Val(X)$ | the set of possible values of a discrete variable $X$ |
| $x, y, z \ldots$ | assignments to random variables |
| $\mathbf{x}, \mathbf{y}, \mathbf{z} \ldots$ | joint assignments to sets of random variables |
| $(\mathbf{X} \perp \mathbf{Y})$ | independence of (sets of) random variables |
| $Ind(\mathbf{X} \perp \mathbf{Y} \mid \mathbf{Z})$ | conditional independence of (sets of) random variables |
| $P(\mathbf{X})$ | probability density of (sets of) random variables ($P$ is used to denote $P(\mathcal{X})$) |
| $P(\mathbf{X}, \mathbf{Y}, \mathbf{Z} \ldots)$ | joint probability density of several (sets of) random variables |
| $P(\mathbf{X} \mid \mathbf{Y})$ | conditional probability density of $\mathbf{X}$ given $\mathbf{Y}$ |
| $\mathcal{B}$ | a Bayesian network |
| $\mathcal{X}$ | the set of all variables in the network $\{X_1, \ldots, X_N\}$ |
| $\mathcal{G}$ | the graph structure of a network |
| $\theta$ | the parameters of a network |
| $\theta_{X_i \mid \mathbf{Pa}_i}$ | parameter of the CPD of $X_i$ |
| $\theta_{x_i \mid \mathbf{pa}_i}$ | parameter corresponding to the values $x_i$ and $\mathbf{pa}_i$ in the CPD of $X_i$ |
| $\mathbf{Pa}_i^{\mathcal{G}}$ | the parents variables of the variable $X_i$ in $\mathcal{G}$ |
| $\mathbf{Ch}_i^{\mathcal{G}}$ | the children variables of the variable $X_i$ in $\mathcal{G}$ |
| $\mathbf{Fam}_i^{\mathcal{G}}$ | the family of $X_i$ in $\mathcal{G}$ (itself and its parents) |
| $\mathbf{Adj}_i^{\mathcal{G}}$ | the adjacent variables to $X_i$ in $\mathcal{G}$ (its parent and children) |
| $\mathbf{MB_i^{\mathcal{G}}}$ | the Markov blanket variables of $X_i$ in $\mathcal{G}$ (its parent, children and their parents) |
| $\mathbf{pa}_i^{\mathcal{G}}$ | an assignment to parents of $X_i$ |
| $N$ | number of variables in the network |
| $\mathcal{D}$ | the training data set |
| $M$ | number of instances in training set |
| $S[x_i, \mathbf{pa}_i]$ | the suffi cient statistics count of $x_i$ and $\mathbf{pa}_i$ in $\mathcal{D}$ |
| $\mathbf{H}$ | hidden variables |
| $\mathbf{O}$ | observed variables |
| $\mathbf{x}[m]$ | the value of $\mathbf{x}$ in the $m$'th sample |
| $\mathbf{o}[m]$ | the $m$'th partially observed instance |
| $L(\theta, \mathcal{G} : \mathcal{D})$ | likelihood of the data given $\theta$ and $\mathcal{G}$ |
| $\ell(\theta, \mathcal{G} : \mathcal{D})$ | log-likelihood of the data given $\theta$ and $\mathcal{G}$ |
| $L_{X_i}(\theta, \mathcal{G} : \mathcal{D})$ | local likelihood of $X_i$'s family |
| $\ell_{X_i}(\theta, \mathcal{G} : \mathcal{D})$ | local log-likelihood of $X_i$'s family |
| $\hat{\theta}$ | estimated parameters |
| $\alpha^j$ | hyper-parameters corresponding to the $j$th value in a multinomial distribution |
| $\alpha_{x_i^j}$ | hyper-parameters corresponding to the $j$th value of $X_i$ |
| $\mathrm{Score}(\mathcal{G} : \mathcal{D})$ | score of $\mathcal{G}$ given $\mathcal{D}$ |

# Bibliography

J. Adachi and M. Hasegawa. Molphy version 2.3, programs for molecular phylogenetics based on maximum likelihood. Technical report, The Institute of Statistical Mathematics, Tokyo, Japan, 1996.

H. Attias. Inferring parameters and structure of latent variable models by variational bayes. In K. Laskey and H. Prade, editors, *Proc. Fifteenth Conference on Uncertainty in Artificial Intelligence (UAI '99)*, pages 21–30, San Francisco, 1999. Morgan Kaufmann.

Y. Barash, G. Bejerano, and N. Friedman. A simple hyper-geometric approach for discovering putative transcription factor binding sites. In O. Gascuel and B. M. E. Moret, editors, *Algorithms in Bioinformatics: Proceedings of the First International Workshop*, number 2149 in LNCS, pages 278–293. Springer, 2001.

Y. Barash and N. Friedman. Context-specific Bayesian clustering for gene expression data. *Journal of Computational Biology*, 9:169–191, 2002.

R. Bareiss and B. Porter. Protos: An exemplar-based learning apprentice. *Proc. 4th International Workshop on Machine Learning*, pages 12–23, 1987.

M. Behr, M. Wilson, W. Gill, H. Salamon, G. Schoolnik, S. Rand, and P. Small. Comparative genomics of bcg vaccines by whole genome dna microarray. *Science*, 284:1520–1523, 1999.

I. Beinlich, G. Suermondt, R. Chavez, and G. Cooper. The ALARM monitoring system: A case study with two probabilistic inference techniques for belief networks. In *Proc. 2'nd European Conference on AI and Medicine*, volume 38, pages 247–256. Springer-Verlag, Berlin, 1989.

J. Binder, D. Koller, S. Russell, and K. Kanazawa. Adaptive probabilistic networks with hidden variables. *Machine Learning*, 29:213–244, 1997.

C. M. Bishop. *Neural Networks for Pattern Recognition*. Oxford University Press, Oxford, United Kingdom, 1995.

C. Boutilier, N. Friedman, M. Goldszmidt, and D. Koller. Context-specific independence in Bayesian networks. In E. Horvitz and F. Jensen, editors, *Proc. Twelfth Conference on Uncertainty in Artificial Intelligence (UAI '96)*, pages 115–123, San Francisco, 1996. Morgan Kaufmann.

X. Boyen, N. Friedman, and D. Koller. Discovering the hidden structure of complex dynamic systems. In K. Laskey and H. Prade, editors, *Proc. Fifteenth Conference on Uncertainty in Artificial Intelligence (UAI '99)*, pages 91–100, San Francisco, 1999. Morgan Kaufmann.

W. Buntine. Learning classification trees. In D. J. Hand, editor, *Artificial Intelligence Frontiers in Statistics*, number III in AI and Statistics, pages 182–201. Chapman & Hall, London, 1993.

W. Buntine. Chain graphs for learning. In P. Besnard and S. Hanks, editors, *Proc. Eleventh Conference on Uncertainty in Artificial Intelligence (UAI '95)*, pages 46–54, San Francisco, 1995. Morgan Kaufmann.

K. Chang and R. Fung. Refinement and coarsening of bayesian networks. In P. P. Bonissone, M. Henrion, L. N. Kanal, and J. F. Lemmer, editors, *Proc. Sixth Annual Conference on Uncertainty Artificial Intelligence (UAI '90)*, pages 475–482, San Francisco, 1990. Morgan Kaufmann.

G. Chechik, A. Globerson, N. Tishby, and Y.Weiss. Gaussian information bottleneck. In S. Thrun, L. K. Saul, and B. Schölkopf, editors, *Advances in Neural Information Processing Systems 16*, Cambridge, Mass., 2003. MIT Press.

P. Cheeseman, J. Kelly, M. Self, J. Stutz, W. Taylor, and D. Freeman. Autoclass: a Bayesian classification system. In *Proc. Fifth International Workshop on Machine Learning*, pages 54–64. Morgan Kaufmann, San Francisco, 1988.

D. M. Chickering. A transformational characterization of equivalent Bayesian network structures. In P. Besnard and S. Hanks, editors, *Proc. Eleventh Conference on Uncertainty in Artificial Intelligence (UAI '95)*, pages 87–98, San Francisco, 1995. Morgan Kaufmann.

D. M. Chickering. Learning Bayesian networks is NP-complete. In D. Fisher and H. J. Lenz, editors, *Learning from Data: Artificial Intelligence and Statistics V*, pages 121–130. Springer-Verlag, New York, 1996a.

D. M. Chickering. Learning equivalence classes of Bayesian network structures. In E. Horvitz and F. Jensen, editors, *Proc. Twelfth Conference on Uncertainty in Artificial Intelligence (UAI '96)*, pages 150–157, San Francisco, 1996b. Morgan Kaufmann.

D. M. Chickering and D. Heckerman. Efficient approximations for the marginal likelihood of incomplete data given a Bayesian network. In E. Horvitz and F. Jensen, editors, *Proc. Twelfth Conference on Uncertainty in Artificial Intelligence (UAI '96)*, pages 158–168, San Francisco, 1996. Morgan Kaufmann.

D. M. Chickering and D. Heckerman. Efficient approximations for the marginal likelihood of Bayesian networks with hidden variables. *Machine Learning*, 29:181–212, 1997.

C. K. Chow and C. N. Liu. Approximating discrete probability distributions with dependence trees. *IEEE Trans. on Info. Theory*, 14:462–467, 1968.

B. Codenotti, G. Manzini, L. Margara, and G. Resta. Perturbation: An efficient technique for the solution of very large instances of the TSP. *INFORMS Journal on Computing*, 8(2):125–133, 1996.

G. F. Cooper. The computational complexity of probabilistic inference using Bayesian belief networks. *Artificial Intelligence*, 42:393–405, 1990.

G. F. Cooper and E. Herskovits. A Bayesian method for the induction of probabilistic networks from data. *Machine Learning*, 9:309–347, 1992.

A. Corduneanu and T. Jaakkola. Continuation methods for mixing heterogeneous sources. In A. Darwich and N. Friedman, editors, *Proc. Eighteenth Conference on Uncertainty in Artificial Intelligence (UAI '02)*, pages 111–118, San Francisco, 2002. Morgan Kaufmann.

T. H. Cormen, C. E. Leiserson, and R. L. Rivest. *Introduction to Algorithms*. MIT Press, Cambridge, Massachusetts, 1990.

T. M. Cover and J. A. Thomas. *Elements of Information Theory*. John Wiley & Sons, New York, 1991.

P. Dagum and M. Luby. An optimal approximation algorithm for Baysian inference. *Artificial Intelligence*, 93(1–2):1–27, 1997.

T. Dean and K. Kanazawa. A model for reasoning about persistence and causation. *Computational Intelligence*, 5:142–150, 1989.

R. Dechter. Bucket elimination: A unifying framework for probabilistic inference. In E. Horvitz and F. Jensen, editors, *Proc. Twelfth Conference on Uncertainty in Artificial Intelligence (UAI '96)*, pages 211–219, San Francisco, 1996. Morgan Kaufmann.

M. H. DeGroot. *Probability and Statistics*. Addison Wesley, Reading, MA, 1989.

A. P. Dempster, N. M. Laird, and D. B. Rubin. Maximum likelihood from incomplete data via the EM algorithm. *Journal of the Royal Statistical Society*, B 39:1–39, 1977.

F. J. Diez. Parameter adjustment in Bayes networks: The generalized noisy or-gate. In D. Heckerman and A. Mamdani, editors, *Proc. Ninth Conference on Uncertainty in Artificial Intelligence (UAI '93)*, pages 99–105, San Francisco, 1993. Morgan Kaufmann.

R. O. Duda and P. E. Hart. *Pattern Classification and Scene Analysis*. John Wiley & Sons, New York, 1973.

R. Durbin, S. Eddy, A. Krogh, and G. Mitchison. *Biological Sequence Analysis : Probabilistic Models of Proteins and Nucleic Acids*. Cambridge University Press, 1998.

B. Efron and R. J. Tibshirani. *An Introduction to the Bootstrap*. Chapman & Hall, London, 1993.

T. El-Hay and N Friedman. Incorporating expressive graphical models in variational approximations: Chain-graphs and hidden variables. In J.S. Breese and D. Koller, editors, *Proc. Seventeenth Conference on Uncertainty in Artificial Intelligence (UAI '01)*, pages 136–143, San Francisco, 2001. Morgan Kaufmann.

G. Elidan and N. Friedman. Learning the dimensionality of hidden variables. In J.S. Breese and D. Koller, editors, *Proc. Seventeenth Conference on Uncertainty in Artificial Intelligence (UAI '01)*, pages 144–151, San Francisco, 2001. Morgan Kaufmann.

G. Elidan and N. Friedman. The information bottleneck EM algorithm. In C. Meek and U. Kjærulff, editors, *Proc. Nineteenth Conference on Uncertainty in Artificial Intelligence (UAI '03)*, pages 200–208, San Francisco, 2003. Morgan Kaufmann.

G. Elidan, N. Lotner, N. Friedman, and D. Koller. Discovering hidden variables: A structure-based approach. In T. K. Leen, T. G. Dietterich, and V. Tresp, editors, *Advances in Neural Information Processing Systems 13*, pages 479–485, Cambridge, Mass., 2001. MIT Press.

G. Elidan, M. Ninio, N. Friedman, and D. Schuurmans. Data perturbation for escaping local maxima in learning. In *Proc. National Conference on Artificial Intelligence (AAAI '02)*, pages 132–139. AAAI Press, Menlo Park, CA, 2002.

N. Friedman. Learning belief networks in the presence of missing values and hidden variables. In D. Fisher, editor, *Proc. Fourteenth International Conference on Machine Learning*, pages 125–133. Morgan Kaufmann, San Francisco, 1997.

N. Friedman. The Bayesian structural EM algorithm. In G. F. Cooper and S. Moral, editors, *Proc. Fourteenth Conference on Uncertainty in Artificial Intelligence (UAI '98)*, pages 129–138, San Francisco, 1998. Morgan Kaufmann.

N. Friedman, D. Geiger, and M. Goldszmidt. Bayesian network classifiers. *Machine Learning*, 29: 131–163, 1997.

N. Friedman, L. Getoor, D. Koller, and A. Pfeffer. Learning probabilistic relational models. In *Proc. Sixteenth International Joint Conference on Artificial Intelligence (IJCAI '99)*, pages 1300–1309. Morgan Kaufmann, San Francisco, 1999a.

N. Friedman and M. Goldszmidt. Discretization of continuous attributes while learning Bayesian networks. In L. Saitta, editor, *Proc. Thirteenth International Conference on Machine Learning*, pages 157–165. Morgan Kaufmann, San Francisco, 1996a.

N. Friedman and M. Goldszmidt. Learning Bayesian networks with local structure. In E. Horvitz and F. Jensen, editors, *Proc. Twelfth Conference on Uncertainty in Artificial Intelligence (UAI '96)*, pages 252–262, San Francisco, 1996b. Morgan Kaufmann.

N. Friedman, M. Goldszmidt, and A. Wyner. Data analysis with Bayesian networks: A bootstrap approach. In K. Laskey and H. Prade, editors, *Proc. Fifteenth Conference on Uncertainty in Artificial Intelligence (UAI '99)*, pages 196–205, San Francisco, 1999b. Morgan Kaufmann.

N. Friedman and D. Koller. Being Bayesian about Bayesian network structure: A Bayesian approach to structure discovery in Bayesian networks. *Machine Learning*, 50:95–126, 2003.

N. Friedman, M. Linial, I. Nachman, and D. Pe'er. Using Bayesian networks to analyze expression data. *Computational Biology*, 7:601–620, 2000.

N. Friedman, O. Mosenzon, N. Slonim, and N. Tishby. Multivariate information bottleneck. In J.S. Breese and D. Koller, editors, *Proc. Seventeenth Conference on Uncertainty in Artificial Intelligence (UAI '01)*, pages 152–161, San Francisco, 2001. Morgan Kaufmann.

N. Friedman, I. Nachman, and D. Pe'er. Learning bayesian network structure from massive datasets: The "sparse candidate" algorithm. In K. Laskey and H. Prade, editors, *Proc. Fifteenth Conference on Uncertainty in Artificial Intelligence (UAI '99)*, pages 206–215, San Francisco, 1999c. Morgan Kaufmann.

N. Friedman, M. Ninio, I. Peer, and T. Pupko. A structural EM algorithm for phylogentic inference. *Journal of Computational Biology*, 9:331–353, 2002.

A. P. Gasch, P. T. Spellman, C. M. Kao, O. Carmel-Harel, M. B. Eisen, G. Storz, D. Botstein, and P. O. Brown. Genomic expression program in the response of yeast cells to environmental changes. *Molecular Biology of the Cell*, 11:4241–4257, 2000.

D. Geiger and D. Heckerman. Learning gaussian networks. In R. López de Mantarás and D. Poole, editors, *Proc. Tenth Conference on Uncertainty in Artificial Intelligence (UAI '94)*, pages 235–243, San Francisco, 1994. Morgan Kaufmann.

D. Geiger and D. Heckerman. Knowledge representation and inference in similarity networks and Bayesian multinets. *Artificial Intelligence*, 82:45–74, 1996.

D. Geiger, D. Heckerman, and C. Meek. Asymptotic model selection for directed networks with hidden variables. In E. Horvitz and F. Jensen, editors, *Proc. Twelfth Conference on Uncertainty in Artificial Intelligence (UAI '96)*, pages 283–290, San Francisco, 1996. Morgan Kaufmann.

D. Geiger and C. Meek. Graphical models and exponential families. In G. F. Cooper and S. Moral, editors, *Proc. Fourteenth Conference on Uncertainty in Artificial Intelligence (UAI '98)*, pages 156–165, San Francisco, 1998. Morgan Kaufmann.

D. Geiger, T. S. Verma, and J. Pearl. Identifying independence in bayesian networks. *Networks*, 20: 507–534, 1990.

A. Gelman, J. B. Carlin, H. S. Stern, and D. B. Rubin. *Bayesian Data Analysis*. Chapman & Hall, London, 1995.

W.R. Gilks, S. Richardson, and D.J. Spiegelhalter. *Markov Chain Monte Carlo Methods in Practice*. CRC Press, 1996.

F. Glover and M. Laguna. Tabu search. In C. Reeves, editor, *Modern Heuristic Techniques for Combinatorial Problems*, Oxford, England, 1993. Blackwell Scientific Publishing.

P.J. Green. Reversible jump Markov chain Monte Carlo computation and Bayesian model determination. *Biometrika*, 82:711–732, 1995.

D. Heckerman. A tutorial on learning with Bayesian networks. In M. I. Jordan, editor, *Learning in Graphical Models*. Kluwer, Dordrecht, Netherlands, 1998.

D. Heckerman and D. Geiger. Learning Bayesian networks: a unification for discrete and Gaussian domains. In P. Besnard and S. Hanks, editors, *Proc. Eleventh Conference on Uncertainty in Artificial Intelligence (UAI '95)*, pages 274–284, San Francisco, 1995. Morgan Kaufmann.

D. Heckerman, D. Geiger, and D. M. Chickering. Learning Bayesian networks: The combination of knowledge and statistical data. In R. López de Mantarás and D. Poole, editors, *Proc. Tenth Conference on Uncertainty in Artificial Intelligence (UAI '94)*, pages 293–301, San Francisco, 1994. Morgan Kaufmann.

D. Heckerman, D. Geiger, and D. M. Chickering. Learning Bayesian networks: The combination of knowledge and statistical data. *Machine Learning*, 20:197–243, 1995a.

D. Heckerman, A. Mamdani, and M. P. Wellman. Real-world applications of Bayesian networks. *Communications of the ACM*, 38, 1995b.

T. Hofmann and J. M. Buhmann. Pairwise data clustering by deterministic annealing. *IEEE Transactions on Pattern Analysis and Machine Intelligence*, 19:1–14, 1997.

T. R. Hughes, M. J. Marton, A. R. Jones, C. J. Roberts, R. Stoughton, C. D. Armour, H. A. Bennett, E. Coffey, H. Dai, Y. D. He, M. J. Kidd, A. M. King, M. R. Meyer, D. Slade, P. Y. Lum, S. B. Stepaniants, D. D. Shoemaker, D. Gachotte, K. Chakraburtty, J. Simon, M. Bard, and S. H. Friend. Functional discovery via a compendium of expression profiles. *Cell*, 102(1):109–26, 2000.

E. T. Jaynes. Information theory and statistical mechanics. *Physical Review*, 106:620–630, 1957.

F. V. Jensen. *An introduction to Bayesian Networks*. University College London Press, London, 1996.

F. V. Jensen, S. L. Lauritzen, and K. G. Olesen. Bayesian updating in causal probabilistic networks by local computations. *Computational Statistics Quarterly*, 5(4):269–282, 1990.

M. I. Jordan, Z. Ghahramani, T. Jaakkola, and L. K. Saul. An introduction to variational approximations methods for graphical models. In M. I. Jordan, editor, *Learning in Graphical Models*. Kluwer, Dordrecht, Netherlands, 1998.

S. Kirkpatrick, C. D. Gelatt, and M. P. Vecchi. Optimization by simulated annealing. *Science*, 220 (4598):671–680, 1983.

S. Kirpatrick, C.D. Gelatt, Jr., and M.P. Vecchi. Optimization by simulated annealing. *Science*, 220: 671–680, May 1994.

J. Kivinen and M. Warmuth. Exponentiated gradient versus gradient descent for linear predictors. *Information and Computation*, 132:1–63, 1997.

T. Kocka and N. L. Zhang. Dimension correction for hierarchical latent class models. In A. Darwich and N. Friedman, editors, *Proc. Eighteenth Conference on Uncertainty in Artificial Intelligence (UAI '02)*, pages 267–274, San Francisco, 2002. Morgan Kaufmann.

S. Kullback and R. A. Leibler. On information and sufficiency. *Annals of Mathematical Statistics*, 22:76–86, 1951.

P. Laarhoven and E. Aarts. *Simulated Annealing: Theory and Applications*. John Wiley & Sons, New York, 1987.

W. Lam and F. Bacchus. Learning Bayesian belief networks: An approach based on the MDL principle. *Computational Intelligence*, 10:269–293, 1994.

K. Lang. Learning to filter netnews. In *12th International Conference on Machine Learning*, pages 331–339. Morgan Kaufmann, San Francisco, California, 1995.

S. L. Lauritzen. The EM algorithm for graphical association models with missing data. *Computational Statistics and Data Analysis*, 19:191–201, 1995.

S. L. Lauritzen and D. J. Spiegelhalter. Local computations with probabilities on graphical structures and their application to expert systems. *Journal of the Royal Statistical Society*, B 50(2):157–224, 1988.

S. L. Lauritzen and N. Wermuth. Graphical models for associations between variables, some of which are qualitative and some quantitative. *Annals of Statistics*, 17:31–57, 1989.

U. N. Lerner. *Hybrid Bayesian Networks for Reasoning about Complex Systems*. PhD thesis, Dept. of Computer Science, Stanford University, 2002.

J. Martin and K. VanLehn. Discrete factor analysis: Learning hidden variables in Bayesian networks. Technical report, Department of Computer Science, University of Pittsburgh, 1995.

L. Mason, J. Baxter, P. Bartlett, and M. Frean. Functional gradient techniques for combining hypotheses. In *Advances in Large Margin Classifiers*. MIT Press, 2000.

P. McCullagh and J.A. Nelder. *Generalized Linear Models*. Chapman & Hall, London, 1989.

M. Meila and M. I. Jordan. Estimating dependency structure as a hidden variable. In M. I. Jordan, M. J. Kearns, and S. A. Solla, editors, *Advances in Neural Information Processing Systems 10*, pages 584–590, Cambridge, Mass., 1998. MIT Press.

N. Metropolis, A.W. Rosenbluth, M.N. Rosenbluth, A.H. Teller, and E. Teller. Equation of state calculation by fast computing machines. *Journal of Chemical Physics*, 21:1087–1092, 1953.

R. Michalski and R. Chilausky. Learning by being told and learning from examples: An experimental comparison of the two methods of knowledge acquisition in the context of developing an expert system for soybean disease diagnosis. *International Journal of Policy Analysis and Information Systems*, 4(2), 1980.

G. W. Milligan and M. C. Cooper. An examination of procedures for determining the number of clusters in a data set. *Psychometrika*, 50:159–179, 1985.

K. Murphy and Y. Weiss. Loopy belief propagation for approximate inference: An empirical study. In K. Laskey and H. Prade, editors, *Proc. Fifteenth Conference on Uncertainty in Artificial Intelligence (UAI '99)*, pages 467–475, San Francisco, 1999. Morgan Kaufmann.

I. Nachman, A. Regev, and N. Friedman. Inferring quantitative models of regulatory networks from expression data. *Bioinformatics*, 20(Suppl 1):S1248–1256, 2004.

R. M. Neal. Connectionist learning of belief networks. *Artificial Intelligence*, 56:71–113, 1992.

R. M. Neal. Probabilistic inference using Markov chain Monte Carlo methods. Technical Report CRG-TR-93-1, Department of Computer Science, University of Toronto, 1993.

R. M. Neal and G. E. Hinton. A new view of the EM algorithm that justifies incremental and other variants. In M. I. Jordan, editor, *Learning in Graphical Models*. Kluwer, Dordrecht, Netherlands, 1998.

K. C. Nixon. The parsimony ratchet, a new method for rapid parsimony analysis. *Cladistics*, 15: 407–414, 1999.

J. Pearl. *Probabilistic Reasoning in Intelligent Systems*. Morgan Kaufmann, 1988.

J. Pearl. Graphs, causality, and structural equation models. *Socioligical Methods and Research*, 1998.

J. Pearl. *Causality: Models, Reasoning, and Inference*. Cambridge Univ. Press, 2000.

D. Pe'er, A. Regev, G. Elidan, and N. Friedman. Inferring subnetworks from perturbed expression profiles. *Bioinformatics*, 17(Suppl 1):S215–24, 2001.

Fernando Pereira, Naftali Tishby, and Lillian Lee. Distributional clustering of English words. In *31st Annual Meeting of the ACL*, pages 183–190, 1993.

Kim Leng Poh and Eric J. Horvitz. Reasoning about the value of decision-model refinement: Methods and application. In D. Heckerman and A. Mamdani, editors, *Proc. Ninth Conference on Uncertainty in Artificial Intelligence (UAI '93)*, pages 174–182, San Francisco, 1993. Morgan Kaufmann.

W. H. Price. *Numerical Recipes in C*. Cambridge University Press, Cambridge, 1992.

J. R. Quinlan. *C4.5: Programs for Machine Learning*. Morgan Kaufmann, San Francisco, California, 1993.

L. R. Rabiner. A tutorial on hidden Markov models and selected applications in speech recognition. *Proc. IEEE*, 77(2):257–286, 1990.

K. Rose. Deterministic annealing for clustering, compression, classification, regression, and related optimization problems. *Proc. IEEE*, 86:2210–2239, 1998.

D. R. Rubin. Inference and missing data. *Biometrica*, 63:581–592, 1976.

S. Russell and P. Norwig. *Artificial Intelligence: A Modern Approach*. Parentice Hall, 1995.

L. Saul, T. Jaakkola, and M. Jordan. Mean field theory for sigmoid belief networks. *Journal of Artificial Intelligence Research*, 4:61–76, 1996.

R. E. Schapire and Y. Singer. Improved boosting algorithms using confidence-rated predictions. *Machine Learning*, 37(3):297–336, 1999.

D. Schuurmans, F. Southey, and R. Holte. The exponentiated subgradient algorithm for heuristic Boolean programming. In *Proc. Seventeenth International Joint Conference on Artificial Intelligence (IJCAI '01)*, pages 334–341, San Francisco, 2001. Morgan Kaufmann.

G. Schwarz. Estimating the dimension of a model. *Annals of Statistics*, 6:461–464, 1978.

E. Segal, Y. Barash, I. Simon, N. Friedman, and D. Koller. From promoter sequence to expression: A probabilistic framekwork. In Gene Myers, Sridhar Hannenhalli, Sorin Istrail, Pavel Pevzner, and Michael Waterman, editors, *Proceedings of the Sixth Annual International Conference on Computational Biology (RECOMB '02)*, pages 263–272. ACM Press, New York, 2002.

R. Settimi and J. Q. Smith. On the geometry of bayesian graphical models with hidden variables. In G. F. Cooper and S. Moral, editors, *Proc. Fourteenth Conference on Uncertainty in Artificial Intelligence (UAI '98)*, pages 472–479, San Francisco, 1998. Morgan Kaufmann.

M.A. Shwe, B. Middleton, D.E. Heckerman, M. Henrion, E.J. Horvitz, H.P. Lehmann, and G.F. Cooper. Probabilistic diagnosis using a reformulation of the INTERNIST-1/QMR knowledge base. I. The probabilistic model and inference algorithms. *Methods of Information in Medicine*, 30:241–55, 1991.

I. Simon, J. Barnett, N. Hannett, C.T. Harbison, N.J. Rinaldi, T.L. Volkert, J.J. Wyrick, J. Zeitlinger, D.K. Gifford, T.S. Jaakkola, and R.A. Young. Serial regulation of transcriptional regulators in the yeast cell cycle. *Cell*, 106:697–708, 2001.

N. Slonim, N.Friedman, and T.Tishby. Agglomerative multivariate information bottleneck. In T. G. Dietterich, S. Becker, and Z. Ghahramani, editors, *Advances in Neural Information Processing Systems 14*, pages 929–936, Cambridge, Mass., 2002. MIT Press.

N. Slonim and N. Tishby. Agglomerative information bottleneck. In S. A. Solla, T. K. Leen, and K. Müller, editors, *Advances in Neural Information Processing Systems 12*, pages 617–623, Cambridge, Mass., 2000. MIT Press.

N. Slonim and N. Tishby. Data clustering by markovian relaxation and the information bottleneck method. In T. K. Leen, T. G. Dietterich, and V. Tresp, editors, *Advances in Neural Information Processing Systems 13*, pages 640–646, Cambridge, Mass., 2001. MIT Press.

N. Slonim and Y. Weiss. Maximum likelihood and the information bottleneck. In S. Becker, S. Thrun, and K. Obermayer, editors, *Advances in Neural Information Processing Systems 15*, pages 351–358, Cambridge, Mass., 2002. MIT Press.

N. A. Smith and J. Eisner. Annealing techniques for unsupervised statistical language learning. In *Proc. 42nd Annual Meeting of the Association for Computational Linguistics*, 2004.

P. T. Spellman, G. Sherlock, M. Q. Zhang, V. R. Iyer, K. Anders, M. B. Eisen, P. O. Brown, D. Botstein, and B. Futcher. Comprehensive identification of cell cycle-regulated genes of the yeast saccharomyces cerevisiae by microarray hybridization. *Molecular Biology of the Cell*, 9(12): 3273–97, 1998.

D. J. Spiegelhalter and S. L. Lauritzen. Sequential updating of conditional probabilities on directed graphical structures. *Networks*, 20:579–605, 1990.

P. Spirtes, C. Glymour, and R. Scheines. *Causation, Prediction and Search*. Number 81 in Lecture Notes in Statistics. Springer-Verlag, New York, 1993.

P. Spirtes, C. Meek, and T. Richardson. Causal inference in the presence of latent variables and selection bias. In P. Besnard and S. Hanks, editors, *Proc. Eleventh Conference on Uncertainty in Artificial Intelligence (UAI '95)*, pages 499–506, San Francisco, 1995. Morgan Kaufmann.

A. Stolcke and S. Omohundro. Hidden Markov Model induction by bayesian model merging. In Stephen José Hanson, Jack D. Cowan, and C. Lee Giles, editors, *Advances in Neural Information Processing Systems*, volume 5, pages 11–18. Morgan Kaufmann, San Mateo, CA, 1993.

A. Stolcke and S. Omohundro. Inducing probabilistic grammars by bayesian model merging. In *Proc. Second International Conference on Grammatical Inference*, pages 106–118, New York, 1994. Springer-Verlag.

M. Szummer and T. Jaakkola. Information regularization with partially labeled data. In S. Becker, S. Thrun, and K. Obermayer, editors, *Advances in Neural Information Processing Systems 15*, pages 640–646, Cambridge, Mass., 2002. MIT Press.

B. Thiesson, C. Meek, D. M. Chickering, and D. Heckerman. Learning mixtures of Bayesian networks. In G. F. Cooper and S. Moral, editors, *Proc. Fourteenth Conference on Uncertainty in Artificial Intelligence (UAI '98)*, pages 504–513, San Francisco, 1998. Morgan Kaufmann.

N. Tishby, F. Pereira, and W. Bialek. The information bottleneck method. In B. Hajek and R. S. Sreenivas, editors, *Proc. 37th Allerton Conference on Communication, Control and Computation*, pages 368–377. University of Illinois, 1999.

R. Parr U. Lerner and D. Koller. Bayesian fault detection and diagnosis in dynamic systems. In *Proc. of the Seventeenth National Conference on Artificial Intelligence (AAAI)*, pages 531–537, 2000.

N. Ueda and R. Nakano. Deterministic annealing EM algorithm. *Neural Networks*, 11(2):271–282, 1998.

S. Waterhouse, D. Mackay, and T. Robinson. Bayesian methods for mixtures of experts. In D. S. Touretzky, M. Mozer, and M. E. Hasselmo, editors, *Advances in Neural Information Processing Systems 8*, pages 351–357, Cambridge, Massachusetts, 1996. MIT Press.

L. T. Watson. Theory of globally convergent probability-one homotopies for non-linear programming. Technical Report TR-00-04, Department of Computer Science, Virginia Tech, 2000.

M. P. Wellman and C.-L. Liu. State-space abstraction for anytime evaluation of probabilistic networks. In R. López de Mantarás and D. Poole, editors, *Proc. Tenth Conference on Uncertainty in Artificial Intelligence (UAI '94)*, pages 567 – 574, San Francisco, 1994. Morgan Kaufmann.

M. Whiley and D. M. Titterington. Applying the deterministic annealing expectation maximization algorithm to Naive Bayes networks. Technical Report 02-5, Department of Statistics, University of Glasgow, 2002.

J. Wilkinson. *The algebric eigenvalue problem*. Claderon Press, Oxford, 1965.

S. Wright. Correlation and causation. *Journal of Agricultural Research*, 20:557–585, 1921.

N.L. Zhang. Hierarchical latent class models for cluster analysis. *Journal of Machine Learning Research*, 5:697–723, 2004.